DRUG RESISTANCE AND IMMUNE MODULATION: NEW ISSUES IN CANCER SYSTEMIC THERAPY

EDITED BY: Yunpeng Hua, Yu Guo, Kui Wang, Cheng Huang, Bing Han and Bei Liu

PUBLISHED IN: Frontiers in Molecular Biosciences

frontiers Research Topics

frontiers

ISSN 1664-8714
ISBN 978-2-88976-259-0
DOI 10.3389/978-2-88976-259-0

About Frontiers

Frontiers is more than just an open-access publisher of scholarly articles: it is a pioneering approach to the world of academia, radically improving the way scholarly research is managed. The grand vision of Frontiers is a world where all people have an equal opportunity to seek, share and generate knowledge. Frontiers provides immediate and permanent online open access to all its publications, but this alone is not enough to realize our grand goals.

Frontiers Journal Series

The Frontiers Journal Series is a multi-tier and interdisciplinary set of open-access, online journals, promising a paradigm shift from the current review, selection and dissemination processes in academic publishing. All Frontiers journals are driven by researchers for researchers; therefore, they constitute a service to the scholarly community. At the same time, the Frontiers Journal Series operates on a revolutionary invention, the tiered publishing system, initially addressing specific communities of scholars, and gradually climbing up to broader public understanding, thus serving the interests of the lay society, too.

Dedication to Quality

Each Frontiers article is a landmark of the highest quality, thanks to genuinely collaborative interactions between authors and review editors, who include some of the world's best academicians. Research must be certified by peers before entering a stream of knowledge that may eventually reach the public - and shape society; therefore, Frontiers only applies the most rigorous and unbiased reviews.
Frontiers revolutionizes research publishing by freely delivering the most outstanding research, evaluated with no bias from both the academic and social point of view. By applying the most advanced information technologies, Frontiers is catapulting scholarly publishing into a new generation.

What are Frontiers Research Topics?

Frontiers Research Topics are very popular trademarks of the Frontiers Journals Series: they are collections of at least ten articles, all centered on a particular subject. With their unique mix of varied contributions from Original Research to Review Articles, Frontiers Research Topics unify the most influential researchers, the latest key findings and historical advances in a hot research area! Find out more on how to host your own Frontiers Research Topic or contribute to one as an author by contacting the Frontiers Editorial Office: frontiersin.org/about/contact

DRUG RESISTANCE AND IMMUNE MODULATION: NEW ISSUES IN CANCER SYSTEMIC THERAPY

Topic Editors:
Yunpeng Hua, The First Affiliated Hospital of Sun Yat-sen University, China
Yu Guo, The First Affiliated Hospital of Sun Yat-sen University, China
Kui Wang, Eastern Hepatobiliary Surgery Hospital, China
Cheng Huang, Fudan University, China
Bing Han, The Affiliated Hospital of Qingdao University, China
Bei Liu, The Ohio State University, United States

Citation: Hua, Y., Guo, Y., Wang, K., Huang, C., Han, B., Liu, B., eds. (2022). Drug Resistance and Immune Modulation: New Issues in Cancer Systemic Therapy. Lausanne: Frontiers Media SA. doi: 10.3389/978-2-88976-259-0

Table of Contents

frontiers in Molecular Biosciences

REVIEW
published: 23 August 2021
doi: 10.3389/fmolb.2021.717038

Possible Immunotherapeutic Strategies Based on Carcinogen-Dependent Subgroup Classification for Oral Cancer

Jiwei Sun[1,2,3†], *Qingming Tang*[1,2,3†], *Junyuan Zhang*[1,2,3], *Guangjin Chen*[1,2,3], *Jinfeng Peng*[1,2,3] *and Lili Chen*[1,2,3*]

[1]Department of Stomatology, Union Hospital, Tongji Medical College, Huazhong University of Science and Technology, Wuhan, China, [2]School of Stomatology, Tongji Medical College, Huazhong University of Science and Technology, Wuhan, China, [3]Hubei Province Key Laboratory of Oral and Maxillofacial Development and Regeneration, Wuhan, China

The oral cavity serves as an open local organ of the human body, exposed to multiple external factors from the outside environment. Coincidentally, initiation and development of oral cancer are attributed to many external factors, such as smoking and drinking, to a great extent. This phenomenon was partly explained by the genetic abnormalities traditionally induced by carcinogens. However, more and more attention has been attracted to the influence of carcinogens on the local immune status. On the other hand, immune heterogeneity of cancer patients is a huge obstacle for enhancing the clinical efficacy of tumor immunotherapy. Thus, in this review, we try to summarize the current opinions about variant genetic changes and multiple immune alterations induced by different oral cancer carcinogens and discuss the prospects of targeted immunotherapeutic strategies based on specific immune abnormalities caused by different carcinogens, as a predictive way to improve clinical outcomes of immunotherapy-treated oral cancer patients.

Keywords: immunotherapies, oral squamous cell carcinoma, immune microenvironment, smoking, areca nut

OPEN ACCESS

Edited by:
Yu Guo,
The First Affiliated Hospital of Sun Yat-Sen University, China

Reviewed by:
Xiqiang Liu,
Southern Medical University, China
Yujie Liang,
Sun Yat-Sen University, China

****Correspondence:***
Lili Chen
chenlili1030@hust.edu.cn

†These authors have contributed equally to this work

Specialty section:
This article was submitted to Molecular Diagnostics and Therapeutics, a section of the journal Frontiers in Molecular Biosciences

Received: *30 May 2021*
Accepted: *23 July 2021*
Published: *23 August 2021*

Citation:
Sun J, Tang Q, Zhang J, Chen G, Peng J and Chen L (2021) Possible Immunotherapeutic Strategies Based on Carcinogen-Dependent Subgroup Classification for Oral Cancer. Front. Mol. Biosci. 8:717038. doi: 10.3389/fmolb.2021.717038

INTRODUCTION

Oral squamous cell carcinoma (OSCC) serves as one of the most important subtypes in head and neck squamous cell carcinoma (HNSCC), diagnosed cases of which have mounted to more than 600,000 worldwide, along with 50,000 new cases each year (Rahman et al., 2019). Unlike many other types of cancers whose pathogenesis is mainly explained by innate genetic alterations, OSCC is mainly related to some classical environmental risk factors such as tobacco and alcohol (Solomon et al., 2018). This phenomenon is easy to understand as the oral cavity is an open organ exposed to the outside environment and has broad interactions with environmental factors. On the other hand, with the development of oncogenic studies, the role of abnormality in the tumor microenvironment has been identified to be more and more important (Binnewies et al., 2018). Recently, many types of immune cells, such as M2 macrophages, regulatory T (Treg) cells, and myeloid-derived suppressor cells (MDSCs), were discovered to exert a pro-tumor influence on oral carcinogenesis (Dar et al., 2020; Li et al., 2020). The cell–cell communications mediated by extracellular vesicles have been identified as crucial mechanisms contributing to tumor progression in many types of carcinomas. Similarly, extracellular vesicles from multiple origins could get involved in many tumor-associated

processes, including proliferation, metastasis, and drug resistance during oral cancer development (Xie et al., 2019). The above clues together indicated whether environmental risk factors could promote OSCC progress *via* deregulation of the tumor microenvironment. In the perspective of tumor therapy, immunotherapies, including check-point therapy and molecule-targeted strategy, have been making significant advances and improving the prognostic outcome of tumor patients to a great extent (Kennedy and Salama, 2020). However, immunotherapy has failed to be the prior strategy for OSCC treatment, partly due to the heterogeneity of OSCC patients, as multiple types of risk factors, for example, smoking and drinking, were involved in the initiation and progression of OSCC. Considering the fact that the huge financial burden and surgical complications are the main blockades for favorable clinical outcomes of OSCC patients, a therapeutic strategy based on patient-specific risk factors is extremely necessary to direct the application of different types of immunotherapies to different patients. This kind of strategy might overcome the heterogeneity of OSCC patients and realize individual-based diagnosis and therapy for OSCC patients, paving the way for the future of OSCC immune therapies.

POSSIBLE CARCINOGENS FOR THE DEVELOPMENT OF OSCC

Exogenous carcinogen-induced tumorigenesis acts as a significant feature of OSCC, distinguishing it from other cancers. Until now, multiple kinds of substances were regarded as possible OSCC carcinogens.

Among all the possible carcinogens for OSCC, cigarette, alcohol, and areca nuts were the most prevalent and well-acknowledged carcinogens (Kumar et al., 2016). Lots of clinical and epidemiological research has identified the strong relationship between smoking and OSCC. Results of a study based on 1,114 participants showed that the risk of OSCC among non-drinkers amounted to the quantity of smoking (Blot et al., 1988). In different regions, such as East Asia, Iran, and Brazil, OSCC patients all exhibited a high percentage of smoking habits, indicating a general influence of smoking on OSCC initiation (Razavi et al., 2015; Bezerra et al., 2018; Hashibe et al., 2019). Furthermore, OSCC patients with a smoking habit showed more aggressive disease features and poorer prognostic outcomes than non-smoking OSCC patients, indicating that smoking might also contribute to the progression and aggression of OSCC (Al Feghali et al., 2019). Alcohol abuse has been implicated as a high risk factor in many types of cancers, including OSCC (Ng et al., 1993), esophageal cancer (Castellsagué et al., 1999), larynx cancer (Bosetti et al., 2002), colorectal cancer (Cho et al., 2004), and pancreatic cancer (Korc et al., 2017). For OSCC, alcoholic beverages have been implicated as an important carcinogen in the etiology of oral cancer since the 1980s (Kabat and Wynder, 1989). Risk of OSCC among non-smokers was also confirmed to increase along with alcohol consumption (Blot et al., 1988). Specifically, a combination of alcohol abuse and smoking could enhance the carcinogenic effect of each other, suggesting a synergistic effect of alcoholism during OSCC development (Castellsagué et al., 2004). It is well known that the habit of chewing areca nuts is widely popular in Southeast Asia, and its positive role in the development of oral precancerous lesions and OSCC has been fully accepted as well (Li et al., 2016). As the areca nut industry was growing fast worldwide, more and more public and medical sources were paid due to betel chewing–induced OSCC (Hu et al., 2017).

Besides the above carcinogens, periodontal infection was also reported to be associated with OSCC development. Lower frequency of tooth-brushing and fewer dental visits, which were highly related with periodontal infection, were all associated with OSCC development. The poorer overall survival of OSCC patients with poor periodontal hygiene further suggested possible roles of periodontal infection in OSCC. With the development of society and subsequent changes in traditional concepts, the frequency of oral sexual behavior has mounted to a high level, especially in young adults (Holway and Hernandez, 2018). This behavior shift makes the oral cavity exposed to a totally new environment. Clinical trials have revealed that changes in sexual behaviors trend toward a higher incidence of oral human papillomavirus (HPV) infection (Chaturvedi et al., 2015). This phenomenon just coincides with the conclusion that the percentage of HPV-positive oropharyngeal carcinomas has risen from 16.3% in the 1980s to 72.7% in the 2000s (Chow, 2020). Obviously, oral sex–mediated HPV exposure has become a newly emerging risk factor for oral and pharyngeal carcinomas.

In addition, some novel perspectives about OSCC-related external carcinogens have been implicated. The presence of some unhealthy components inside the oral cavity, including residue dental roots and crowns, as well as improper dental prothesis, was identified to promote the malignant transformation of the normal oral epithelium due to its persistent physical stimulus. Besides, global nutrition deficiency might also be related to OSCC. Deficiency of vitamin A was identified to have a correlation with the occurrence of oral leukoplakia, a type of oral precancerous lesion (Sankaranarayanan et al., 1997). Loss of vitamin D might also act as a contributor to OSCC progression (Verma et al., 2020). Persistent intake of hot water and food is an acknowledged risk factor for esophagus carcinoma, and this stimulus, along with other stimulatory factors including pungent passing through the oral cavity, might also promote the formation of malignant oral lesions. In some special regions of the world, for example, New Zealand, where strong illumination exists throughout the year, UV radiation was also considered a possible carcinogen for skin carcinoma and OSCC (Yakin et al., 2017).

ABNORMALITY OF GENOME LANDSCAPE IN OSCC

Traditional concepts claimed that initiation and development of oral cancer are due to a sum of self- or risk factor–induced genetic changes that would lead to alterations in the activation of oncogenes and inactivation of tumor suppressor genes (Pérez-Sayáns et al., 2009; Irimie et al., 2016). Multiple types of genes controlling cell proliferation, DNA repair, angiogenesis, and

other pro-tumor biological processes have manifested significant variations between OSCC and normal oral tissues.

ABNORMALITY OF IMMUNE MICROENVIRONMENT IN OSCC

The current hot spot in cancer oncology research, apart from genetic variations, mainly lies in the tumor microenvironment, which contributes a lot to local tumorigenesis by promoting cellular proliferation, metabolism, metastasis, and so on (Casey et al., 2015). In the perspective of OSCC, although the heterogeneity of immune cell infiltration in the OSCC microenvironment makes it difficult to describe the total immunological landscape, more and more studies have been dedicated to figuring out this challenge.

Abnormal Production of Cytokines

Abnormal expression of chemokines plays an important part in the immunomodulation of the tumor microenvironment as recruitment and activation of immune cell subtypes are largely mediated by the interaction between chemokines and chemokine receptors (Nagarsheth et al., 2017). The chemokine-mediated regulating network exhibited its complexity *via* bidirectional pro-tumor and anti-tumor functions (**Figure 1**).

IL-2 functions as an important growth factor for T cell subpopulations, and activation of $CD4^+$ T cell differentiation by IL-2 has been verified. In addition, effector and memory $CD8^+$ T cell responses could also be induced by IL-2 (Spolski et al., 2018), indicating its crucial role in the T cell–mediated anti-tumor process.

A large amount of evidence indicated crucial roles of IL-10 in the anti-tumor process. $CD8^+$ T cell function and memory could be ignited by IL-10 exposure (Foulds et al., 2006). Elevation of granzyme B and activation and interferon-γ (IFN-γ) expression, along with subsequent CTL infiltration, have also been identified (Emmerich et al., 2012). Direct stimulation of NK cells by IL-10 would contribute to its anti-tumor effects (Lauw et al., 2000), while IL-10 could also indirectly mediate NK cell activation *via* inhibition of ROS secretion by TAMs (Mocellin et al., 2004).

IL-35 is another commonly acknowledged regulator in the tumor microenvironment. As a member of the IL-12 family, its immune suppressive role would render a pro-tumor status. Pro-tumor neutrophils induced by IL-35 could result in malignant progression of local tumor tissues (Zou et al., 2017). In addition, Tregs accumulated in tumor sites are the main resource of IL-35, and anti-IL35 treatment showed a similar effect to that of the depletion of Tregs. Inhibition of Th17 cell growth and function by IL-35 were also discovered (Niedbala et al., 2007), indicating that IL-35 might inhibit anti-tumor effects partially through a Th17 blockade.

IL-6 is a crucial chronic inflammatory mediator, higher levels of which have been observed in multiple types of cancers. Several major pro-tumor activities, including growth, invasion, and angiogenesis, have been identified to be closely correlated with IL-6 overexpression. In addition, the blockade of type 1 immune response (Tsukamoto et al., 2018), elevation of Treg cells (Kato et al., 2018), expansion of MDSCs, and activation of stromal fibroblasts could also be induced by IL-6, thus contributing to tumor development (Hanazawa et al., 2018).

IL-8 normally acts as a kind of chemokine, recruiting the accumulation of leukocytes (Alfaro et al., 2017). While in the tumor microenvironment, the high affinity of IL-8 to CXCR1 and CXCR2, the activation of which has been demonstrated to play an important role in tumor progression (Campbell et al., 2013; David et al., 2016), would contribute a great deal to the malignant process. Besides, an IL-8–induced increase in MDSC recruitment would accelerate the chronic inflammatory status of local tumor sites (Chi et al., 2014).

Similarly, IL-17 also played pro-tumor roles during tumor progression. Chronic exposure of IL-17 would lead to a pro-tumor microenvironment *via* production of inflammatory mediators, mobilizing myeloid cells and a phenotypic switch of stromal cells (Zhao et al., 2020).

TNF-α is a key pro-inflammatory cytokine, which exhibited a dual function in tumor progression. Stromal cells and cancer cells could both be sources of TNF-α. On the one hand, high levels of cytotoxic potential from TNF-α could render destruction of tumor vasculature, necrosis and apoptosis of cancer cells, and facilitation of drug accumulation inside tumor sites. On the other hand, studies also showed that TNF-α secreted by host cells surrounding tumor tissues could instead construct an inflammatory status and promote tumor progression (Egberts et al., 2008; Sethi et al., 2008).

As for OSCC, differential production of some types of chemokines is significantly associated with carcinogenesis.

When it comes to chemokines, accumulations of CCL20, CCL18, CCL4, and CCL2 were identified to promote tumor progression in OSCC (Li et al., 2014; Lee et al., 2017; Wang et al., 2017; Lien et al., 2018). Meanwhile, gene polymorphisms of CCL4 and CCL5 were highly associated with OSCC susceptibility (Weng et al., 2010; Lien et al., 2017). These deregulated chemokines have been shown to play roles in microenvironmental immunomodulation *via* recruitment of Treg cells, macrophages, MDSCs, and so on (Nagarsheth et al., 2017). As for inflammatory cytokines, interleukin (IL) 6, IL-8, and tumor necrosis factor-alpha (TNF-α) have been identified in terms of their potential roles as diagnostic biomarkers for OSCC (Sahibzada et al., 2017). Association between the gene polymorphism of IL-2 and OSCC has also been discovered (Singh et al., 2017). IL-23 could contribute to the progression of premalignant oral lesions to OSCC (Caughron et al., 2018), while IL-17 was significantly linked to the overall survival status of HNSCC (Lee et al., 2018). It is widely acknowledged that complex interacting networks of inflammatory cytokines could control recruitment, activation, and suppression of immune cells. Thus, the discussed abnormality of inflammatory cytokines in OSCC might result in a pro-tumor immune landscape in OSCC.

Abnormal Tumor-Infiltrating Immune Cells

Tumor-infiltrating cells are those immune cells located in the local tumor microenvironment, which have been identified to play crucial roles in either pro-tumorigenesis or anti-tumorigenesis and have significant prognostic value in cancer development (Shang et al., 2015). Immune cells inside the tumor

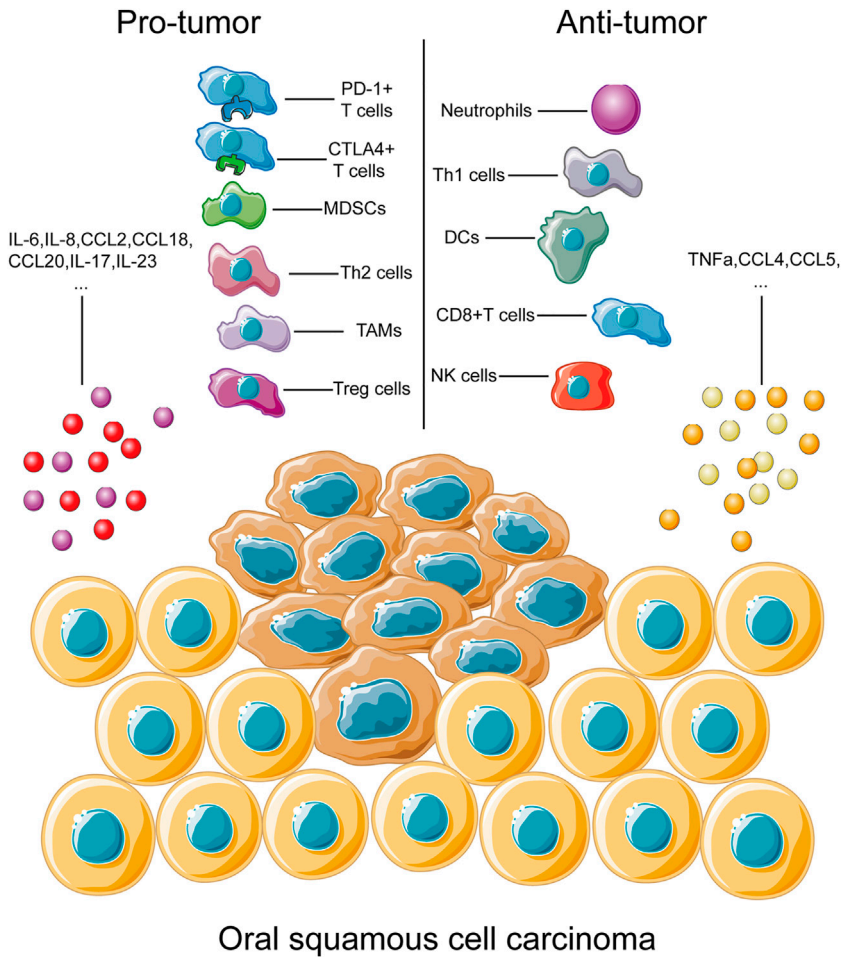

FIGURE 1 | Immune cells and cytokines associated with OSCC progression. This figure depicts the main types of immune cells and cytokines associated with progression of OSCC development. During OSCC progression, immune cells and cytokines could be divided into two groups, the pro-tumor part and the anti-tumor part. Immune cells, including PD-1$^+$ and CTLA4$^+$ T cells and TAMs, have been identified to play roles in tumor progression through multiple pathways, as discussed above. Similarly, immune cells contributing to the anti-tumor process, Th1 cells and NK cells, for example, were also listed inside. A complete overview of immune cells involved in tumor development would help us better understand the complexity of immune regulation of OSCC.

microenvironment could commonly be divided into two groups, the myeloid cell subgroup and the lymphocyte subgroup, all of which work together to form a comprehensive and interactive immune regulating network to influence the complexity of the tumor immune microenvironment.

Tumor-Related Myeloid Cells

Traditionally, myeloid cells acted as major components for host protection. They have changed evolutionally as barriers against variant infections and contributors to tissue remolding. However, during tumor development, myeloid cells would play complicated roles (Gabrilovich, 2017).

Myeloid-Derived Suppressor Cells

Myeloid cells which are CD11b- and Gr-1–positive and exhibited a strong immune suppressive effect have now been defined as myeloid-derived suppressor cells (MDSCs). Main subtypes of MDSCs are polymorphonuclear (PMN-MDSCs) and mononuclear (M-MDSCs). Although the suppressive effect of MDSCs could cover multiple types of immune cells, T cells are their main targets (Gabrilovich et al., 2012). Production of NO and variant cytokines induced by M-MDSCs could efficiently suppress T cell activity, as a NO-associated T cell receptor blockade would reduce the antigen presentation process (Koehn et al., 2015), while formation of antigen-specific T cell tolerance is a main mechanism for PMN-MDSCs (Gabrilovich et al., 2012). Besides, production of reactive oxygen species (ROS) is also essential for this process. On the other hand, MDSCs could also participate in the remolding process of the tumor microenvironment and tumor angiogenesis *via* VEGF, bFGF, and MMP9 (Casella et al., 2003; Shojaei et al., 2009).

Neutrophils

Neutrophils are the first line against multiple infections of the host. However, their plasticity in the tumor microenvironment puts them into both pro-tumor and anti-tumor roles (Giese et al.,

2019). Generation of ROS, reactive nitrogen species (RNS), and hydrogen peroxide could direct cancer cell–specific death, which is the main mechanism for neutrophil-induced anti-tumor roles (Granot et al., 2011), while in addition to their cytotoxic effect, abnormal production of ROS and RNS would result in oxidative DNA damage and genetic variations (Güngör et al., 2010). It is also well known that neutrophil-extracellular traps (NETs) generated in the tumor microenvironment would result in migration and invasion of cancer cells (Park et al., 2016). Secretion of MMPs from neutrophil granules might promote malignant development *via* migration, proliferation, and angiogenesis (Ardi et al., 2007; Das et al., 2017).

Dentritic Cells

Dendritic cells (DCs) are commonly regarded as the activator of T cells *via* transporting cancer-associated antigens. Initiation, polarization, and direction of T cells in the tumor microenvironment as well as recycling lymph nodes by DCs are the main mechanisms for DC-induced tumor suppression, during which the $CD8^+$T cell is their main target (Gardner et al., 2016). However, suppression of DCs in the tumor microenvironment would block this process, rendering a non-immunogenic DC phenotype switch. Thus, stimulatory and suppressive signals in the tumor microenvironment aiming at DCs, cytokines, and cell–cell communication, for example, would regulate DC-related T cell immunogenic functions.

Tumor-Associated Macrophages

Tumor-associated macrophage (TAM) is a subtype of infiltrating macrophage contributing to local tumor growth, metastasis, and neovascularization (Zhu et al., 2017). Infiltrating TAMs in OSCC is also associated with tumorigenesis. CD163, a common marker for TAMs, was observed to be elevated in OSCC tissues (Stasikowska-Kanicka et al., 2018a), suggesting its possible relationship with oral carcinogenesis. Coincidentally, the same phenomenon was observed in oral precancerous lesions (Boas et al., 2013). Besides, CD204, another TAM marker, was shown to be linked to the progress from oral premalignant lesions to OSCC (Kouketsu et al., 2019). Using a xenograft model, irradiation-induced M2 macrophage accumulation showed the potential to promote oral tumor recurrence *via* enhancement of neovascularization (Okubo et al., 2016). The *in vitro* experiment remodeling the tumor environment confirmed the mutual promoting effect between oral cancer cells and TAMs (Essa et al., 2016), and the Gas6/Axl signaling pathway was further confirmed to enhance the epithelial-mesenchymal-transition of oral cancer cells (Lee et al., 2014). Apart from M2 macrophages, M1 subtype TAMs also played a positive role in OSCC (Xiao et al., 2018). In the early tumor stage, local resident macrophages act in cooperation with other innate immune cells to initiate inflammatory responses to reduce tumor progression, through some direct effects, for example, ROS generation, and some indirect pathways, such as regulation of Th1 responses (Joyce and Pollard, 2009; Murray and Wynn, 2011). It could be concluded from the above that TAM is significantly involved in the pathogenesis of OSCC.

Tumor-Related Lymphocytes

$CD8^+$T Cell

The $CD8^+$T cell is a generally recognized anti-tumor defender of the host and serves as one of the most crucial effector cells in anti-cancer immunity, dysfunction of which would result in a severe barrier for cancer elimination (He et al., 2019). Loss of $CD8^+$T cells has contributed to tumorigenesis in many types of cancers. In OSCC, the $CD8^+$T cell was shown to decrease in either OSCC tissues or precancerous lesions (Stasikowska-Kanicka et al., 2018a). High $CD8^+$T cell percentage could also predict a better overall survival and disease-specific survival rate in OSCC (Shimizu et al., 2019). Immunological staining further revealed an increase in $CD8^+$T cells in OSCC with better prognosis (Stasikowska-Kanicka et al., 2018b). The expression level of PD-L1, an immune checkpoint blockade targeting cytotoxic T cells, was highly unregulated in OSCC (Stasikowska-Kanicka et al., 2018a; Stasikowska-Kanicka et al., 2018b), indicating a loss-of-function status of T cells in OSCC. In the translational medical perspective, the anti-tumor effect of radiotherapy in OSCC was also verified to be partly attributed to the activation of $CD8^+$ T cells (Suwa et al., 2006). These clinical experimental results together come to the conclusion that $CD8^+$ T cells play an anti-tumor role in OSCC, the abnormality of which would help in tumorigenesis.

$CD4^+$T Cells

T cells expressing CD4 glycoprotein are another crucial T cell subtype called the $CD4^+$T cell, and their functions in the tumor microenvironment are extremely complicated, due to multiple subgroups of $CD4^+$T cells, including Th (T helper)1 cells, Th2 cells, Th9, Th17, Th22, and T regular cells (Treg).

Th1 cells show some anti-tumor effects mainly *via* their large amount of IFN-γ production, along with some chemokines to recruit and prime effector $CD8^+$T cells. Also, NK cells and M1 macrophages could be recruited and activated by Th1 cells in local tumor sites for tumor elimination (Nishimura et al., 1999). By targeting of tumor stroma and subsequent angiogenesis blockade, tumor growth could be inhibited in an IFN-γ–mediated way by $CD4^+$T cells (Qin and Blankenstein, 2000).

Th2 cells have been verified to play some contradictory roles in tumor progression. Secretion of IL-4 by Th2 cells would mediate transport of macrophages and eosinophils into tumor sites for anti-tumor actions (Tepper et al., 1989), and this immune transfer function is the main mechanism for the Th2-mediated anti-tumor effect. On the other hand, antigen-specific effector Th2 cells have been reported to promote cancer development, and IL-5 secreted by them might be the reason behind this pro-tumor effect (Tatsumi et al., 2002).

Th17 cells are an important subgroup participating in the anti-infection process. A pro-inflammatory microenvironment induced by secreted IL-17a and IL-23 would promote tumor progression *via* elevating angiogenesis and inhibiting infiltration of $CD8^+$T cells. Only a small amount of Th17-associated cytokine exposure could remarkably facilitate cancer progression (Lee et al., 2012), while some studies support that a high level of IL-17 would result in an anti-tumor immune status (Numasaki

et al., 2005). This contradictory phenomenon suggested that the role of Th17 in tumor progression largely depends on the host status and local context.

Treg is a negative regulator in the adaptive immune system, suppressing the activation of immune responses and maintaining the immune balance (Sakaguchi, 2004). During tumor progress, excessive upregulation and activation of Treg cells would result in immune deficiency and subsequent immune escape of tumor cells, thus facilitating the development of tumorigenesis (Smigiel et al., 2014). In OSCC patients, elevated levels of Treg cell–associated cytokines were observed in peripheral blood (Gaur et al., 2014), while a higher frequency of Treg cells was also discovered in OSCC samples (Schwarz et al., 2008). Animal experiments using mice and dogs further verified an increase in Treg cells in OSCC (Horiuchi et al., 2010; De Costa et al., 2012). In tongue squamous cell carcinoma, a higher level of expression of Treg cells was significantly associated with a poorer survival rate, and accumulation of Treg cells was used to predict bad prognosis of patients (Hanakawa et al., 2014). Compared with healthy donors, levels of circulating Treg cells were also much higher in OSCC patients, along with a higher level of TGF-β, a Treg-associated cytokine (Lim et al., 2014). The above evidence together confirmed the pro-tumorigenesis value of Treg cells in OSCC.

Natural Killer Cells

The anti-tumor immunity of natural killer (NK) cells has long been regarded as a predominant effector against metastasis or hematological cancers, and more and more efforts have been applied to fully understand properties of NK cells (Guillerey et al., 2016). Escape of NK cell immune surveillance in OSCC tissues and inactivation of the NK cell status in peripheral circulation of OSCC patients has been recorded in clinical research (Dutta et al., 2015). Similarly, the downregulated NK cell status was also observed to be linked to higher invasive oral tumor areas (Türkseven and Oygür, 2010). A newly published meta-analysis indicated the possibility of the NK cell marker being a prognostic marker, considering the negative correlation between NK cell markers and the OSCC patient survival rate (Huang et al., 2019). The successful curative effect of NK cell immunotherapy in OSCC identified in an *in vivo* model further confirmed the crucial anti-tumor role of NK cells in OSCC (Greene et al., 2020).

OSCC CARCINOGEN-INDUCED IMMUNE ABNORMALITIES

As predominant contributors to the progress of OSCC, multiple OSCC-related carcinogens, including smoking, drinking alcohol, chewing areca nuts, periodontal infection, and oral sexual behavior, have all been proven to be related to local immune abnormality to a great extent. A complete understanding of the immune status induced by carcinogens would help in possible recognition of the immune landscape of carcinogen-induced OSCC.

Cigarette

Cigarettes are a well-known risk factor for many oral diseases, including periodontitis (Kinane et al., 2017), halitosis (Jiun et al., 2015), oral leukoplakia (Granero Fernandez and Lopez-Jornet, 2017), and OSCC (Blot et al., 1988). Previous studies about the effect of smoking on carcinogenesis mainly focused on aberrant genetic alterations brought on by harmful compounds inside cigarettes. Accumulation of DNA adducts and oxidative DNA damage induced by tobacco smoking have been identified for a while (Phillips, 2002), and the subsequent genetic mutational signatures, such as TP53, P73, and MDM2 (Misra et al., 2009), were listed clearly, using sequencing methods (Alexandrov et al., 2016). However, little attention was cast onto the influence of microenvironmental changes caused by tobacco. The oral cavity is a local microenvironment whose stability would be extremely changed due to tobacco smoking (**Figure 2**). Thousands of reactive oxygen species (ROS) are generated in burning cigarettes (Huang et al., 2005), and ROS-attacked epithelial cells and cancer cells in the oral cavity would secrete lots of inflammatory mediators, thus leading to imbalance of host immunity in the oral cavity. It is evidenced that cigarette smoke could result in upregulation of IL-8 (Barnes, 2016) and downregulation of IL-12 by the oral epithelium (Vassallo et al., 2005a). As IL-12 is a main inducer of the Th1 response (Trinchieri, 2003), the phenomenon coincides with the observation that cigarette smoking would result in suppression of Th1 responses and generation of Th2 inflammatory reaction

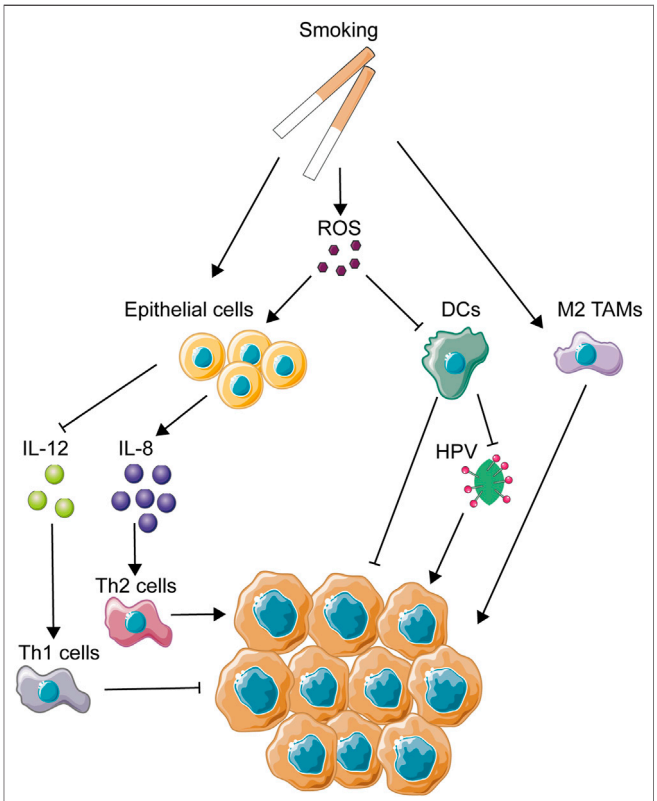

FIGURE 2 | Mechanisms of smoking-related immune regulation in OSCC. This figure depicts several main immune-regulating activities associated with smoking. As one of the most important OSCC carcinogens, smoking could directly or indirectly regulate immune activities through activation of epithelial cells and immune cells and the production of ROS.

(Cozen et al., 2004), and excessive Th2 response would break the balance between Th1 and Th2. As has been known, Th2 immune polarization might result in some unexpected effects in carcinogenesis. CCL5-mediated recruitment and differentiation of Th2 cells enhanced the primary tumor burden and pulmonary metastases of luminal breast cancer (Zhang et al., 2015). NLRP3-activated polarization of Th2 cells also had a tumor-promoting impact on pancreatic cancer (Daley et al., 2017), further identifying the immunosuppressive role of Th2 in carcinogenesis. On the other hand, patients with higher accumulation of Th1 exhibited better and prolonged survival (Tosolini et al., 2011), precise evidence for the anti-tumor effect of Th1. Furthermore, some chemotherapies targeted at the tumor microenvironment also aim to enhance Th1 cytokine levels as an anti-tumor pathway (Berlato et al., 2017). Thus, smoking-induced imbalance of Th1/Th2 might be speculated to play a role in development of OSCC from an immunological perspective. Besides, IL-8 could act as a pro-tumorigenesis cytokine with its promotion of tumor proliferation, migration, and maintaining of stemness (Chen et al., 2014; Huang et al., 2015; Ding et al., 2017). As reported, the release of IL-8 induced by cigarette smoke (CS) was mainly from macrophages (Facchinetti et al., 2007) and airway epithelial cells (Mio et al., 1997). Interestingly, several research studies have reported that IL-8 was induced in oral squamous cell carcinoma cells (Tsunoda et al., 2016) and gingival epithelial cells (Mahanonda et al., 2009). Thus, upregulation of IL-8 by CS might play an important role in CS-induced tumorigenesis.

CS could also impose a great influence on immunological functions of dendritic cells. It has been reported that some components of CS, such as ROS, nicotine, and other chemicals inside, were involved in the influence on DCs (dendric cells), causing the suppression of DC-induced T cell activation and proliferation (Vassallo et al., 2005b; Kroening et al., 2008; Vassallo et al., 2008). DCs are considered to be main activators for both innate immunity and adaptive immunity, being highly efficient in generating fast and fierce immunological responses (Constantino et al., 2017). However, under the immunosuppressive influence of the tumor microenvironment, DCs always show a biological dysfunction in the cancerous background, as a way to help tumor evasion (Tang et al., 2017). Due to its central role in the initial phase of immunity activation, DC-based immunotherapy has been used in clinical trials since the mid-1990s and has been applied in many types of cancers such as melanoma, prostate cancer, malignant glioma, and renal cell carcinoma (Anguille et al., 2014). Thus, CS-induced dysfunction of DCs is considered as a contributor to the malignant development of the tumor microenvironment. In addition, CS extract has also been found to suppress production of antiviral cytokines from DCs (Mortaz et al., 2009). In nasopharyngeal carcinoma, CS extract has been proved to promote the infection of the Epstein–Barr virus (EBV), the enhancement of which is closely associated with the malignant development of nasopharyngeal carcinoma (Huang et al., 2017). The proportion of HPV-related OSCC has increased in the past 30 years in a longitude clinical survey in America (Chaturvedi et al., 2008), emphasizing the importance of HPV infection in OSCC development. Thus, it could be speculated that the decrease in antiviral capacity caused by CS might promote the colonization and replication of HPV in the oral cavity.

Smoking was found to increase the aggregation of alveolar macrophages but impair the normal functions of macrophages (Kotani et al., 2000; Hodge et al., 2003). The same phenomenon was identified *in vitro* (Kirkham et al., 2004). As is known to all, dysfunction of macrophages might help to promote the development of tumors. In addition, smoking could induce the polarization of M2 macrophages in alveoli (Bazzan et al., 2017). In an *in vivo* mouse model, smoking was identified to induce the polarization of tumor-associated macrophages and promote the development of pancreatic cancer in this way (Kumar et al., 2015). Thus, the dysfunction and M2 polarization of macrophages caused by smoking might partly explain the malignant transformation of the tumor microenvironment, leading to OSCC development as a result.

On the other hand, CS is a crucial modulator of host response to pathogens (Nuorti et al., 2000). Smokers are shown to be more likely to get infection of *Streptococcus pneumoniae* and *Tuberculosis* (Padrao et al., 2018). This feasibility of pathogen colonization might suggest a dysfunction of host immunity and destruction of microbial balance, leading to a low resistance to extraneous pathogens. Recently, the relationship between oral microbial dysbiosis and tumor development has been a hot topic, and a lot of evidence has revealed microbial dysbiosis as a contributor to carcinogenesis. Smoking was strongly identified to be involved in oral microbial variations through some clinical trials with large amounts of samples (Wu et al., 2016; Yu et al., 2017). Microbial diversity was decreased in smokers, and there were a reduction of phylum Proteobacteria and genera *Capnocytophaga*, *Peptostreptococcus*, and *Leptotrichia* and enhancement of *Atopobium* and *Streptococcus*. These abnormal changes of host microbial composition caused by smoking might be one of the reasons for the CS-induced effect of carcinogenesis.

Alcohol

Alcohol abuse has been implicated as a high risk factor in many types of cancers, including OSCC (Ng et al., 1993), esophageal cancer (Castellsagué et al., 1999), larynx cancer (Bosetti et al., 2002), colorectal cancer (Cho et al., 2004), and pancreatic cancer (Korc et al., 2017). Alcohol dehydrogenase (ADH) and aldehyde dehydrogenase (ALDH) play crucial roles in the regular conversion of ethanol to acetate. When it comes to carcinogenesis, traditional opinions about alcohol-induced carcinogenesis support the abnormal metabolism of ethanol caused by variations of ADH- and ALDH-encoding genes serving as main contributors (Jelski et al., 2009). For example, this abnormality of ethanol metabolism could lead to increased generation of ROS from epithelial cells, which then activates cellular pathways, such as the nuclear factor κB (NF-κB) pathway and the mitogen-activated protein kinase (MAPK) pathway (Wu, 2006; Morgan and Liu, 2011), causing the malignant transformation of tumor cells. In addition, the RNS level of the epithelium was also elevated by alcohol stimulation. Accumulation of ROS and RNS would indirectly modify the

immune microenvironment *via* its suppressive effect on T cells, NK cells, and macrophages (**Figure 3**). Besides this direct carcinogenic effect of alcohol, the function of host immunity is also under significant burden due to alcohol intake, which might partly explain the carcinogenesis of alcohol.

Alcohol intake, either acute or chronic, poses a great burden on NK cells. Alcohol abuse has long been regarded as a promoter for the development of hepatic diseases, such as hepatitis viral infection and liver fibrosis. It is reported that chronic ethanol consumption would accelerate virus-induced hepatitis through suppression of NK cell accumulation and cytotoxicity ability (Pan et al., 2006). Similarly, ADH3, a crucial enzyme in the metabolic process of alcohol, has great correlation with the development of hepatic fibrosis due to its suppression of NK cells (Yi et al., 2014). Abrogation of the antifibrotic effect of NK cells caused by alcohol was seen to increase the severity of alcoholic liver fibrosis (Jeong et al., 2008). In alcoholic hepatitis, a decreased frequency and reduction of the degranulation capacity of NK cells were also observed compared with healthy ones (Støy et al., 2015). When it comes to cancer development, alcohol abuse could also explain its carcinogenesis through NK cell variation, as acute alcohol ingestion has been demonstrated to cause a marked reduction of NK cell activity and, in this way, promote the tumor metastasis *in vivo* (Ben-Eliyahu et al., 1996). Metastasis of colon cancer cells into the liver was also increased by treatment of chronic alcohol consumption in a preclinical model (Im et al., 2016). In perspective of the count variation of NK cells, alcohol consumption has been identified to decrease the number of NK cells in the spleen (Blank et al., 1991) and peripheral lymph nodes (Zhang et al., 2011). Furthermore, the balance of thymus-derived and bone marrow–derived NK cells was also destroyed by alcohol intake (Zhang and Meadows, 2008). Besides, cytotoxicity and cell activity of NK cells was downregulated by treatment of alcohol (Wu et al., 1994), and enzymatic activity of granzyme A and B expressed by NK cells was suppressed, resulting in the loss of cell viability of NK cells (Spitzer and Meadows, 1999). On the other hand, some research focused on the explanations for alcohol-induced suppression of NK cells. Alcohol consumption could render a variation of the autonomic nervous system and reduction of pro-inflammatory cytokines from neuroendocrine and immune cells, leading to suppression of NK cell cytolytic activity (Boyadjieva et al., 2006; Chen et al., 2006). Downregulation of IL15 induced by alcohol consumption seemed like a way to suppress the availability of NK cells (Zhang et al., 2017), and this observation has been confirmed by a rescue experiment (Zhang and Meadows, 2009). Moreover, activity of the NF-κB pathway in NK cells, a crucial pathway for immune activation, was also suppressed by alcohol treatment (Zhou and Meadows, 2003).

T cell function is also under the influence of alcohol drinking. Alcohol-derived acetaldehyde has been proved to pose severe toxicity to the immune system, and recent study has confirmed its role in the downregulation of T cell function *via* inhibiting aerobic glycolysis and hampering the energy source of T cells (Gao et al., 2019). An *in vivo* experiment using ethanol-fed mice proved that ethanol could enhance the antibody-induced $CD4^+$ T cell immunosuppression and thus promote tumorigenesis (Hunt et al., 2000). A chronic alcohol treatment was identified to accelerate the immunosenescence process of $CD8^+$ T cells of rhesus macaques (Katz et al., 2015). Besides, an *in vitro* experiment showed that alcohol consumption could inhibit the T cell proliferation rate compared with water consumption, and an increase in some pro-tumor immune groups of cells, such as Treg cells and MDSCs, might also impair the function of T cells (Zhang and Meadows, 2010). The apoptosis of T cells would also be activated by the alcohol treatment *via* downregulation of the vitamin D receptor (Rehman et al., 2013).

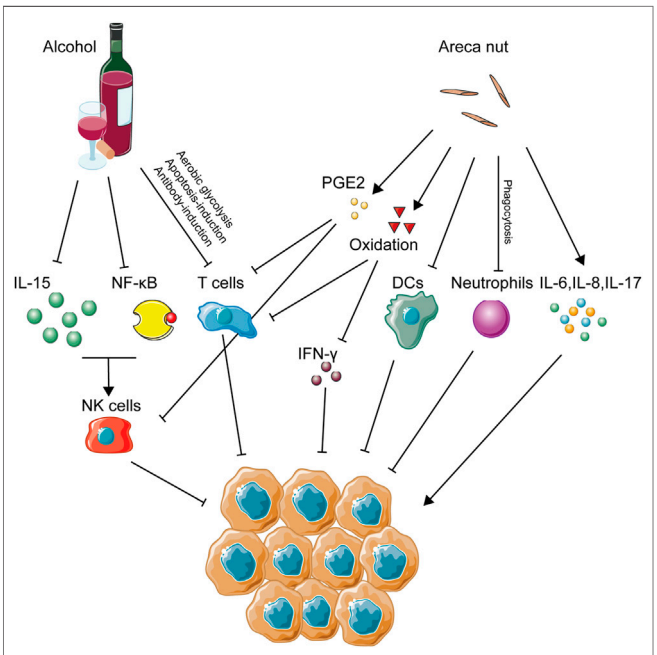

FIGURE 3 | Immune activities caused by alcohol and areca nut consumption in OSCC. This figure depicts the immune-regulating networks induced by alcohol and areca nuts during OSCC development according to related studies. Specifically, inhibition of NK cells, T cells, DCs, and neutrophils, several main anti-tumor immune cells, was a remarkable feature of immune abnormalities induced by alcohol and areca nuts, indicating that immune inhibition might be excessively crucial in OSCC associated with these two carcinogens.

Areca Nuts

It is well known that the habit of chewing Areca nuts has been widely popular in Southeast Asia, and its positive role in the development of oral precancerous lesion and OSCC has been fully accepted as well (Li et al., 2016). Apart from its genotoxicity, the areca nut might also affect the progress of oral malignant transformation *via* immunomodulation (**Figure 3**). For lymphocytes, the DNA synthesis process was identified to get inhibited long before (Yang et al., 1979). This phenomenon posed the hypothesis that areca nuts might decrease the immunity of lymphocytes. Further study confirmed that T cell activation and IFN-γ production were suppressed by areca nut treatment through induction of oxidative stress (Wang et al., 2007). When it comes to immune cell function, the phagocytosis of neutrophils (Hung et al., 2006), the adhesion and migration of

mononuclear leukocytes (Chang et al., 2014), and the differentiation of dendric cells from monocytes (Wang et al., 2012) were all proven to decrease due to areca nuts. In the perspective of inflammatory cytokines, treatment of human immune cells using areca nut extract was identified to increase multiple inflammatory cytokines, such as TNF-α, IL6, IL8, cyclooxygenase-2 (COX2), and prostaglandin E2 (PGE2) (Chang et al., 2009; Chang et al., 2013; Faouzi et al., 2018), as well as decrease the level of IL2 production by spleen cells (Selvan et al., 1991). As for oral keratinocytes, production of PGE2, Prostaglandin I2 (PGI2), IL-6, and TNF-a was also enhanced due to areca components (Jeng et al., 2000; Jeng et al., 2003). Expressions of IL-2 and IL-2 receptor by $CD8^+$ cytotoxic T lymphocytes (CTLs) and tumor-infiltrating lymphocytes (TILs) were also reduced under the influence of PGE2, while PGE2 induced $CD4^+$ Th2 cell activation (Wustrow and Mahnke, 1996; Li et al., 2013). As mentioned above, TILs are lymphocytes that migrate from the blood to the tumor, playing crucial roles in either pro-tumorigenesis or anti-tumorigenesis. Among them, $CD4^+$Th2 cells promote tumor growth, while CTLs inhibit tumorigenesis (Lauerova et al., 2002; Farhood et al., 2019). In other words, PGE2 serves as an immunosuppressor contributing to the induction of $CD4^+$ Th2 cells and the pro-tumor efficacy of TILs. Circulating the immune complex, known to exhibit an immunosuppressive effect on NK cells and CTLs, was detected to accumulate more frequently in areca chewers than in healthy controls (Remani et al., 1988). A large-population experiment using flow cytometry and immune-staining reveals that IL-17 was highly expressed in areca chewers (Quan et al., 2020). Exposure of areca extracts was shown to induce the increasing secretion of IL-6 and IL-8 by peripheral blood mononuclear cells (Chang et al., 2006). In an animal model, arecoline receivers exhibited a low splenic lymphocyte proliferation rate and a high apoptosis rate (Dasgupta et al., 2006). Similarly, production of IL-8 from oral squamous cancer cells was also increased due to exposure of arecoline (Cheng et al., 2000). PBMC isolated from areca chewers exhibited a higher level of DNA damage markers in circulating lymphocytes (Liu et al., 2004).

Periodontal Infection

Periodontitis, one of the most common diseases inside the oral cavity, is largely caused by poor oral hygiene status and oral microbial dysbiosis (Lertpimonchai et al., 2017; Meuric et al., 2017). Periodontitis is featured by the dysbiotic inflammatory status (Hajishengallis, 2015), which is highly associated with inflammatory microenvironmental abnormality (**Figure 4**). Most of pathogenic oral bacteria are Gram negative ones, sharing a similar ability to induce higher concentration of cytokines from oral epithelial cells, such as IL-6, IL-1β, TNF-α, and IL-8 (Ha et al., 2016; Cardoso et al., 2018), and overexpression of these inflammatory cytokines contributes to the abnormality of the microenvironment as discussed above. In particular, some periodontal pathogenic microbiota has been reported to impose immunosuppression on the local focus. *F. nucleatum,* a common periodontitis-associated bacterium, was identified to recruit MDSCs, a kind of tumor-infiltrating immune cell with anti-immunity ability (Kostic et al., 2013). M2

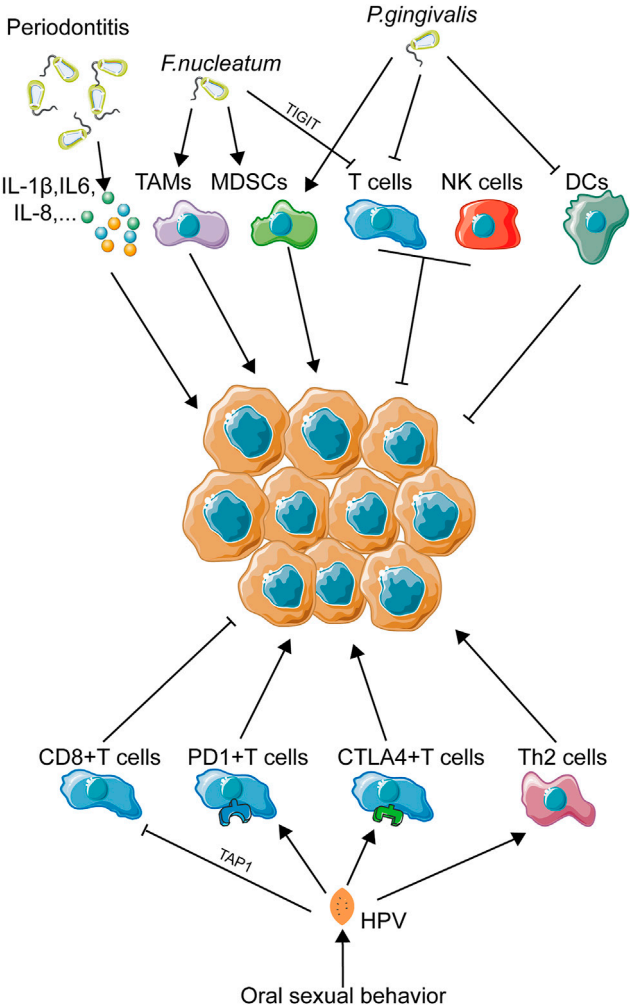

FIGURE 4 | Immune landscape in oral pathogen–related OSCC. This figure depicts the immune landscape caused by oral pathogens, including bacteria and viruses, in OSCC development. Immune regulation was the main activity upon oral pathogen exposure. As infectious factors have been proven to be more and more important in OSCC initiation and progression, immune activities induced by OSCC-related pathogenic bacteria and viruses might also be a crucial part contributing to OSCC progression.

polarization, leading to the differentiation of tumor-associated macrophages, was also observed to be induced by *F. nucleatum* (Chen et al., 2018). TIGIT, a membrane protein of many immune cells, such as NK cells and T cells, could also be modulated by *F. nucleatum,* resulting in loss of function of NK cells and cytotoxic T cells (Gur et al., 2015). Another common periodontal pathogen, *P. gingivalis*, is also involved in immunomodulation. *P. gingivalis* was identified to silence innate immune response partly by inactivating DCs (Abdi et al., 2017). *In vivo* experiment exhibited that *P. gingivalis* infection promoted the expansion of MDSCs (Su et al., 2017). Disturbance of the Th1/Th17 balance was also induced by *P. gingivalis* (Monasterio et al., 2019), while suppression of IL-2 accumulation in T cells (Khalaf and Bengtsson, 2012) and reduction of CXCL10 expression caused by *P. gingivalis* infection (Jauregui et al., 2013) might be used to

partly explain this phenomenon. M2 polarization was also elicited by *P. gingivalis* and could promote carcinogenesis in HNSCC (Utispan et al., 2018).

Oral Sexual Behavior

With the development of society and subsequent changes in traditional concepts, the frequency of oral sexual behavior has mounted to a high level, especially in young adults (Holway and Hernandez, 2018). This behavior shift makes the oral cavity exposed to a totally new environment. Clinical trials have revealed that changes in sexual behaviors trend toward a higher incidence of oral HPV infection (Chaturvedi et al., 2015). This phenomenon just coincides with the conclusion that the percentage of HPV-positive oropharyngeal carcinomas has risen from 16.3% in the 1980s to 72.7% in the 2000s (Chow, 2020). Obviously, oral sex–mediated HPV exposure has become a newly emerging risk factor for oral and pharyngeal carcinomas. It is worth noting that HPV infection has been identified to play a crucial role in local immune disruption (**Figure 4**). Studies have revealed that HPV^+ HNSCC patients are more likely to exhibit an abnormal tumor immune microenvironment (Gameiro et al., 2018). A meta-analysis concludes that dysfunction of T cells plays a great part in HPV-induced immune deficiency, while the abnormality of macrophages, Tregs, and MDSCs remains unclear (Lechien et al., 2019). Viral protein E7 could reduce expression of TAP1, as a way to inactivate cytotoxic T cells (Einstein et al., 2009). Infection of HPV would result in downregulation of pro-inflammatory cytokines and upregulation of anti-inflammatory cytokines, such as IL-10 (Mota et al., 1999). In cervical cancer, another HPV-associated carcinoma, loss of T cell cytotoxicity, increase in immunosuppressive Th cell infiltrating, and secretion of immunosuppressive cytokines are all associated with HPV infection (Piersma, 2011). In HNSCC, a large-population transcriptome analysis revealed a T cell dysfunction and T cell exhaustion signatures in HPV-positive patients (Krishna et al., 2018). Furthermore, overexpression of PD-1 and CTLA-4 was observed in HPV-positive HNSCC tissues, which indicated a loss-of-function status of $CD8^+$ T cells due to HPV infection (Kansy et al., 2017). In short, abnormality of the T cell status induced by HPV infection might be closely related to OSCC development.

RISK FACTOR–BASED IMMUNOTHERAPEUTIC STRATEGY

Until now, surgical operation is still the first choice for OSCC treatment. Heterogeneity acts as one of the main traits in head and neck squamous cell carcinoma (HNSCC) (Schubert et al., 2020), and poor clinical outcomes of radiation and chemical treatment were partly due to the heterogeneity of OSCC patients (Kagohara et al., 2020). Immune phenotypes of HNSCC classified by the heterogeneity of immune landscapes among HNSCC patients have been built up successfully (Feng et al., 2020). This result further indicated that immune heterogeneity of HNSCC might be summarized into a statistical rule, which might be used for classification of HNSCC patients with different immune statuses. A recent study has identified that smoking could exert an immunosuppressive effect on the HNSCC tumor microenvironment with the help of multi-omics analysis (de la Iglesia et al., 2020). This discovery just coincides with the above hypothesis that oral cancer–related risk factors might greatly account for the abnormality of the immune status. In the perspective of tumor therapy, immunotherapeutic strategies for OSCC ought to be dependent on intratumor heterogeneity to achieve better clinical outcomes (Mroz et al., 2020). Thus, in consideration of the correlation between risk factors and immune variations, a new concept is brought out that combination of patient risk factor information and immune status detection might be valuable for directing individual-based immunotherapy for OSCC patients (**Figure 5**).

Check Point Blockade Therapy

Anti–PD-(L)1 Treatment

Programmed death ligand 1 (PD-L1) is often expressed on the surface of antigen-presenting cells (APCs), tumor cells, etc., and it can bind to PD-1 on the surface of activated T cells, leading to the exhausted status of T cells (Goodman et al., 2017). Anti–PD-(L)1 treatment could be applied due to its role in reducing T cell apoptosis and enhancing recruitment of T effector cells to tumor sites (Dong et al., 2002). Downregulation of T cell function is a significant feature in OSCC, which is a plausible reason for possible application of anti–PD-(L)1 treatment in OSCC. As reported, anti–PD-1 (aPD1) immunotherapy has been proven to be effective in lymphomas (Goodman et al., 2017), melanoma (Wang et al., 2016), and non–small-cell lung cancer (Xia et al., 2019). Increased expression of PD-1 and PD-L1 was observed in oral lesions progressing to OSCC compared to non-progressing dysplasia (Dave et al., 2020). In addition, several reports revealed that recurrent/metastatic HNSCC patients treated with anti-PD1 showed a significantly prolonged survival compared with standard treatment (Ghanizada et al., 2019). Additionally, high expression of PD-1 was observed in exhausted NK cells, and anti-PD1 therapy could reverse this condition in many cancers (Romero, 2016; Li et al., 2018). So the anti–PD-(L)1 method might also be used as the NK cell–targeted method in alcohol-related OSCC. Subsequent clinical experiments identified that anti-PD1 therapy achieved a better prognostic outcome in HPV^+ cancer patients than HPV^- controls (Ferris et al., 2016). Besides, a systemic meta-analysis confirmed that HPV^+ HNSCC patients could benefit more from anti-PD1 immunotherapy, further ensuring the role of the PD1 blocking method in the treatment of HPV^+ OSCC patients (Galvis et al., 2020). In conclusion, anti–PD-(L)1 treatment is an optional method for all subgroups of OSCC discussed above.

Anti–CTLA-4 Treatment

The cytotoxic T-lymphocyte–associated antigen 4 (CTLA-4) is a critical receptor for the negative regulation of T cell activation (Rowshanravan et al., 2018). Although elimination of CTLA-4 can result in several diseases including autoimmune diseases, effective anti-tumor immunity sometimes requires the blockade of CTLA-4 (Brunner-Weinzierl and Rudd, 2018; Hosseini et al., 2020).

Risk factor-based Immunotherapeutic Strategy

Possible Immunotherapeutic Strategies			Recommended OSCC Subgroups
Check-point therapy		Anti-PD-(L)1 treatment	Smoking-related OSCC Alcohol-related OSCC Periodontitis-related OSCC Areca nut-related OSCC HPV-related OSCC
		Anti-CTLA-4 treatment	Smoking-related OSCC Alcohol-related OSCC Periodontitis-related OSCC Areca nut-related OSCC HPV-related OSCC
		Anti-TIGIT treatment	Alcohol-related OSCC Periodontitis-related OSCC
Immune agonist therapy		TLR agonist	Smoking-related OSCC
		CD40/CD40L agonist	
Cytokine therapy	Exogenous cytokines	IL-2	Alcohol-related OSCC Areca nut-related OSCC
		IL-12	
		IL-15	
		Type I and type II IFNs	
		GM-CSF	
	Anti-cytokine therapy	IL-6,IL-8,IL-1β inhibitors	Periodontitis-related OSCC
		STAT3,MAPK inhibitors	
		EGFR inhibitors	Smoking-related OSCC Periodontitis-related OSCC
		VEGF inhibitors	
		TGF-β inhibitors	
		CSF/CSF1R inhibitors	
		CCR2 inhibitors	
		PI3K inhibitors	
Adoptive cell therapy			Smoking-related OSCC Alcohol-related OSCC Periodontitis-related OSCC Areca nut-related OSCC HPV-related OSCC

FIGURE 5 | Immunotherapeutic strategies based on the specific carcinogen-related immune status. This figure depicts multiple types of immunotherapeutic strategies and subsequent OSCC subgroups suitable for each kind of strategy. As discussed in this manuscript, carcinogens would result in a specific aberrant immune status for OSCC patients, which just explained drug resistance and individual variations of immunotherapeutic responses. Thus, possible personalized immunotherapeutic strategies based on different carcinogen-induced types of the OSCC local immune status were listed above and might achieve a better clinical outcomes.

Wang et al. (2019) found that syngeneic animal models of tobacco-associated oral cancers have higher response rates to anti–CTLA-4 immunotherapy than to anti-PD1 treatment. Anti–CTLA-4 treatment could also increase IFN-γ–producing $CD4^+$ Th1 cells, which is necessary for overcoming the imbalance of Th1/Th2 caused by smoking (Chen et al., 2009). On the other hand, downregulation of T cell function was also observed in alcohol-drinking patients. Depending on this point, anti–PD-(L)1 and anti-CTLA4, two common check-point inhibitors for T cells, could be used as discussed above. In addition, based on the overexpression of CTLA-4 observed in HPV^+ HNSCC tissue samples, a combination of anti-PD1 and anti–CTLA-4 therapies might be likely to achieve a better clinical outcome in HPV-related OSCC patients.

Anti-TIGIT Treatment

The T cell immunoreceptor with immunoglobulin and ITIM domain (TIGIT) is a promising new target along with PD-(L)1 and CTLA-4 for cancer immunotherapy, and the blockade of TIGIT and PD-L1 were found to act synergistically on T cells and NK cells' effector functions (Johnston et al., 2014). Zhang et al. (2018) found that the inhibition of TIGIT could prevent NK cell exhaustion and promote NK cell–dependent tumor immunity in several tumor mouse models. Since the dysfunction of NK cells plays an important pathogenic role in drinking patients, anti-TIGIT therapy might be effective in the treatment of alcohol-related OSCC. In addition, due to the binding ability of *F. nucleatum* to TIGIT and subsequent downregulation of NK cells and T cells, some anti-TIGIT antibodies, MK-7684, for example, might work against the tumorigenesis effect of *F. nucleatum* specifically. As anti-tumor therapies targeting TIGIT have achieved great success recently, this method might also be useful in OSCC patients with high *F. nucleatum* abundance (Solomon and Garrido-Laguna, 2018).

Immune Agonist Therapies

Although many patients have benefited from checkpoint-blockade immunotherapies, and the overall survival of patients was significantly prolonged due to these therapies, substantial patients do not respond to these strategies, and several drug-resistance mechanisms have been identified (Dempke et al., 2017). To overcome low efficiency of checkpoint-blockade immunotherapies for some OSCC patients, more and more investigations begin to focus on co-stimulatory agents. Toll-like-receptor (TLR) agonists could promote innate immune cells (e.g., macrophages and plasmacytoid DCs), while PD-1

inhibitors act on adoptive immune cells (e.g., activated T cells). Sato-Kaneko et al. (2017) identified that combination therapy with TLR agonists and anti–PD-1 increased antigen-presenting functions of TAMs and the infiltration of IFNγ+CD8+T cells in head and neck tumors, thus suppressing tumor growth. CD40 is a TNF receptor superfamily member expressed on both immune and non-immune cells, and CD40/CD40L agonists could upregulate antigen presentation machinery, enhance T cell proliferation and cytokine production, thus acting in the regression of tumors (Bennett et al., 1998; Mayes et al., 2018; Vonderheide, 2020). Considering the contribution of CS-induced dysfunction of DCs to the development of smoking-related OSCC, these immunotherapies might be effective strategies targeted at these subgroups.

Cytokine Therapy

Exogenous Cytokines

IL-2 was the first approved cytokine for boosting NK cells clinically (Floros and Tarhini, 2015) and was mainly used to produce lymphokine-activated NK cells. Similarly, IL-15 and IL-12 were also pro-inflammatory cytokines playing important roles in the development, homeostasis, and cytotoxicity of NK cells (Floros and Tarhini, 2015). For OSCC patients with a drinking habit, a great burden on NK cells was a significant feature, and these cytokines were the most commonly applied cytokines for NK cell activation, clinically. Apart from their roles in the maturation of NK cells, IL-15 and IL-12 can also lead to IFNγ production (Berraondo et al., 2019). Both type I and type II IFNs have been reported to induce the anti-tumor activities of almost all immune cells, especially the maturation of DCs for antigen presentation and the negative regulation of MDSCs (Parker et al., 2016). Besides, oncolytic virus talimogene laherperepvec (T-VEC), which could express myeloid cell growth and survival factor GM-CSF (Andtbacka et al., 2019), might also be used to ameliorate the loss of DCs in smoking OSCC patients. Considering that inactivation of DCs and induction of MDSCs were both related to high abundance of *P. gingivalis* and areca-chewing habits, these cytokines mentioned above might be effective for those OSCC patients. In addition, owing to the significant decrease in IL-2 induced by areca-chewing, an extraordinary supplementation of IL-2 might also help to some extent.

Anti-Cytokine Therapy

Anti-cytokine therapy here refers to blockades of cytokines, cytokine receptors, and the subsequent signaling pathways. Overexpression of some crucial pro-inflammatory cytokines, including IL-6, IL-8, and IL-1β, was a shared phenomenon during periodontitis. These cytokines were reported to promote tumorigenesis (Kumari et al., 2016; Berraondo et al., 2019), so monoclonal antibody therapy against them or their signaling downstream molecules such as STAT3 and MAPK might help a lot (Johnson et al., 2018).

Tumor-associated macrophages (TAMs), which contribute to local tumor growth, often express some angiogenesis-promoting factors (e.g., EGFR ligands and VEGF) and immune-suppressing factors (e.g., TGF-β and IL-10), contributing to tumor growth and metastasis. Thus, monoclonal antibody therapies targeting these molecules could relieve the tumor burden to some extent. Inhibition of CSF1/CSF1R could suppress proliferation, differentiation, and survival of monocytes and macrophages and has been examined through multiple types of cancers (Strachan et al., 2013; Chitu and Stanley, 2017). In addition, CCR2 inhibition and PI3K inhibition, which could be used to restrict TAM recruitment into tumor sites (Okkenhaug, 2013; Le et al., 2018), might also reduce the recruitment and accumulation of TAMs into OSCC local lesions. Since TAMs tend to get accumulated inside tumor sites in OSCC patients with a smoking habit or high abundance of *F. nucleatum*, the strategies targeting TAMs discussed above were necessary.

Adoptive Cell Therapy

Adoptive cell therapy (ACT) is a new form of immunotherapy in which autologous immune cells (mainly T cells) from peripheral blood were engineered *ex vivo* to express tumor-specific transgenic antigen receptors such as chimeric antigen receptors (CARs) or T cell receptors (TCRs) (Wang and Cao, 2020). Despite the application of CD19-directed CAR-T cells having shown remarkable success in the treatment of $CD19^+$ B cell malignancies, there are some obstacles to this method for solid tumors due to the heterogeneity of antigens expressed in solid tumors (Chan et al., 2021) and the immunosuppressive tumor microenvironment (Yeku et al., 2017). However, investigations into its solutions never stop. CAR-T cell therapy targeting ErbB family receptors has attracted a lot of interest in the treatment of head and neck cancer and was evaluated in ongoing phase I clinical trails (van Schalkwyk et al., 2013; Yeku et al., 2017). In addition, engineered T cells expressing the dendritic cell growth factor Flt3L were reported to overcome the clinical problem of antigen-negative tumor escape following ACT (Lai et al., 2020). Besides, many scholars demonstrate that the combination of ACT and approaches targeting immune check-point receptors would enhance anti-tumor immunity *in vivo* (Liu et al., 2017; Chan et al., 2021). Similarly, other therapies, such as NK cell adoptive transferring and NK cell manufacture, which have not been broadly used, might also be applied in clinical treatment in the future. In conclusion, ACT, mentioned above, has a promising future in OSCC treatment and helps solve the T cell and NK cell exhaustion in TME even though more scientific research studies are still necessary.

DISCUSSION

In this review, an abnormal immune status during the progress of OSCC was depicted first. Complete analysis of immune abnormalities caused by different oral cancer–related carcinogens was then accomplished. Based on different types of immune abnormalities induced by different carcinogens, possible individual immunotherapeutic strategies dependent on carcinogen-induced immune abnormalities were figured out as a way to possibly overcome heterogeneity of OSCC patients and enhance clinical efficacy of immunotherapies.

Nowadays, surgical resection still remains the predominant method for treatment of OSCC. However, the heavy financial and physical burden of surgical operation has become an insurmountable hurdle for lots of OSCC patients (Hamoir

et al., 2014). In this condition, some alternative treatment methods, including immunotherapy, deserve further attempts during the treatment process of OSCC. Heterogeneity among different cancer patients acts as a main obstacle for common applications of immunotherapies among multiple cancers, OSCC included (Caswell and Swanton, 2017). Until now, multiple studies have focused on creating personalized therapies for HNSCC (Baird et al., 2018), and subgroup division seems to be an effective way for this. Until now, some subgroup division standards based on HPV status, age, and cetuximab history have failed to contribute greatly to enhancing the efficacy of immunotherapy in OSCC (Cramer et al., 2019). Different types of local immune abnormalities caused by different carcinogens suggest that subgroup division standard based on carcinogens, in combination with specific judgment of the patient immune status, might help achieve individual-targeted immunotherapy and improve the clinical outcome of immunotherapy-treated patients to a great extent.

Nevertheless, lack of systemic studies for influence of different carcinogens on the OSCC local immune status is a defect for our review, so we could only predict possible immune alternations and corresponding therapeutic strategies for OSCC. Further studies are still necessary to verify these possibilities. Besides, occurrence of OSCC depends not only on carcinogens but also genetic abnormalities, which means carcinogen-based immunotherapies might not completely explain and overcome heterogeneity of OSCC patients. In addition, a specific OSCC patient might be under the influence of more than one type of carcinogen, which might render the local immune microenvironment more complex and harder to be predicted. Multiple factor–associated OSCC has long become a challenge for chemotherapy, as different types of carcinogens would produce a complex network regulating patterns, making it an extreme dilemma for researchers. Until now, studies about OSCC chemotherapy have all focused on the influence of a single carcinogenic factor, while no such clinical study aimed at figuring out multiple factor–induced immune variations has been completed yet. Based on this research status, efforts were made in this manuscript to describe and summarize immune status variations induced by every specific OSCC carcinogen and changes of a specific immune status associated with multiple types of OSCC carcinogens. Thus, our review only aimed at a complete analysis and summarization of current knowledge about single-carcinogen–induced immune abnormalities in OSCC. Obviously, more clinical experiments focused on this issue ought to be conducted to confirm our assumption, constructing a better strategy to expand application of immunotherapies during the OSCC treatment process.

AUTHOR CONTRIBUTIONS

All authors listed have made a substantial, direct, and intellectual contribution to the work and approved it for publication.

FUNDING

This work was funded by Young Elite Scientist Sponsorship Program by CAST (2018QNRC001, to QT), and Key Supporting Program by Health Commission of Hubei Province (WJ2019C001, to LC).

REFERENCES

Abdi, K., Chen, T., Klein, B. A., Tai, A. K., Coursen, J., Liu, X., et al. (2017). Mechanisms by Which Porphyromonas Gingivalis Evades Innate Immunity. *PloS one* 12, e0182164. doi:10.1371/journal.pone.0182164

Al Feghali, K. A., Ghanem, A. I., Burmeister, C., Chang, S. S., Ghanem, T., Keller, C., et al. (2019). Impact of Smoking on Pathological Features in Oral Cavity Squamous Cell Carcinoma. *J. Cancer Res. Ther.* 15, 582–588. doi:10.4103/jcrt.JCRT_641_16

Alexandrov, L. B., Ju, Y. S., Haase, K., Van Loo, P., Martincorena, I., Nik-Zainal, S., et al. (2016). Mutational Signatures Associated with Tobacco Smoking in Human Cancer. *Science* 354, 618–622. doi:10.1126/science.aag0299

Alfaro, C., Sanmamed, M. F., Rodríguez-Ruiz, M. E., Teijeira, Á., Oñate, C., González, Á., et al. (2017). Interleukin-8 in Cancer Pathogenesis, Treatment and Follow-Up. *Cancer Treat. Rev.* 60, 24–31. doi:10.1016/j.ctrv.2017.08.004

Andtbacka, R. H. I., Collichio, F., Harrington, K. J., Middleton, M. R., Downey, G., Öhrling, K., et al. (2019). Final Analyses of OPTiM: a Randomized Phase III Trial of Talimogene Laherparepvec versus Granulocyte-Macrophage colony-stimulating Factor in Unresectable Stage III-IV Melanoma. *J. Immunother. Cancer* 7, 145. doi:10.1186/s40425-019-0623-z

Anguille, S., Smits, E. L., Lion, E., van Tendeloo, V. F., and Berneman, Z. N. (2014). Clinical Use of Dendritic Cells for Cancer Therapy. *Lancet Oncol.* 15, e257–e267. doi:10.1016/s1470-2045(13)70585-0

Ardi, V. C., Kupriyanova, T. A., Deryugina, E. I., and Quigley, J. P. (2007). Human Neutrophils Uniquely Release TIMP-free MMP-9 to Provide a Potent Catalytic Stimulator of Angiogenesis. *Proc. Natl. Acad. Sci.* 104, 20262–20267. doi:10.1073/pnas.0706438104

Baird, J. R., Bell, R. B., Troesch, V., Friedman, D., Bambina, S., Kramer, G., et al. (2018). Evaluation of Explant Responses to STING Ligands: Personalized Immunosurgical Therapy for Head and Neck Squamous Cell Carcinoma. *Cancer Res.* 78, 6308–6319. doi:10.1158/0008-5472.can-18-1652

Barnes, P. J. (2016). Inflammatory Mechanisms in Patients with Chronic Obstructive Pulmonary Disease. *J. Allergy Clin. Immunol.* 138, 16–27. doi:10.1016/j.jaci.2016.05.011

Bazzan, E., Turato, G., Tinè, M., Radu, C. M., Balestro, E., Rigobello, C., et al. (2017). Dual Polarization of Human Alveolar Macrophages Progressively Increases with Smoking and COPD Severity. *Respir. Res.* 18, 40. doi:10.1186/s12931-017-0522-0

Ben-Eliyahu, S., Page, G. G., Yirmiya, R., and Taylor, A. N. (1996). Acute Alcohol Intoxication Suppresses Natural Killer Cell Activity and Promotes Tumor Metastasis. *Nat. Med.* 2, 457–460. doi:10.1038/nm0496-457

Bennett, S. R. M., Carbone, F. R., Karamalis, F., Flavell, R. A., Miller, J. F. A. P., and Heath, W. R. (1998). Help for Cytotoxic-T-Cell Responses Is Mediated by CD40 Signalling. *Nature* 393, 478–480. doi:10.1038/30996

Berlato, C., Khan, M. N., Schioppa, T., Thompson, R., Maniati, E., Montfort, A., et al. (2017). A CCR4 Antagonist Reverses the Tumor-Promoting Microenvironment of Renal Cancer. *J. Clin. Invest.* 127, 801–813. doi:10.1172/jci82976

Berraondo, P., Sanmamed, M. F., Ochoa, M. C., Etxeberria, I., Aznar, M. A., Pérez-Gracia, J. L., et al. (2019). Cytokines in Clinical Cancer Immunotherapy. *Br. J. Cancer* 120, 6–15. doi:10.1038/s41416-018-0328-y

Bezerra, N. V., Leite, K. L., de Medeiros, M. M., Martins, M. L., Cardoso, A. M., Alves, P. M., et al. (2018). Impact of the Anatomical Location, Alcoholism and Smoking on the Prevalence of Advanced Oral Cancer in Brazil. *Med. Oral Patol Oral Cir Bucal* 23, e295–e301. doi:10.4317/medoral.22318

Binnewies, M., Roberts, E. W., Kersten, K., Chan, V., Fearon, D. F., Merad, M., et al. (2018). Understanding the Tumor Immune Microenvironment (TIME) for Effective Therapy. *Nat. Med.* 24, 541–550. doi:10.1038/s41591-018-0014-x

Blank, S. E., Duncan, D. A., and Meadows, G. G. (1991). Suppression of Natural Killer Cell Activity by Ethanol Consumption and Food Restriction. *Alcohol. Clin. Exp. Res.* 15, 16–22. doi:10.1111/j.1530-0277.1991.tb00514.x

Blot, W. J., McLaughlin, J. K., Winn, D. M., Austin, D. F., Greenberg, R. S., Preston-Martin, S., et al. (1988). Smoking and Drinking in Relation to Oral and Pharyngeal Cancer. *Cancer Res.* 48, 3282–3287.

Boas, D. S. V., Takiya, C. M., Gurgel, C. A. S., Cabral, M. G., and Santos, J. N. d. (2013). Tumor-infiltrating Macrophage and Microvessel Density in Oral Squamous Cell Carcinoma. *Braz. Dent. J.* 24, 194–199. doi:10.1590/0103-6440201302049

Bosetti, C., Gallus, S., Franceschi, S., Levi, F., Bertuzzi, M., Negri, E., et al. (2002). Cancer of the Larynx in Non-smoking Alcohol Drinkers and in Non-drinking Tobacco Smokers. *Br. J. Cancer* 87, 516–518. doi:10.1038/sj.bjc.6600469

Boyadjieva, N., Advis, J. P., and Sarkar, D. K. (2006). Role of ?-Endorphin, Corticotropin-Releasing Hormone, and Autonomic Nervous System in Mediation of the Effect of Chronic Ethanol on Natural Killer Cell Cytolytic Activity. *Alcohol. Clin. Exp. Res.* 30, 1761–1767. doi:10.1111/j.1530-0277.2006.00209.x

Brunner-Weinzierl, M. C., and Rudd, C. E. (2018). CTLA-4 and PD-1 Control of T-Cell Motility and Migration: Implications for Tumor Immunotherapy. *Front. Immunol.* 9, 2737. doi:10.3389/fimmu.2018.02737

Campbell, L., Maxwell, P., and Waugh, D. (2013). Rationale and Means to Target Pro-inflammatory Interleukin-8 (CXCL8) Signaling in Cancer. *Pharmaceuticals* 6, 929–959. doi:10.3390/ph6080929

Cardoso, E. M., Reis, C., and Manzanares-Céspedes, M. C. (2018). Chronic Periodontitis, Inflammatory Cytokines, and Interrelationship with Other Chronic Diseases. *Postgrad. Med.* 130, 98–104. doi:10.1080/00325481.2018.1396876

Casella, I., Feccia, T., Chelucci, C., Samoggia, P., Castelli, G., Guerriero, R., et al. (2003). Autocrine-paracrine VEGF Loops Potentiate the Maturation of Megakaryocytic Precursors through Flt1 Receptor. *Blood* 101, 1316–1323. doi:10.1182/blood-2002-07-2184

Casey, S. C., Amedei, A., Aquilano, K., Azmi, A. S., Benencia, F., Bhakta, D., et al. (2015). Cancer Prevention and Therapy through the Modulation of the Tumor Microenvironment. *Semin. Cancer Biol.* 35 (35 Suppl. l), S199–s223. doi:10.1016/j.semcancer.2015.02.007

Castellsagué, X., Muñoz, N., De Stefani, E., Victora, C. G., Castelletto, R., Rolón, P. A., et al. (1999). Independent and Joint Effects of Tobacco Smoking and Alcohol Drinking on the Risk of Esophageal Cancer in Men and Women. *Int. J. Cancer* 82, 657–664. doi:10.1002/(sici)1097-0215(19990827)82:5<657::aid-ijc7>3.0.co;2-c

Castellsagué, X., Quintana, M. J., Martínez, M. C., Nieto, A., Sánchez, M. J., Juan, A., et al. (2004). The Role of Type of Tobacco and Type of Alcoholic Beverage in Oral Carcinogenesis. *Int. J. Cancer* 108, 741–749. doi:10.1002/ijc.11627

Caswell, D. R., and Swanton, C. (2017). The Role of Tumour Heterogeneity and Clonal Cooperativity in Metastasis, Immune Evasion and Clinical Outcome,. *BMC Med.* 15, 133. doi:10.1186/s12916-017-0900-y

Caughron, B., Yang, Y., and Young, M. R. I. (2018). Role of IL-23 Signaling in the Progression of Premalignant Oral Lesions to Cancer. *PloS one* 13, e0196034. doi:10.1371/journal.pone.0196034

Chan, J. D., Lai, J., Slaney, C. Y., Kallies, A., Beavis, P. A., and Darcy, P. K. (2021). Cellular Networks Controlling T Cell Persistence in Adoptive Cell Therapy. *Nat. Rev. Immunol.* doi:10.1038/s41577-021-00539-6

Chang, L.-Y., Lai, Y.-L., Yu, T.-H., Chen, Y.-T., and Hung, S.-L. (2014). Effects of Areca Nut Extract on Lipopolysaccharides-Enhanced Adhesion and Migration of Human Mononuclear Leukocytes. *J. Periodontol.* 85, 859–867. doi:10.1902/jop.2013.130198

Chang, L.-Y., Wan, H.-C., Lai, Y.-L., Chou, I.-C., Chen, Y.-T., and Hung, S.-L. (2013). Areca Nut Extracts Increased the Expression of Cyclooxygenase-2, Prostaglandin E2 and Interleukin-1α in Human Immune Cells via Oxidative Stress. *Arch. Oral Biol.* 58, 1523–1531. doi:10.1016/j.archoralbio.2013.05.006

Chang, L.-Y., Wan, H.-C., Lai, Y.-L., Kuo, Y.-F., Liu, T.-Y., Chen, Y.-T., et al. (2009). Areca Nut Extracts Increased Expression of Inflammatory Cytokines, Tumor Necrosis Factor-α, Interleukin-1β, Interleukin-6 and Interleukin-8, in Peripheral Blood Mononuclear Cells. *J. Periodont Res.* 44, 175–183. doi:10.1111/j.1600-0765.2008.01104.x

Chang, L.-Y., Wan, H.-C., Lai, Y.-L., Liu, T.-Y., and Hung, S.-L. (2006). Enhancing Effects of Areca Nut Extracts on the Production of Interleukin-6 and Interleukin-8 by Peripheral Blood Mononuclear Cells. *J. Periodontol.* 77, 1969–1977. doi:10.1902/jop.2006.060039

Chaturvedi, A. K., Engels, E. A., Anderson, W. F., and Gillison, M. L. (2008). Incidence Trends for Human Papillomavirus-Related and -Unrelated Oral Squamous Cell Carcinomas in the United States. *Jco* 26, 612–619. doi:10.1200/jco.2007.14.1713

Chaturvedi, A. K., Graubard, B. I., Broutian, T., Pickard, R. K. L., Tong, Z.-y., Xiao, W., et al. (2015). NHANES 2009-2012 Findings: Association of Sexual Behaviors with Higher Prevalence of Oral Oncogenic Human Papillomavirus Infections in U.S. Men. *Cancer Res.* 75, 2468–2477. doi:10.1158/0008-5472.can-14-2843

Chen, C. P., Boyadjieva, N. I., Advis, J. P., and Sarkar, D. K. (2006). Ethanol Suppression of the Hypothalamic Proopiomelanocortin Level and the Splenic NK Cell Cytolytic Activity Is Associated with a Reduction in the Expression of Proinflammatory Cytokines but Not Anti-inflammatory Cytokines in Neuroendocrine and Immune Cells. *Alcohol. Clin. Exp. Res.* 30, 1925–1932. doi:10.1111/j.1530-0277.2006.00237.x

Chen, H., Liakou, C. I., Kamat, A., Pettaway, C., Ward, J. F., Tang, D. N., et al. (2009). Anti-CTLA-4 Therapy Results in Higher CD4+ICOShiT Cell Frequency and IFN-γ Levels in Both Nonmalignant and Malignant Prostate Tissues. *Pnas* 106, 2729–2734. doi:10.1073/pnas.0813175106

Chen, L., Fan, J., Chen, H., Meng, Z., Chen, Z., Wang, P., et al. (2014). The IL-8/CXCR1 axis Is Associated with Cancer Stem Cell-like Properties and Correlates with Clinical Prognosis in Human Pancreatic Cancer Cases,. *Scientific Rep.* 4, 5911. doi:10.1038/srep05911

Chen, T., Li, Q., Wu, J., Wu, Y., Peng, W., Li, H., et al. (2018). Fusobacterium Nucleatum Promotes M2 Polarization of Macrophages in the Microenvironment of Colorectal Tumours via a TLR4-dependent Mechanism. *Cancer Immunol. Immunother.* 67, 1635–1646. doi:10.1007/s00262-018-2233-x

Cheng, Y. A., Shiue, L. F., Yu, H. S., Hsieh, T. Y., and Tsai, C. C. (2000). Interleukin-8 Secretion by Cultured Oral Epidermoid Carcinoma Cells Induced with Nicotine And/or Arecoline Treatments. *Kaohsiung J. Med. Sci.* 16, 126–133.

Chi, N., Tan, Z., Ma, K., Bao, L., and Yun, Z. (2014). Increased Circulating Myeloid-Derived Suppressor Cells Correlate with Cancer Stages, Interleukin-8 and -6 in Prostate Cancer. *Int. J. Clin. Exp. Med.* 7, 3181–3192.

Chitu, V., and Stanley, E. R. (2017). Regulation of Embryonic and Postnatal Development by the CSF-1 Receptor. *Curr. Top. Dev. Biol.* 123, 229–275. doi:10.1016/bs.ctdb.2016.10.004

Cho, E., Smith-Warner, S. A., Ritz, J., van den Brandt, P. A., Colditz, G. A., Folsom, A. R., et al. (2004). Alcohol Intake and Colorectal Cancer: a Pooled Analysis of 8 Cohort Studies. *Ann. Intern. Med.* 140, 603–613. doi:10.7326/0003-4819-140-8-200404200-00007

Chow, L. Q. M. (2020). Head and Neck Cancer. *N. Engl. J. Med.* 382, 60–72. doi:10.1056/NEJMra1715715

Constantino, J., Gomes, C., Falcão, A., Neves, B. M., and Cruz, M. T. (2017). Dendritic Cell-Based Immunotherapy: a Basic Review and Recent Advances. *Immunol. Res.* 65, 798–810. doi:10.1007/s12026-017-8931-1

Cozen, W., Diaz-Sanchez, D., James Gauderman, W., Zadnick, J., Cockburn, M. G., Gill, P. S., et al. (2004). Th1 and Th2 Cytokines and IgE Levels in Identical Twins with Varying Levels of Cigarette Consumption. *J. Clin. Immunol.* 24, 617–622. doi:10.1007/s10875-004-6247-0

Cramer, J. D., Burtness, B., and Ferris, R. L. (2019). Immunotherapy for Head and Neck Cancer: Recent Advances and Future Directions. *Oral Oncol.* 99, 104460. doi:10.1016/j.oraloncology.2019.104460

Daley, D., Mani, V. R., Mohan, N., Akkad, N., Pandian, G. S. D. B., Savadkar, S., et al. (2017). NLRP3 Signaling Drives Macrophage-Induced Adaptive Immune Suppression in Pancreatic Carcinoma. *J. Exp. Med.* 214, 1711–1724. doi:10.1084/jem.20161707

Dar, A. A., Patil, R. S., Pradhan, T. N., Chaukar, D. A., D'Cruz, A. K., and Chiplunkar, S. V. (2020). Myeloid-derived Suppressor Cells Impede T Cell Functionality and Promote Th17 Differentiation in Oral Squamous Cell Carcinoma, Cancer Immunology, Immunotherapy. *Cancer Immunol. Immunother.* 69, 1071–1086. doi:10.1007/s00262-020-02523-w

Das, A., Monteiro, M., Barai, A., Kumar, S., and Sen, S. (2017). MMP Proteolytic Activity Regulates Cancer Invasiveness by Modulating Integrins. *Scientific Rep.* 7, 14219. doi:10.1038/s41598-017-14340-w

Dasgupta, R., Saha, I., Pal, S., Bhattacharyya, A., Sa, G., Nag, T. C., et al. (2006). Immunosuppression, Hepatotoxicity and Depression of Antioxidant Status by

Arecoline in Albino Mice. *Toxicology* 227, 94–104. doi:10.1016/j.tox.2006.07.016

Dave, K., Ali, A., and Magalhaes, M. (2020). Increased Expression of PD-1 and PD-L1 in Oral Lesions Progressing to Oral Squamous Cell Carcinoma: a Pilot Study. *Sci. Rep.* 10, 9705. doi:10.1038/s41598-020-66257-6

David, J. M., Dominguez, C., Hamilton, D. H., and Palena, C. (2016). The IL-8/IL-8R Axis: A Double Agent in Tumor Immune Resistance,. *Vaccines* 4, 22. doi:10.3390/vaccines4030022

De Costa, A.-M. A., Schuyler, C. A., Walker, D. D., and Young, M. R. I. (2012). Characterization of the Evolution of Immune Phenotype during the Development and Progression of Squamous Cell Carcinoma of the Head and Neck. *Cancer Immunol. Immunother.* 61, 927–939. doi:10.1007/s00262-011-1154-8

de la Iglesia, J. V., Slebos, R. J. C., Martin-Gomez, L., Wang, X., Teer, J. K., Tan, A. C., et al. (2020). Effects of Tobacco Smoking on the Tumor Immune Microenvironment in Head and Neck Squamous Cell Carcinoma. *Clin. Cancer Res.* 26, 1474–1485. doi:10.1158/1078-0432.ccr-19-1769

Dempke, W. C. M., Fenchel, K., Uciechowski, P., and Dale, S. P. (2017). Second- and Third-Generation Drugs for Immuno-Oncology Treatment-The More the Better? *Eur. J. Cancer* 74, 55–72. doi:10.1016/j.ejca.2017.01.001

Ding, S., Tang, Z., Jiang, Y., Huang, H., Luo, P., Qing, B., et al. (2017). IL-8 Is Involved in Estrogen-Related Receptor α-Regulated Proliferation and Migration of Colorectal Cancer Cells. *Dig. Dis. Sci.* 62, 3438–3446. doi:10.1007/s10620-017-4779-4

Dong, H., Strome, S. E., Salomao, D. R., Tamura, H., Hirano, F., Flies, D. B., et al. (2002). Tumor-associated B7-H1 Promotes T-Cell Apoptosis: a Potential Mechanism of Immune Evasion. *Nat. Med.* 8, 793–800. doi:10.1038/nm730

Dutta, A., Banerjee, A., Saikia, N., Phookan, J., Baruah, M. N., and Baruah, S. (2015). Negative Regulation of Natural Killer Cell in Tumor Tissue and Peripheral Blood of Oral Squamous Cell Carcinoma. *Cytokine* 76, 123–130. doi:10.1016/j.cyto.2015.09.006

Egberts, J.-H., Cloosters, V., Noack, A., Schniewind, B., Thon, L., Klose, S., et al. (2008). Anti-tumor Necrosis Factor Therapy Inhibits Pancreatic Tumor Growth and Metastasis. *Cancer Res.* 68, 1443–1450. doi:10.1158/0008-5472.can-07-5704

Einstein, M. H., Leanza, S., Chiu, L. G., Schlecht, N. F., Goldberg, G. L., Steinberg, B. M., et al. (2009). Genetic Variants in TAP Are Associated with High-Grade Cervical Neoplasia. *Clin. Cancer Res.* 15, 1019–1023. doi:10.1158/1078-0432.ccr-08-1207

Emmerich, J., Mumm, J. B., Chan, I. H., LaFace, D., Truong, H., McClanahan, T., et al. (2012). IL-10 Directly Activates and Expands Tumor-Resident CD8+ T Cells without De Novo Infiltration from Secondary Lymphoid Organs. *Cancer Res.* 72, 3570–3581. doi:10.1158/0008-5472.can-12-0721

Essa, A. A. M., Yamazaki, M., Maruyama, S., Abé, T., Babkair, H., Raghib, A. M., et al. (2016). Tumour-associated Macrophages Are Recruited and Differentiated in the Neoplastic Stroma of Oral Squamous Cell Carcinoma. *Pathology* 48, 219–227. doi:10.1016/j.pathol.2016.02.006

Facchinetti, F., Amadei, F., Geppetti, P., Tarantini, F., Di Serio, C., Dragotto, A., et al. (2007). α,β-Unsaturated Aldehydes in Cigarette Smoke Release Inflammatory Mediators from Human Macrophages. *Am. J. Respir. Cel Mol Biol* 37, 617–623. doi:10.1165/rcmb.2007-0130oc

Faouzi, M., Neupane, R. P., Yang, J., Williams, P., and Penner, R. (2018). Areca Nut Extracts Mobilize Calcium and Release Pro-inflammatory Cytokines from Various Immune Cells. *Sci. Rep.* 8, 1075. doi:10.1038/s41598-017-18996-2

Farhood, B., Najafi, M., and Mortezaee, K. (2019). CD8 + Cytotoxic T Lymphocytes in Cancer Immunotherapy: A Review. *J. Cel Physiol* 234, 8509–8521. doi:10.1002/jcp.27782

Feng, B., Shen, Y., Pastor, X., Bieg, M., Plath, M., Ishaque, N., et al. (2020). Integrative Analysis of Multi-Omics Data Identified EGFR and PTGS2 as Key Nodes in a Gene Regulatory Network Related to Immune Phenotypes in Head and Neck Cancer. *Clin. Cancer Res.* 26, 3616–3628. doi:10.1158/1078-0432.CCR-19-3997

Ferris, R. L., Blumenschein, G., Jr., Fayette, J., Guigay, J., Colevas, A. D., Licitra, L., et al. (2016). Nivolumab for Recurrent Squamous-Cell Carcinoma of the Head and Neck. *N. Engl. J. Med.* 375, 1856–1867. doi:10.1056/nejmoa1602252

Floros, T., and Tarhini, A. A. (2015). Anticancer Cytokines: Biology and Clinical Effects of Interferon-A2, Interleukin (IL)-2, IL-15, IL-21, and IL-12. *Semin. Oncol.* 42, 539–548. doi:10.1053/j.seminoncol.2015.05.015

Foulds, K. E., Rotte, M. J., and Seder, R. A. (2006). IL-10 Is Required for Optimal CD8 T Cell Memory followingListeria monocytogenesInfection. *J. Immunol.* 177, 2565–2574. doi:10.4049/jimmunol.177.4.2565

Gabrilovich, D. I. (2017). Myeloid-Derived Suppressor Cells. *Cancer Immunol. Res.* 5, 3–8. doi:10.1158/2326-6066.cir-16-0297

Gabrilovich, D. I., Ostrand-Rosenberg, S., and Bronte, V. (2012). Coordinated Regulation of Myeloid Cells by Tumours. *Nat. Rev. Immunol.* 12, 253–268. doi:10.1038/nri3175

Galvis, M. M., Borges, G. A., Oliveira, T. B. d., Toledo, I. P. d., Castilho, R. M., Guerra, E. N. S., et al. (2020). Immunotherapy Improves Efficacy and Safety of Patients with HPV Positive and Negative Head and Neck Cancer: A Systematic Review and Meta-Analysis. *Crit. Rev. oncology/hematology* 150, 102966. doi:10.1016/j.critrevonc.2020.102966

Gameiro, S. F., Ghasemi, F., Barrett, J. W., Koropatnick, J., Nichols, A. C., Mymryk, J. S., et al. (2018). Treatment-naïve HPV+ Head and Neck Cancers Display a T-Cell-Inflamed Phenotype Distinct from Their HPV- Counterparts that Has Implications for Immunotherapy. *Oncoimmunology* 7, e1498439. doi:10.1080/2162402x.2018.1498439

Gao, Y., Zhou, Z., Ren, T., Kim, S.-J., He, Y., Seo, W., et al. (2019). Alcohol Inhibits T-Cell Glucose Metabolism and Hepatitis in ALDH2-Deficient Mice and Humans: Roles of Acetaldehyde and Glucocorticoids. *Gut* 68, 1311–1322. doi:10.1136/gutjnl-2018-316221

Gardner, A., Ruffell, B., Cells, Dendritic., and Immunity, Cancer. (2016). Dendritic Cells and Cancer Immunity. *Trends Immunology* 37, 855–865. doi:10.1016/j.it.2016.09.006

Gaur, P., Singh, A. K., Shukla, N. K., and Das, S. N. (2014). Inter-relation of Th1, Th2, Th17 and Treg Cytokines in Oral Cancer Patients and Their Clinical Significance. *Hum. Immunol.* 75, 330–337. doi:10.1016/j.humimm.2014.01.011

Ghanizada, M., Jakobsen, K. K., Grønhøj, C., and von Buchwald, C. (2019). The Effects of Checkpoint Inhibition on Head and Neck Squamous Cell Carcinoma: A Systematic Review. *Oral Oncol.* 90, 67–73. doi:10.1016/j.oraloncology.2019.01.018

Giese, M. A., Hind, L. E., and Huttenlocher, A. (2019). Neutrophil Plasticity in the Tumor Microenvironment. *Blood* 133, 2159–2167. doi:10.1182/blood-2018-11-844548

Goodman, A., Patel, S. P., and Kurzrock, R. (2017). PD-1-PD-L1 Immune-Checkpoint Blockade in B-Cell Lymphomas. *Nat. Rev. Clin. Oncol.* 14, 203–220. doi:10.1038/nrclinonc.2016.168

Granero Fernandez, M., and Lopez-Jornet, P. (2017). Association between Smoking, Glycaemia, Blood Lipoproteins and Risk of Oral Leukoplakia. *Aust. Dent J.* 62, 47–51. doi:10.1111/adj.12431

Granot, Z., Henke, E., Comen, E. A., King, T. A., Norton, L., and Benezra, R. (2011). Tumor Entrained Neutrophils Inhibit Seeding in the Premetastatic Lung. *Cancer cell* 20, 300–314. doi:10.1016/j.ccr.2011.08.012

Greene, S., Robbins, Y., Mydlarz, W. K., Huynh, A. P., Schmitt, N. C., Friedman, J., et al. (2020). Inhibition of MDSC Trafficking with SX-682, a CXCR1/2 Inhibitor, Enhances NK-Cell Immunotherapy in Head and Neck Cancer Models. *Clin. Cancer Res.* 26, 1420–1431. doi:10.1158/1078-0432.ccr-19-2625

Guillerey, C., Huntington, N. D., and Smyth, M. J. (2016). Targeting Natural Killer Cells in Cancer Immunotherapy. *Nat. Immunol.* 17, 1025–1036. doi:10.1038/ni.3518

Güngör, N., Knaapen, A. M., Munnia, A., Peluso, M., Haenen, G. R., Chiu, R. K., et al. (2010). Genotoxic Effects of Neutrophils and Hypochlorous Acid. *Mutagenesis* 25, 149–154. doi:10.1093/mutage/gep053

Gur, C., Ibrahim, Y., Isaacson, B., Yamin, R., Abed, J., Gamliel, M., et al. (2015). Binding of the Fap2 Protein of Fusobacterium Nucleatum to Human Inhibitory Receptor TIGIT Protects Tumors from Immune Cell Attack. *Immunity* 42, 344–355. doi:10.1016/j.immuni.2015.01.010

Ha, N. H., Park, D. G., Woo, B. H., Kim, D. J., Choi, J. I., Park, B. S., et al. (2016). Porphyromonas Gingivalis Increases the Invasiveness of Oral Cancer Cells by Upregulating IL-8 and MMPs. *Cytokine* 86, 64–72. doi:10.1016/j.cyto.2016.07.013

Hajishengallis, G. (2015). Periodontitis: from Microbial Immune Subversion to Systemic Inflammation. *Nat. Rev. Immunol.* 15, 30–44. doi:10.1038/nri3785

Hamoir, M., Schmitz, S., and Gregoire, V. (2014). The Role of Neck Dissection in Squamous Cell Carcinoma of the Head and Neck. *Curr. Treat. Options. Oncol.* 15, 611–624. doi:10.1007/s11864-014-0311-7

Hanakawa, H., Orita, Y., Sato, Y., Takeuchi, M., Ohno, K., Gion, Y., et al. (2014). Regulatory T-Cell Infiltration in Tongue Squamous Cell Carcinoma. *Acta oto-laryngologica* 134, 859–864. doi:10.3109/00016489.2014.918279

Hanazawa, A., Ito, R., Katano, I., Kawai, K., Goto, M., Suemizu, H., et al. (2018). Generation of Human Immunosuppressive Myeloid Cell Populations in Human Interleukin-6 Transgenic NOG Mice. *Front. Immunol.* 9, 152. doi:10.3389/fimmu.2018.00152

Hashibe, M., Li, Q., Chen, C.-J., Hsu, W.-L., Lou, P.-J., Zhu, C., et al. (2019). Involuntary Smoking and the Risk of Head and Neck Cancer in an East Asian Population. *Cancer Epidemiol.* 59, 173–177. doi:10.1016/j.canep.2019.01.020

He, Q.-F., Xu, Y., Li, J., Huang, Z.-M., Li, X.-H., and Wang, X. (2019). CD8+ T-Cell Exhaustion in Cancer: Mechanisms and New Area for Cancer Immunotherapy. *Brief. Funct. genomics* 18, 99–106. doi:10.1093/bfgp/ely006

Hodge, S., Hodge, G., Scicchitano, R., Reynolds, P. N., and Holmes, M. (2003). Alveolar Macrophages from Subjects with Chronic Obstructive Pulmonary Disease Are Deficient in Their Ability to Phagocytose Apoptotic Airway Epithelial Cells. *Immunol. Cel Biol* 81, 289–296. doi:10.1046/j.1440-1711.2003.t01-1-01170.x

Holway, G. V., and Hernandez, S. M. (2018). Oral Sex and Condom Use in a U.S. National Sample of Adolescents and Young Adults. *J. Adolesc. Health* 62, 402–410. doi:10.1016/j.jadohealth.2017.08.022

Horiuchi, Y., Tominaga, M., Ichikawa, M., Yamashita, M., Okano, K., Jikumaru, Y., et al. (2010). Relationship between Regulatory and Type 1 T Cells in Dogs with Oral Malignant Melanoma. *Microbiol. Immunol.* 54, 152–159. doi:10.1111/j.1348-0421.2009.00194.x

Hosseini, A., Gharibi, T., Marofi, F., Babaloo, Z., and Baradaran, B. (2020). CTLA-4: From Mechanism to Autoimmune Therapy. *Int. Immunopharmacology* 80, 106221. doi:10.1016/j.intimp.2020.106221

Hu, Y. J., Chen, J., Zhong, W. S., Ling, T. Y., Jian, X. C., Lu, R. H., et al. (2017). Trend Analysis of Betel Nut-associated Oral Cancer and Health Burden in China. *Chin. J. Dent Res.* 20, 69–78. doi:10.3290/j.cjdr.a38271

Huang, D., Song, S.-J., Wu, Z.-Z., Wu, W., Cui, X.-Y., Chen, J.-N., et al. (2017). Epstein-Barr Virus-Induced VEGF and GM-CSF Drive Nasopharyngeal Carcinoma Metastasis via Recruitment and Activation of Macrophages. *Cancer Res.* 77, 3591–3604. doi:10.1158/0008-5472.can-16-2706

Huang, M.-F., Lin, W.-L., and Ma, Y.-C. (2005). A Study of Reactive Oxygen Species in Mainstream of Cigarette. *Indoor air* 15, 135–140. doi:10.1111/j.1600-0668.2005.00330.x

Huang, W., Chen, Z., Zhang, L., Tian, D., Wang, D., Fan, D., et al. (2015). Interleukin-8 Induces Expression of FOXC1 to Promote Transactivation of CXCR1 and CCL2 in Hepatocellular Carcinoma Cell Lines and Formation of Metastases in Mice. *Gastroenterology* 149, 1053–1067. e1014. doi:10.1053/j.gastro.2015.05.058

Huang, Z., Xie, N., Liu, H., Wan, Y., Zhu, Y., Zhang, M., et al. (2019). The Prognostic Role of Tumour-infiltrating Lymphocytes in Oral Squamous Cell Carcinoma: A Meta-analysis. *J. Oral Pathol. Med.* 48, 788–798. doi:10.1111/jop.12927

Hung, S.-L., Lee, Y.-Y., Liu, T.-Y., Peng, J.-L., Cheng, Y.-Y., and Chen, Y.-T. (2006). Modulation of Phagocytosis, Chemotaxis, and Adhesion of Neutrophils by Areca Nut Extracts. *J. Periodontol.* 77, 579–585. doi:10.1902/jop.2006.050217

Hunt, J. D., Robert, E. G., Zieske, A. W., Bautista, A. P., Bukara, M., Lei, D., et al. (2000). Orthotopic Human Lung Carcinoma Xenografts in BALB/c Mice Immunosuppressed with Anti-CD4 Monoclonal Antibodies and Chronic Alcohol Consumption. *Cancer* 88, 468–479. doi:10.1002/(sici)1097-0142(20000115)88:2<468::aid-cncr30>3.0.co;2-#

Im, H.-J., Kim, H.-G., Lee, J.-S., Kim, H.-S., Cho, J.-H., Jo, I.-J., et al. (2016). A Preclinical Model of Chronic Alcohol Consumption Reveals Increased Metastatic Seeding of Colon Cancer Cells in the Liver. *Cancer Res.* 76, 1698–1704. doi:10.1158/0008-5472.can-15-2114

Irimie, A. I., Braicu, C., Pileczki, V., Petrushev, B., Soritau, O., Campian, R. S., et al. (2016). Knocking Down of P53 Triggers Apoptosis and Autophagy, Concomitantly with Inhibition of Migration on SSC-4 Oral Squamous Carcinoma Cells. *Mol. Cel Biochem* 419, 75–82. doi:10.1007/s11010-016-2751-9

Jauregui, C. E., Wang, Q., Wright, C. J., Takeuchi, H., Uriarte, S. M., and Lamont, R. J. (2013). Suppression of T-Cell Chemokines by Porphyromonas Gingivalis. *Infect. Immun.* 81, 2288–2295. doi:10.1128/iai.00264-13

Jelski, W., Kozlowski, M., Laudanski, J., Niklinski, J., and Szmitkowski, M. (2009). Alcohol Dehydrogenase Isoenzymes and Aldehyde Dehydrogenase Activity in the Sera of Patients with Esophageal Cancer. *Clin. Exp. Med.* 9, 131–137. doi:10.1007/s10238-008-0028-7

Jeng, J.-H., Wang, Y.-J., Chiang, B.-L., Lee, P.-H., Chan, C.-P., Ho, Y.-S., et al. (2003). Roles of Keratinocyte Inflammation in Oral Cancer: Regulating the Prostaglandin E2, Interleukin-6 and TNF- Production of Oral Epithelial Cells by Areca Nut Extract and Arecoline. *Carcinogenesis* 24, 1301–1315. doi:10.1093/carcin/bgg083

Jeng, J. H., Ho, Y. S., Chan, C. P., Wang, Y. J., Hahn, L. J., Lei, D., et al. (2000). Areca Nut Extract Up-Regulates Prostaglandin Production, Cyclooxygenase-2 mRNA and Protein Expression of Human Oral Keratinocytes. *Carcinogenesis* 21, 1365–1370. doi:10.1093/carcin/21.5.365

Jeong, W. I., Park, O., and Gao, B. (2008). Abrogation of the Antifibrotic Effects of Natural Killer Cells/Interferon-γ Contributes to Alcohol Acceleration of Liver Fibrosis. *Gastroenterology* 134, 248–258. doi:10.1053/j.gastro.2007.09.034

Jiun, I. L., Siddik, S. N., Malik, S. N., Tin-Oo, M. M., Alam, M. K., Khan, M. M., et al. (2015). Association between Oral Hygiene Status and Halitosis Among Smokers and Nonsmokers. *Oral Health Prev. Dent* 13, 395–405. doi:10.3290/j.ohpd.a33920

Johnson, D. E., O'Keefe, R. A., and Grandis, J. R. (2018). Targeting the IL-6/JAK/STAT3 Signalling axis in Cancer. *Nat. Rev. Clin. Oncol.* 15, 234–248. doi:10.1038/nrclinonc.2018.8

Johnston, R. J., Comps-Agrar, L., Hackney, J., Yu, X., Huseni, M., Yang, Y., et al. (2014). The Immunoreceptor TIGIT Regulates Antitumor and Antiviral CD8 + T Cell Effector Function. *Cancer Cell* 26, 923–937. doi:10.1016/j.ccell.2014.10.018

Joyce, J. A., and Pollard, J. W. (2009). Microenvironmental Regulation of Metastasis. *Nat. Rev. Cancer* 9, 239–252. doi:10.1038/nrc2618

Kabat, G. C., and Wynder, E. L. (1989). Type of Alcoholic Beverage and Oral Cancer. *Int. J. Cancer* 43, 190–194. doi:10.1002/ijc.2910430203

Kagohara, L. T., Zamuner, F., Davis-Marcisak, E. F., Sharma, G., Considine, M., Allen, J., et al. (2020). Integrated Single-Cell and Bulk Gene Expression and ATAC-Seq Reveals Heterogeneity and Early Changes in Pathways Associated with Resistance to Cetuximab in HNSCC-Sensitive Cell Lines. *Br. J. Cancer* 123, 101–113. doi:10.1038/s41416-020-0851-5

Kansy, B. A., Concha-Benavente, F., Srivastava, R. M., Jie, H.-B., Shayan, G., Lei, Y., et al. (2017). PD-1 Status in CD8+ T Cells Associates with Survival and Anti-PD-1 Therapeutic Outcomes in Head and Neck Cancer. *Cancer Res.* 77, 6353–6364. doi:10.1158/0008-5472.can-16-3167

Kato, T., Noma, K., Ohara, T., Kashima, H., Katsura, Y., Sato, H., et al. (2018). Cancer-Associated Fibroblasts Affect Intratumoral CD8+ and FoxP3+ T Cells via IL6 in the Tumor Microenvironment. *Clin. Cancer Res.* 24, 4820–4833. doi:10.1158/1078-0432.ccr-18-0205

Katz, P. S., Siggins, R. W., Porretta, C., Armstrong, M. L., Zea, A. H., Mercante, D. E., et al. (2015). Chronic Alcohol Increases CD8+ T-Cell Immunosenescence in Simian Immunodeficiency Virus-Infected Rhesus Macaques. *Alcohol* 49, 759–765. doi:10.1016/j.alcohol.2015.09.003

Kennedy, L. B., and Salama, A. K. S. (2020). A Review of Cancer Immunotherapy Toxicity,. *CA Cancer J. Clin.* 70. doi:10.3322/caac.21596

Khalaf, H., and Bengtsson, T. (2012). Altered T-Cell Responses by the Periodontal Pathogen Porphyromonas Gingivalis. *PloS one* 7, e45192. doi:10.1371/journal.pone.0045192

Kinane, D. F., Stathopoulou, P. G., and Papapanou, P. N. (2017). Periodontal Diseases, Nature Reviews. *Dis. primers* 3, 17038. doi:10.1038/nrdp.2017.38

Kirkham, P. A., Spooner, G., Rahman, I., and Rossi, A. G. (2004). Macrophage Phagocytosis of Apoptotic Neutrophils Is Compromised by Matrix Proteins Modified by Cigarette Smoke and Lipid Peroxidation Products. *Biochem. biophysical Res. Commun.* 318, 32–37. doi:10.1016/j.bbrc.2004.04.003

Koehn, B. H., Apostolova, P., Haverkamp, J. M., Miller, J. S., McCullar, V., Tolar, J., et al. (2015). GVHD-associated, Inflammasome-Mediated Loss of Function in Adoptively Transferred Myeloid-Derived Suppressor Cells. *Blood* 126, 1621–1628. doi:10.1182/blood-2015-03-634691

Korc, M., Jeon, C. Y., Edderkaoui, M., Pandol, S. J., and Petrov, M. S. (2017). Tobacco and Alcohol as Risk Factors for Pancreatic Cancer. *Best Pract. Res. Clin. Gastroenterol.* 31, 529–536. doi:10.1016/j.bpg.2017.09.001

Kostic, A. D., Chun, E., Robertson, L., Glickman, J. N., Gallini, C. A., Michaud, M., et al. (2013). Fusobacterium Nucleatum Potentiates Intestinal Tumorigenesis and Modulates the Tumor-Immune Microenvironment. *Cell Host & Microbe* 14, 207–215. doi:10.1016/j.chom.2013.07.007

Kotani, N., Hashimoto, H., Sessler, D. I., Yoshida, H., Kimura, N., Okawa, H., et al. (2000). Smoking Decreases Alveolar Macrophage Function during Anesthesia and Surgery. *Anesthesiology* 92, 1268–1277. doi:10.1097/00000542-200005000-00014

Kouketsu, A., Sato, I., Oikawa, M., Shimizu, Y., Saito, H., Tashiro, K., et al. (2019). Regulatory T Cells and M2-Polarized Tumour-Associated Macrophages Are Associated with the Oncogenesis and Progression of Oral Squamous Cell Carcinoma. *Int. J. Oral Maxill. Surg.* 48, 1279–1288. doi:10.1016/j.ijom.2019.04.004

Krishna, S., Ulrich, P., Wilson, E., Parikh, F., Narang, P., Yang, S., et al. (2018). Human Papilloma Virus Specific Immunogenicity and Dysfunction of CD8+ T Cells in Head and Neck Cancer. *Cancer Res.* 78, 6159–6170. doi:10.1158/0008-5472.can-18-0163

Kroening, P. R., Barnes, T. W., Pease, L., Limper, A., Kita, H., and Vassallo, R. (2008). Cigarette Smoke-Induced Oxidative Stress Suppresses Generation of Dendritic Cell IL-12 and IL-23 through ERK-dependent Pathways. *J. Immunol.* 181, 1536–1547. doi:10.4049/jimmunol.181.2.1536

Kumar, M., Nanavati, R., Modi, T., and Dobariya, C. (2016). Oral Cancer: Etiology and Risk Factors: A Review. *J. Can. Res. Ther.* 12, 458–463. doi:10.4103/0973-1482.186696

Kumar, S., Torres, M. P., Kaur, S., Rachagani, S., Joshi, S., Johansson, S. L., et al. (2015). Smoking Accelerates Pancreatic Cancer Progression by Promoting Differentiation of MDSCs and Inducing HB-EGF Expression in Macrophages. *Oncogene* 34, 2052–2060. doi:10.1038/onc.2014.154

Kumari, N., Dwarakanath, B. S., Das, A., and Bhatt, A. N. (2016). Role of Interleukin-6 in Cancer Progression and Therapeutic Resistance. *Tumor Biol.* 37, 11553–11572. doi:10.1007/s13277-016-5098-7

Lai, J., Mardiana, S., House, I. G., Sek, K., Henderson, M. A., Giuffrida, L., et al. (2020). Adoptive Cellular Therapy with T Cells Expressing the Dendritic Cell Growth Factor Flt3L Drives Epitope Spreading and Antitumor Immunity. *Nat. Immunol.* 21, 914–926. doi:10.1038/s41590-020-0676-7

Lauerova, L., Dusek, L., Simickova, M., Kocák, I., Vagundová, M., Zaloudík, J., et al. (2002). Malignant Melanoma Associates with Th1/Th2 Imbalance that Coincides with Disease Progression and Immunotherapy Response. *Neoplasma* 49, 159–166.

Lauw, F. N., Pajkrt, D., Hack, C. E., Kurimoto, M., van Deventer, S. J. H., and van der Poll, T. (2000). Proinflammatory Effects of IL-10 during Human Endotoxemia. *J. Immunol.* 165, 2783–2789. doi:10.4049/jimmunol.165.5.2783

Le, D., Gutierrez, M. E., Saleh, M., Chen, E., Mallick, A. B., Pishvaian, M. J., et al. (2018). Abstract CT124: A Phase Ib/II Study of BMS-813160, a CC Chemokine Receptor (CCR) 2/5 Dual Antagonist, in Combination with Chemotherapy or Nivolumab in Patients (Pts) with Advanced Pancreatic or Colorectal Cancer,. *Cancer Res.* 78, CT124. doi:10.1158/1538-7445.AM2018-CT124

Lechien, J. R., Seminerio, I., Descamps, G., Mat, Q., Mouawad, F., Hans, S., et al. (2019). Impact of HPV Infection on the Immune System in Oropharyngeal and Non-oropharyngeal Squamous Cell Carcinoma: A Systematic Review,. *Cells* 8. doi:10.3390/cells8091061

Lee, C.-H., Liu, S.-Y., Chou, K.-C., Yeh, C.-T., Shiah, S.-G., Huang, R.-Y., et al. (2014). Tumor-associated Macrophages Promote Oral Cancer Progression through Activation of the Axl Signaling Pathway. *Ann. Surg. Oncol.* 21, 1031–1037. doi:10.1245/s10434-013-3400-0

Lee, J.-J., Kao, K.-C., Chiu, Y.-L., Jung, C.-J., Liu, C.-J., Cheng, S.-J., et al. (2017). Enrichment of Human CCR6+ Regulatory T Cells with Superior Suppressive Activity in Oral Cancer. *J.I.* 199, 467–476. doi:10.4049/jimmunol.1601815

Lee, M.-H., Tung-Chieh Chang, J., Liao, C.-T., Chen, Y.-S., Kuo, M.-L., and Shen, C.-R. (2018). Interleukin 17 and Peripheral IL-17-expressing T Cells Are Negatively Correlated with the Overall Survival of Head and Neck Cancer Patients. *Oncotarget* 9, 9825–9837. doi:10.18632/oncotarget.23934

Lee, Y., Awasthi, A., Yosef, N., Quintana, F. J., Xiao, S., Peters, A., et al. (2012). Induction and Molecular Signature of Pathogenic TH17 Cells. *Nat. Immunol.* 13, 991–999. doi:10.1038/ni.2416

Lertpimonchai, A., Rattanasiri, S., Arj-Ong Vallibhakara, S., Attia, J., and Thakkinstian, A. (2017). The Association between Oral hygiene and Periodontitis: a Systematic Review and Meta-Analysis. *Int. dental J.* 67, 332–343. doi:10.1111/idj.12317

Li, B., Ren, M., Zhou, X., Han, Q., and Cheng, L. (2020). Targeting Tumor-Associated Macrophages in Head and Neck Squamous Cell Carcinoma. *Oral Oncol.* 106, 104723. doi:10.1016/j.oraloncology.2020.104723

Li, C., Zhang, N., Zhou, J., Ding, C., Jin, Y., Cui, X., et al. (2018). Peptide Blocking of PD-1/pd-L1 Interaction for Cancer Immunotherapy. *Cancer Immunol. Res.* 6, 178–188. doi:10.1158/2326-6066.cir-17-0035

Li, H., Edin, M. L., Gruzdev, A., Cheng, J., Bradbury, J. A., Graves, J. P., et al. (2013). Regulation of T Helper Cell Subsets by Cyclooxygenases and Their Metabolites. *Prostaglandins & Other Lipid Mediators* 104-105, 74–83. doi:10.1016/j.prostaglandins.2012.11.002

Li, X., Xu, Q., Wu, Y., Li, J., Tang, D., Han, L., et al. (2014). A CCL2/ROS Autoregulation Loop Is Critical for Cancer-Associated Fibroblasts-Enhanced Tumor Growth of Oral Squamous Cell Carcinoma. *Carcinogenesis* 35, 1362–1370. doi:10.1093/carcin/bgu046

Li, Y.-C., Chang, J. T., Chiu, C., Lu, Y.-C., Li, Y.-L., Chiang, C.-H., et al. (2016). Areca Nut Contributes to Oral Malignancy through Facilitating the Conversion of Cancer Stem Cells. *Mol. Carcinog.* 55, 1012–1023. doi:10.1002/mc.22344

Lien, M.-Y., Lin, C.-W., Tsai, H.-C., Chen, Y.-T., Tsai, M.-H., Hua, C.-H., et al. (2017). Impact of CCL4 Gene Polymorphisms and Environmental Factors on Oral Cancer Development and Clinical Characteristics. *Oncotarget* 8, 31424–31434. doi:10.18632/oncotarget.15615

Lien, M. Y., Tsai, H. C., Chang, A. C., Tsai, M. H., Hua, C. H., Wang, S. W., et al. (2018). Chemokine CCL4 Induces Vascular Endothelial Growth Factor C Expression and Lymphangiogenesis by miR-195-3p in Oral Squamous Cell Carcinoma. *Front. Immunol.* 9, 412. doi:10.3389/fimmu.2018.00412

Lim, K. P., Chun, N. A., Ismail, S. M., Abraham, M. T., Yusoff, M. N., Zain, R. B., et al. (2014). CD4+CD25hiCD127low Regulatory T Cells Are Increased in Oral Squamous Cell Carcinoma Patients. *PloS one* 9, e103975. doi:10.1371/journal.pone.0103975

Liu, T.-Y., Chung, Y.-T., Wang, P.-F., Chi, C.-W., and Hsieh, L.-L. (2004). Safrole-DNA Adducts in Human Peripheral Blood-An Association with Areca Quid Chewing and CYP2E1 Polymorphisms. *Mutat. Research/Genetic Toxicol. Environ. Mutagenesis* 559, 59–66. doi:10.1016/j.mrgentox.2003.12.013

Liu, X., Zhang, Y., Cheng, C., Cheng, A. W., Zhang, X., Li, N., et al. (2017). CRISPR-Cas9-mediated Multiplex Gene Editing in CAR-T Cells. *Cell Res* 27, 154–157. doi:10.1038/cr.2016.142

Mahanonda, R., Sa-Ard-Iam, N., Eksomtramate, M., Rerkyen, P., Phairat, B., Schaecher, K. E., et al. (2009). Cigarette Smoke Extract Modulates Human β-defensin-2 and Interleukin-8 Expression in Human Gingival Epithelial Cells. *J. Periodontal Res.* 44, 557–564. doi:10.1111/j.1600-0765.2008.01153.x

Mayes, P. A., Hance, K. W., and Hoos, A. (2018). The Promise and Challenges of Immune Agonist Antibody Development in Cancer. *Nat. Rev. Drug Discov.* 17, 509–527. doi:10.1038/nrd.2018.75

Meuric, V., Le Gall-David, S., Boyer, E., Acuna-Amador, L., Martin, B., Fong, S. B., et al. (2017). Signature of Microbial Dysbiosis in Periodontitis. *Appl. Environ. Microbiol.* 83. doi:10.1128/aem.00462-17

Mio, T., Romberger, D. J., Thompson, A. B., Robbins, R. A., Heires, A., and Rennard, S. I. (1997). Cigarette Smoke Induces Interleukin-8 Release from Human Bronchial Epithelial Cells. *Am. J. Respir. Crit. Care Med.* 155, 1770–1776. doi:10.1164/ajrccm.155.5.9154890

Misra, C., Majumder, M., Bajaj, S., Ghosh, S., Roy, B., and Roychoudhury, S. (2009). Polymorphisms Atp53,p73, andMDM2loci Modulate the Risk of Tobacco Associated Leukoplakia and Oral Cancer. *Mol. Carcinog.* 48, 790–800. doi:10.1002/mc.20523

Mocellin, S., Marincola, F., Riccardo Rossi, C., Nitti, D., and Lise, M. (2004). The Multifaceted Relationship between IL-10 and Adaptive Immunity: Putting Together the Pieces of a Puzzle. *Cytokine Growth Factor. Rev.* 15, 61–76. doi:10.1016/j.cytogfr.2003.11.001

Monasterio, G., Fernández, B., Castillo, F., Rojas, C., Cafferata, E. A., Rojas, L., et al. (2019). Capsular-defectivePorphyromonas Gingivalismutant Strains Induce Less Alveolar Bone Resorption Than W50 Wild-type Strain Due to a Decreased Th1/Th17 Immune Response and Less Osteoclast Activity. *J. Periodontol.* 90, 522–534. doi:10.1002/jper.18-0079

Morgan, M. J., and Liu, Z.-g. (2011). Crosstalk of Reactive Oxygen Species and NF-Kb Signaling. *Cel Res* 21, 103–115. doi:10.1038/cr.2010.178

Mortaz, E., Lazar, Z., Koenderman, L., Kraneveld, A. D., Nijkamp, F. P., and Folkerts, G. (2009). Cigarette Smoke Attenuates the Production of Cytokines by Human Plasmacytoid Dendritic Cells and Enhances the Release of IL-8 in Response to TLR-9 Stimulation. *Respir. Res.* 10, 47. doi:10.1186/1465-9921-10-47

Mota, F., Rayment, N., Chong, S., Singer, A., and Chain, B. (1999). The Antigen-Presenting Environment in normal and Human Papillomavirus (HPV)-related Premalignant Cervical Epithelium. *Clin. Exp. Immunol.* 116, 33–40. doi:10.1046/j.1365-2249.1999.00826.x

Mroz, E. A., Patel, K. B., and Rocco, J. W. (2020). Intratumor Heterogeneity Could Inform the Use and Type of Postoperative Adjuvant Therapy in Patients with

Head and Neck Squamous Cell Carcinoma. *Cancer* 126, 1895–1904. doi:10.1002/cncr.32742

Murray, P. J., and Wynn, T. A. (2011). Protective and Pathogenic Functions of Macrophage Subsets. *Nat. Rev. Immunol.* 11, 723–737. doi:10.1038/nri3073

Nagarsheth, N., Wicha, M. S., and Zou, W. (2017). Chemokines in the Cancer Microenvironment and Their Relevance in Cancer Immunotherapy. *Nat. Rev. Immunol.* 17, 559–572. doi:10.1038/nri.2017.49

Ng, S. K. C., Kabat, G. C., and Wynder, E. L. (1993). Oral Cavity Cancer in Non-users of Tobacco. *JNCI J. Natl. Cancer Inst.* 85, 743–745. doi:10.1093/jnci/85.9.743

Niedbala, W., Wei, X.-q., Cai, B., Hueber, A. J., Leung, B. P., McInnes, I. B., et al. (2007). IL-35 Is a Novel Cytokine with Therapeutic Effects against Collagen-Induced Arthritis through the Expansion of Regulatory T Cells and Suppression of Th17 Cells. *Eur. J. Immunol.* 37, 3021–3029. doi:10.1002/eji.200737810

Nishimura, T., Iwakabe, K., Sekimoto, M., Ohmi, Y., Yahata, T., Nakui, M., et al. (1999). Distinct Role of Antigen-specific T Helper Type 1 (Th1) and Th2 Cells in Tumor Eradication *In Vivo*. *J. Exp. Med.* 190, 617–628. doi:10.1084/jem.190.5.617

Numasaki, M., Watanabe, M., Suzuki, T., Takahashi, H., Nakamura, A., McAllister, F., et al. (2005). IL-17 Enhances the Net Angiogenic Activity and *In Vivo* Growth of Human Non-small Cell Lung Cancer in SCID Mice through Promoting CXCR-2-dependent Angiogenesis. *J. Immunol.* 175, 6177–6189. doi:10.4049/jimmunol.175.9.6177

Nuorti, J. P., Butler, J. C., Farley, M. M., Harrison, L. H., McGeer, A., Kolczak, M. S., et al. (2000). Cigarette Smoking and Invasive Pneumococcal Disease. *N. Engl. J. Med.* 342, 681–689. doi:10.1056/nejm200003093421002

Okkenhaug, K. (2013). Signaling by the Phosphoinositide 3-Kinase Family in Immune Cells. *Annu. Rev. Immunol.* 31, 675–704. doi:10.1146/annurev-immunol-032712-095946

Okubo, M., Kioi, M., Nakashima, H., Sugiura, K., Mitsudo, K., Aoki, I., et al. (2016). M2-polarized Macrophages Contribute to Neovasculogenesis, Leading to Relapse of Oral Cancer Following Radiation. *Scientific Rep.* 6, 27548. doi:10.1038/srep27548

Padrao, E., Oliveira, O., Felgueiras, O., Gaio, A. R., and Duarte, R. (2018). Tuberculosis and Tobacco: Is There Any Epidemiological Association? *Eur. Respir. J.* 51, 1702121. doi:10.1183/13993003.02121-2017

Pan, H.-n., Sun, R., Jaruga, B., Hong, F., Kim, W.-H., and Gao, B. (2006). Chronic Ethanol Consumption Inhibits Hepatic Natural Killer Cell Activity and Accelerates Murine Cytomegalovirus-Induced Hepatitis. *Alcohol. Clin. Exp. Res.* 30, 1615–1623. doi:10.1111/j.1530-0277.2006.00194.x

Park, J., Wysocki, R. W., Amoozgar, Z., Maiorino, L., Fein, M. R., Jorns, J., et al. (2016). Cancer Cells Induce Metastasis-Supporting Neutrophil Extracellular DNA Traps. *Sci. translational Med.* 8, 361ra138. doi:10.1126/scitranslmed.aag1711

Parker, B. S., Rautela, J., and Hertzog, P. J. (2016). Antitumour Actions of Interferons: Implications for Cancer Therapy. *Nat. Rev. Cancer* 16, 131–144. doi:10.1038/nrc.2016.14

Pérez-Sayáns, M., Somoza-Martín, J. M., Barros-Angueira, F., Reboiras-López, M. D., Gándara Rey, J. M., and García-García, A. (2009). Genetic and Molecular Alterations Associated with Oral Squamous Cell Cancer (Review). *Oncol. Rep.* 22, 1277–1282. doi:10.3892/or_00000565

Phillips, D. H. (2002). Smoking-related DNA and Protein Adducts in Human Tissues. *Carcinogenesis* 23, 1979–2004. doi:10.1093/carcin/23.12.1979

Piersma, S. J. (2011). Immunosuppressive Tumor Microenvironment in Cervical Cancer Patients. *Cancer Microenvironment* 4, 361–375. doi:10.1007/s12307-011-0066-7

Qin, Z., and Blankenstein, T. (2000). CD4 + T Cell-Mediated Tumor Rejection Involves Inhibition of Angiogenesis that Is Dependent on IFNγ Receptor Expression by Nonhematopoietic Cells. *Immunity* 12, 677–686. doi:10.1016/s1074-7613(00)80218-6

Quan, H., Shan, Z., Liu, Z., Liu, S., Yang, L., Fang, X., et al. (2020). The Repertoire of Tumor-Infiltrating Lymphocytes within the Microenvironment of Oral Squamous Cell Carcinoma Reveals Immune Dysfunction. *Cancer Immunol. Immunother.* 69, 465–476. doi:10.1007/s00262-020-02479-x

Rahman, S., Kraljevic Pavelic, S., and Markova-Car, E. (2019). Circadian (De) regulation in Head and Neck Squamous Cell Carcinoma. *Int. J. Mol. Sci.* 20. doi:10.3390/ijms20112662

Razavi, S. M., Tahani, B., Nouri, S., and Khazaei, A. (2015). Oral Cancer Knowledge and Practice Among Dental Patients and Their Attitude towards Tobacco Cessation in Iran. *Asian Pac. J. Cancer Prev.* 16, 5439–5444. doi:10.7314/apjcp.2015.16.13.5439

Rehman, S., Chandel, N., Salhan, D., Rai, P., Sharma, B., Singh, T., et al. (2013). Ethanol and Vitamin D Receptor in T Cell Apoptosis. *J. Neuroimmune Pharmacol.* 8, 251–261. doi:10.1007/s11481-012-9393-9

Remani, P., Ankathil, R., Vijayan, K. K., Haseena Beevi, V. M., Rajendran, R., and Vijayakumar, T. (1988). Circulating Immune Complexes as an Immunological Marker in Premalignant and Malignant Lesions of the Oral Cavity. *Cancer Lett.* 40, 185–191. doi:10.1016/0304-3835(88)90009-2

Romero, D. (2016). Immunotherapy: PD-1 Says Goodbye, TIM-3 Says Hello, Nature Reviews. *Clin. Oncol.* 13, 202–203. doi:10.1038/nrclinonc.2016.40

Rowshanravan, B., Halliday, N., and Sansom, D. M. (2018). CTLA-4: a Moving Target in Immunotherapy. *Blood* 131, 58–67. doi:10.1182/blood-2017-06-741033

Sahibzada, H. A., Khurshid, Z., Khan, R. S., Naseem, M., Siddique, K. M., Mali, M., et al. (2017). Salivary IL-8, IL-6 and TNF-α as Potential Diagnostic Biomarkers for Oral Cancer. *Diagnostics (Basel)* 7, 21. doi:10.3390/diagnostics7020021

Sakaguchi, S. (2004). NaturallyArisingCD4+RegulatoryT Cells forImmunologicSelf-Tolerance andNegativeControl ofImmuneResponses. *Annu. Rev. Immunol.* 22, 531–562. doi:10.1146/annurev.immunol.21.120601.141122

Sankaranarayanan, R., Mathew, B., Varghese, C., Sudhakaran, P., Menon, V., Jayadeep, A., et al. (1997). Chemoprevention of Oral Leukoplakia with Vitamin A and Beta Carotene: an Assessment. *Oral Oncol.* 33, 231–236. doi:10.1016/s0964-1955(97)00010-9

Sato-Kaneko, F., Yao, S., Ahmadi, A., Zhang, S. S., Hosoya, T., Kaneda, M. M., et al. (2017). Combination Immunotherapy with TLR Agonists and Checkpoint Inhibitors Suppresses Head and Neck Cancer. *JCI Insight* 2. doi:10.1172/jci.insight.93397

Schubert, A. D., Channah Broner, E., Agrawal, N., London, N., Pearson, A., Gupta, A., et al. (2020). Somatic Mitochondrial Mutation Discovery Using Ultra-deep Sequencing of the Mitochondrial Genome Reveals Spatial Tumor Heterogeneity in Head and Neck Squamous Cell Carcinoma. *Cancer Lett.* 471, 49–60. doi:10.1016/j.canlet.2019.12.006

Schwarz, S., Butz, M., Morsczeck, C., Reichert, T. E., and Driemel, O. (2008). Increased Number of CD25+ FoxP3+ Regulatory T Cells in Oral Squamous Cell Carcinomas Detected by Chromogenic Immunohistochemical Double Staining. *official Publ. Int. Assoc. Oral Pathol. Am. Acad. Oral Pathol.* 37, 485–489. doi:10.1111/j.1600-0714.2008.00641.x

Selvan, R. S., Selvakumaran, M., and Rao, A. R. (1991). Influence of Arecoline on Immune System: II. Suppression of Thymus-dependent Immune Responses and Parameter of Non-specific Resistance after Short-Term Exposure. *Immunopharmacology and Immunotoxicology* 13, 281–309. doi:10.3109/08923979109019706

Sethi, G., Sung, B., and Aggarwal, B. B. (2008). TNF: A Master Switch for Inflammation to Cancer. *Front. Biosci.* Volume, 5094–5107. doi:10.2741/3066

Shang, B., Liu, Y., Jiang, S. J., and Liu, Y. (2015). Prognostic Value of Tumor-Infiltrating FoxP3+ Regulatory T Cells in Cancers: a Systematic Review and Meta-Analysis. *Scientific Rep.* 5, 15179. doi:10.1038/srep15179

Shimizu, S., Hiratsuka, H., Koike, K., Tsuchihashi, K., Sonoda, T., Ogi, K., et al. (2019). Tumor-infiltrating CD8+ T-Cell Density Is an Independent Prognostic Marker for Oral Squamous Cell Carcinoma. *Cancer Med.* 8, 80–93. doi:10.1002/cam4.1889

Shojaei, F., Wu, X., Qu, X., Kowanetz, M., Yu, L., Tan, M., et al. (2009). G-CSF-initiated Myeloid Cell Mobilization and Angiogenesis Mediate Tumor Refractoriness to Anti-VEGF Therapy in Mouse Models. *Proc. Natl. Acad. Sci.* 106, 6742–6747. doi:10.1073/pnas.0902280106

Singh, P. K., Kumar, V., Ahmad, M. K., Gupta, R., Mahdi, A. A., Jain, A., et al. (2017). Association of -330 Interleukin-2 Gene Polymorphism with Oral Cancer. *Indian J. Med. Res.* 146, 730–737. doi:10.4103/ijmr.IJMR_1949_15

Smigiel, K. S., Srivastava, S., Stolley, J. M., and Campbell, D. J. (2014). Regulatory T-Cell Homeostasis: Steady-State Maintenance and Modulation during Inflammation. *Immunol. Rev.* 259, 40–59. doi:10.1111/imr.12170

Solomon, B. L., and Garrido-Laguna, I. (2018). TIGIT: a Novel Immunotherapy Target Moving from Bench to Bedside. *Cancer Immunol. Immunother.* 67, 1659–1667. doi:10.1007/s00262-018-2246-5

Solomon, B., Young, R. J., and Rischin, D. (2018). Head and Neck Squamous Cell Carcinoma: Genomics and Emerging Biomarkers for Immunomodulatory

Cancer Treatments. *Semin. Cancer Biol.* 52, 228–240. doi:10.1016/j.semcancer.2018.01.008

Spitzer, J. H., and Meadows, G. G. (1999). Modulation of Perforin, Granzyme A, and Granzyme B in Murine Natural Killer (NK), IL2 Stimulated NK, and Lymphokine-Activated Killer Cells by Alcohol Consumption. *Cell Immunol.* 194, 205–212. doi:10.1006/cimm.1999.1511

Spolski, R., Li, P., and Leonard, W. J. (2018). Biology and Regulation of IL-2: from Molecular Mechanisms to Human Therapy. *Nat. Rev. Immunol.* 18, 648–659. doi:10.1038/s41577-018-0046-y

Stasikowska-Kanicka, O., Wągrowska-Danilewicz, M., and Danilewicz, M. (2018). CD8+ and CD163+ Infiltrating Cells and PD-L1 Immunoexpression in Oral Leukoplakia and Oral Carcinoma. *Apmis* 126, 732–738. doi:10.1111/apm.12881

Stasikowska-Kanicka, O., Wągrowska-Danilewicz, M., and Danilewicz, M. (2018). Immunohistochemical Analysis of Foxp3+, CD4+, CD8+ Cell Infiltrates and PD-L1 in Oral Squamous Cell Carcinoma. *Pathol. Oncol. Res.* 24, 497–505. doi:10.1007/s12253-017-0270-y

Støy, S., Dige, A., Sandahl, T. D., Laursen, T. L., Buus, C., Hokland, M., et al. (2015). Cytotoxic T Lymphocytes and Natural Killer Cells Display Impaired Cytotoxic Functions and Reduced Activation in Patients with Alcoholic Hepatitis. *Am. J. Physiol. Gastrointest. Liver Physiol.* 308, G269–G276. doi:10.1152/ajpgi.00200.2014

Strachan, D. C., Ruffell, B., Oei, Y., Bissell, M. J., Coussens, L. M., Pryer, N., et al. (2013). CSF1R Inhibition Delays Cervical and Mammary Tumor Growth in Murine Models by Attenuating the Turnover of Tumor-Associated Macrophages and Enhancing Infiltration by CD8(+) T Cells. *Oncoimmunology* 2, e26968. doi:10.4161/onci.26968

Su, L., Xu, Q., Zhang, P., Michalek, S. M., and Katz, J. (2017). Phenotype and Function of Myeloid-Derived Suppressor Cells Induced by Porphyromonas Gingivalis Infection. *Infect. Immun.* 85, e00213–17. doi:10.1128/iai.00213-17

Suwa, T., Saio, M., Umemura, N., Yamashita, T., Toida, M., Shibata, T., et al. (2006). Preoperative Radiotherapy Contributes to Induction of Proliferative Activity of CD8+ Tumor-Infiltrating T-Cells in Oral Squamous Cell Carcinoma. *Oncol. Rep.* 15, 757–763. doi:10.3892/or.15.4.757

Tang, M., Diao, J., and Cattral, M. S. (2017). Molecular Mechanisms Involved in Dendritic Cell Dysfunction in Cancer. *Cell. Mol. Life Sci.* 74, 761–776. doi:10.1007/s00018-016-2317-8

Tatsumi, T., Kierstead, L. S., Ranieri, E., Gesualdo, L., Schena, F. P., Finke, J. H., et al. (2002). Disease-associated Bias in T Helper Type 1 (Th1)/Th2 CD4+ T Cell Responses against MAGE-6 in HLA-Drb1*0401+ Patients with Renal Cell Carcinoma or Melanoma. *J. Exp. Med.* 196, 619–628. doi:10.1084/jem.20012142

Tepper, R. I., Pattengale, P. K., and Leder, P. (1989). Murine Interleukin-4 Displays Potent Anti-tumor Activity *In Vivo*. *Cell* 57, 503–512. doi:10.1016/0092-8674(89)90925-2

Tosolini, M., Kirilovsky, A., Mlecnik, B., Fredriksen, T., Mauger, S., Bindea, G., et al. (2011). Clinical Impact of Different Classes of Infiltrating T Cytotoxic and Helper Cells (Th1, Th2, Treg, Th17) in Patients with Colorectal Cancer. *Cancer Res.* 71, 1263–1271. doi:10.1158/0008-5472.can-10-2907

Trinchieri, G. (2003). Interleukin-12 and the Regulation of Innate Resistance and Adaptive Immunity. *Nat. Rev. Immunol.* 3, 133–146. doi:10.1038/nri1001

Tsukamoto, H., Fujieda, K., Miyashita, A., Fukushima, S., Ikeda, T., Kubo, Y., et al. (2018). Combined Blockade of IL6 and PD-1/pd-L1 Signaling Abrogates Mutual Regulation of Their Immunosuppressive Effects in the Tumor Microenvironment. *Cancer Res.* 78, 5011–5022. doi:10.1158/0008-5472.can-18-0118

Tsunoda, K., Tsujino, I., Koshi, R., Sugano, N., Sato, S., and Asano, M. (2016). Nicotine-Mediated Ca 2+ -Influx Induces IL-8 Secretion in Oral Squamous Cell Carcinoma Cell. *J. Cel. Biochem.* 117, 1009–1015. doi:10.1002/jcb.25387

Türkseven, M. R., and Oygür, T. (2010). Evaluation of Natural Killer Cell Defense in Oral Squamous Cell Carcinoma. *Oral Oncol.* 46, e34–e37. doi:10.1016/j.oraloncology.2010.02.019

Utispan, K., Pugdee, K., and Koontongkaew, S. (2018). Porphyromonas Gingivalis Lipopolysaccharide-Induced Macrophages Modulate Proliferation and Invasion of Head and Neck Cancer Cell Lines. *Biomed. Pharmacother.* 101, 988–995. doi:10.1016/j.biopha.2018.03.033

van Schalkwyk, M. C. I., Papa, S. E., Jeannon, J.-P., Urbano, T. G., Spicer, J. F., and Maher, J. (2013). Design of a Phase I Clinical Trial to Evaluate Intratumoral Delivery of ErbB-Targeted Chimeric Antigen Receptor T-Cells in Locally Advanced or Recurrent Head and Neck Cancer. *Hum. Gene Ther. Clin. Develop.* 24, 134–142. doi:10.1089/humc.2013.144

Vassallo, R., Kroening, P. R., Parambil, J., and Kita, H. (2008). Nicotine and Oxidative Cigarette Smoke Constituents Induce Immune-Modulatory and Pro-inflammatory Dendritic Cell Responses. *Mol. Immunol.* 45, 3321–3329. doi:10.1016/j.molimm.2008.04.014

Vassallo, R., Tamada, K., Lau, J. S., Kroening, P. R., and Chen, L. (2005). Cigarette Smoke Extract Suppresses Human Dendritic Cell Function Leading to Preferential Induction of Th-2 Priming. *J. Immunol.* 175, 2684–2691. doi:10.4049/jimmunol.175.4.2684

Vassallo, R., Tamada, K., Lau, J. S., Kroening, P. R., and Chen, L. (2005). Cigarette Smoke Extract Suppresses Human Dendritic Cell Function Leading to Preferential Induction of Th-2 Priming. *J. Immunol.* 175, 2684–2691. doi:10.4049/jimmunol.175.4.2684

Verma, A., Vincent-Chong, V. K., DeJong, H., Hershberger, P. A., and Seshadri, M. (2020). Impact of Dietary Vitamin D on Initiation and Progression of Oral Cancer. *J. Steroid Biochem. Mol. Biol.* 199, 105603. doi:10.1016/j.jsbmb.2020.105603

Vonderheide, R. H. (2020). CD40 Agonist Antibodies in Cancer Immunotherapy. *Annu. Rev. Med.* 71, 47–58. doi:10.1146/annurev-med-062518-045435

Wang, C.-C., Chen, T.-Y., Wu, H.-Y., Liu, T.-Y., and Jan, T.-R. (2012). Areca Nut Extracts Suppress the Differentiation and Functionality of Human Monocyte-Derived Dendritic Cells. *J. Periodont Res.* 47, 198–203. doi:10.1111/j.1600-0765.2011.01421.x

Wang, C. C., Liu, T. Y., Wey, S. P., Wang, F. I., and Jan, T. R. (2007). Areca Nut Extract Suppresses T-Cell Activation and Interferon-γ Production via the Induction of Oxidative Stress. *Food Chem. Toxicol.* 45, 1410–1418. doi:10.1016/j.fct.2007.02.005

Wang, C., Ye, Y., Hochu, G. M., Sadeghifar, H., and Gu, Z. (2016). Enhanced Cancer Immunotherapy by Microneedle Patch-Assisted Delivery of Anti-PD1 Antibody. *Nano Lett.* 16, 2334–2340. doi:10.1021/acs.nanolett.5b05030

Wang, H., Liang, X., Li, M., Tao, X., Tai, S., Fan, Z., et al. (2017). Chemokine (CCmotif) Ligand 18 Upregulates Slug Expression to Promote Stem-cell like Features by Activating the Mammalian Target of Rapamycin Pathway in Oral Squamous Cell Carcinoma. *Cancer Sci.* 108, 1584–1593. doi:10.1111/cas.13289

Wang, Z., and Cao, Y. J. (2020). Adoptive Cell Therapy Targeting Neoantigens: A Frontier for Cancer Research,. *Front. Immunol.* 11, 176. doi:10.3389/fimmu.2020.00176

Wang, Z., Wu, V. H., Allevato, M. M., Gilardi, M., He, Y., Luis Callejas-Valera, J., et al. (2019). Syngeneic Animal Models of Tobacco-Associated Oral Cancer Reveal the Activity of *In Situ* Anti-CTLA-4. *Nat. Commun.* 10, 5546. doi:10.1038/s41467-019-13471-0

Weng, C.-J., Chien, M.-H., Lin, C.-W., Chung, T.-T., Zavras, A.-I., Tsai, C.-M., et al. (2010). Effect of CC Chemokine Ligand 5 and CC Chemokine Receptor 5 Genes Polymorphisms on the Risk and Clinicopathological Development of Oral Cancer. *Oral Oncol.* 46, 767–772. doi:10.1016/j.oraloncology.2010.07.011

Wu, J., Peters, B. A., Dominianni, C., Zhang, Y., Pei, Z., Yang, L., et al. (2016). Cigarette Smoking and the Oral Microbiome in a Large Study of American Adults. *Isme J.* 10, 2435–2446. doi:10.1038/ismej.2016.37

Wu, W.-S. (2006). The Signaling Mechanism of ROS in Tumor Progression. *Cancer Metastasis Rev.* 25, 695–705. doi:10.1007/s10555-006-9037-8

Wu, W. J., Wolcott, R. M., and Pruett, S. B. (1994). Ethanol Decreases the Number and Activity of Splenic Natural Killer Cells in a Mouse Model for Binge Drinking. *J. Pharmacol. Exp. Ther.* 271, 722–729.

Wustrow, T. P., and Mahnke, C. G. (1996). Causes of Immunosuppression in Squamous Cell Carcinoma of the Head and Neck. *Anticancer Res.* 16, 2433–2468.

Xia, L., Liu, Y., and Wang, Y. (2019). PD-1/PD-L1 Blockade Therapy in Advanced Non-Small-Cell Lung Cancer: Current Status and Future Directions. *Oncol.* 24, S31–s41. doi:10.1634/theoncologist.2019-io-s1-s05

Xiao, M., Zhang, J., Chen, W., and Chen, W. (2018). M1-like Tumor-Associated Macrophages Activated by Exosome-Transferred THBS1 Promote Malignant Migration in Oral Squamous Cell Carcinoma, Journal of Experimental & Clinical Cancer Research. *CR* 37, 143. doi:10.1186/s13046-018-0815-2

Xie, C., Ji, N., Tang, Z., Li, J., and Chen, Q. (2019). The Role of Extracellular Vesicles from Different Origin in the Microenvironment of Head and Neck Cancers,. *Mol. Cancer* 18, 83. doi:10.1186/s12943-019-0985-3

Yakin, M., Gavidi, R. O., Cox, B., and Rich, A. (2017). Oral Cancer Risk Factors in New Zealand. *N. Z. Med. J.* 130, 30–38.

Yang, J. A., Huber, S. A., and Lucas, Z. J. (1979). Inhibition of DNA Synthesis in Cultured Lymphocytes and Tumor Cells by Extracts of Betel Nut, Tobacco, and Miang Leaf, Plant Substances Associated with Cancer of the Ororespiratory Epithelium. *Cancer Res.* 39, 4802–4809.

Yeku, O., Li, X., and Brentjens, R. J. (2017). Adoptive T-Cell Therapy for Solid Tumors. *Am. Soc. Clin. Oncol. Educ. Book* 37, 193–204. doi:10.1200/edbk_180328

Yi, H.-S., Lee, Y.-S., Byun, J.-S., Seo, W., Jeong, J.-M., Park, O., et al. (2014). Alcohol Dehydrogenase III Exacerbates Liver Fibrosis by Enhancing Stellate Cell Activation and Suppressing Natural Killer Cells in Mice. *Hepatology* 60, 1044–1053. doi:10.1002/hep.27137

Yu, G., Phillips, S., Gail, M. H., Goedert, J. J., Humphrys, M. S., Ravel, J., et al. (2017). The Effect of Cigarette Smoking on the Oral and Nasal Microbiota,. *Microbiome* 5, 3. doi:10.1186/s40168-016-0226-6

Zhang, F., Little, A., and Zhang, H. (2017). Chronic Alcohol Consumption Inhibits Peripheral NK Cell Development and Maturation by Decreasing the Availability of IL-15. *J. Leukoc. Biol.* 101, 1015–1027. doi:10.1189/jlb.1a0716-298rr

Zhang, H., and Meadows, G. G. (2010). Chronic Alcohol Consumption Enhances Myeloid-Derived Suppressor Cells in B16BL6 Melanoma-Bearing Mice. *Cancer Immunol. Immunother.* 59, 1151–1159. doi:10.1007/s00262-010-0837-x

Zhang, H., and Meadows, G. G. (2008). Chronic Alcohol Consumption Perturbs the Balance between Thymus-Derived and Bone Marrow-Derived Natural Killer Cells in the Spleen. *J. Leukoc. Biol.* 83, 41–47. doi:10.1189/jlb.0707472

Zhang, H., and Meadows, G. G. (2009). Exogenous IL-15 in Combination with IL-15Rα Rescues Natural Killer Cells from Apoptosis Induced by Chronic Alcohol Consumption. *Clin. Exp. Res.* 33, 419–427. doi:10.1111/j.1530-0277.2008.00852.x

Zhang, H., Zhu, Z., and Meadows, G. G. (2011). Chronic Alcohol Consumption Decreases the Percentage and Number of NK Cells in the Peripheral Lymph Nodes and Exacerbates B16BL6 Melanoma Metastasis into the Draining Lymph Nodes. *Cell Immunol.* 266, 172–179. doi:10.1016/j.cellimm.2010.10.001

Zhang, Q., Bi, J., Zheng, X., Chen, Y., Wang, H., Wu, W., et al. (2018). Blockade of the Checkpoint Receptor TIGIT Prevents NK Cell Exhaustion and Elicits Potent Anti-tumor Immunity. *Nat. Immunol.* 19, 723–732. doi:10.1038/s41590-018-0132-0

Zhang, Q., Qin, J., Zhong, L., Gong, L., Zhang, B., Zhang, Y., et al. (2015). CCL5-Mediated Th2 Immune Polarization Promotes Metastasis in Luminal Breast Cancer. *Cancer Res.* 75, 4312–4321. doi:10.1158/0008-5472.can-14-3590

Zhao, J., Chen, X., Herjan, T., and Li, X. (2020). The Role of Interleukin-17 in Tumor Development and Progression,. *J. Exp. Med.* 217. doi:10.1084/jem.20190297

Zhou, J., and Meadows, G. G. (2003). Alcohol Consumption Decreases IL-2-Induced NF-kappaB Activity in Enriched NK Cells from C57BL/6 Mice. *official J. Soc. Toxicol.* 73, 72–79. doi:10.1093/toxsci/kfg047

Zhu, C., Kros, J. M., Cheng, C., and Mustafa, D. (2017). The Contribution of Tumor-Associated Macrophages in Glioma Neo-Angiogenesis and Implications for Anti-angiogenic Strategies. *Neuro-oncology* 19, 1435–1446. doi:10.1093/neuonc/nox081

Zou, J.-M., Qin, J., Li, Y.-C., Wang, Y., Li, D., Shu, Y., et al. (2017). IL-35 Induces N2 Phenotype of Neutrophils to Promote Tumor Growth. *Oncotarget* 8, 33501–33514. doi:10.18632/oncotarget.16819

Conflict of Interest: The authors declare that the research was conducted in the absence of any commercial or financial relationships that could be construed as a potential conflict of interest.

Publisher's Note: All claims expressed in this article are solely those of the authors and do not necessarily represent those of their affiliated organizations, or those of the publisher, the editors, and the reviewers. Any product that may be evaluated in this article, or claim that may be made by its manufacturer, is not guaranteed or endorsed by the publisher.

frontiers in Molecular Biosciences

ORIGINAL RESEARCH
published: 11 October 2021
doi: 10.3389/fmolb.2021.759495

Tumor Microenvironment Characterization in Breast Cancer Identifies Prognostic and Neoadjuvant Chemotherapy Relevant Signatures

*Fei Ji[1†], Jiao-Mei Yuan[2†], Hong-Fei Gao[1†], Ai-Qi Xu[2†], Zheng Yang[3], Ci-Qiu Yang[1], Liu-Lu Zhang[1], Mei Yang[1], Jie-Qing Li[1], Teng Zhu[1], Min-Yi Cheng[1], Si-Yan Wu[4] and Kun Wang[1]**

[1]Department of Breast Cancer, Cancer Center, Guangdong Provincial People's Hospital, Guangdong Academy of Medical Sciences, Guangzhou, China, [2]School of Medicine, South China University of Technology, Guangzhou University Town, Guangzhou, China, [3]Department of Pathology, Guangdong Provincial People's Hospital, Guangdong Academy of Medical Sciences, Guangzhou, China, [4]Department of Operation Room, Guangdong Provincial People's Hospital, Guangdong Academy of Medical Sciences, Guangzhou, China*

Immune response which involves distinct immune cells is associated with prognosis of breast cancer. Nonetheless, less study have determined the associations of different types of immune cells with patient survival and treatment response. In this study, A total of 1,502 estrogen receptor(ER)-negative breast cancers from public databases were used to infer the proportions of 22 subsets of immune cells. Another 320 ER-negative breast cancer patients from Guangdong Provincial People's Hospital were also included and divided into the testing and validation cohorts. $CD8^+$ T cells, $CD4^+$ T cells, B cells, and M1 macrophages were associated with favourable outcome (all p <0.01), whereas Treg cells were strongly associated with poor outcome (p = 0.005). Using the LASSO model, we classified patients into the stromal immunotype A and B subgroups according to immunoscores. The 10 years OS and DFS rates were significantly higher in the immunotype A subgroup than immunotype B subgroup. Stromal immunotype was identified as an independent prognostic indicator in multivariate analysis in all cohorts and was also related to pathological complete response(pCR) after neoadjuvant chemotherapy. The nomogram that integrated the immunotype and clinicopathologic features showed good predictive accuracy for pCR and discriminatory power. The stromal immunotype A subgroup had higher expression levels of immune checkpoint molecules (PD-L1, PD-1, and CTLA-4) and cytokines (IL-2, INF-γ, and TGF-β). In addition, patients with immunotype A and B diseases had distinct mutation signatures. Therefore, The stromal immunotypes could predict survival and responses of ER-negative breast cancer patients to neoadjuvant chemotherapy.

Keywords: breast cancer, stromal immunotype, prognosis, biomarker, neoadjuvant chemotherapy

OPEN ACCESS

Edited by:
Yu Guo,
The First Affiliated Hospital of Sun Yat-sen University, China

Reviewed by:
Ke-Da Yu,
Fudan University, China
Yingying Xu,
The First Affiliated Hospital of China Medical University, China

****Correspondence:***
Kun Wang
gzwangkun@126.com

[†]These authors have contributed equally to this work

Specialty section:
This article was submitted to Molecular Diagnostics and Therapeutics, a section of the journal Frontiers in Molecular Biosciences

Received: *16 August 2021*
Accepted: *20 September 2021*
Published: *11 October 2021*

Citation:
Ji F, Yuan J-M, Gao H-F, Xu A-Q, Yang Z, Yang C-Q, Zhang L-L, Yang M, Li J-Q, Zhu T, Cheng M-Y, Wu S-Y and Wang K (2021) Tumor Microenvironment Characterization in Breast Cancer Identifies Prognostic and Neoadjuvant Chemotherapy Relevant Signatures. Front. Mol. Biosci. 8:759495. doi: 10.3389/fmolb.2021.759495

INTRODUCTION

Breast cancer is the most common cancer in women and a leading cancer worldwide. Genomic changes in cancer cells may be used to predict prognosis and treatment responses as well as to develop new targeted therapy (Cancer Genome Altas Network, 2012; Curtis et al., 2012; Ali et al., 2014; Ji et al., 2019). Recently, it has been reported that the tumor microenvironment also played an important role in tumor progression and chemotherapy efficacy. breast cancer is composed of a mixtures of cancer cells and non-cancer cells such as stromal cells, vascular cells, and tumor-infiltrating lymphocytes (TILs), with the roles of non-cancer cells remain unclear. Among the non-cancer cells, TIL values have been reported to be associated with pathologically complete response (pCR) and prolonged overall survival (OS) in patients with breast cancer (Ladoire et al., 2008; Kitano et al., 2017; Luen et al., 2017), it also could be used as a drug target, but the roles of specific immune cells have not been well clarified. To better understand the diverse immune cells of breast cancer to the response of treatment and construct the classification of stromal immunotype for survival prediction, we enumerate immune cells in a way that accounts for the breadth of their specialized functions, and to reliably investigate the interaction of the immune response with breast cancer, and finally find the effective parameters to support the personalized therapy.

Therefore, the aim of this study was to quantify the composition of immune cells and investigate their relationships with responses to neoadjuvant chemotherapy and survival of breast cancer patients.

PATIENTS AND METHODS

Study Population

The present study was approved by the Ethics Committee of the Guangdong Provincial People's Hospital. Three independent cohorts of patients with breast cancer were included. The training cohort was comprised of 1,502 estrogen receptor(ER)-negative breast cancer patients with gene expression data from the public studies, details of patients from public studies can be found in corresponding publications(**Supplementary Table S1**), some data were compiled and created as previously described (Haibe-Kains et al., 2012; Ali et al., 2016). some data were downloaded from Gene Expression Omnibus and ArrayExpress(TCGA and METABRIC). After excluding patients with comorbidities (e.g., other malignant tumors), incomplete follow-up data, and metastatic disease, 320 patients with pathologically diagnosed ER-negative breast cancer using needle core biopsy at the Guangdong Provincial People's Hospital between June 2009 and December 2015 were selected and randomly divided into the testing cohort (n = 218) and the validation cohort (n = 102) by using computer-generated random numbers. pCR was defined as the absence of any residual invasive carcinoma or DCIS on pathologic review of a surgical specimen following neoadjuvant chemotherapy. The study design is shown in Supplementary Figure S1. Informed consent was signed by each patient to allow the use of their data in clinical researches.

Immunoscore Establishment

Normalized gene expression data were used to infer the relative proportions of 22 types of infiltrating immune cells using the CIBERSORT algorithm. For the TCGA dataset, RNA sequencing data were transformed using voom, converting count data to values more similar to those resulting from microarrays (Cancer Genome Altas Network, 2012; Law et al., 2014). The CIBERSORT is a well-designed method for the analysis of microarray gene expression profiles (Ali et al., 2016; Li et al., 2019). The LM22 file covers 547 genes that can be used to accurately discriminate 22 distinct functional subsets of immune cells and activation states including seven T cell types, naive and memory B cells, plasma cells, NK cells, and myeloid subsets. So in our study, we used the CIBERSORT and the LM22 gene signature file to estimate the fractions of diverse immune cells in the patients. The associations of immune cells with the OS and disease-free survival (DFS) of patients in the training cohort were analyzed using the estimated fractions by univariate analysis. The COX regression analysis with the least absolute shrinkage and selection operator (LASSO) model was used to develop an immunoscore for the classification of immunotypes A and B breast cancer (**Figures 1A–C**).

Immunohistochemistry and Evaluation of Immunostaining

The identified survival-associated immune cells were stained with different antibodies in the testing and validation cohorts. IHC was performed as described in our previous studies (Ji et al., 2015; Ji et al., 2018). The following markers were used: CD4 (for $CD4^+$ T cells, ab133616, Abcam, MA, United States), CD8 (for $CD8^+$ T cells, ab93278, Abcam, MA, United States), CD20 (for B cells, ab78237, Abcam, MA, United States), CD80 (for M1 macrophages, ab134120, Abcam, MA, United States), and FOXP3 (for regulatory T cells, ab215206, Abcam, MA, United States). The following antibodies were used for staining: interleukin-2(IL-2,ab92381,Abcam, MA, United States), interferon-gamma (INF-γ, ab231036,Abcam, MA, United States), transforming growth factor-β2(TGF-β2, ab53778, Abcam, MA, United States), programmed cell death 1 ligand 1, (PD-L1,ab228415, Abcam, MA, United States), programmed cell death-1(PD-1, ab234444, Abcam, MA, United States), cytotoxic T lymphocyte-associated antigen-4(CTLA-4,ab228229,Abcam, MA, United States). The sections were incubated with pre-diluted primary polyclonal antibodies at 4°C overnight. The sections stained without primary antibodies were used as negative controls. The stained immune cells in three random areas of stroma and tumor core at ×200 magnification were counted. Two pathologists blinded to the clinicopathological data scored all samples independently, and the mean count was adopted.

Statistical Analysis

The coefficients and partial likelihood deviance for each prognostic feature were calculated with the "glmnet" package in the R program. The LASSO Cox regression model was used to estimate the ideal coefficient and likelihood deviance. Restricted cubic spline regression was used to characterize the relationship between immune score and patient survival in all three cohorts. Besides, The nomogram integrating immune type and clinical parameters was constructed according to results of the

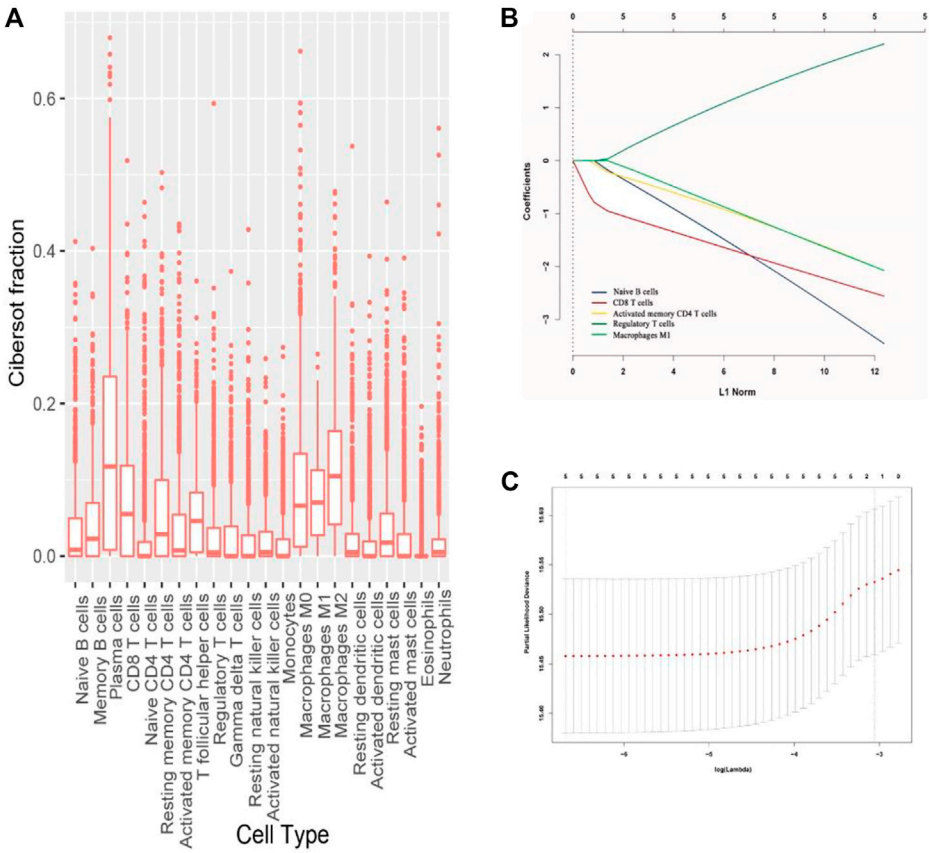

FIGURE 1 | (A) Fraction data of the 22 types of immune cells. **(B)** LASSO coefficient profiles of the five selected stromal features for overall survival. **(C)** Partial likelihood deviance of the LASSO coefficient profiles for overall survival.

multivariate logistic regression models. Based on the identified prognostic factors, the nomogram could be utilized to predict pCR after neoadjuvant chemotherapy. The discriminative capabilities of the nomogram was assessed by the area under the receiver operating characteristic curve (ROC). The differentially enriched pathways between stromal immunotypes A and B breast cancer were identified using the Gene Set Enrichment Analysis. Statistical analyses were performed using the MedCalc software (version 18; MedCalc, Mariakerke, Belgium), Stata (vension 14; StataCorp, College Station, TX), and R software packages (version 3.4.2; The R foundation for Statistical Computing, http://www.-rproject.org/).

RESULTS

Stromal Immunoscore and Stromal Immunotype

The fractions of the 22 types of immune cells are showed in **Figure 1**. Among them, five types ($CD8^+$ T cells, $CD4^+$ T cells, B cells, M1 macrophages, and Treg cells) were significantly associated with OS and DFS (**Supplementary Figure S2**), so we chose these five types as research cells. In the testing and validation cohorts, the mean densities of B cells, $CD8^+$ T cells, $CD4^+$ T cells, Treg cells, and M1 macrophages in the stroma were higher than the densities in tumor core (38.320, 77.234, 45.291, 26.291, and 71.248 cells/mm^2 Vs 9.580, 25.745, 10.065,6.5728, and 24.568 cells/mm^2, respectively). (**Figure 2**). The immune cell infiltration in the stroma was significantly associated with the OS of ER-negative breast cancer (**Supplementary Table S2**). The representative images of these immune cells are shown in **Figure 2**. We built prognostic classifiers by using the LASSO COX model in the training cohort (**Supplementary Table S1**; **Figure 1**) and calculated the coefficients using the following formulas: IS = 2.202 × Treg cell count—3.455 × B cell count—2.559 × $CD8^+$ T cell count—2.077 × $CD4^+$ T cell count—2.074 × M1 macrophage count. Therefore, We classified patients into immunotype A and immunotype B groups based on the median immunoscore. Clinical characteristics of patients with breast cancer of stromal immunotypes A and B in the training cohort and the testing and validation cohorts did not vary significantly (**Table 1**).

Association of Stromal Immunotype With Patient Survival

As shown in **Figure 3**, tumors with high immunoscore generally contained increased Treg cells and reduced B cells, $CD8^+$ T cells,

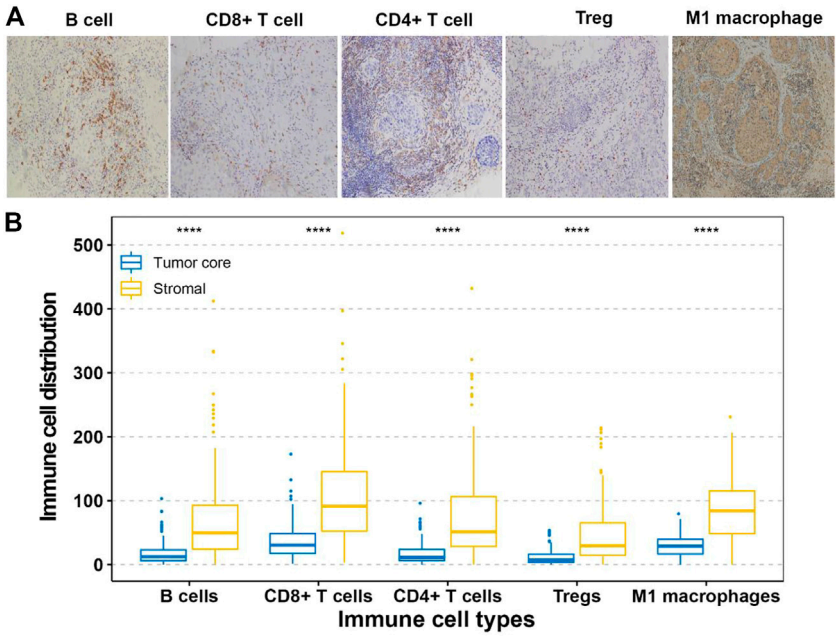

FIGURE 2 | (A) Tumor infiltration of B cells, CD8$^+$ T cells, CD4$^+$ T cells, Treg cells and M1 macrophage cells in breast cancer patients. **(B)** Tumor infiltration density of B cells, CD8$^+$ T cells, CD4$^+$ T cells, Treg cells and M1 macrophage cells in testing and validation cohorts.

TABLE 1 | Clinical characteristics of patients according to the stromal immunotype in the training, testing and validation cohorts.

Variables	Training cohort (*N* = 1,502)				Testing cohort (*N* = 218)				Validation cohort (*N* = 102)			
	N	Immunotype A (%)	Immunotype B (%)	*p*	*N*	Immunotype A (%)	Immunotype B (%)	*p*	*N*	Immunotype A (%)	Immunotype B (%)	*p*
Age(yrs)		52.56 ± 12.20	53.02 ± 12.63	0.495		53.11 ± 11.1	53.21 ± 12.6	0.954		51.86 ± 12.71	52.86 ± 11.30	0.671
Axillary lymph nodes				0.293				0.643				0.251
Positive	398	190 (12.6%)	208 (13.8%)		92	46 (21.1%)	46 (21.1%)		47	22 (21.6%)	25 (24.5%)	
Negative	1,104	561 (37.4%)	543 (36.2%)		126	67 (30.7%)	59 (27.1%)		55	32 (31.4%)	23 (22.5%)	
TNM stage				0.101				0.477				0.561
I-II	1,108	540 (36.0%)	568 (37.8%)		183	87 (39.9%)	76 (34.9%)		88	41 (40.2%)	34 (33.3%)	
III-IV	394	211 (14.0%)	183 (12.2%)		35	26 (11.9%)	29 (13.3%)		14	13 (12.7%)	14 (13.8%)	
Tumor size				0.241				0.2860				0.300
0–20 mm	462	246 (16.4%)	216(14.4%)		67	18 (8.3%)	18 (8.3%)		29	7 (6.9%)	11 (10.8%)	
21–50 mm	782	381 (25.4%)	401 (26.7%)		122	78 (35.8%)	63 (28.9%)		48	39 (38.2%)	28 (27.5%)	
>50 mm	258	124(8.3%)	134(8.8%)		29	17 (7.8%)	24(10.9%)		25	8 (7.8%)	9 (8.8%)	
HER2 status by Fish				0.101				0.056				0.168
No amplification	1,057	543 (36.2%)	514 (34.2%)		161	97 (44.5%)	64 (29.4%)		84	23 (22.5%)	27 (26.5%)	
Ampification	445	208 (13.8%)	237 (15.8%)		57	26 (11.9%)	31 (14.2%)		18	31 (30.4%)	21 (20.6%)	

CD4$^+$ T cells, and M1 macrophages. Therefore, patients in each of the three cohorts were divided into a stromal immunotype A subgroup (CD8$^+$ T cells^{high}, CD4$^+$ T cells^{high}, B cells^{high}, M1 macrophages^{high}, and Treg cells^{low}) and a stromal immunotype B subgroup (CD8$^+$ T cells^{low}, CD4$^+$ T cells^{low}, B cells^{low}, M1 macrophages^{low}, and Treg cells^{high}). Patients in the immunotype B subgroup had a higher death rate as well as shorter DFS and OS than patients in the immunotype A subgroup. The 10-years DFS and OS rates were significantly higher in patients immunotype A disease than in those with immunotype B disease in the training (DFS: 63.7 vs. 44.5%, $p < 0.001$; OS: 66.0 vs. 49.9%, $p < 0.001$), testing (DFS: 40.2 vs. 17.6%, $p = 0.025$;

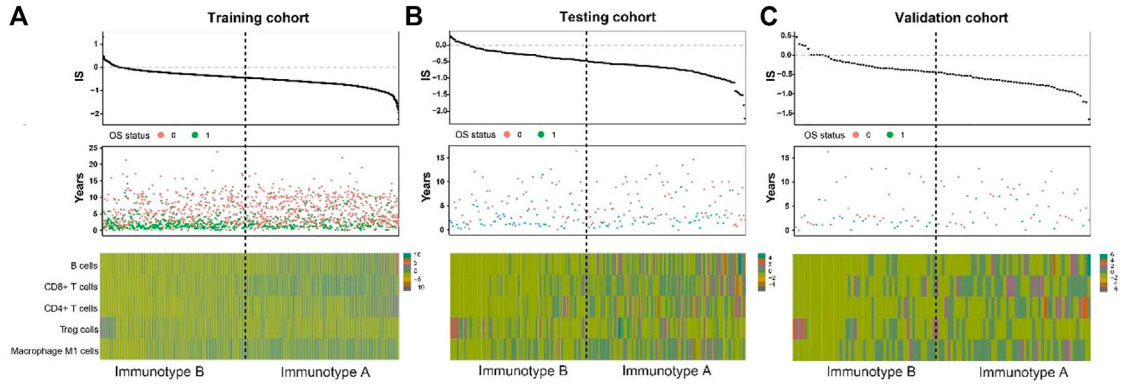

FIGURE 3 | Correlate immunotype with overall survival in training cohort, testing cohort and validation cohort. Hierarchical tree structure classifying the patients of the training cohort **(A)** the patients of the testing cohort. **(B)** and the patients of the validation cohort. **(C)** according to the levels of five immune cell cluster features: high expression (green) and low expression (brown). OS status showed 0: survival; 1: death.

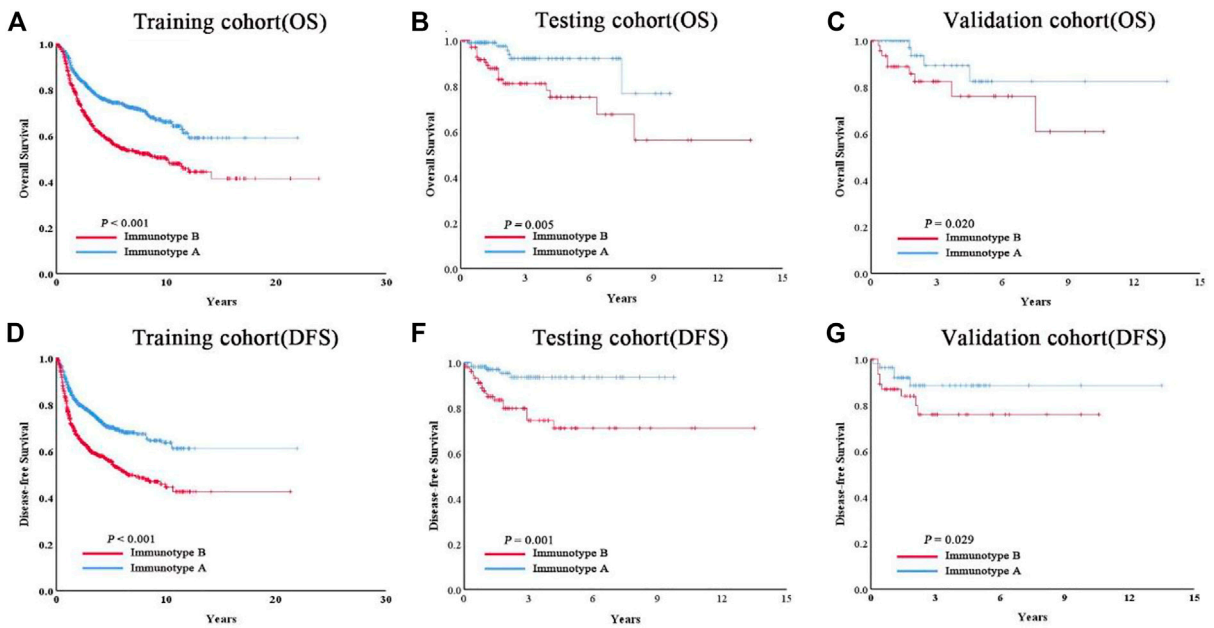

FIGURE 4 | Patients with immunotype B had significantly worse overall survival **(A–C)** and disease-free survival **(D–F)** than patients with immunotype A in all three cohorts.

OS: 32.0 vs. 20.7%, $p = 0.034$), and validation cohorts (DFS: 66.5 vs. 27.0%, $p = 0.020$; OS: 61.7 vs. 34.4%, $p = 0.029$) (**Figure 4**).

Association of Stromal Immunotype With Response to Neoadjuvant Chemotherapy

To quantitatively predict responses to neoadjuvant chemotherapy, we constructed a nomogram which integrated both stromal immunotype and clinicopathological factors using the data from the testing cohort and validated it using the data from the validation cohort. First, we analyzed the relationships between pCR and clinicopathologic characteristics and found that the rate of pCR was associated with tumor size, histologic grade, HER2 status, TNM stage, immunotype in the testing cohort and the validation cohort (all $p < 0.05$) (**Table 2**). Multivariate logistic analyses in both cohorts showed that histologic grade, TNM stage, HER2 status, and immunotype were independent predictors for pCR (all $p < 0.05$) (**Table 3**). Therefore, we constructed a nomogram using these factors (**Figure 5**). The calibration plots and ROC curve (AUC: 0.8128) showed that the derived nomogram performed well, with a high pCR-predictive ability in the validation cohort

TABLE 2 | The relationship between pCR and clinicopathologic characters in testing cohort and validation cohort.

Variables	Testing cohort				Validation cohort			
	Cases	pCR	nonpCR	*p* value	Cases	pCR	nonpCR	*p* value
Age(yrs)				0.393				0.119
>60	36	19 (8.7%)	17(7.8%)		21	9(8.8%)	12(11.8%)	
≤60	182	110(50.5%)	72(33.0%)		81	50(49.0%)	31(30.4%)	
Tumor size				<0.001				0.039
T1-T2	177	116(53.2%)	61(30.0%)		84	53(52.0%)	32(31.4%)	
T3-T4	41	13(6.0%)	28(10.8%)		18	6(5.9%)	11(10.7%)	
Nodal status				0.040				0.487
negative	89	60(27.5%)	29(13.3%)		42	26(25.5%)	16(15.7%)	
positive	129	69(31.7%)	60(27.5%)		60	33(32.4%)	27(26.4%)	
Histologic grade				0.019				0.013
G1-G2	92	46(21.1%)	46(21.1%)		47	21(20.6%)	26(25.5%)	
G3	126	83(38.1%)	43(19.7%)		55	38(37.3%)	17(16.6%)	
HER2 status by FISH				0.008				0.005
No amplification	99	49(22.5%)	50(22.9%)		50	22(21.6%)	28(27.5%)	
Amplification	119	80(36.7%)	39(17.9%)		52	37(36.3%)	15(14.6%)	
TNM				0.001				0.011
I-II	163	107(49.1%)	56(25.7%)		75	49(48.0%)	26(25.5%)	
III-IV	55	22(10.1%)	33(15.1%)		27	10(9.8%)	17(16.7%)	
Risk score				<0.001				
Immunotype A	113	82(37.6%)	31(14.2%)		54	39(38.2%)	15(14.7%)	0.002
Immunotype B	105	47(21.6%)	58(26.6%)		48	20(19.6%)	28(27.5%)	

TABLE 3 | Multivariate logistic regression analysis.

Variables	Testing cohort				Validation cohort			
	βvalue	OR value	95%CI	*p* value	βvalue	OR value	95%CI	*p* value
Grade	0.843	2.323	1.196–4.512	0.013	1.720	5.583	1.808–17.240	0.003
TNM	−1.329	0.265	0.121–0.580	0.001	−1.657	0.191	0.059–0.614	0.005
HER2 status By Fish	−1.105	0.331	0.169–0.647	0.001	−2.137	0.118	0.036–0.387	<0.001
Immunotype	−0.904	0.405	0.218–0.750	0.004	−1.657	0.191	0.059–0.614	0.005

(AUC: 0.7199). Interestingly, the predictive accuracy of our nomogram was higher than that of the TNM staging system in both cohorts (AUC: 0.6129 and 0.6043).

Identification of Stromal Immunotype-Associated Biological Pathways and Immune Checkpoint Molecules

By IHC staining, we found three important cytokines (IL-2, INF-γ, and TGF-β) that were differently expressed between immunotype A and B subgroups. IL-2, INF-γ expression was significantly higher in the immunotype A subgroup, and TGF-β expression was significantly higher in the immunotype B subgroup (**Figure 6**). Furthermore, the expression levels of several immune checkpoint molecules (PD-L1, PD-1, and CTLA-4) were significantly higher in the immunotype A subgroup than in the immunotype B subgroup (**Figure 6**). The Gene Set Enrichment Analysis showed that the T-cell receptor signaling pathway, B-cell receptor signaling pathway, and NK cell-mediated immunity were highly enriched in the immunotype A subgroup (**Figure 6**).

DISCUSSION

Tumor microenvironment is involved in not only the progression but also the responses to anticancer therapies and outcomes of breast cancer (Yu et al., 2017). TILs in the microenvironment can be used to monitor the immune response and are important in predicting treatment responses in many cancers (Asano et al., 2016). Denkert et al. (Denkert et al., 2018) have demonstrated that increased TIL concentration was associated with good response to neoadjuvant chemotherapy in all molecular subtypes of breast cancer and with a survival benefit in HER2-positive and triple-negative breast cancer. TILs include various types of immune cells. Some types of TILs have been shown to be associated with survival or proliferation of cancer cells, for example, high Treg cell count was related to poor clinical outcomes (McCoy et al., 2015). However, not all TILs have definitive prognostic values. Therefore, we applied the CIBERSORT algorithm (Ali et al., 2016) to estimate the relative proportions of 22 distinct functional subsets of immune cells in ER-negative breast cancer patients. $CD8^+$ T cells, $CD4^+$ T cells, B cells, M1 macrophages, and Treg cells with significant prognostic values were selected using univariate cox regression. Then five selected types of immune cells were used to build a stromal immunotype. The immunotype not only

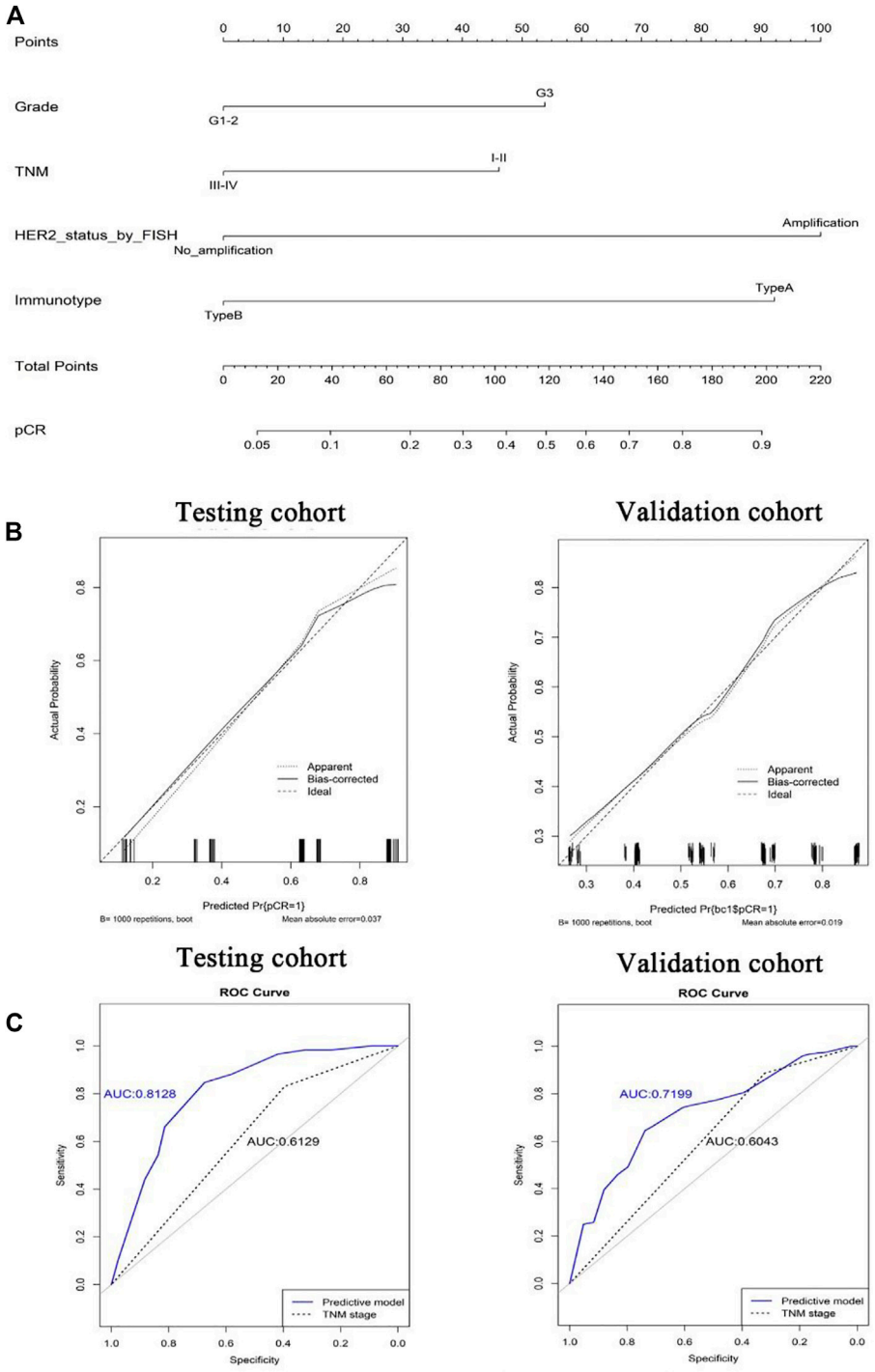

FIGURE 5 | Nomograms (for pCR) that integrated the immunotype and clinicopathologic risk factors **(A)**. Calibration curves showing the discriminatory power of the nomogram for pCR in testing and validation cohorts **(B)**. ROC curves showing the predictive accuracy of the nomogram for pCR and the predictive accuracy was higher than that of the TNM staging system in both testing and validation cohorts **(C)**.

indicated the bio-immunological information of breast cancer but also showed the location information of immune cell infiltration, giving us a clear preview of immune contexture. With further analysis, tumors with high immunoscore (immunotype B) consisted of high levels of Treg cells and low levels of B cells, $CD8^+$ T cells, $CD4^+$ T cells, and M1 macrophages, while tumors with low immunoscore (immunotype A) consisted of low levels of Treg cells and high levels of B cells, $CD8^+$ T cells, $CD4^+$ T cells, and M1 macrophages. Patients in the

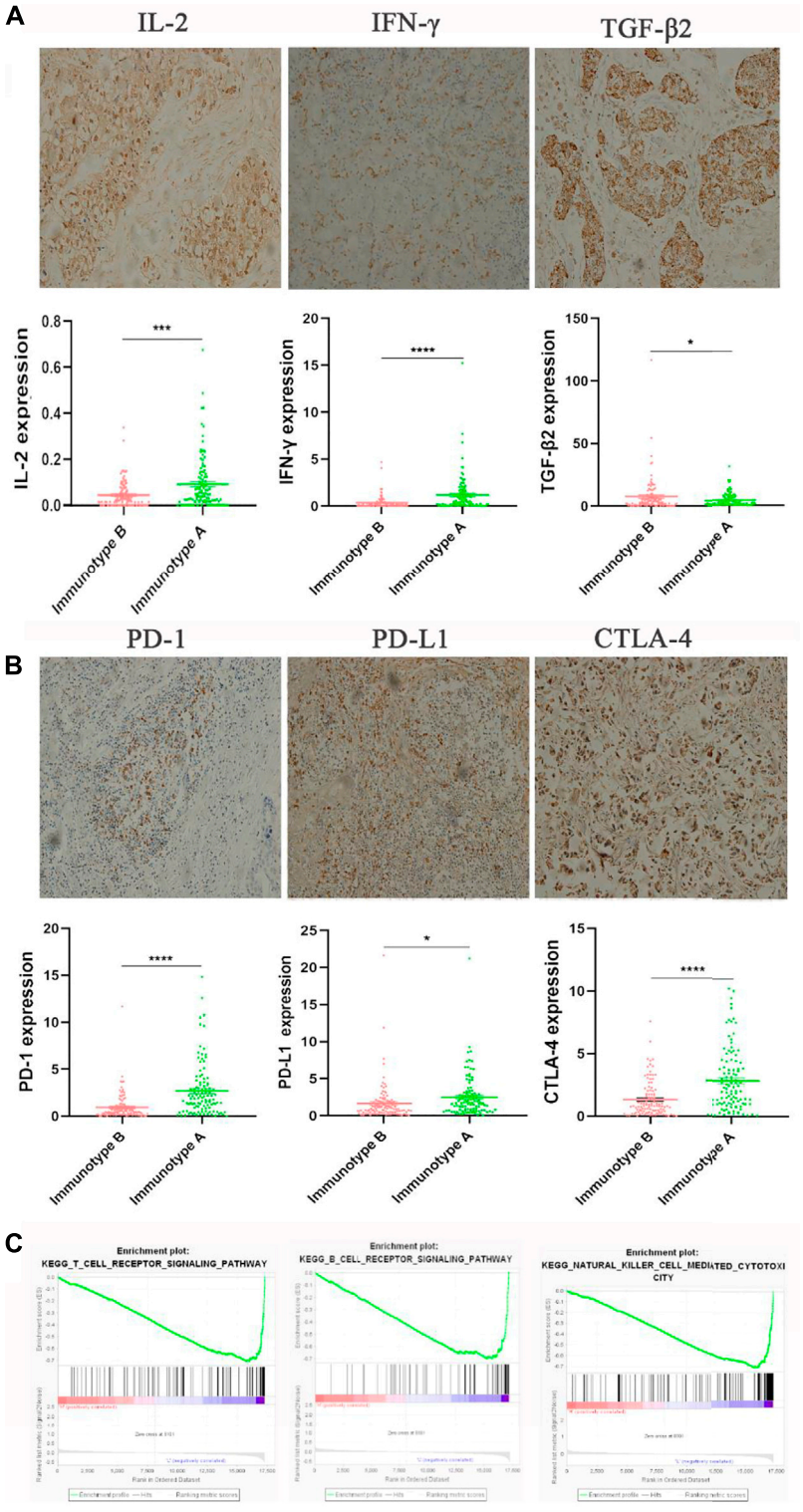

FIGURE 6 | The expression of immunomarkers and signal pathway of stromal immunotypes. The representative immunohistochemistry images of IL-2, IFN-γ, TGF-β2 **(A)**. The associations of immunotype with the immune check-point markers **(B)**. Three enriched biology pathways related with different stromal immunotypes **(C)**.

immunotype B subgroup had significantly shorter OS and DFS than those in the immunotype A subgroup.

Interleukin-2 (IL-2), a cell growth factor in the immune system, can promote the proliferation of Th0 and CTL. IFN-γ, a multifunctional cytokine, plays an important role in promoting antigen presentation and enhancing the activity of macrophages and natural killer cells. TGF-β regulates tumor-stroma interactions, angiogenesis, and metastasis and shows an immunosuppressive function, inhibiting the proliferation and activity of CTL and B cells, while promoting the proliferation of M2 macrophages (Sia et al., 2017; Xue et al., 2020). Interestingly, in the present study, we found that IL-2 and IFN-γ were increased in the immunotype A patients, whereas the TGF-β-mediated immunosuppression pathway was elevated in immunotype B patients. What's more, the Gene Set Enrichment Analysis showed that the B-cell receptor signaling pathway, T cell-mediated pathway, and NK cell-mediated immunity were highly enriched in immunotype A patients. All these findings suggest that immunotype A indicates a hyperimmune state, with a strong tumor-immune cell interaction. $CD4^+$ T-cells in immunotype A may play an important role in recruiting and modulating cytotoxic T-cells in antitumor immunity and $CD4^+$ T-cell activity contributes to the full function of $CD8^+$ cytotoxic T-cells, which is effective for tumor control. While immunotype B indicates a status of immunosuppression for the level of Tregs. These may also explain the prognostic heterogeneity in patients with different immunotypes. In addition, we found that immunotype A was associated with high expression levels of immune checkpoint molecules and cytokines, suggesting that immune checkpoint inhibitor might work well in this subgroup. Therefore, the stromal immunotype might be used to predict responses to immunotherapy.

Recently, many studies focused on biomarkers that were highly associated with treatment responses such as chemotherapy (Lee et al., 2019; Al Amri et al., 2020; Jiao et al., 2020; Valdés-Ferrada et al., 2020; Zhao et al., 2020), and most of them focused on signatures of genes, microRNAs, lncRNAs, and epigenetic biomarkers for the prediction of long-term survival in patients with tumor. However, these signatures cannot be widely used in clinic because of the variability in gene sequencing methods, the inconvenience in the use of assay platforms, and the requirement for specialized analyses. In the present study, we quantified immune cells using IHC staining, which might be easily applied in clinical practice. Moreover, breast cancer has heterogeneous prognosis. To better predict the responses after neoadjuvant chemotherapy, we constructed a nomogram combining clinical characteristics and immunotype. The calibration plots and ROC curve showed that the derived nomogram outperformed the TNM staging system (the 7^{th} edition).

The present study had several limitations. First, as a retrospective study with relatively small sample sizes, our results need to be validated in a prospective study with larger cohorts. Second, not all of the 22 subsets of immune cells were analyzed. We selected only five subsets using the CIBERSORT method. Other important immunotypes such as neutrophil infiltration might also be valuable, but were not analyzed in the present study. The immunotype classification needs to be optimized with more important immune markers being identified. Third, the underlying mechanisms of the relationship between immunotype and patient prognosis were not well investigated. The role of the immune profile in the development and invasion of breast cancer needs to be further investigated.

In conclusion, immune cell infiltration in breast cancer is associated with prognosis. We defined two immunotypes by integrating the indicators of the immune cell infiltration, which could be used to predict survival and responses of breast cancer patients to neoadjuvant treatment. The immunotypes might also have significant implications in immunotherapy for the patients who are insensitive to chemotherapy.

DATA AVAILABILITY STATEMENT

The original contributions presented in the study are included in the article/**Supplementary Material**, further inquiries can be directed to the corresponding author.

ETHICS STATEMENT

The present study was approved by the Ethics Committee of the Guangdong Provincial People's Hospital. The patients/participants provided their written informed consent to participate in this study.

AUTHOR CONTRIBUTIONS

This study was designed by FJ, J-MY, A-QX, and KW. The manuscript was written by FJ. Experiments and data analysis were performed by ZY, L-LZ, MY, H-FG, and J-QL. Imaging was carried out by ZT, M-YC, and S-YW. All authors provided input and feedback.

FUNDING

This study was funded by Grants from National Natural Science Foundation of China (82171898, 82103093), Guangdong Basic and Applied Basic Research Foundation (Grant number 2020A1515010346, 2021A1515011570) Science and Technology Planning Project of Guangzhou City (202002030236, 202102021055), The Fundamental Research Funds for the Central Universities (NO: 2020ZYGXZR017, y2syD2200440), Science and Technology Special Fund of Guangdong Provincial People's Hospital (2017zh01), CSCO-Hengrui Cancer Research Fund (Y-HR2016-067), and Guangdong Provincial Department of Education Characteristic Innovation Project (2015KTSCX080). Funding Nursing research fund of Guangdong Provincial People's Hospital (DFJH2020010). The funders had no role in study design, data collection and analysis, decision to publish, or preparation of the manuscript.

SUPPLEMENTARY MATERIAL

The Supplementary Material for this article can be found online at: https://www.frontiersin.org/articles/10.3389/fmolb.2021.759495/full#supplementary-material

REFERENCES

Al Amri, W. S., Baxter, D. E., Hanby, A. M., Stead, L. F., Verghese, E. T., Thorne, J. L., et al. (2020). Identification of Candidate Mediators of Chemoresponse in Breast Cancer Through Therapy-Driven Selection of Somatic Variants. *Breast Cancer Res. Treat.* 183, 607–616. doi:10.1007/s10549-020-05836-7

Ali, H. R., Chlon, L., Pharoah, P. D., Markowetz, F., and Caldas, C. (2016). Patterns of Immune Infiltration in Breast Cancer and Their Clinical Implications: A Gene-Expression-Based Retrospective Study. *Plos Med.* 13, e1002194–24. doi:10.1371/journal.pmed.1002194

Ali, H. R., Rueda, O. M., Chin, S.-F., Curtis, C., Dunning, M. J., Aparicio, S. A., et al. (2014). Genome-Driven Integrated Classification of Breast Cancer Validated in Over 7,500 Samples. *Genome Biol.* 15, 431. doi:10.1186/s13059-014-0431-1

Asano, Y., Kashiwagi, S., Goto, W., Kurata, K., Noda, S., Takashima, T., et al. (2016). Tumour-Infiltrating CD8 to FOXP3 Lymphocyte Ratio in Predicting Treatment Responses to Neoadjuvant Chemotherapy of Aggressive Breast Cancer. *Br. J. Surg.* 103, 845–854. doi:10.1002/bjs.10127

Cancer Genome Altas Network (2012). Comprehensive Molecular Portraits of Human Breast Tumours. *Nature.* 490, 61–70. doi:10.1038/nature11412

Curtis, C., Shah, S. P., Shah, S. P., Chin, S.-F., Turashvili, G., Rueda, O. M., et al. (2012). The Genomic and Transcriptomic Architecture of 2,000 Breast Tumours Reveals Novel Subgroups. *Nature.* 486, 346–352. doi:10.1038/nature10983

Denkert, C., von Minckwitz, G., Darb-Esfahani, S., Lederer, B., Heppner, B. I., Weber, K. E., et al. (2018). Tumour-infiltrating Lymphocytes and Prognosis in Different Subtypes of Breast Cancer: a Pooled Analysis of 3771 Patients Treated With Neoadjuvant Therapy. *Lancet Oncol.* 19, 40–50. doi:10.1016/s1470-2045(17)30904-x

Haibe-Kains, B., Desmedt, C., Loi, S., Culhane, A. C., Bontempi, G., Quackenbush, J., et al. (2012). A Three-Gene Model to Robustly Identify Breast Cancer Molecular Subtypes. *J. Natl. Cancer Inst.* 104, 311–325. doi:10.1093/jnci/djr545

Ji, F., Fu, S.-J., Shen, S.-L., Zhang, L.-J., Cao, Q.-H., Li, S.-Q., et al. (2015). The Prognostic Value of Combined TGF-B1 and ELF in Hepatocellular Carcinoma. *BMC Cancer.* 15, 116. doi:10.1186/s12885-015-1127-y

Ji, F., Xiao, W.-K., Yang, C.-Q., Yang, M., Zhang, L.-L., Gao, H.-F., et al. (2019). Tumor Location of the Central and Nipple Portion Is Associated With Impaired Survival for Women With Breast Cancer. *Cancer Manage. Res.* Vol. 11, 2915–2925. doi:10.2147/cmar.s186205

Ji, F., Zhang, Z.-h., Zhang, Y., Shen, S.-L., Cao, Q.-H., Zhang, L.-J., et al. (2018). Low Expression of C-Myc Protein Predicts Poor Outcomes in Patients With Hepatocellular Carcinoma After Resection. *BMC Cancer.* 18, 460. doi:10.1186/s12885-018-4379-5

Jiao, R., Zheng, X., Sun, Y., Feng, Z., Song, S., and Ge, H. (2020). Ido1 Expression Increased After Neoadjuvant Therapy Predicts Poor Pathologic Response and Prognosis in Esophageal Squamous Cell Carcinoma. *Front. Oncol.* 10, 1099. doi:10.3389/fonc.2020.01099

Kitano, A., Ono, M., Yoshida, M., Noguchi, E., Shimomura, A., Shimoi, T., et al. (2017). Tumour-Infiltrating Lymphocytes Are Correlated With Higher Expression Levels of PD-1 and PD-L1 in Early Breast Cancer. *ESMO Open.* 2, e000150–8. doi:10.1136/esmoopen-2016-000150

Ladoire, S., Arnould, L., Apetoh, L., Coudert, B., Martin, F., Chauffert, B., et al. (2008). Pathologic Complete Response to Neoadjuvant Chemotherapy of Breast Carcinoma Is Associated With the Disappearance of Tumor-Infiltrating Foxp3+ Regulatory T Cells. *Clin. Cancer Res.* 14, 2413–2420. doi:10.1158/1078-0432.ccr-07-4491

Law, C. W., Chen, Y., Shi, W., and Smyth, G. K. (2014). Voom: Precision Weights Unlock Linear Model Analysis Tools for RNA-Seq Read Counts. *Genome Biol.* 15, R29. doi:10.1186/gb-2014-15-2-r29

Lee, J., Kim, D.-M., and Lee, A. (2019). Prognostic Role and Clinical Association of Tumor-Infiltrating Lymphocyte, Programmed Death Ligand-1 Expression With Neutrophil-Lymphocyte Ratio in Locally Advanced Triple-Negative Breast Cancer. *Cancer Res. Treat.* 51, 649–663. doi:10.4143/crt.2018.270

Li, W., Xu, L., Han, J., Yuan, K., and Wu, H. (2019). Identification and Validation of Tumor Stromal Immunotype in Patients With Hepatocellular Carcinoma. *Front. Oncol.* 9, 664. doi:10.3389/fonc.2019.00664

Luen, S. J., Salgado, R., Fox, S., Savas, P., Eng-Wong, J., Clark, E., et al. (2017). Tumour-Infiltrating Lymphocytes in Advanced HER2-Positive Breast Cancer Treated With Pertuzumab or Placebo in Addition to Trastuzumab and Docetaxel: a Retrospective Analysis of the CLEOPATRA Study. *Lancet Oncol.* 18, 52–62. doi:10.1016/S1470-2045(16)30631-3

McCoy, M. J., Hemmings, C., Miller, T. J., Austin, S. J., Bulsara, M. K., Zeps, N., et al. (2015). Low Stromal Foxp3+ Regulatory T-Cell Density Is Associated With Complete Response to Neoadjuvant Chemoradiotherapy in Rectal Cancer. *Br. J. Cancer.* 113, 1677–1686. doi:10.1038/bjc.2015.427

Sia, D., Jiao, Y., Martinez-Quetglas, I., Kuchuk, O., Villacorta-Martin, C., Castro de Moura, M., et al. (2017). Identification of an Immune-Specific Class of Hepatocellular Carcinoma, Based on Molecular Features. *Gastroenterology.* 153, 812–826. doi:10.1053/j.gastro.2017.06.007

Valdés-Ferrada, J., Muñoz-Durango, N., Pérez-Sepulveda, A., Muñiz, S., Coronado-Arrázola, I., Acevedo, F., et al. (2020). Peripheral Blood Classical Monocytes and Plasma Interleukin 10 Are Associated to Neoadjuvant Chemotherapy Response in Breast Cancer Patients. *Front. Immunol.* 11, 1413. doi:10.3389/fimmu.2020.01413

Xue, L., Bi, G., Zhan, C., Zhang, Y., Yuan, Y., and Fan, H. (2020). Development and Validation of a 12-Gene Immune Relevant Prognostic Signature for Lung Adenocarcinoma Through Machine Learning Strategies. *Front. Oncol.* 10, 835. doi:10.3389/fonc.2020.00835

Yu, T., Di, G., and Di, G. (2017). Role of Tumor Microenvironment in Triple-Negative Breast Cancer and its Prognostic Significance. *Chin. J. Cancer Res.* 29, 237–252. doi:10.21147/j.issn.1000-9604.2017.03.10

Zhao, J., Meisel, J., Guo, Y., Nahta, R., Hsieh, K. L., Peng, L., et al. (2020). Evaluation of PD-L1, Tumor-Infiltrating Lymphocytes, and CD8+ and FOXP3+ Immune Cells in HER2-Positive Breast Cancer Treated With Neoadjuvant Therapies. *Breast Cancer Res. Treat.* 183, 599–606. doi:10.1007/s10549-020-05819-8

Conflict of Interest: The authors declare that the research was conducted in the absence of any commercial or financial relationships that could be construed as a potential conflict of interest.

frontiers in Molecular Biosciences

ORIGINAL RESEARCH
published: 20 October 2021
doi: 10.3389/fmolb.2021.751506

Creation of a Novel Nomogram Based on the Direct Bilirubin-To-Indirect Bilirubin Ratio and Lactate Dehydrogenase Levels in Resectable Colorectal Cancer

Yifei Ma[1,2,3†], *Lulu Shi*[2,3†], *Ping Lu*[2,3,4], *Shuang Yao*[2,3], *Hongli Xu*[2,3,4], *Junjie Hu*[1,2,3], *Xin Liang*[1,2,3], *Xinjun Liang*[2,3,4*] *and Shaozhong Wei*[1,2,3*]

[1]Department of Gastrointestinal Oncology Surgery, Hubei Cancer Hospital, Wuhan, China, [2]Colorectal Cancer Clinical Research Center of Hubei Province, Wuhan, China, [3]Colorectal Cancer Clinical Research Center of Wuhan, Wuhan, China, [4]Department of Abdominal Oncology, Hubei Cancer Hospital, Wuhan, China

OPEN ACCESS

Edited by:
Yu Guo,
The First Affiliated Hospital of Sun Yat-sen University, China

Reviewed by:
Guoxian Long,
Huazhong University of Science and Technology, China
Ding Lin Xiaoxiao,
Sun Yat-sen Memorial Hospital, China

***Correspondence:**
Xinjun Liang
doctorlxj@163.com
Shaozhong Wei
weishaozhong@163.com

[†]These authors have contributed equally to this work

Specialty section:
This article was submitted to Molecular Diagnostics and Therapeutics, a section of the journal Frontiers in Molecular Biosciences

Received: 01 August 2021
Accepted: 04 October 2021
Published: 20 October 2021

Citation:
Ma Y, Shi L, Lu P, Yao S, Xu H, Hu J, Liang X, Liang X and Wei S (2021) Creation of a Novel Nomogram Based on the Direct Bilirubin-To-Indirect Bilirubin Ratio and Lactate Dehydrogenase Levels in Resectable Colorectal Cancer. Front. Mol. Biosci. 8:751506. doi: 10.3389/fmolb.2021.751506

Background: Recently, many studies have suggested that bilirubin is associated with the prognosis of colorectal cancer (CRC). Conversely, there is substantial evidence that lactate dehydrogenase (LDH) levels are associated with the prognosis of cancer. Therefore, we sought to find a novel marker based on the above to predict prognosis in patients with resectable CRC.

Methods: A total of 702 patients from Hubei Cancer Hospital were included. The whole population was randomly divided into training (n = 491) and testing (n = 211) cohorts. Next, we established a new index based on direct bilirubin, indirect bilirubin and LDH levels. Chi-square tests, Kaplan-Meier survival analyses, and Cox regression analyses were used to evaluate prognosis. The prediction accuracies of models for overall survival (OS) and disease-free survival (DFS) were estimated through Harrell's concordance index (C-index) and the Brier score.

Results: The median DFS duration was 32 months (range: 0–72.6 months), whereas the median OS duration was 35 months (range: 0 months–73.8 months). In addition, a new indicator, (DIR.LDH) (HR: 1.433; 95% CI, 1.069–1.920) could independently predict outcomes in CRC patients. Moreover, the module based on DIR. LDH was found to have exceptional performance for predicting OS and DFS. The C-index of the nomogram for OS was 0.802 (95% CI, 0.76–0.85) in the training cohort and 0.829 (95% CI, 0.77–0.89) in the testing cohort. The C-index of the nomogram for DFS was 0.774 (95% CI, 0.74–0.81) in the training cohort and 0.775 (95% CI, 0.71–0.84) in the testing cohort.

Conclusion: We successfully established a novel module to guide clinical decision-making for CRC.

Keywords: colorectal cancer, prognosis, nomogram, bilirubin, lactate dehydrogenase

Abbreviations: AUC, area under the curve; CA199, carbohydrate antigen 19-9; CEA, carcinoembryonic antigen; C-index, Harrell's concordance index; CRC, colorectal cancer; DBIL, direct bilirubin; DFS, disease-free survival; DIR, direct bilirubin to indirect bilirubin ratio; DIR.LDH, the combination of DIR and LDH; IDBIL, indirect bilirubin; LDH, lactate dehydrogenase; OS, overall survival; ROC, receiver operating characteristic curve; UCB, unconjugated bilirubin.

INTRODUCTION

Colorectal cancer (CRC) is the second most common cause of cancer-related death in the United States. In 2020, there were approximately 147,950 new cases and 53,200 deaths (Siegel et al., 2020). In China, it is the fifth most commonly diagnosed cancer and the fifth most common cause cancer-related death. The incidence of CRC has risen over the past decade, making it the third most common cancer in men (12.8%) and women (11.3%) (Chen et al., 2019). CRC is the fifth leading cause of cancer-related death in men (8.0%) (the top three being lung, liver, and stomach cancer), whereas among women, it is the third leading cause (9.8%) (the top two being lung and stomach cancer) (Feng et al., 2019). At present, surgical treatment is still the most important and decisive method for the treatment of CRC, but the effect of single surgical resection is often not satisfactory. Radiotherapy and chemotherapy, immunotherapy, and targeted therapy are becoming increasingly important colorectal cancer treatment options. However, there are still few predictors of efficacy that can truly guide clinical decision making. Therefore, there is an urgent need to identify effective prognostic markers for the stratified management of cancer patients.

Bilirubin is the main metabolite of iron porphyrin compounds in the body. It is toxic and can cause irreversible damage to the brain and nervous system, but it also has antioxidant functions and can inhibit the oxidation of linoleic acid and phospholipids. Studies from the past decade have indicated that mildly elevated serum bilirubin levels are closely associated with a reduced prevalence of chronic diseases, such as cardiovascular disease (Wagner et al., 2015). Recent data have suggested that bilirubin levels are associated with cancer prognosis. Therefore, bilirubin levels, as a biomarker of some diseases, have important clinical significance.

Lactate dehydrogenase (LDH) is a well-known diagnostic marker for myocardial infarction, liver dysfunction and various types of myopathies (Wróblewski and Gregory, 1961; Mg and Mj, 1964; Kopperschläger and Kirchberger, 1996a). However, some researchers found that LDH levels were also elevated in cancer patients. Elevated LDH levels are associated with the recurrence and metastasis of several tumours, such as pancreatic carcinoma, non-small-cell lung cancer, hepatocellular carcinoma and CRC (Tas et al., 2001a; Danner et al., 2010).

Therefore, we attempted to combine serum bilirubin and LDH levels to explore a new prognostic marker for CRC patients and establish a prognostic model with resectable colorectal cancer patients.

MATERIALS AND METHODS

Study Population

In total, 702 patients with histopathologically confirmed CRC who had undergone resection of the primary lesion at Hubei Cancer Hospital, Hubei, China, between January 2013 and December 2016 were enrolled in our retrospective study. The following baseline indicators were analysed: age, sex, family history, history of smoking and drinking, stage of TNM and some pathological conditions, including tumour differentiation, location, nerve infiltration status, circumferential margin status, and vascular cancer embolus status. Importantly, LDH, direct bilirubin (DBIL), indirect bilirubin (IDBIL), carcinoembryonic antigen (CEA), and carbohydrate antigen 19-9 (CA199) levels were also retrieved the week before surgery. The following inclusion criteria were used: 1) age ≥18 years; 2) primary CRC patients; and 3) patients who had radical surgery. The exclusion criteria were as follows: 1) cooccurrence of other cancers and 2) patients lacking clinical data. This study was supported by the Ethics Committee and Institutional Review Board of Hubei Cancer Hospital. In addition, all patients provided informed consent.

Blood Sample Analysis

Routine preoperative blood examinations were performed within 1 week before surgery. The DIR was defined as the level of direct bilirubin divided by the level of indirect bilirubin. Next, we divided patients into a high-level group or a low-level group according to the cut-off values of the DIR and LDH levels. Patients with low DIR and LDH levels were assigned a score of 0, those with a high DIR level or a high LDH level were assigned a score of 1, and those with high DIR and LDH levels were assigned a score of 2.

We randomly divided the total sample into a training cohort (70%) and a testing cohort (30%). The training group was used to determine the cut-off values and establish the prediction model, while the validation group was used to test the performance of the new index and the prediction model.

Statistical Analyses

The chi-square test or Fisher's exact test was used to compare differences between groups. By using cut-off values obtained via receiver operating characteristic (ROC) curve analyses, continuous variables were transformed into categorical variables. The Kaplan-Meier method was used to establish the survival curves, and the log-rank test was used to analyse the differences between groups. Multivariate Cox regression analyses were performed to identify independent prognostic factors. Harrell's concordance index (the C-index) and the Brier score were used to estimate the efficacy of the models. Time-dependent ROC curves, calibration curves, and nomograms were plotted to visualize the performance of the models. Differences with a two-tailed p value < 0.05 were considered statistically significant. The time-dependent ROC curve, calibration curve, and nomogram were generated using the "survival ROC," "time ROC," "pec" and "regplot" packages of R 3.6.0 (The R Foundation for Statistical Computing, Vienna, Austria).

RESULTS

Pooled Population

Our study included a cohort of 702 patients with a diagnosis of CRC (clinical and pathological characteristics are listed in **Table 1**). In the whole cohort, 22.5% of patients had rectal cancer, and 59.6% had right-sided colon cancer. Approximately 64.1% of patients had negative lymph nodes.

TABLE 1 | Demographic and tumor characteristics of colorectal cancer patients.

		DIR.LDH			
		0	1	2	P
Age(years)	<65	353 (50.2)	93 (13.2)	15 (2.1)	0.389
	≥65	182 (25.9)	51 (7.3)	8 (5.5)	
Sex	Male	345 (49.1)	84 (12.0)	12 (1.7)	0.389
	Female	190 (27.1)	60 (8.5)	11 (1.6)	
Family history of CRC	no	469 (66.8)	122 (17.4)	20 (2.8)	0.461
	yes	66 (9.4)	22 (3.1)	3 (0.5)	
BMI(kg/m2)	<25	404 (57.5)	116 (16.5)	17 (2.4)	0.429
	≥25	131 (18.7)	28 (4.0)	6 (0.9)	
Smoking	No	351 (50.0)	107 (15.2)	21 (3.0)	0.007
	Yes	184 (26.2)	37 (5.3)	2 (0.3)	
Drink	No	414 (58.9)	27 (3.8)	21 (3.0)	0.122
	Yes	121 (17.2)	117 (16.7)	2 (3.37)	
Lymph node ratio	<0.07	353 (50.3)	84 (12.0)	13 (1.9)	0.176
	≥0.07	182 (26.0)	60 (8.5)	10 (1.3)	
Location	Left colon	87 (12.4)	37 (5.2)	5 (0.7)	<0.001
	Right colon	339 (48.3)	32 (4.6)	8 (1.1)	
	Rectal	109 (15.5)	39 (5.6)	10 (6.6)	
postoperation radiotherapy	No	504 (71.8)	134 (19.1)	22 (3.1)	0.845
	Yes	31 (4.4)	10 (1.4)	1 (0.2)	
TNM stage	1	63 (9.0)	11 (1.6)	2 (0.3)	<0.001
	2	194 (27.6)	39 (5.6)	4 (0.6)	
	3	211 (30.1)	44 (6.3)	1 (0.1)	
	4	67 (9.5)	50 (7.1)	16 (2.2)	
Cea (ng/ml)	<3.5	308 (43.9)	54 (7.7)	5 (0.7)	<0.001
	≥3.5	227 (32.3)	90 (12.8)	18 (2.6)	
Ca199 (ng/ml)	<35.5	413 (58.8)	94(13.4)	10 (1.4)	<0.001
	≥35.5	122 (17.4)	50 (7.1)	13 (1.9)	
Circumferential margin	No	527 (75.1)	140 (20.0)	21 (3.0)	0.027
	Yes	8 (1.1)	4 (0.6)	2 (0.2)	
Vascular cancer embolus	No	383 (54.6)	103 (14.7)	14 (2.0)	0.537
	Yes	152 (21.6)	41 (5.8)	9 (1.3)	
Nerve infiltration	No	412 (58.7)	121 (17.2)	17 (2.4)	0.273
	Yes	123 (17.5)	23 (3.3)	6 (0.9)	
Differentiation	Poor	68 (9.7)	19 (2.7)	9 (1.3)	0.032
	Moderate	408 (58.1)	110 (15.7)	13 (1.9)	
	Well	59 (8.4)	15 (2.1)	1 (0.1)	
neoadjuvant	No	166 (23.4)	39 (5.6)	7 (0.9)	0.658
	Yes	369 (52.6)	105 (15.0)	16 (2.5)	

Abbreviation: CEA, carcinoembryonic antigen; CA199, carbohydrate antigen 19-9; DIR, direct bilirubin/indirect bilirubin; LDH, lactate dehydrogenase; DIR.LDH, the combination of DIR and LDH.

Of note, 13.6 and 75.6% of patients had poorly differentiated and moderately differentiated tumours, respectively. In addition, 10.8% of patients had stage 1 disease, 33.7% had stage 2 disease, and 36.4% had stage 3 disease. Moreover, 69.8% of patients received neoadjuvant chemotherapy, and 5.9% of patients received postoperative adjuvant radiotherapy. According to the ROC curve, the optimal cut-off values for the DIR and LDH levels were 0.42 and 221 (IU/L), respectively.

Training Cohort

The training cohort included 491 patients. We found that OS and DFS differed in the total cohort, the training cohort or the validation cohort according to the DIR and LDH levels (DIR.LDH) (**Figure 1**). In addition, we found that the DIR. LDH was associated with the TNM stage ($p < 0.001$), the tumour location ($p < 0.001$), a history of smoking ($p = 0.007$), and CEA ($p < 0.001$) and CA199 levels ($p < 0.001$) (**Table 1**). In contrast, differentiation was not associated with DIR.LDH. In the univariate regression analysis, we found that the DIR.LDH, lymph node ratio, differentiation, TNM stage, circumferential margin, vascular cancer embolus, nerve infiltration, and CEA and CA199 levels might be independent prognostic factors for DFS and OS, and we included the above indicators in the multivariate regression analysis and found that DIR.LDH was indeed an independent prognostic factor for patients with CRC (**Table 2**). Next, we added the above significant indicators and some baseline indicators to our nomogram plot. Finally, we established two prognostic models for OS and DFS based on DIR.LDH.

Ultimately, age, sex, TNM stage, status of circumferential margin, status of vascular cancer embolus, status of nerve infiltration, differentiation, DIR.LDH, lymph node ratio, and CEA and CA199 levels were included in the nomogram. In the training cohort, the C-index of the prognostic model for

TABLE 2 | Univariate and multivariate analyses of the factors affecting overall survival and disease-free survival by Cox proportional hazard model.

Characteristic		N	Disease-free survival				Overall survival			
			Univariate analysis HR (95%CI)	P	Multivariate analysis[a] HR (95%CI)	P	Univariate analysis HR (95%CI)	P	Multivariate analysis[b] HR (95%CI)	P
Age(years)	<65	458	1	0.878	—	—	1	0.063	1	0.047
	≥65	244	0.978 (0.740–1.293)		—		1.398 (0.982–1.989)		1.435 (1.005–2.047)	
Sex	Male	444	1	0.339	—	—	1	0.429	—	—
	Female	258	0.873 (0.660–1.153)		—		0.861 (0.595–1.247)		—	
Family history of CRC	No	611	1	0.617	—	—	1	0.412	—	—
	Yes	91	0.908 (0.621–1.327)		—		1.262 (0.724–2.199)		—	
BMI(kg/m^2)	<25	537	1	0.560	—	—	1	0.750	—	—
	≥25	165	0.910 (0.662–1.250)		—		0.935 (0.618–1.415)		—	
Smoking	No	479	1	0.952	—	—	1	0.821	—	—
	Yes	223	0.991 (0.747–1.315)		—		0.958 (0.660–1.390)		—	
Drink	No	552	1	0.206	—	—	1	0.774	—	—
	Yes	145	1.223(0.895–1.670)		—		0.938(0.609–1.447)		—	
Lymph node ratio	<0.07	450	1	<0.001	1	0.086	1	<0.001	1	<0.001
	≥0.07	252	2.819 (2.158–3.683)		1.283 (0.965–1.705)		4.774 (3.273–6.964)		2.503 (1.690–3.708)	
Location	Left colon	125	1	0.214	—	—	1	0.039	—	—
	Right colon	419			—				—	
	Rectal	158	0.904 (0.772–1.060)		—		0.808 (0.661–0.989)		—	
Differentiation	Poor	96	1	<0.001	1	0.011	1	<0.001	—	—
	Moderate	531							—	
	Well	75	0.513 (0.393–0.670)		0.693 (0.523–0.918)		0.568 (0.401–0.803)		—	
TNM stage	1	76	1	<0.001	1	<0.001	1	<0.001	1	<0.001
	2	237								
	3	256								
	4	133	2.296 (2.452–3.491)		2.180 (1.777–2.673)		3.166 (2.495–4.017)		2.307 (1.737–3.063)	
Cea (ng/ml)	<3.5	367	1	<0.001	1	0.013	1	<0.001	1	0.023
	≥3.5	335	2.586 (1.954–3.421)		1.466 (1.084–1.982)		2.869 (1.962–4.196)		1.588 (1.065–2.370)	
Ca199 (ng/ml)	<35.5	517	1	<0.001	1	0.002	1	<0.001	—	—
	≥35.5	185	2.639 (2.019–3.450)		1.579 (1.190–2.094)		2.678 (1.888–3.798)		—	
Circumferential margin	No	668	1	0.002	—	—	1	<0.001	—	—
	Yes	14	2.821 (1.446–5.503)		—		4.212 (2.056–8.628)		—	
Vascular cancer embolus	No	500	1	<0.001	—	—	1	0.274	—	—
	Yes	202	1.589 (1.206–2.094)		—		1.233 (0.847–1.794)		—	
Nerve infiltration	No	550	1	<0.001	—	—	1	0.029	—	-
	Yes	152	1.677 (1.253–2.245)		—		1.539 (1.046–2.266)		—	
postoperation radiotherapy	No	660	1	0.108	—	—	1	0.391	—	—
	Yes	42	1.501 (0.915–2.464)		—		1.346 (0.683–2.654)		—	
neoadjuvant	No	212	1	<0.001	—	—	1	0.224	—	—
	Yes	490	2.147 (1.524–3.025)		—		1.282 (0.859–1.914)		—	
DIR.LDH	0	535	1	<0.001	1	0.057	1	<0.001	1	0.016
	1	144								
	2	23	1.907 (1.526–2.383)		1.257 (0.993–1.590)		2.250 (1.710–2.960)		1.433 (1.069–1.920)	

[a]*The multivariate Cox regression model included DIR.LDH, lymph node ratio, differentiation, TNM stage, circumferential margin, vascular cancer embolus, nerve infiltration, CEA, CA199 and neoadjuvant.*

[b]*The multivariate Cox regression model included DIR.LDH, lymph node ratio, location, differentiation, TNM stage, circumferential margin, nerve infiltration, CEA, CA199 and age.*

Abbreviation: CEA: carcinoembryonic antigen; CA199: carbohydrate antigen 19-9; DIR: direct bilirubin/indirect bilirubin; LDH: lactate dehydrogenase; DIR.LDH: the combination of DIR and LDH.

OS based on age, sex, TNM stage, circumferential margin status, vascular cancer embolus status, nerve infiltration status, differentiation, DIR.LDH, lymph node ratio, location, CEA and CA199 levels was 0.802 (95% CI, 0.76–0.85). The C-index of the prognostic model for DFS based on age, sex, TNM stage, circumferential margin status, nerve infiltration status, differentiation, DIR. LDH, lymph node ratio, location, CEA and CA199 levels was 0.774 (95% CI, 0.74–0.81). We used

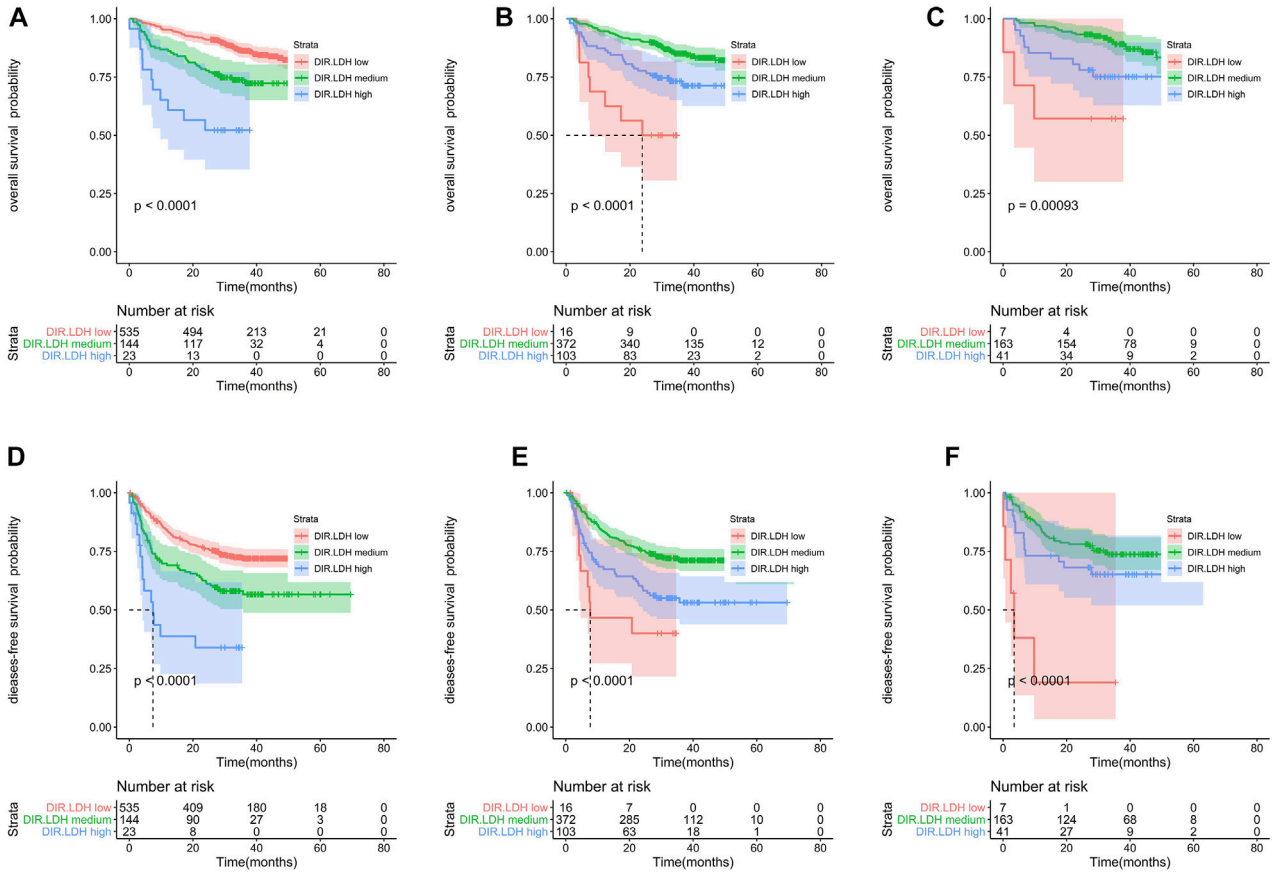

FIGURE 1 | Kaplan-Meier survival analyses of DIR.LDH in the whole cohort **(A,D)**, training cohort **(B,E)** and testing cohort **(C,F)**. Abbreviations: DIR, direct bilirubin/indirect bilirubin; LDH, lactate dehydrogenase; DIR.LDH, the combination of DIR and LDH.

one- and 3-year time-dependent ROC curves to determine the performance of the two models (**Figures 2A,C**). The area under the curve (AUC) values, which were 0.813 for 1-year OS and 0.825 for 3-year OS in the training set, were used to illustrate the predictive power of the two models. Furthermore, the AUC values for 1-year and 3-year DFS were 0.814 and 0.815 in the training set, respectively. In addition, the AUC values (95% CIs) of the two models were stable (**Figures 2E,G**), and the calibration curves showed good consistency between the predictions and observations in the 1-year and 3-year OS and DFS probabilities, with Brier scores of 0.034 and 0.069 for OS and 0.078 and 0.122 for DFS, respectively (**Figures 3A,C,E,G**).

Nomograms for OS and DFS were plotted, as shown in **Figures 4**, **5**, respectively.

Testing Cohort

The testing cohort included 211 patients. The C-indices of the two models for DFS and OS were 0.775 (95% CI, 0.71–0.84) and 0.829 (95% CI, 0.77–0.89), respectively. One- and 3-year time-dependent ROC curves were used to verify the performance of the models (**Figures 2B,D**). Meanwhile, the AUC values of the 1-year and 3-year OS rates were 0.927 and 0.863 in the testing cohort, respectively. Furthermore, the AUC values of the 1-year and 3-year DFS rates were 0.827 and 0.795, respectively. The AUC values were stable over time (**Figures 2F,H**), and the calibration curves showed good consistency between the predictions and observations in the 1-year and 3-year OS and DFS probabilities, with Brier scores of 0.024 and 0.055 for OS and 0.070 and 0.113 for DFS, respectively (**Figures 3D,F,H**).

DISCUSSION

We found a new indicator, DIR. LDH, which was correlated not only with DFS but also with OS. More importantly, the prognostic model created with this metric in combination with other baseline values has high predictive performance for OS.

Bilirubin is involved in antioxidation and stress. Bilirubin inhibits complement induction by inhibiting the interaction between complement C1q and immunoglobulin, thereby inhibiting initial complement activation via classic pathways (Basiglio et al., 2010). However, few studies have reported that bilirubin is associated with the prognosis of CRC. It was reported that serum bilirubin was inversely related to total cancer mortality in a population-based cohort from Belgium (Temme et al., 2001). In addition, an association between baseline bilirubin levels and lung cancer

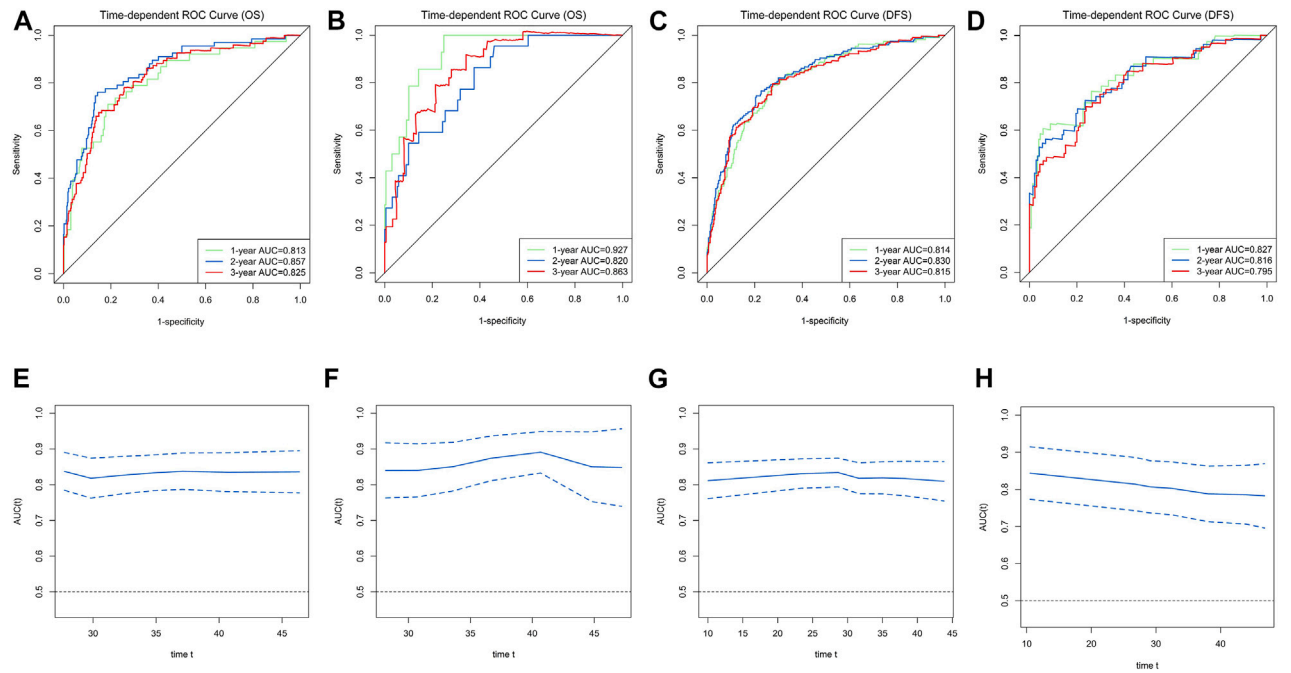

FIGURE 2 | Time-dependent receiver operating characteristic (ROC) curves for the overall survival (OS) and disease-free survival (DFS)-associated nomograms for predicting 1-, 2- and 3-year survival rates and time-AUCs of the model. Time-dependent ROC curves from the nomograms for the prediction of OS and DFS rates in the training **(A,C)** and testing **(B,D)** sets. Time-AUCs from the nomograms for the prediction of OS and DFS rates in the training **(E,G)** and testing **(F,H)** sets.

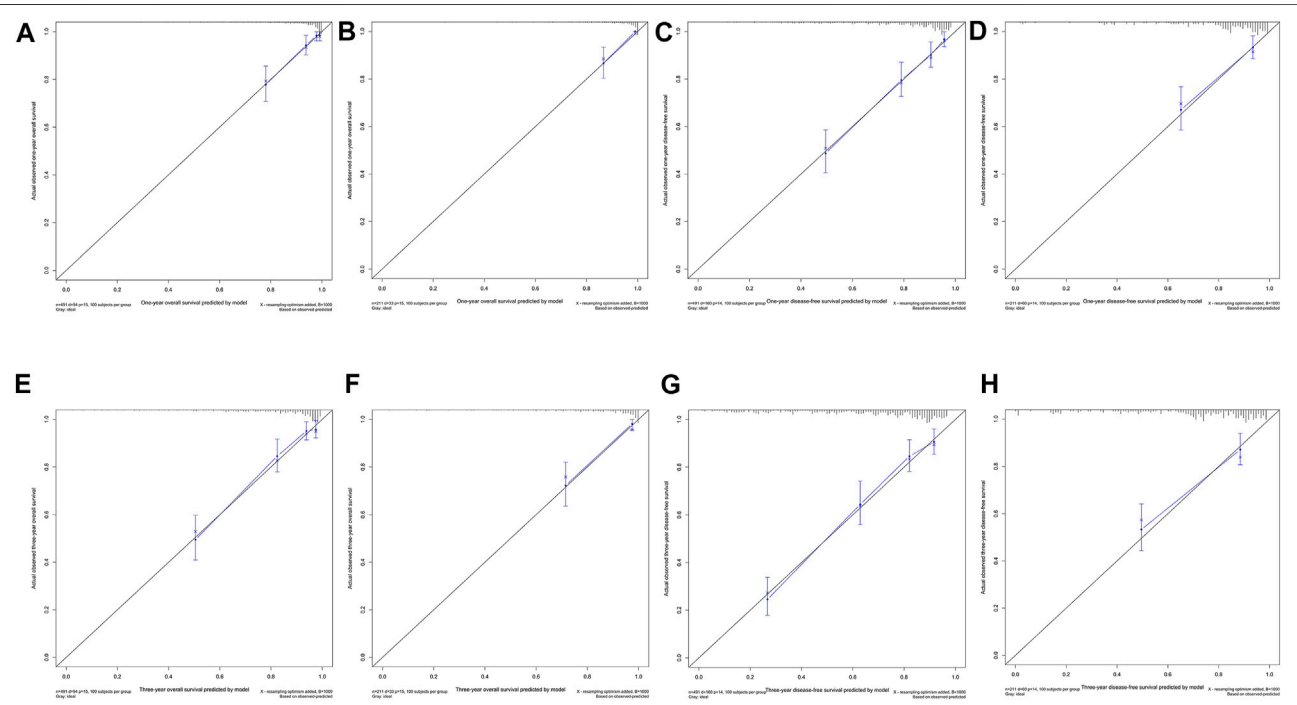

FIGURE 3 | One-year and 3-year calibration curves of the model. One-year calibration curves from the nomograms for the prediction of OS and DFS rates in the training **(A,C)** and testing **(B,D)** sets. Three-year calibration curves from the nomograms for the prediction of OS and DFS rates in the training **(E,G)** and testing **(F,H)** sets.

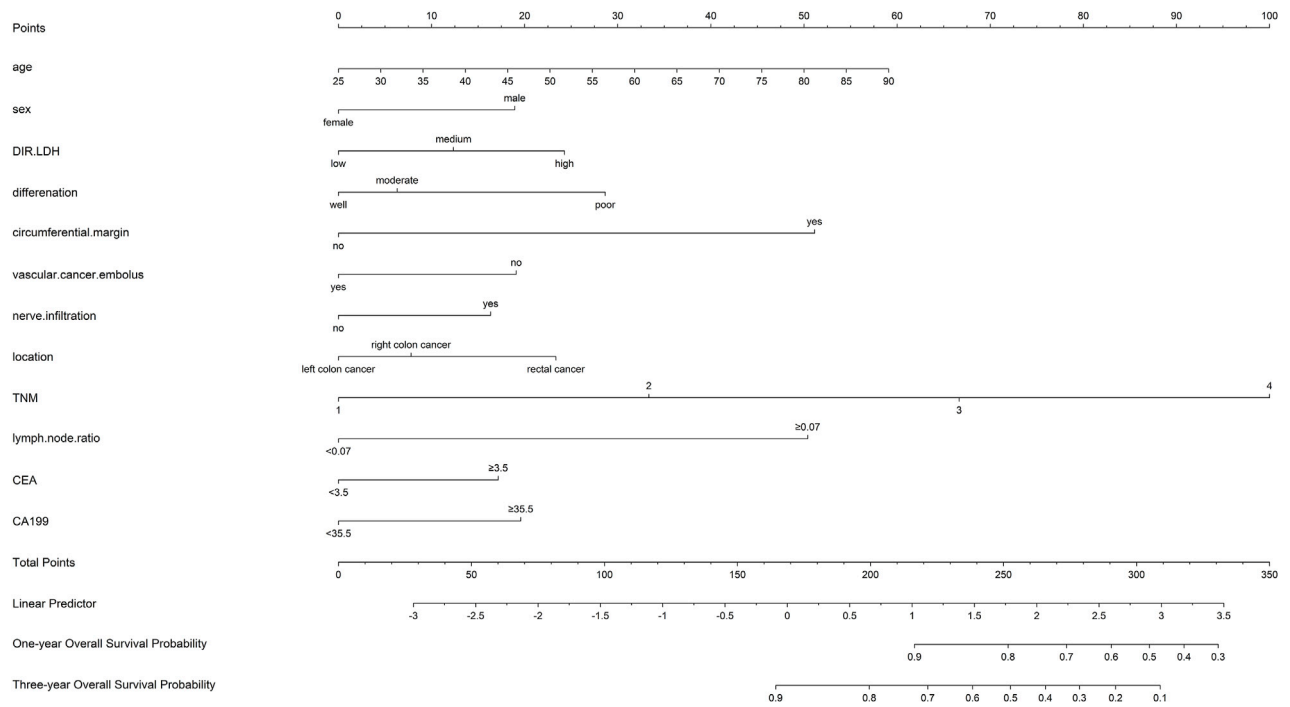

FIGURE 4 | Nomogram of the prognostic model for the OS of patients with colorectal cancer.

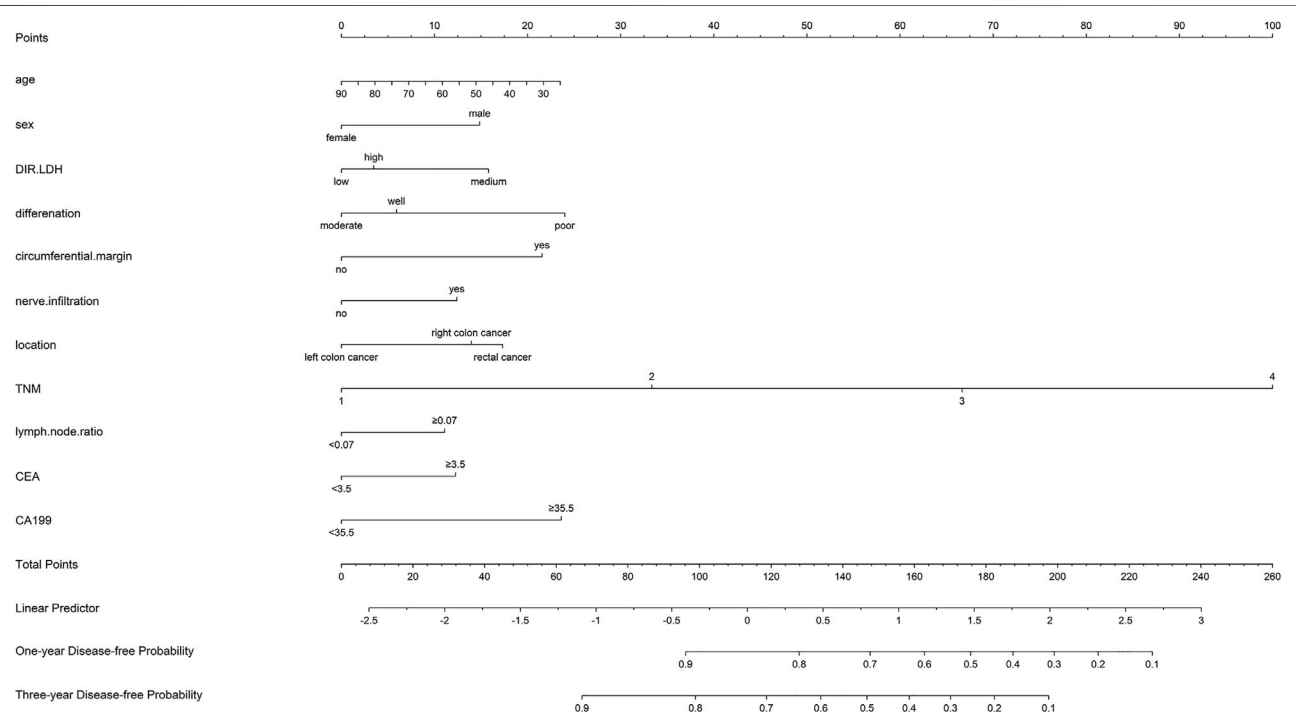

FIGURE 5 | Nomogram of the prognostic model for the DFS of patients with colorectal cancer.

has been reported (Horsfall et al., 2011; Wulaningsih et al., 2015). A real-world study showed that the cancer-related mortality risk of males linearly decreased as bilirubin increased, especially with reference to non-lung cancers (Temme et al., 2001). Another study showed that the relationship between unconjugated bilirubin (UCB) levels and CRC risk was related to sex, with high UCB levels being positively associated with CRC risk in men, and the opposite was true in women (Seyed Khoei et al., 2020). Therefore, our study combined the two and redefined new prognostic indicators, and the surprising findings have good prognostic value.

Some studies have shown that the glycolysis rate of malignant tumours is much higher than that of normal tissues in the tumour microenvironment, so the level of LDH will increase in malignant tumours. LDH can also participate in the formation of tumour blood vessels by mediating VEGF-A and VEGF receptor 1 overexpression (Tas et al., 2001b; Faloppi et al., 2016). Most importantly, LDH mediates immune escape from tumour cells by inhibiting immune function (Husain et al., 2013; Brand et al., 2016). Therefore, an increase in LDH levels through enzyme or gene regulation is considered to be beneficial to tumour growth (Certo et al., 2021). Moreover, for testicular cancer patients, LDH can be used to monitor patient outcomes and make decisions about therapeutic management (Hughes and Bishop, 1996; Shin and Kim, 2013). In the case of Wilms' tumour, LDH is used as a marker in both diagnosis and monitoring the response to therapy (Schwartz, 1991; Kopperschläger and Kirchberger, 1996b; Pandian et al., 1997). Therefore, an elevated serum LDH level is an adverse prognostic factor for tumours.

In recent years, many studies have established prognostic models based on blood biomarkers. There is a very important reason why blood-based biomarkers are very reproducible, very quick to analyse and easy to use in clinical practice. We attempted to combine direct bilirubin, indirect bilirubin and LDH to explore a new predictor and establish a new prognostic model. Data analysis showed that our ideas are logical. A prognostic model based on age, sex, TNM stage, circumferential margin status, vascular cancer embolus status, nerve infiltration status, differentiation, DIR. LDH, lymph node ratio, location, CEA and CA199 levels was found to exhibit excellent predictive performance for OS [C-index: 0.802 (95% CI, 0.76–0.85) and Brier score: 0.034]. Another model based on age, sex, TNM stage, circumferential margin status, nerve infiltration status, differentiation, DIR.LDH, lymph node ratio, location, CEA and CA199 levels also exhibited excellent performance for DFS [C-index: 0.774 (95% CI, 0.74–0.81) and Brier score: 0.078]. More importantly, the model also showed good predictive performance in the testing sets. A previous model considering the mutation status and other parameters presented C-indices of 0.68 and 0.62 for progression-free survival (You et al., 2020).

There are some limitations to this study that should be mentioned. Most importantly, because this was a retrospective study, we did not include the genetic status of patients in our study. For RAS wild-type patients, there was a significant correlation between the efficacy of anti-EGFR mAb (cetuximab) and the tumour site, while no significant correlation between the efficacy of anti-VEGF mAb (bevacizumab) and the tumour site was observed. Cetuximab was superior to bevacizumab in objective response rate and overall survival in left colorectal cancer. In right-sided colon cancer, cetuximab is inferior to bevacizumab in terms of overall survival, although it may show an advantage with regard to the objective response rate (Tejpar et al., 2017). The 2020 NCCN recommended that patients with MSI-H/dMMR advanced colorectal cancer be treated with pembrolizumab and navurliumab (LE et al., 2015; Overman et al., 2016; Overman et al., 2018). Moreover, we did not consider the treatment modalities or the effects of targeted therapy and immunotherapy on prognostic markers. It is worth considering whether immunotherapy would have any effect on these blood-based indicators. In addition, due to the lack of relevant data, we regret that there is no external set to further verify our conclusions.

The advantages of this study are that we jointly considered changes in direct bilirubin, indirect bilirubin and LDH to establish two models that have excellent predictive performance, which has never been done before.

In conclusion, we innovatively combined the potential blood markers direct bilirubin, indirect bilirubin and LDH and further verified that our indicators were meaningful at different stages. Most importantly, we built a novel prognostic model based on direct bilirubin, indirect bilirubin and LDH to efficiently and practically predict the prognosis of CRC patients, and this model exhibited good predictive performance.

DATA AVAILABILITY STATEMENT

The raw data supporting the conclusion of this article will be made available by the authors, without undue reservation.

ETHICS STATEMENT

This study was supported by the Ethics Committee and Institutional Review Board of Hubei Cancer Hospital. In addition, all patients provided informed consent. Written informed consent was obtained from the individual(s) for the publication of any potentially identifiable images or data included in this article.

AUTHOR CONTRIBUTIONS

All authors made a significant contribution to the work reported, whether that is in the conception, study design, execution, acquisition of data, analysis and interpretation, or in all these areas; took part in drafting, revising or critically reviewing the article; gave final approval of the version to be published; have agreed on the journal to which the article has been submitted; and agree to be accountable for all aspects of the work.

FUNDING

This work was supported by the Natural Science Foundation of Hubei Province (Grant No. 2019ACA135), the National Natural Sciences Foundation of China (Grants No. 81772499), the National Key R&D Program of China (Grant No. 2017YFC0908204), the

Health commission of Hubei Province scientific research project (Grant Nos WJ2017Z020, WJ2019H121, WJ 2017M142, WJ2021Z001), Applied Basic Research Program of Wuhan Science and Technology bureau (Grant No. 2020020601012250).

ACKNOWLEDGMENTS

The authors would like to thank all participants who volunteered to provide data and samples in this study.

REFERENCES

Basiglio, C. L., Arriaga, S. M., Pelusa, F., Almará, A. M., Kapitulnik, J., and Mottino, A. D. (2010). Complement Activation and Disease: Protective Effects of Hyperbilirubinaemia. *Clin. Sci.* 118, 99–113. doi:10.1042/CS20080540

Brand, A., Singer, K., Koehl, G. E., Kolitzus, M., Schoenhammer, G., Thiel, A., et al. (2016). LDHA-associated Lactic Acid Production Blunts Tumor Immunosurveillance by T and NK Cells. *Cel Metab.* 24, 657–671. doi:10.1016/j.cmet.2016.08.011

Certo, M., Tsai, C.-H., Pucino, V., Ho, P.-C., and Mauro, C. (2021). Lactate Modulation of Immune Responses in Inflammatory versus Tumour Microenvironments. *Nat. Rev. Immunol.* 21 (3), 151–161. doi:10.1038/s41577-020-0406-2

Chen, H., Li, N., Ren, J., Feng, X., Lyu, Z., Wei, L., et al. (2019). Participation and Yield of a Population-Based Colorectal Cancer Screening Programme in China. *Gut* 68 (8), 1450–1457. doi:10.1136/gutjnl-2018-317124

Danner, B. C., Didilis, V. N., Wiemeyer, S., Stojanovic, T., Kitz, J., Emmert, A., et al. (2010). Long-term Survival Is Linked to Serum LDH and Partly to Tumour LDH-5 in NSCLC. *Anticancer Res.* 30 (4), 1347–1351. doi:10.1159/000135492PMID: 20530451

Faloppi, L., Bianconi, M., Memeo, R., Casadei Gardini, A., Giampieri, R., Bittoni, A., et al. (2016). Lactate Dehydrogenase in Hepatocellular Carcinoma: Something Old, Something New. *Biomed. Res. Int.* 2016, 1–7. doi:10.1155/2016/7196280

Feng, R.-M., Zong, Y.-N., Cao, S.-M., and Xu, R.-H. (2019). Current Cancer Situation in China: Good or Bad News from the 2018 Global Cancer Statistics? *Cancer Commun.* 39 (1), 22. doi:10.1186/s40880-019-0368-6

Horsfall, L. J., Rait, G., Walters, K., Swallow, D. M., Pereira, S. P., Nazareth, I., et al. (2011). Serum Bilirubin and Risk of Respiratory Disease and Death. *JAMA* 305 (7), 691–697. doi:10.1001/jama.2011.124

Hughes, O., and Bishop, M. (1996). Lactate Dehydrogenase Should Be Used as Marker in Testicular Tumours. *BMJ* 313 (7057), 625. doi:10.1136/bmj.313.7057.625b

Husain, Z., Huang, Y., Seth, P., and Sukhatme, V. P. (2013). Tumor-derived Lactate Modifies Antitumor Immune Response: Effect on Myeloid-Derived Suppressor Cells and NK Cells. *J.I.* 191, 1486–1495. doi:10.4049/jimmunol.1202702

Kopperschläger, G., and Kirchberger, J. (1996). Methods for the Separation of Lactate Dehydrogenases and Clinical Significance of the Enzyme. *J. Chromatogr. B Biomed. Appl.* 684 (1–2), 25–49. doi:10.1016/0378-4347(96)00133-8

Kopperschläger, G., and Kirchberger, J. (1996). Methods for the Separation of Lactate Dehydrogenases and Clinical Significance of the Enzyme. *J. Chromatogr. B Biomed. Appl.* 684 (1–2), 25–49. doi:10.1016/0378-4347(96)00133-8

LE, D. T., Uram, J. N., Wang, H., Bartlett, B. R., Kemberling, H., Eyring, A. D., et al. (2015). PD-1 Blockade in Tumors with Mismatch-Repair Deficiency. *N. Engl. J. Med.* 372 (26), 2509–2520. doi:10.1056/NEJMoa1500596

Mg, L., and Mj, L. (1964). Electrophoretic Distribution Pattern of Lactate Dehydrogenase in Mouse and Human Muscular Dystrophy. *Clin. Chim. Acta* 9, 276–284. doi:10.1016/0009-8981(64)90108-1

Overman, M. J., Kopetz, S., Mcdermott, R. S., Leach, J., Lonardi, S., Lenz, H.-J., et al. (2016). Nivolumab ± Ipilimumab in Treatment (Tx) of Patients (Pts) with Metastatic Colorectal Cancer (mCRC) with and without High Microsatellite Instability (MSI-H): CheckMate-142 Interim Results. *Jco* 34 (15), 3501. doi:10.1200/jco.2016.34.15_suppl.3501

Overman, M. J., Lonardi, S., Wong, K. Y. M., Lenz, H.-J., Gelsomino, F., Aglietta, M., et al. (2018). Durable Clinical Benefit with Nivolumab Plus Ipilimumab in DNA Mismatch Repair-Deficient/Microsatellite Instability-High Metastatic Colorectal Cancer. *Jco* 36 (8), 773–779. doi:10.1200/JCO.2017.76.9901

Pandian, S. S., McClinton, S., Bissett, D., and Ewen, S. W. B. (1997). Lactate Dehydrogenase as a Tumour Marker in Adult Wilm's Tumour. *BJU Int.* 80 (4), 670–671. doi:10.1046/j.1464-410x.1997.00312.x

Schwartz, M. K. (1991). Lactic Dehydrogenase: An Old Enzyme Reborn as a Cancer Marker? *Am. J. Clin. Pathol.* 96 (4), 441–443. doi:10.1093/ajcp/96.4.441

Seyed Khoei, N., Anton, G., Peters, A., Freisling, H., and Wagner, K.-H. (2020). The Association between Serum Bilirubin Levels and Colorectal Cancer Risk: Results from the Prospective Cooperative Health Research in the Region of Augsburg (KORA) Study in Germany. *Antioxidants* 9 (10), 908. doi:10.3390/antiox9100908

Shin, Y. S., and Kim, H. J. (2013). Current Management of Testicular Cancer. *Korean J. Urol.* 54 (1), 2–10. doi:10.4111/kju.2013.54.1.2

Siegel, R. L., Miller, K. D., Goding Sauer, A., Fedewa, S. A., Butterly, L. F., Anderson, J. C., et al. (2020). Colorectal Cancer Statistics, 2020. *CA A. Cancer J. Clin.* 70 (3), 145–164. doi:10.3322/caac.21601

Tas, F., Aykan, F., Alici, S., Kaytan, E., Aydiner, A., and Topuz, E. (2001). Prognostic Factors in Pancreatic Carcinoma. *Am. J. Clin. Oncol.* 24 (6), 547–550. doi:10.1097/00000421-200112000-00003

Tas, F., Aykan, F., Alici, S., Kaytan, E., Aydiner, A., and Topuz, E. (2001). Prognostic Factors in Pancreatic Carcinoma. *Am. J. Clin. Oncol.* 24, 547–550. doi:10.1097/00000421-200112000-00003

Tejpar, S., Stintzing, S., Ciardiello, F., Tabernero, J., Van Cutsem, E., Beier, F., et al. (2017). Prognostic and Predictive Relevance of Primary Tumor Location in Patients with RAS Wild-type Metastatic Colorectal Cancer. *JAMA Oncol.* 3 (2), 194–201. doi:10.1001/jamaoncol.2016.3797

Temme, E. H. M., Zhang, J., Schouten, E. G., and Kesteloot, H. (2001). Serum Bilirubin and 10-year Mortality Risk in a Belgian Population. *Cancer Causes Control* 12 (10), 887–894. doi:10.1023/a:1013794407325

Wagner, K.-H., Wallner, M., Mölzer, C., Gazzin, S., Bulmer, A. C., Tiribelli, C., et al. (2015). Looking to the Horizon: the Role of Bilirubin in the Development and Prevention of Age-Related Chronic Diseases. *Clin. Sci. (Lond).* 129 (1), 1–25. doi:10.1042/CS20140566

Wróblewski, F., and Gregory, K. F. (1961). Lactic Dehydrogenase Isozymes and Their Distribution in Normal Tissues and Plasma and in Disease States*. *Ann. N. Y Acad. Sci.* 94, 912–932. doi:10.1111/j.1749-6632.1961.tb35584.x

Wulaningsih, W., Holmberg, L., Garmo, H., Malmstrom, H., Lambe, M., Hammar, N., et al. (2015). Prediagnostic Serum Inflammatory Markers in Relation to Breast Cancer Risk, Severity at Diagnosis and Survival in Breast Cancer Patients. *Carcin* 36 (10), 1121–1128. doi:10.1093/carcin/bgv096

You, W., Yan, L., Cai, Z., Xie, L., Sheng, N., Wang, G., et al. (2020). Clinical Significances of Positive Postoperative Serum CEA and Post-preoperative CEA Increment in Stage II and III Colorectal Cancer: A Multicenter Retrospective Study. *Front. Oncol.* 10, 671. doi:10.3389/fonc.2020.00671

Conflict of Interest: The authors declare that the research was conducted in the absence of any commercial or financial relationships that could be construed as a potential conflict of interest.

Publisher's Note: All claims expressed in this article are solely those of the authors and do not necessarily represent those of their affiliated organizations, or those of the publisher, the editors and the reviewers. Any product that may be evaluated in this article, or claim that may be made by its manufacturer, is not guaranteed or endorsed by the publisher.

frontiers in Molecular Biosciences

ORIGINAL RESEARCH
published: 05 November 2021
doi: 10.3389/fmolb.2021.745990

Hepatitis B Virus Promotes Hepatocellular Carcinoma Progression Synergistically With Hepatic Stellate Cells *via* Facilitating the Expression and Secretion of ENPP2

Wanyu Deng[1,2,3], *Fu Chen*[3], *Ziyu Zhou*[1,2], *Yipei Huang*[1,2], *Junlong Lin*[1,2], *Fapeng Zhang*[1,2], *Gang Xiao*[1,2], *Chaoqun Liu*[1,2], *Chao Liu*[1]* *and Leibo Xu*[1]*

[1]*Department of Biliary Pancreatic Surgery, Sun Yat-sen Memorial Hospital, Sun Yat-sen University, Guangzhou, China,* [2]*Guangdong Provincial Key Laboratory of Malignant Tumor Epigenetics and Gene Regulation, Sun Yat-sen Memorial Hospital, Sun Yat-sen University, Guangzhou, China,* [3]*College of Life Science, Shangrao Normal University, Shangrao, China*

OPEN ACCESS

Edited by:
Yunpeng Hua,
The First Affiliated Hospital of Sun Yat-sen University, China

Reviewed by:
Vikas Singh,
The Rockefeller University, United States
Shihai Liu,
The Affiliated Hospital of Qingdao University, China

***Correspondence:**
Leibo Xu
xuleibo3@mail.sysu.edu.cn
Chao Liu
liuchao3@mail.sysu.edu.cn

Specialty section:
This article was submitted to Molecular Diagnostics and Therapeutics, a section of the journal Frontiers in Molecular Biosciences

Received: *23 July 2021*
Accepted: *13 October 2021*
Published: *05 November 2021*

Citation:
Deng W, Chen F, Zhou Z, Huang Y, Lin J, Zhang F, Xiao G, Liu C, Liu C and Xu L (2021) Hepatitis B Virus Promotes Hepatocellular Carcinoma Progression Synergistically With Hepatic Stellate Cells via Facilitating the Expression and Secretion of ENPP2. Front. Mol. Biosci. 8:745990. doi: 10.3389/fmolb.2021.745990

Background: Hepatitis B virus (HBV) infection is a major risk factor causing hepatocellular carcinoma (HCC) development, but the molecular mechanisms are not fully elucidated. It has been reported that virus infection induces ectonucleotide pyrophosphatase-phosphodiesterase 2 (ENPP2) expression, the latter participates in tumor progression. Therefore, the aim of the present study was to investigate whether HBV induced HCC malignancy *via* ENPP2.

Methods: HCC patient clinical data were collected and prognosis was analyzed. Transient transfection and stable ectopic expression of the HBV genome were established in hepatoma cell lines. Immunohistochemical staining, RT-qPCR, western blot, and ELISA assays were used to detect the expression and secretion of ENPP2. Finally, CCK-8, colony formation, and migration assays as well as a subcutaneous xenograft mouse model were used to investigate the influence of HBV infection, ENPP2 expression, and activated hepatic stellate cells (aHSCs) on HCC progression *in vitro* and *in vivo*.

Results: The data from cancer databases indicated that the level of ENPP2 was significant higher in HCC compared within normal liver tissues. Clinical relevance analysis using 158 HCC patients displayed that ENPP2 expression was positively correlated with poor overall survival and disease-free survival. Statistical analysis revealed that compared to HBV-negative HCC tissues, HBV-positive tissues expressed a higher level of ENPP2. *In vitro*, HBV upregulated ENPP2 expression and secretion in hepatoma cells and promoted hepatoma cell proliferation, colony formation, and migration *via* enhancement of ENPP2; downregulation of ENPP2 expression or inhibition of its function suppressed HCC progression. In addition, aHSCs strengthened hepatoma cell proliferation, migration *in vitro*, and promoted tumorigenesis synergistically with HBV *in vivo*; a loss-function assay further verified that ENPP2 is essential for HBV/aHSC-induced HCC progression.

Conclusion: HBV enhanced the expression and secretion of ENPP2 in hepatoma cells, combined with aHSCs to promote HCC progression *via* ENPP2.

Keywords: hepatitis B virus-related hepatocellular carcinoma, prognosis, ectonucleotide pyrophosphatase-phosphodiesterase 2, hepatic stellate cells, progression

INTRODUCTION

Globally, hepatocellular carcinoma (HCC) is the dominant type of liver cancer, accounting for approximately 75% of the total (McGlynn et al., 2021). Although there have been improvements in treatments for HCC, the prognosis and survival rate for patients remain unsatisfying due to limited effective therapeutic options (Zhong et al., 2021). Hepatitis B virus (HBV) infection is the most prominent risk factor causing HCC occurrence and development in developing countries (Yang et al., 2019; Llovet et al., 2021). Viral infection causes the transformation of the liver to benefit hepatocyte malignancy *via* genome integration, activating oncogenes (Levrero and Zucman-Rossi, 2016), and changing the immune response process to an immunosuppressive microenvironment, especially in HCC patients (Liu et al., 2016; Wang et al., 2018; Li et al., 2020), resulting in virus persistence and reactivation (Shi and Zheng, 2020). HBV reactivation is an independent risk factor for HCC patient survival and antiviral treatment is associated with prolonging the overall survival (OS) (Liu S. et al., 2020) and risk reduction of tumor recurrence after curative treatment for HBV-related HCC patients (Huang et al., 2017; Huang et al., 2018), while the exact molecular mechanisms for HCC aggressiveness induced by HBV are still unclear.

Ectonucleotide pyrophosphatase-phosphodiesterase 2 (ENPP2) is a secreted lysophospholipase D and is largely responsible for converting extracellular lysophosphatidylcholine (LPC) into lysophosphatidic acid (LPA) (Salgado-Polo et al., 2018). ENPP2 is essential for normal development, is implicated in various physiological processes, and is also associated with pathological conditions including cancer (Nishimasu et al., 2012). For instance, inhibiting ENPP2 decreases initial breast tumor growth and subsequent lung metastatic nodules in mice (Benesch et al., 2014), ENPP2 is highly secreted from ovarian cancer stem cells (CSC) (Seo et al., 2016), and the ENPP2/LPA signaling axis is critical for maintaining CSC characteristics (Seo et al., 2016), facilitating estrogen-induced endometrial cancer cell proliferation (Zhang et al., 2018) and promoting K-ras-(G12D)-driven lung cancer pathogenesis (Magkrioti et al., 2018). Aberrant ENPP2 expression has been observed in several chronic inflammatory diseases or malignant diseases (Barbayianni et al., 2015), such as in chronic liver disease patients of different etiologies. ENPP2 in turn activates hepatic stellate cells (HSCs) and promotes HCC development (Enooku et al., 2016; Kaffe et al., 2017). Besides, in Hodgkin lymphoma, high levels of ENPP2 are strongly positivity associated with Epstein-Barr virus (EBV), EBV infection results in the induction of ENPP2 and leads to the enhanced growth and survival of Hodgkin lymphoma cells *via* the ENPP2/LPA axis (Baumforth et al., 2005). During hepatitis C virus infection, the plasma level of ENPP2 and LPA in patients are elevated (Kostadinova et al., 2016). It has been reported that increases in serum ENPP2 activity and protein levels have been found in patients with chronic hepatitis B (Joshita et al., 2018). This means virus infection may enhance ENPP2 expression. However, whether HBV infection regulates the expression of ENPP2 in hepatocytes and the role of ENPP2 in HBV-related HCC malignancy are still unknown. Herein, we want to verify whether ENPP2 is a factor that connects HBV infection and tumor progression in HBV-related HCC.

In the present study, we firstly analyzed the expression differences of ENPP2 between normal liver and HCC tissue, especially comparing the differences in HBV-positive and -negative HCC tissues. The prognostic correlations of ENPP2 expression and HCC patients were analyzed. We then designed a series of *in vitro* and *in vivo* studies to observe whether HBV induced HCC progression *via* enhancement of the expression and secretion of ENPP2. Finally, since in liver tissue HBV infection not only transforms host cell hepatocytes and activates HSC through viral antigens (Martin-Vilchez et al., 2008; Zan et al., 2013; Gong et al., 2016; Zhang et al., 2020) and possibly through ENPP2 from hepatocytes (Kaffe et al., 2017), we analyzed the role of activated HSC (aHSC) in HBV-related HCC progression. These data can improve our understanding of the molecular mechanisms in HBV-related HCC malignancy.

MATERIALS AND METHODS

Hepatocellular Carcinoma Patients and Tumor Tissues

The clinicopathologic information of HCC patients and tumor tissues (n = 158) was obtained from Sun Yat-sen Memorial Hospital, Sun Yat-sen University. Patient informed consent was obtained and the procedure of human sample collection was approved by the Ethics Committee of Sun Yat-sen Memorial Hospital (ethical number 202101). Data including primary HCC and adjacent noncancerous liver tissues were obtained from Oncomine (https://www.oncomine.org) and GEPIA (http://gepia.cancer-pku.cn) databases. OS was defined as the interval between the date of surgery and the date of either death or the last follow-up. Disease-free survival (DFS) was defined as the interval between the date of surgery and the date of either tumor recurrence or metastasis.

Reagents

HBV replication-competent clone pSM2-HBV harboring a head-to-tail tandem dimer of the HBV genome (GenBank accession number: V01460) was provided by Dr. Hans Will (Heinrich-Pette-Institute, Germany). Small interfering RNAs (siRNAs)

targeting ENPP2 were synthesized by Genepharma, Shanghai (sequences are listed in **Supplementary Table S1**). Secreted HBV surface antigen (HBsAg) and HBV e antigen (HBeAg) from cell culture media were detected by Roche Diagnostics (36461400, 33448500, respectively). Cultrex pathclear basement membrane extract (3432-010-01), an ELISA kit for detection of secreted ENPP2 (DENP20), and ENPP2 inhibitor PF-8380 (4078) were purchased from R&D system, United States. Cell counting kit-8 (CCK-8, 40203ES80) was purchased from Yeasen, China.

Cell Culture and Transfection

Human hepatoma cell lines HepG2, Huh7, immortalized hepatocyte L02, and immortalized activated hepatic stellate cell line LX-2 were maintained in DMEM supplemented with 1% penicillin/streptomycin, 10% fetal bovine serum (FBS, Gibco), and maintained at 37°C in a humidified 5% CO_2 atmosphere. HepG2.2.15 was cultured with an additional 500 μg/ml of G418 (Apexbio, United States). Plasmid pSM2-HBV (1.5 μg) and siRNAs (30 nM) were transfected into cells seeded in 6-well culture plates using lipofectamine 3000 (Invitrogen, United States) according to the manufacturer's instructions. The plasmid transfection and HBV expression efficiency were assessed according to published protocols (Deng et al., 2017).

Western Blotting Analysis

Whole cells were harvested 72 h after transfection and protein samples were subjected to sodium dodecyl sulfate-polyacrylamide gel electrophoresis (SDS-PAGE) and blotted with primary antibodies recognizing ENPP2 (ab77104, Abcam, British) and β-actin (Cell Signing, United States), respectively. Protein bands were visualized using ECL Plus western blotting detection reagents (Millipore, United States).

Enzyme-Linked Immunosorbent Assay

Secreted HBsAg and HBeAg in culture media from HCC cells were quantified by a double-antibody sandwich ELISA and compared to the cutoff value (the cutoff values were 0.05 for HBsAg and 1 for HBeAg). As for detection of secreted ENPP2, after balancing all reagents in the kit and samples to room temperature (RT), we added 100 μl of assay diluent RD1-34 to each well and then added 50 μl of standard, control, or sample per well in duplicate. The solutions were incubated for 2 h at RT on a horizontal orbital microplate shaker set at 500 rpm. Each well was aspirated and washed with wash buffer (400 μl) four times. A total of 200 μl of human ENPP2 conjugate was added to each well and incubated for 2 h at RT on the shaker. The solutions were aspirated and washed with wash buffer (400 μl) four times. A total of 200 μl of substrate solution was added to each well and incubated for 30 min at RT without light. Then, 50 μl of stop solution was added to each well and the optical density at 450 nm was detected with correction at 540 nm. A standard curve was constructed by plotting the mean absorbance for each standard on the y-axis against the concentration on the x-axis, and the concentration of ENPP2 for each sample was calculated according to the standard curve.

Quantitative Real-Time Polymerase Chain Reaction

Total RNAs were extracted using TRIzol reagent (Invitrogen, United States) and were reverse-transcribed with a PrimeScriptTM RT Reagent kit (Takara, Japan). RT-qPCR was performed with a 7500 Real-Time PCR system (Thermo Scientific, United States) using TB Green® Premix Ex Taq™ II as described by the manufacturer's protocol (Takara, Japan). The *enpp2* mRNA expression level was normalized to *gapdh* and quantified by the comparative CT ($2^{-\Delta\Delta CT}$) method and then multiplied by 10^6. All primers used for RT-qPCR are listed in **Supplementary Table S1**.

Cell Viability and Proliferation Assay

Cells were seeded in 96-well culture plates (Corning, United States) at a density of 5,000-10,000 cells/well, each sample seeded two wells. In order to detect the inhibitory ability of PF-8380, hepatoma cells were exposed to PF-8380 on the following day at various concentrations for 48 h. Cell proliferation was then measured by the CCK-8 assay according to the manufacturer's instructions. The absorbance was determined at 450 nm with a SPARK 10M Microplate Reader (Tecan, Switzerland). The percentage of cell growth inhibition was calculated and the concentration of PF-8380 resulting in a 50% reduction in cell viability was denoted as the 50% inhibitory concentration (IC_{50}).

Cell Migration Assay

The Transwell insert chambers (Corning, United States) was used to assess tumor cell migration ability. Briefly, after having assessed the cell viability, approximately 5–10×10^4 cells were suspended in serum-free DMEM and seeded into each well of the upper chamber for migration, and DMEM with 20% FBS or conditional media (CM) from LX-2 was added to the lower chamber as a chemoattractant. After 24/48 h of incubation, cells remaining in the upper chamber were removed with cotton swabs. The cells that passed through the membrane were fixed in 4% formaldehyde and stained with 0.1% crystal violet. Cells in at least three random microscopic fields (magnification, ×100) were counted.

Colony Formation Assay

For the colony formation assay, hepatoma cells were seeded in 6-well culture plates (500-1,000 cells/well), the culture medium or the LX-2 CM was replaced every 48 h. After 2 weeks of incubation, the number of colonies were counted in each well. A colony was counted as such when it had more than 50 cells. The capability of colony formation was evaluated by the colony formation number.

Immunohistochemistry

The expression of ENPP2 in the paraffin-embedded HCC samples was examined by IHC analysis. IHC experiments were performed as described previously (Xu et al., 2020), and sections were incubated with ENPP2 antibody (ab137590, Abcam, British, 1:400 dilution) overnight at 4°C. To evaluate ENPP2 expression, the scores were determined by the staining intensity and the percentage of positively stained areas. The final staining index

was the sum of the staining intensity and extent scores. Staining intensity was scored according to the following standard: zero (negative), one (weak), two (moderate), or three (strong). Scores zero and one and scores two and three were divided into low and high ENPP2 expression groups, respectively. In addition, the extent of staining was scored as follows: zero (0%), one (<10%), two (10–35%), three (36–75%), or four (>75%). Scores zero, one, and two and scores three and four were divided into low and high ENPP2 expression groups, respectively. The clinical samples were reviewed and scored separately by two experienced pathologists.

In vivo Tumor Xenograft Formation

Four-week-old male BALB/c nude mice were purchased from Slyke, Shanghai, China and acclimated to their surroundings for approximately 1 week with food and water before experiments. Animal studies were carried out in the South China University of Technology and approved by the Laboratory Animal Welfare and Ethics Committee of the South China University of Technology (ethical number 2021046). All animal experiments conformed to the approved guidelines of Animal Care and Use Committee of South China University of Technology. All efforts were made to minimize suffering. Mice were randomly divided into six groups (six mice per group): HepG2, LX-2, HepG2+LX-2, HepG2.2.15, HepG2.2.15+LX-2+DMSO, and HepG2.2.15+LX-2+PF-8380. Cells suspended in PBS were mixed with Matrigel with a ratio of 1:1 on ice, and then 200 μl of the cell mixture was seeded into the right flank *via* subcutaneous injection (5×10^6 cells/mouse and hepatoma cell: LX-2 = 3 : 1). Once tumors were palpable, HepG2.2.15+LX-2 groups were injected intraperitoneally with vehicle (DMSO) or PF-8380 at 30 mg/kg body weight twice daily for 2 weeks. The length and the width of tumors were measured every 3 days. Tumor volume was calculated using the formula (volume = $0.5\times$length $\times$ width^2). Mice were anesthetized with isoflurane gas, and sacrificed by cervical dislocation. Tumors were excised, weighed, and their volumes were measured.

Statistical Analysis

All data are shown as mean ± standard deviation (SD). Statistical significance of differences was detected by Student's two-tailed *t*-test between two groups and the ANOVA test for multiple comparisons using GraphPad Prism 5 software. Log-rank tests of Kaplan-Meier survival curves were conducted to elucidate the relationship between gene expression and patient survival. Differences were considered statistically significant at $p < 0.05$ ($^*p < 0.05$, $^{**}p < 0.01$, and $^{***}p < 0.001$).

RESULTS

Ectonucleotide Pyrophosphatase-Phosphodiesterase 2 Expression Is Positively Correlated to Poor Prognosis in Hepatocellular Carcinoma Patients

Oncomine and GEPIA databases indicated that ENPP2 expression was higher in HCC compared within normal liver tissues ($p < 0.05$; **Figures 1A,B**). Consistent with clinical data, ENPP2 expression and secretion were significant higher in hepatoma cells, including Huh7 and HepG2, compared within normal hepatocytes both in RNA and protein level (**Figures 1C,E**). Then liver tissues were collected for IHC from 158 HCC patients who underwent surgery, and the samples were classified into the ENPP2 high expression group ($ENPP2^{high}$, n = 106) and ENPP2 low expression group ($ENPP2^{low}$, n = 52). The OS and DFS were both worse in $ENPP2^{high}$ than $ENPP2^{low}$ ($p = 0.0445$ for OS, $p = 0.0071$ for DFS; **Figures 1F,G**).

Hepatitis B Virus Enhances Ectonucleotide Pyrophosphatase-Phosphodiesterase 2 Expression and Secretion

In the above 158 HCC patients, 25 patients were HBV-negative (HBV-, both HBV DNA and HBsAg were negative in patient serum) and 133 patients were HBV-positive (HBV+, HBV DNA load was more than 5×10^2, and HBsAg was positive in patient serum). In the HBV + cohort, 72.2% of patients had high ENPP2 expression, while only 40.0% of patients displayed high ENPP2 expression in the HBV- cohort, the expression difference between the two cohorts was significant ($p = 0.003$; **Figures 2A,B**). In order to illuminate the correlation between HBV infection and ENPP2 expression, plasmid pSM2-HBV was transfected into hepatoma cells, then ENPP2 expression and secretion was tested. RT-qPCR results showed that enpp2 mRNA was enhanced by HBV transfection both in Huh7 and HepG2 (**Figures 2C,D**); western blot and ELISA assays displayed that the intracellular and secreted ENPP2 were also upregulated significantly in the HBV transfected group compared to the control group transfected with the empty vector (**Figures 2E–H**).

Hepatitis B Virus Induces Hepatoma Cell Proliferation, Colony Formation, and Migration *via* Upregulation of Ectonucleotide Pyrophosphatase-Phosphodiesterase 2

Next, in order to elucidate whether HBV induces HCC progression *via* regulation of ENPP2, plasmid pSM2-HBV was transfected into hepatoma cells to express the HBV genome, then cells were re-transfected with siRNAs to knock down ENPP2 expression. The knockdown efficiencies for the two selected siRNAs targeting ENPP2 (siENPP2-1 and siENPP2-4) were more than 70% (**Supplementary Figure S1**). The immunoblotting results confirmed that HBV transfection enhanced ENPP2 expression and secretion both at the RNA and protein level, while knocking down of ENPP2 weakened these phenomena both in Huh7 and HepG2 (**Figures 3A–E**). The CCK-8 assay displayed that compared to those transfected with control vector, hepatoma cells transfected with pSM2-HBV had a stronger ability of proliferation, while

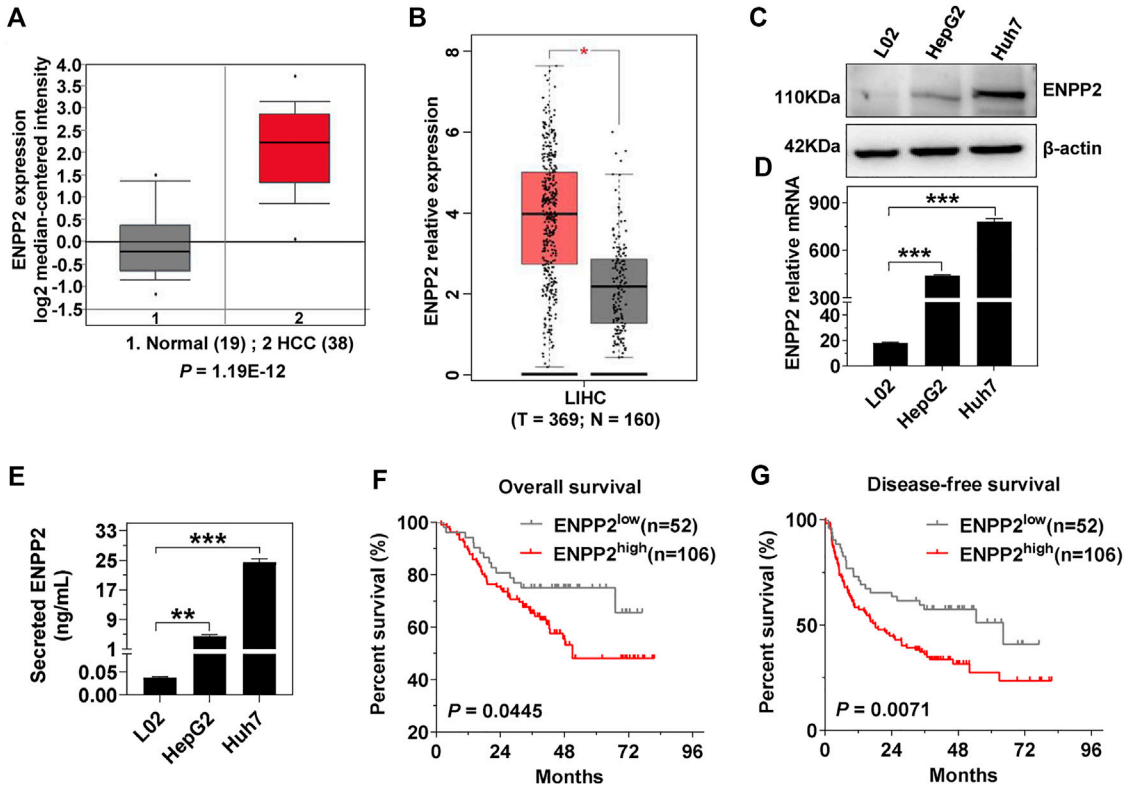

FIGURE 1 | ENPP2 expression is positively correlated with poor patient prognosis. **(A)** Oncomine database analysis of the ENPP2 median-centered intensity in normal (n = 19) and HCC tissue (n = 38). **(B)** GEPIA database analysis of the relative mRNA expression of enpp2 in matched HCC tissues (n = 369) and adjacent normal tissues (n = 160). **(C)** The intracellular ENPP2 protein expression in L02, HepG2, and Huh7, respectively. **(D)** The level of enpp2 mRNA in L02, HepG2, and Huh7, respectively. **(E)** The secreted ENPP2 in supernatants from L02, HepG2, and Huh7, respectively. **(F, G)** Overall survival (F) and disease-free survival (G) for $ENPP2^{high}$ (n = 106) and $ENPP2^{low}$ (n = 52) expression patients, respectively. The statistical analysis was based on three independent experiments. *, $p < 0.05$; **, $p < 0.01$; ***, $p < 0.001$.

knocking down of ENPP2 could inhibit cell proliferation significantly (**Figures 3F,G**). The colony formation assay confirmed that HBV enhanced hepatoma cell proliferation and this phenomenon could be weakened by knocking down ENPP2 expression both in Huh7 and HepG2 (**Figures 3H,I**). HBV also promoted hepatoma cell migration, while knocking down of ENPP2 could inhibit hepatoma cell migration even though cells were transfected with pSM2-HBV (**Figures 3J,K**).

Then PF-8380, a small molecule inhibitor that suppresses the activity of ENPP2 and has a reported IC_{50} of 1.7 nM on natural LPC substrates, was used (Gierse et al., 2010). *In vitro,* the inhibition on hepatoma cell viability was tested, and the IC_{50} on Huh7 and HepG2 were 44.2 and 45.6 nM, respectively (**Figures 4A,B**). PF-8380 inhibited Huh7 and HepG2 proliferation obviously even though the hepatoma cells were under the condition of HBV transfection (**Figures 4C,D**). The colony formation assay confirmed that HBV was enhanced, but PF-8380 inhibited hepatoma cell colony formation obviously (**Figures 4E,F**). The cell migration assay showed that PF-8380 impeded the ability of migration for Huh7 and HepG2 even though the cells were transfected with pSM2-HBV (**Figures 4G,H**).

Hepatocellular Carcinoma Progression Induced by Hepatitis B Virus Is Strengthened by Activated Hepatic Stellate Cells

The above results confirmed that HBV promoted tumor cell proliferation and migration *via* enhancement of ENPP2 expression and secretion in hepatoma cells. A major contributor to tumor progression is the cross talk between tumor cells and the surrounding stroma. HSC is the major surrounding cell in the liver tumor microenvironment and aHSC normally promotes HCC progression (Barry et al., 2020; Ruan et al., 2020). So co-culture assays were performed between hepatoma cells and aHSC, the effects of these interactions were then studied by a series of functional assays. The CCK-8 assay showed that cell proliferation was enhanced obviously when co-culturing HepG2 or Huh7 with LX-2 compared to cultured hepatoma cells alone, especially when hepatoma cells were transfected with pSM2-HBV (**Figures 5A,B**). While the inhibitor PF-8380 could suppress cell proliferation even though the hepatoma cells were both under pSM2-HBV transfection and co-cultured with LX-2 (**Figures 5A,B**). Hepatoma cells were also incubated with LX-2 CM and the

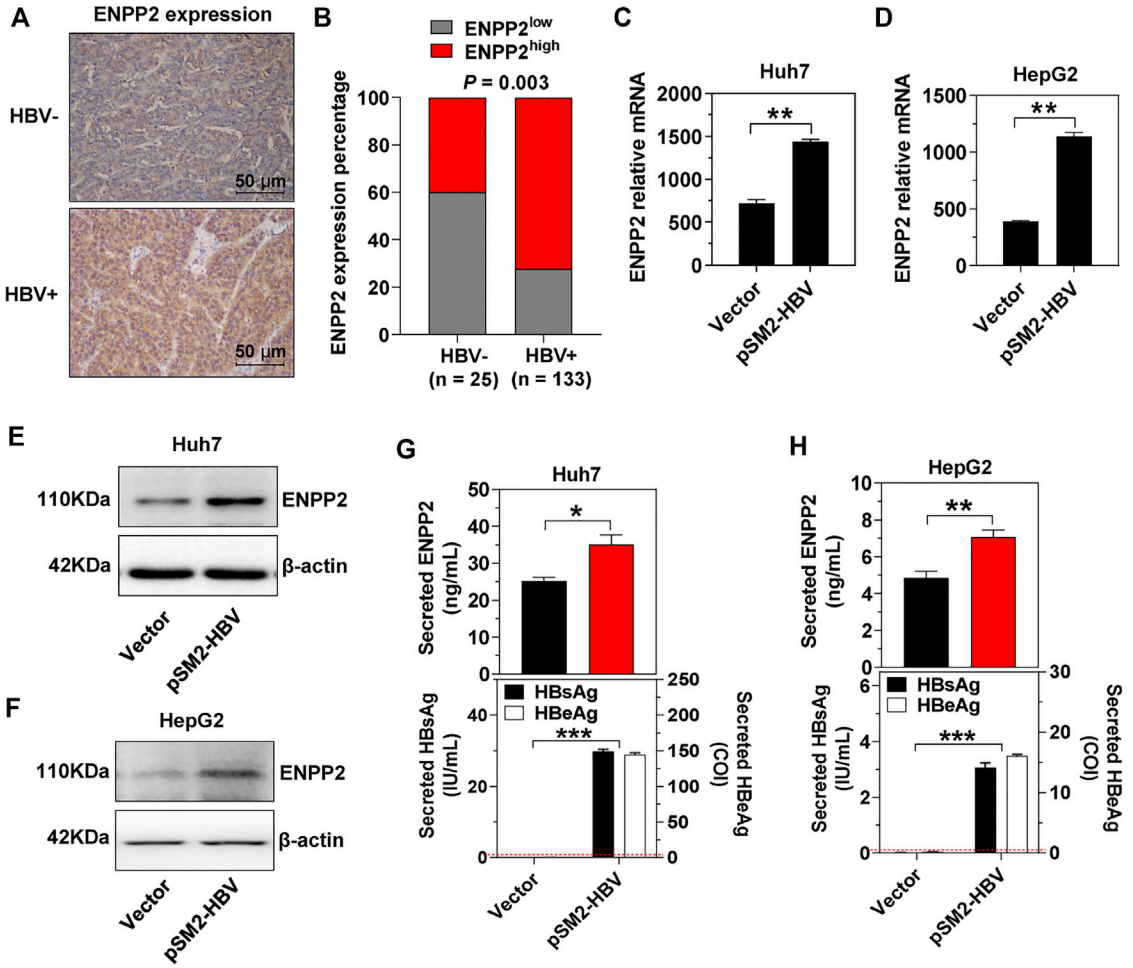

FIGURE 2 | HBV enhances ENPP2 expression and secretion. **(A)** Representative IHC images of ENPP2 staining in HBV- and HBV + HCC tissues (magnification ×200). **(B)** ENPP2 expression percentage in HBV- (n = 25) and HBV + HCC tissues (n = 133), respectively. **(C, D)** The level of enpp2 mRNA in Huh7 (C) and HepG2 (D) after being transfected with vector or pSM2-HBV for 3 days. **(E, F)** The intracellular ENPP2 protein in Huh7 (E) and HepG2 (F) after being transfected with vector or pSM2-HBV for 3 days. **(G, H)** The secreted ENPP2, HBsAg, and HBeAg in supernatants from Huh7 (G) and HepG2 (H) after being transfected with vector or pSM2-HBV for 3 days, respectively. The red dotted line in the graph represents the cutoff for HBsAg and HBeAg. The statistical analysis was based on three independent experiments. *, $p < 0.05$; **, $p < 0.01$.

results showed that LX-2 CM significantly enhanced the colony formation for Huh7 and HepG2, especially when hepatoma cells were transfected with pSM2-HBV, while these phenomena were suppressed by PF-8380 (**Figures 5C,D**). In addition to cell proliferation, LX-2 CM also enhanced Huh7 and HepG2 migration, especially when hepatoma cells were transfected with pSM2-HBV, while these phenomena were also suppressed by PF-8380 (**Figures 5E,F**).

Hepatitis B Virus and Activated Hepatic Stellate Cells Induce Hepatocellular Carcinoma Progression Synergistically *in vivo*

To explore whether HBV determined the tumorigenicity of HCC *in vivo*, we used HepG2.2.15, a cell line derived from HepG2, to integrate and express the HBV whole genome stably. Compared to HepG2, there was much more intracellular and secretory ENPP2 in HepG2.2.15 (**Figures 6A–C**). The proliferation, colony formation, and migration ability of HepG2.2.15 were stronger than HepG2 or HepG2 transfected with pSM2-HBV, especially when HepG2.2.15 was incubated with LX-2 CM, while PF-8380 could inhibit HepG2.2.15 proliferation and migration even though the cells were incubated with LX-2 CM (**Figures 6D–H**).

Then subcutaneous transplantation of HepG2 and HepG2.2.15, or co-transplantation of HepG2 and HepG2.2.15 with LX-2 into immune-compromised nude mice was carried out to observe tumor growth. There was no tumor formation in mice injected either with HepG2 or LX-2 alone, while mice co-injected with HepG2 and LX-2 (HepG2+LX-2) had obvious tumor formations on day 10 (**Figure 6I**). Mice injected with HepG2.2.15 alone also formed tumors, the tumors in mice co-injected with

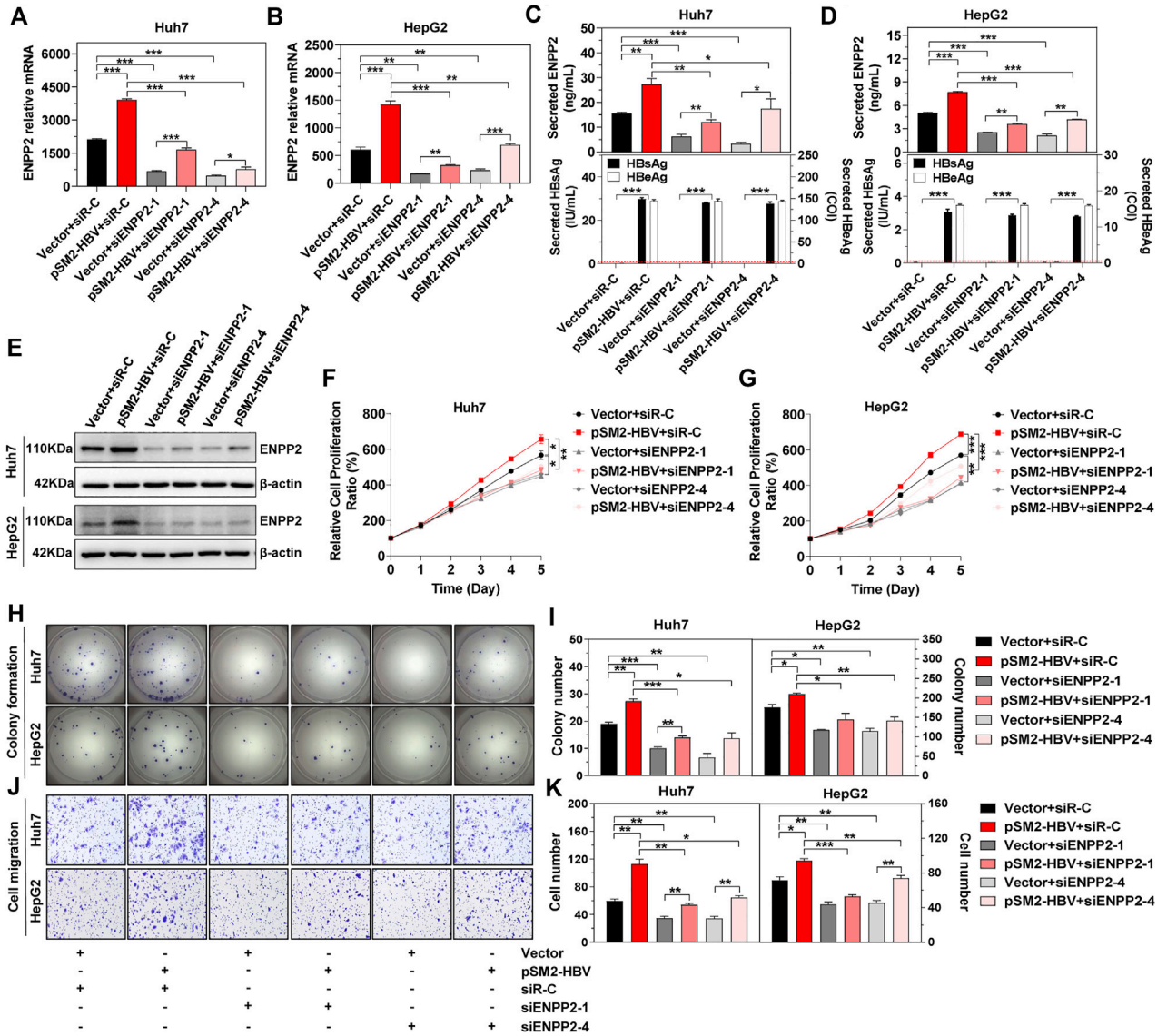

FIGURE 3 | HBV enhances hepatoma cell proliferation, colony formation, and migration, and was impeded by knocking down of ENPP2 expression. Hepatoma cells were firstly transfected with vector or pSM2-HBV for 1 day (set as day 0), and then transfected with siR-C or siENPP2. **(A, B)** The level of enpp2 mRNA in Huh7 (A) and HepG2 (B) after being transfected with siRNAs for 3 days. **(C, D)** Secreted ENPP2, HBsAg, and HBeAg in supernatants from Huh7 (C) and HepG2 (D) after being transfected with siRNAs for 3 days. The red dotted line in the graph represents the cutoff for HBsAg and HBeAg. **(E)** The intracellular ENPP2 expression in Huh7 **(upper panels)** and HepG2 **(below panels)** after being transfected with siRNAs for 3 days. **(F, G)** The cell proliferation ability for Huh7 (F) and HepG2 (G), respectively. **(H)** Representative images of colony formation for Huh7 **(upper panels)** and HepG2 **(below panels)**, respectively. **(I)** The bar graph of colony number indicated quantitative analysis data for Huh7 **(left panel)** and HepG2 **(right panel)**, respectively. **(J)** Representative images of the cell migration assay for Huh7 **(upper panels)** and HepG2 **(below panels)**, respectively (magnification ×100). **(K)** The bar graph of cell number migrated from Transwell indicated quantitative analysis data for Huh7 **(left panel)** and HepG2 **(right panel)**, respectively. The statistical analysis was based on three replicates. *, $p < 0.05$; **, $p < 0.01$; ***, $p < 0.001$.

HepG2.2.15 and LX-2 (HepG2.2.15+LX-2) were larger than those injected with HepG2.2.15 alone on day 10 ($p < 0.001$) (**Figure 6I**). To further assess that ENPP2 was the key factor in liver tumor formation in this mouse model, intraperitoneal injection of PF-8380 or DMSO was conducted in mice subcutaneously transplanted with HepG2.2.15+LX-2. Compared to DMSO, intraperitoneal injection of PF-8380 significantly suppressed tumor growth ($p < 0.05$ on day-13), and after injection of an inhibitor for two consecutive weeks, the tumors in the HepG2.2.15+LX-2+PF-8380 group were almost undetectable. While the average size of tumors in the HepG2.2.15+LX-2+DMSO group was 232 mm^3 ($p < 0.001$), other groups, including the HepG2+LX-2 and HepG2.2.15 groups also had growing tumors, and the volume of tumors among these four groups had significant differences on day 25 (**Figures 6I,J**). The tumor weight among these four groups also had statistic differences except between HepG2+LX-2 and HepG2.2.15 groups (**Figure 6K**).

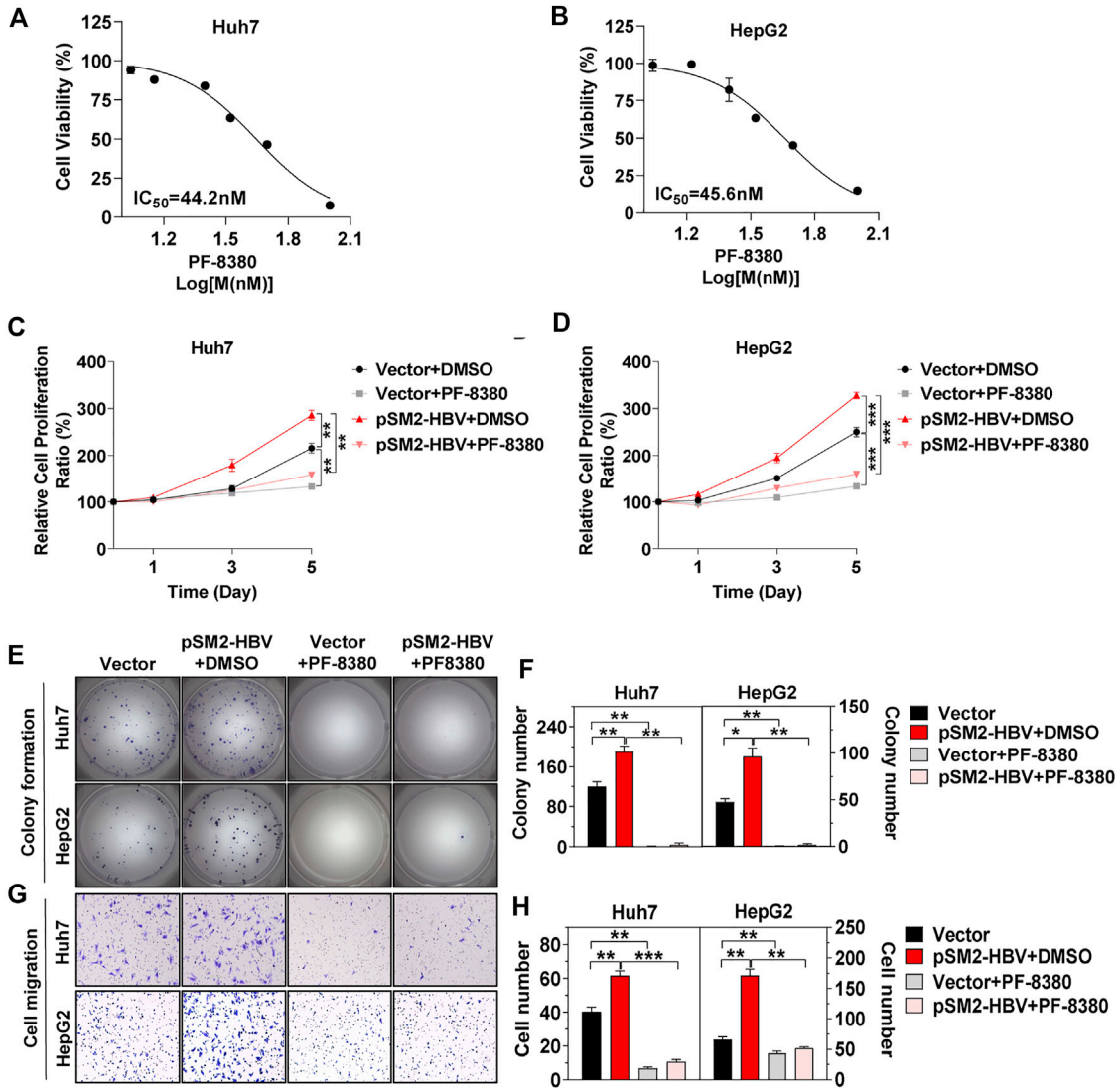

FIGURE 4 | HCC progression induced by HBV is impeded by inhibitor PF-8380. Hepatoma cells were transfected with vector or pSM2-HBV for 1 day (set as day 0) and then treated cells with vehicle DMSO or ENPP2 inhibitor PF-8380. **(A, B)** Antiproliferative activity of PF-8380 against Huh7 (A) and HepG2 (B) *in vitro*. **(C, D)** A CCK-8 assay was carried out to detect cell proliferation for Huh7 (C) and HepG2 (D), respectively. **(E)** Representative images of colony formation for Huh7 **(upper panels)** and HepG2 **(below panels)**, respectively. **(F)** The bar graph of colony number indicated quantitative analysis data for Huh7 **(left panel)** and HepG2 **(right panel)**, respectively. **(G)** Representative images of the cell migration assay for Huh7 **(upper panels)** and HepG2 **(below panels)**, respectively (magnification ×100). **(H)** The bar graph of cell number migrated from Transwell indicated quantitative analysis data for Huh7 **(left panel)** and HepG2 **(right panel)**, respectively. The statistical analysis was based on three replicates. *, $p < 0.05$; **, $p < 0.01$; ***, $p < 0.001$.

DISCUSSION

Differences in the etiologies and pathogenic mechanisms of hepatocarcinogenesis may reflect the unique clinical characteristics and prognosis in patients with HCC, and patients with negative HBV infection normally have better prognosis and lower risk of tumor recurrence than HBV-positive patients (Utsunomiya et al., 2015; Liu A. P. Y. et al., 2020). In the present study, our *in vitro* and *in vivo* results verified that transient transfection or stable expression of the HBV genome enhanced hepatoma cell proliferation and migration and also promoted xenograft tumor formation in nude mice. These mean antiviral treatments still act as key approaches to improve patient prognosis and could significantly decrease tumor recurrence and tumor-related death for HBV-related HCC patients.

Increased ENPP2 expression is detected in chronic liver disease patients of different etiologies, including HBV-associated liver disease (Kaffe et al., 2017; She et al., 2018). The data from cancer databases confirmed that ENPP2 was highly expressed in HCC tissue compared within normal liver tissues, our clinical data displayed that HCC patients with high ENPP2 level normally had poor prognosis, and ENPP2 expression was positively correlated with HBV infection.

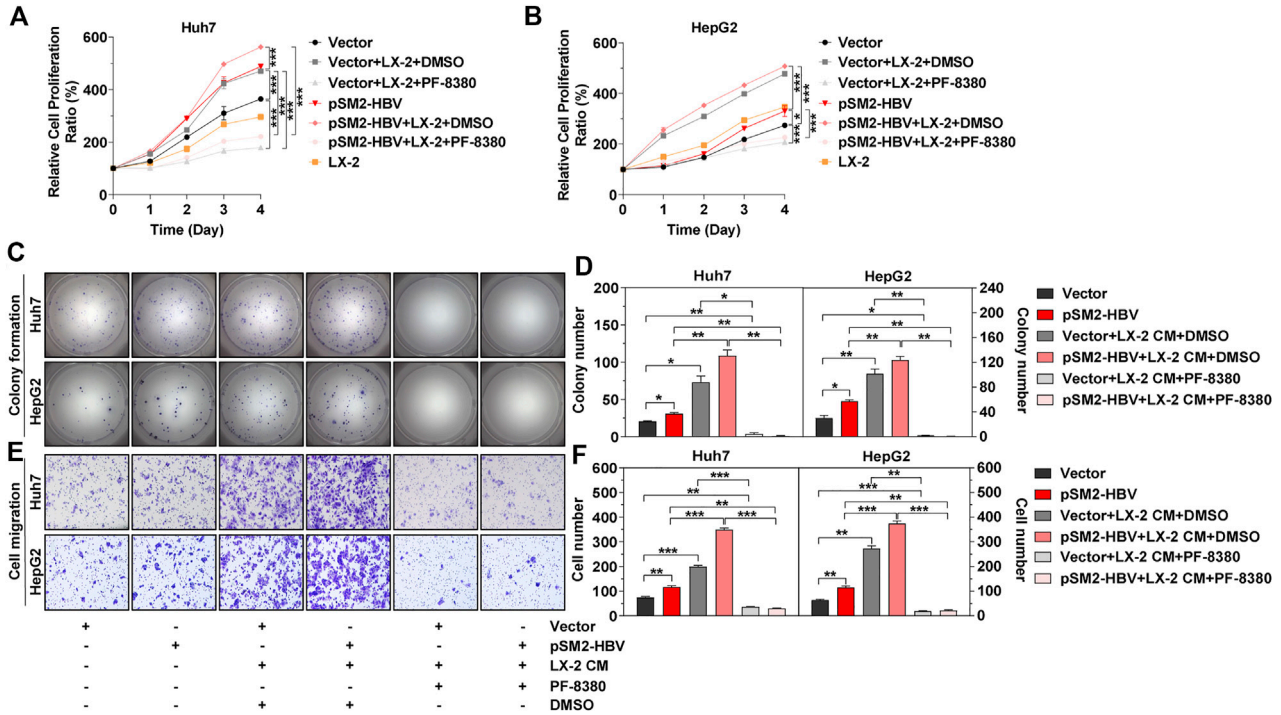

FIGURE 5 | Activated HSC strengthens HCC progression induced by HBV. Hepatoma cells were transfected with vector or pSM2-HBV for 1 day (set as day 0) and then co-cultured with LX-2 or treated with LX-2 CM containing DMSO or PF-8380. **(A, B)** Cell proliferation abilities for Huh7 (A) or HepG2 (B), respectively. **(C)** Representative images of colony formation for Huh7 **(upper panels)** and HepG2 **(below panels)**, respectively. **(D)** The bar graph of colony number indicated quantitative analysis data for Huh7 **(left panel)** and HepG2 **(right panel)**, respectively. **(E)** Representative images of the cell migration assay for Huh7 **(upper panels)** and HepG2 **(below panels)**, respectively (magnification ×100). **(F)** The bar graph of cell number migrated from Transwell indicated quantitative analysis data for Huh7 **(left panel)** and HepG2 **(right panel)**, respectively. The statistical analysis was based on three replicates. *, $p < 0.05$; **, $p < 0.01$; ***, $p < 0.001$.

Besides, our results indicated that knocking down of ENPP2 expression or inhibiting ENPP2 function could impede hepatoma cell proliferation, migration, and xenograft tumor formation induced by HBV. Mechanistically, ENPP2 hydrolyzes LPC to produce LPA (Salgado-Polo et al., 2018), a lipid mediator that functions as a mitogen and motility factor to stimulate proliferation, migration, and survival of cancer cells through combination with the LPA receptors (LPAR) (Houben and Moolenaar, 2011), which are overlapping specificities and have widespread distribution (Choi et al., 2010). Bioinformatics analysis suggests that lipid metabolisms are strongly activated by HBV-associated proteins and lead to the progression of liver tumors (Xu et al., 2016). These indicate that ENPP2 induced by HBV may promote HCC progression *via* downstream LPA/LPAR in HBV-related HCC patients.

Besides altering gene expressions in host cells, virus infection often transfers environment. It is reported that HBV infection causes liver fibrosis *via* activation of HSC (Zan et al., 2013; Gong et al., 2016; Zhang et al., 2020). In our results, we confirmed that HBV enhanced the secretion of ENPP2 in hepatoma cells, and ENPP2 is reported to have the function to activate HSC (Kaffe et al., 2017), these points imply that HBV may activate HSC *via* ENPP2. On the other hand, approximately 90% of HCC cases arise in the context of liver fibrosis (Seitz and Stickel, 2006), during the hepatic fibrotic process, activation of HSC drives fibrogenesis, changes the composition of the extracellular matrix, and is considered to be the central event that contributes to hepatic malignancies (Santamato et al., 2011; Zhang and Friedman, 2012; Coulouarn and Clement, 2014). Our co-culture assays showed that aHSC could strengthen hepatoma cell proliferation, colony formation, migration, and tumor formation induced by HBV *via* ENPP2 both *in vitro* and *in vivo*. In pancreatic ductal adenocarcinoma (PDAC), LPCs secreted from activated pancreatic stellate cells could be hydrolyzed by ENPP2, which was produced by PDAC, and finally promoted pancreatic tumor progression *via* the ENPP2/LPA axis (Auciello et al., 2019; Biffi and Tuveson, 2019), so in future, we need to clarify if aHSC may also secrete LPCs acting as a major substrate for ENPP2, and if HBV induces HCC progression not only by autocrine ENPP2, but also transfers the microenvironment to benefit HCC survival *via* the LPC/ENPP2/LPA axis in HBV-related HCC patients.

In summary, this study clarified that HBV infection induced ENPP2 expression and secretion in hepatocytes. HSC could synergistically enhance hepatoma cell proliferation, migration, and liver tumor formation with HBV *via* ENPP2. These indicate that besides antiviral therapy, ENPP2 could also be considered as a key regulation factor in improving prognosis for HBV-related HCC patients.

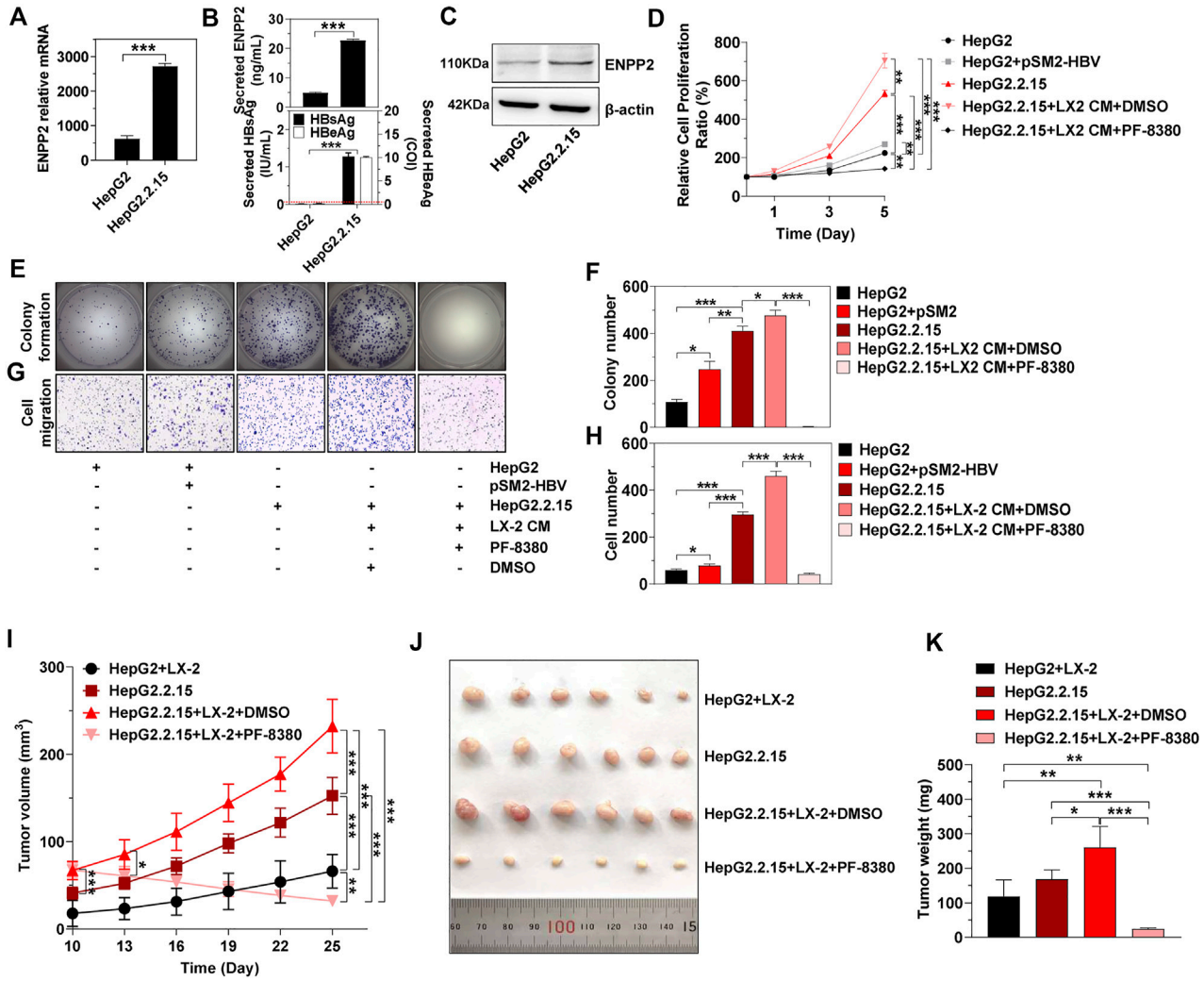

FIGURE 6 | HBV and aHSC induce HCC progression synergistically *in vivo*. **(A)** The level of enpp2 mRNA in HepG2 and HepG2.2.15. **(B)** The secretory ENPP2, HBsAg, and HBeAg in supernatants from HepG2 and HepG2.2.15. The red dotted line in the graph represented the cutoff for HBsAg and HBeAg. The statistical analysis was based on three independent experiments. **(C)** The intracellular ENPP2 protein in HepG2 and HepG2.2.15. HepG2.2.15 and HepG2, transfected with vector or pSM2-HBV for 1 day (set as day 0), were treated with LX-2 CM containing DMSO or PF-8380, and then hepatoma cell function was detected. **(D)** Cell proliferation for each group. The statistical analysis was based on three replicates. **(E)** Representative images of colony formation for each group cells. (**F**) The bar graph of colony number indicated quantitative analysis data based on three independent experiments for each group of cells. **(G)** Representative images of the cell migration assay for each group of cells (magnification ×100). **(H)** The bar graph of cell number migrated from Transwell indicated quantitative analysis data based on three independent experiments for each group of cells. **(I)** Tumor growth at different times in each group in nude mice (error bars, SD of six mice per group). **(J)** The final tumor size in nude mice upon subcutaneous transplantation with hepatoma cells or co-transplantation with hepatoma cells with LX-2 (3:1 ratio). Indicated groups were treated with vehicle DMSO or PF-8380 for two consecutive weeks. **(K)** Bar charts show the final tumor weight of each group of mice. *, $p < 0.05$; **, $p < 0.01$; ***, $p < 0.001$.

DATA AVAILABILITY STATEMENT

The original contributions presented in the study are included in the article/**Supplementary Material**, further inquiries can be directed to the corresponding authors.

ETHICS STATEMENT

The studies involving human participants were reviewed and approved by Sun Yat-sen Memorial Hospital, Sun Yat-sen University. The patients/participants provided their written informed consent to participate in this study. The animal study was reviewed and approved by South China University of Technology.

AUTHOR CONTRIBUTIONS

WD designed the research, carried out the experiments, and wrote the first draft of the manuscript. YH helped with the experiments. ZZ and FC helped in analyzing the data. FZ and

JL provided the HCC tissue samples and patient information. CQL and GX contributed to statistical analysis. CL supervised the project. CL and LX read and approved the manuscript. All authors contributed to the article and approved the submitted version.

FUNDING

This work was supported by grants from the National Natural Science Foundation of China (No. 81801999, 81772597, 81672412, 81972255); the Guangdong Basic and Applied Basic Research Foundation (No. 2021A1515010095); the Shangrao Science and Technology Department (No. 2020D001); the Natural Science Foundation of Jiangxi Province (No. 20181BAB214002); Education Department Science and Technology Foundation of Jiangxi Province (No. 6000216); and the Guangdong Science and Technology Department (No. 2017B030314026).

SUPPLEMENTARY MATERIAL

The Supplementary Material for this article can be found online at: https://www.frontiersin.org/articles/10.3389/fmolb.2021.745990/full#supplementary-material

REFERENCES

Auciello, F. R., Bulusu, V., Oon, C., Tait-Mulder, J., Berry, M., Bhattacharyya, S., et al. (2019). A Stromal Lysolipid-Autotaxin Signaling Axis Promotes Pancreatic Tumor Progression. *Cancer Discov.* 9, 617–627. doi:10.1158/2159-8290.CD-18-1212

Barbayianni, E., Kaffe, E., Aidinis, V., and Kokotos, G. (2015). Autotaxin, a Secreted Lysophospholipase D, as a Promising Therapeutic Target in Chronic Inflammation and Cancer. *Prog. Lipid Res.* 58, 76–96. doi:10.1016/j.plipres.2015.02.001

Barry, A. E., Baldeosingh, R., Lamm, R., Patel, K., Zhang, K., Dominguez, D. A., et al. (2020). Hepatic Stellate Cells and Hepatocarcinogenesis. *Front. Cel Dev. Biol.* 8, 709. doi:10.3389/fcell.2020.00709

Baumforth, K. R. N., Flavell, J. R., Reynolds, G. M., Davies, G., Pettit, T. R., Wei, W., et al. (2005). Induction of Autotaxin by the Epstein-Barr Virus Promotes the Growth and Survival of Hodgkin Lymphoma Cells. *Blood* 106, 2138–2146. doi:10.1182/blood-2005-02-0471

Benesch, M. G. K., Tang, X., Maeda, T., Ohhata, A., Zhao, Y. Y., Kok, B. P. C., et al. (2014). Inhibition of Autotaxin Delays Breast Tumor Growth and Lung Metastasis in Mice. *FASEB j.* 28, 2655–2666. doi:10.1096/fj.13-248641

Biffi, G., and Tuveson, D. A. (2019). A FATal Combination: Fibroblast-Derived Lipids and Cancer-Derived Autotaxin Promote Pancreatic Cancer Growth. *Cancer Discov.* 9, 578–580. doi:10.1158/2159-8290.CD-19-0273

Choi, J. W., Herr, D. R., Noguchi, K., Yung, Y. C., Lee, C.-W., Mutoh, T., et al. (2010). LPA Receptors: Subtypes and Biological Actions. *Annu. Rev. Pharmacol. Toxicol.* 50, 157–186. doi:10.1146/annurev.pharmtox.010909.105753

Coulouarn, C., and Clément, B. (2014). Stellate Cells and the Development of Liver Cancer: Therapeutic Potential of Targeting the Stroma. *J. Hepatol.* 60, 1306–1309. doi:10.1016/j.jhep.2014.02.003

Deng, W., Zhang, X., Ma, Z., Lin, Y., and Lu, M. (2017). MicroRNA-125b-5p Mediates post-transcriptional Regulation of Hepatitis B Virus Replication via the LIN28B/let-7 axis. *RNA Biol.* 14, 1389–1398. doi:10.1080/15476286.2017.1293770

Enooku, K., Uranbileg, B., Ikeda, H., Kurano, M., Sato, M., Kudo, H., et al. (2016). Higher LPA2 and LPA6 mRNA Levels in Hepatocellular Carcinoma Are Associated with Poorer Differentiation, Microvascular Invasion and Earlier Recurrence with Higher Serum Autotaxin Levels. *PLoS One* 11, e0161825. doi:10.1371/journal.pone.0161825

Gierse, J., Thorarensen, A., Beltey, K., Bradshaw-Pierce, E., Cortes-Burgos, L., Hall, T., et al. (2010). A Novel Autotaxin Inhibitor Reduces Lysophosphatidic Acid Levels in Plasma and the Site of Inflammation. *J. Pharmacol. Exp. Ther.* 334, 310–317. doi:10.1124/jpet.110.165845

Gong, J., Tu, W., Han, J., He, J., Liu, J., Han, P., et al. (2016). Hepatic SATB1 Induces Paracrine Activation of Hepatic Stellate Cells and Is Upregulated by HBx. *Sci. Rep.* 6, 37717. doi:10.1038/srep37717

Houben, A. J. S., and Moolenaar, W. H. (2011). Autotaxin and LPA Receptor Signaling in Cancer. *Cancer Metastasis Rev.* 30, 557–565. doi:10.1007/s10555-011-9319-7

Huang, G., Li, P.-p., Lau, W. Y., Pan, Z.-y., Zhao, L.-h., Wang, Z.-g., et al. (2018). Antiviral Therapy Reduces Hepatocellular Carcinoma Recurrence in Patients with Low HBV-DNA Levels. *Ann. Surg.* 268, 943–954. doi:10.1097/SLA.0000000000002727

Huang, S., Xia, Y., Lei, Z., Zou, Q., Li, J., Yang, T., et al. (2017). Antiviral Therapy Inhibits Viral Reactivation and Improves Survival after Repeat Hepatectomy for Hepatitis B Virus-Related Recurrent Hepatocellular Carcinoma. *J. Am. Coll. Surgeons* 224, 283–293 e4. doi:10.1016/j.jamcollsurg.2016.11.009

Joshita, S., Ichikawa, Y., Umemura, T., Usami, Y., Sugiura, A., Shibata, S., et al. (2018). Serum Autotaxin Is a Useful Liver Fibrosis Marker in Patients with Chronic Hepatitis B Virus Infection. *Hepatol. Res.* 48, 275–285. doi:10.1111/hepr.12997

Kaffe, E., Katsifa, A., Xylourgidis, N., Ninou, I., Zannikou, M., Harokopos, V., et al. (2017). Hepatocyte Autotaxin Expression Promotes Liver Fibrosis and Cancer. *Hepatology* 65, 1369–1383. doi:10.1002/hep.28973

Kostadinova, L., Shive, C. L., Judge, C., Zebrowski, E., Compan, A., Rife, K., et al. (2016). During Hepatitis C Virus (HCV) Infection and HCV-HIV Coinfection, an Elevated Plasma Level of Autotaxin Is Associated with Lysophosphatidic Acid and Markers of Immune Activation that Normalize during Interferon-free HCV Therapy. *J. Infect. Dis.* 214, 1438–1448. doi:10.1093/infdis/jiw372

Levrero, M., and Zucman-Rossi, J. (2016). Mechanisms of HBV-Induced Hepatocellular Carcinoma. *J. Hepatol.* 64, S84–S101. doi:10.1016/j.jhep.2016.02.021

Li, B., Yan, C., Zhu, J., Chen, X., Fu, Q., Zhang, H., et al. (2020). Anti-PD-1/PD-L1 Blockade Immunotherapy Employed in Treating Hepatitis B Virus Infection-Related Advanced Hepatocellular Carcinoma: A Literature Review. *Front. Immunol.* 11, 1037. doi:10.3389/fimmu.2020.01037

Liu, A. P. Y., Soh, S.-Y., Cheng, F. W. C., Pang, H. H., Luk, C.-W., Li, C.-H., et al. (2020a). Hepatitis B Virus Seropositivity Is a Poor Prognostic Factor of Pediatric Hepatocellular Carcinoma: a Population-Based Study in Hong Kong and Singapore. *Front. Oncol.* 10, 570479. doi:10.3389/fonc.2020.570479

Liu, S., Lai, J., Lyu, N., Xie, Q., Cao, H., Chen, D., et al. (2020b). Effects of Antiviral Therapy on HBV Reactivation and Survival in Hepatocellular Carcinoma Patients Undergoing Hepatic Artery Infusion Chemotherapy. *Front. Oncol.* 10, 582504. doi:10.3389/fonc.2020.582504

Liu, Y., Cheng, L.-s., Wu, S.-d., Wang, S.-q., Li, L., She, W.-m., et al. (2016). IL-10-producing Regulatory B-Cells Suppressed Effector T-Cells but Enhanced Regulatory T-Cells in Chronic HBV Infection. *Clin. Sci. (Lond)* 130, 907–919. doi:10.1042/CS20160069

Llovet, J. M., Kelley, R. K., Villanueva, A., Singal, A. G., Pikarsky, E., Roayaie, S., et al. (2021). Hepatocellular Carcinoma. *Nat. Rev. Dis. Primers* 7, 6. doi:10.1038/s41572-020-00240-3

Magkrioti, C., Oikonomou, N., Kaffe, E., Mouratis, M.-A., Xylourgidis, N., Barbayianni, I., et al. (2018). The Autotaxin - Lysophosphatidic Acid axis Promotes Lung Carcinogenesis. *Cancer Res.* 78, 3797–3644. doi:10.1158/0008-5472.CAN-17-3797

Martín-Vílchez, S., Sanz-Cameno, P., Rodríguez-Muñoz, Y., Majano, P. L., Molina-Jiménez, F., López-Cabrera, M., et al. (2008). The Hepatitis B Virus X Protein Induces Paracrine Activation of Human Hepatic Stellate Cells. *Hepatology* 47, 1872–1883. doi:10.1002/hep.22265

McGlynn, K. A., Petrick, J. L., and El-Serag, H. B. (2021). Epidemiology of Hepatocellular Carcinoma. *Hepatology* 73 (Suppl. 1), 4–13. doi:10.1002/hep.31288

Nishimasu, H., Ishitani, R., Aoki, J., and Nureki, O. (2012). A 3D View of Autotaxin. *Trends Pharmacol. Sci.* 33, 138–145. doi:10.1016/j.tips.2011.12.004

Ruan, Q., Wang, H., Burke, L. J., Bridle, K. R., Li, X., Zhao, C. X., et al. (2020). Therapeutic Modulators of Hepatic Stellate Cells for Hepatocellular Carcinoma. *Int. J. Cancer* 147, 1519–1527. doi:10.1002/ijc.32899

Salgado-Polo, F., Fish, A., Matsoukas, M.-T., Heidebrecht, T., Keune, W.-J., and Perrakis, A. (2018). Lysophosphatidic Acid Produced by Autotaxin Acts as an Allosteric Modulator of its Catalytic Efficiency. *J. Biol. Chem.* 293, 14312–14327. doi:10.1074/jbc.RA118.004450

Santamato, A., Fransvea, E., Dituri, F., Caligiuri, A., Quaranta, M., Niimi, T., et al. (2011). Hepatic Stellate Cells Stimulate HCC Cell Migration via Laminin-5 Production. *Clin. Sci. (Lond).* 121, 159–168. doi:10.1042/CS20110002

Seitz, H. K., and Stickel, F. (2006). Risk Factors and Mechanisms of Hepatocarcinogenesis with Special Emphasis on Alcohol and Oxidative Stress. *Biol. Chem.* 387, 349–360. doi:10.1515/BC.2006.047

Seo, E. J., Kwon, Y. W., Jang, I. H., Kim, D. K., Lee, S. I., Choi, E. J., et al. (2016). Autotaxin Regulates Maintenance of Ovarian Cancer Stem Cells through Lysophosphatidic Acid-Mediated Autocrine Mechanism. *Stem Cells* 34, 551–564. doi:10.1002/stem.2279

She, S., Yang, M., Hu, H., Hu, P., Yang, Y., and Ren, H. (2018). Proteomics Based Identification of Autotaxin as an Anti-hepatitis B Virus Factor and a Promoter of Hepatoma Cell Invasion and Migration. *Cell Physiol Biochem* 45, 744–760. doi:10.1159/000487166

Shi, Y., and Zheng, M. (2020). Hepatitis B Virus Persistence and Reactivation. *BMJ* 370, m2200. doi:10.1136/bmj.m2200

Utsunomiya, T., Shimada, M., Kudo, M., Ichida, T., Matsui, O., Izumi, N., et al. (2015). A Comparison of the Surgical Outcomes Among Patients with HBV-Positive, HCV-Positive, and Non-B Non-C Hepatocellular Carcinoma. *Ann. Surg.* 261, 513–520. doi:10.1097/Sla.0000000000000821

Wang, S., Li, J., Wu, S., Cheng, L., Shen, Y., Ma, W., et al. (2018). Type 3 Innate Lymphoid Cell: a New Player in Liver Fibrosis Progression. *Clin. Sci. (Lond).* 132, 2565–2582. doi:10.1042/CS20180482

Xu, L., Lin, J., Deng, W., Luo, W., Huang, Y., Liu, C.-Q., et al. (2020). EZH2 Facilitates BMI1-dependent Hepatocarcinogenesis through Epigenetically Silencing microRNA-200c. *Oncogenesis* 9, 101. doi:10.1038/s41389-020-00284-w

Xu, Z., Zhai, L., Yi, T., Gao, H., Fan, F., Li, Y., et al. (2016). Hepatitis B Virus X Induces Inflammation and Cancer in Mice Liver through Dysregulation of Cytoskeletal Remodeling and Lipid Metabolism. *Oncotarget* 7, 70559–70574. doi:10.18632/oncotarget.12372

Yang, F., Ma, L., Yang, Y., Liu, W., Zhao, J., Chen, X., et al. (2019). Contribution of Hepatitis B Virus Infection to the Aggressiveness of Primary Liver Cancer: A Clinical Epidemiological Study in Eastern China. *Front. Oncol.* 9, 370. doi:10.3389/fonc.2019.00370

Zan, Y., Zhang, Y., and Tien, P. (2013). Hepatitis B virus e antigen induces activation of rat hepatic stellate cells. *Biochem. Biophysical Res. Commun.* 435, 391–396. doi:10.1016/j.bbrc.2013.04.098

Zhang, D. Y., and Friedman, S. L. (2012). Fibrosis-dependent Mechanisms of Hepatocarcinogenesis. *Hepatology* 56, 769–775. doi:10.1002/hep.25670

Zhang, G., Cheng, Y., Zhang, Q., Li, X., Zhou, J., Wang, J., et al. (2018). ATX LPA axis F acilitates Estrogen induced Endometrial Cancer Cell Proliferation via MAPK/ERK Signaling Pathway. *Mol. Med. Rep.* 17, 4245–4252. doi:10.3892/mmr.2018.8392

Zhang, H., Yan, X., Yang, C., Zhan, Q., Fu, Y., Luo, H., et al. (2020). Intrahepatic T Helper 17 Cells Recruited by Hepatitis B Virus X Antigen-activated Hepatic Stellate Cells Exacerbate the Progression of Chronic Hepatitis B Virus Infection. *J. Viral Hepat.* 27, 1138–1149. doi:10.1111/jvh.13352

Zhong, C., Li, Y., Yang, J., Jin, S., Chen, G., Li, D., et al. (2021). Immunotherapy for Hepatocellular Carcinoma: Current Limits and Prospects. *Front. Oncol.* 11, 589680. doi:10.3389/fonc.2021.589680

Conflict of Interest: The authors declare that the research was conducted in the absence of any commercial or financial relationships that could be construed as a potential conflict of interest.

Publisher's Note: All claims expressed in this article are solely those of the authors and do not necessarily represent those of their affiliated organizations, or those of the publisher, the editors and the reviewers. Any product that may be evaluated in this article, or claim that may be made by its manufacturer, is not guaranteed or endorsed by the publisher.

frontiers in Molecular Biosciences

ORIGINAL RESEARCH
published: 12 November 2021
doi: 10.3389/fmolb.2021.749313

An lncRNA Model for Predicting the Prognosis of Hepatocellular Carcinoma Patients and ceRNA Mechanism

Hao Zhang[1], *Renzheng Liu*[1], *Lin Sun*[2] *and Xiao Hu*[1]*

[1]Department of Hepatobiliary Pancreatic Surgery, The Affiliated Hospital of Qingdao University, Qingdao, China, [2]Department of ICU, The Affiliated Hospital of Qingdao University, Qingdao, China

Liver cancer is a highly malignant tumor. Notably, recent studies have found that long non-coding RNAs (lncRNAs) play a prominent role in the prognosis of patients with liver cancer. Herein, we attempted to construct an lncRNA model to accurately predict the survival rate in liver cancer. Based on The Cancer Genome Atlas (TCGA) database, we first identified 1066 lncRNAs with differential expression. The patient data obtained from TCGA were divided into the experimental group and the verification group. According to the difference in lncRNAs, we used single-factor and multi-factor Cox regression to select the genes needed to build the model in the experimental group, which were verified in the verification group. The results showed that the model could accurately predict the survival rate of patients in the high and low risk groups. The reliability of the model was also confirmed by the area under the receiver operating characteristic curve. Our model is significantly correlated with different clinicopathological features. Finally, we built a ceRNA network based on lncRNAs, which was used to display miRNAs and mRNAs related to lncRNAs. In summary, we constructed an lncRNA model to predict the survival rate of patients with hepatocellular carcinoma.

Keywords: lncRNA, model, prognosis, hepatocellular carcinoma, ceRNA

OPEN ACCESS

Edited by:
Yunpeng Hua,
The First Affiliated Hospital of Sun Yat-sen University, China

Reviewed by:
Gao Liu,
Meizhou People's Hospital, China
Shunli Shen,
The First Affiliated Hospital of Sun Yat-sen University, China

***Correspondence:**
Xiao Hu
8371270@qq.com

Specialty section:
This article was submitted to Molecular Diagnostics and Therapeutics, a section of the journal Frontiers in Molecular Biosciences

Received: *29 July 2021*
Accepted: *08 October 2021*
Published: *12 November 2021*

Citation:
Zhang H, Liu R, Sun L and Hu X (2021) An lncRNA Model for Predicting the Prognosis of Hepatocellular Carcinoma Patients and ceRNA Mechanism. Front. Mol. Biosci. 8:749313. doi: 10.3389/fmolb.2021.749313

INTRODUCTION

Hepatocellular carcinoma (HCC) is the most common type of primary liver cancer, with high mortality (Farazi and DePinho, 2006). Despite several available treatment methods for HCC, patients in different stages require different treatment measures and the long-term survival remains poor. At present, the staging and grading of HCC is not comprehensive (Zhu et al., 2011), which makes assessment of prognosis difficult. Therefore, it is important to identify predictive indicators and develop a prognostic model for patients with HCC.

As the biological functions of long non-coding RNAs (lncRNAs) have been gradually uncovered, they have become a research hotspot. The function of lncRNAs can be divided into two types: regulating the local chromatin structure and/or gene expression of cis vs. trans, and those leaving the transcription site and performing cell function with trans transcripts (Gil and Ulitsky, 2020). After

Abbreviations: HCC, hepatocellular carcinoma; lncRNAs, long non-coding RNAs; qPCR, quantitative real-time PCR; ROC, receiver operating characteristic; TCGA, The Cancer Genome Atlas.

TABLE 1 | Primer sequences used in the study.

AC016717.2	Forward:5′-GATGCTGATGCTGCCTGTCCATAG-3′
	Reverse:5′-ATGCTGTGCTGTTGGTCTCTGAAG-3′
DDX11-AS1	Forward:5′-CTGGCTACTCTTCCTCCTGG-3′
	Reverse:5′-CAGAGGACATGTGGGAGGTT-3′
LINC00462	Forward:5′-ACTAGGTCCTTCTGGTGTT-3′
	Reverse:5′-GTAAAACTTGCTGCTGATG-3′
ZFPM2-AS1	Forward:5′-GGTGGCACCTGAAATCACAGA-3′
	Reverse:5′-TGCAAGATGACGCTCAGTCG-3′
GAPDH	Forward:5′-TCGGAGTCAACGGATTTGGT-3′
	Reverse:5′-TTCCCGTTCTCAGCCTTGAC-3′

the role of lncRNAs in regulating tumorigenesis and oncoprotein expression was established, lncRNAs were also found to alter the prognosis of numerous human cancers. Various studies have shown the effect of lncRNAs on the survival of patients with HCC. However, there is no effective prognostic model to evaluate the prognosis and guide the treatment of HCC. The Cancer Genome Atlas (TCGA) database has abundant transcriptome expression profiles of different cancers. Bioinformatics facilitates screening of biomarkers and constructing prediction models using public databases. Through the analysis of gene transcription level using TCGA and bioinformatics, this study found new molecular markers related to HCC survival and established a prognosis model of lncRNAs in HCC. Cox regression analysis, and least absolute shrinkage and selection operator were implemented to validate the lncRNAs associated with prognosis. The power of the prognostic model including four lncRNAs was tested by the receiver operating characteristic (ROC) curve. Statistics and graphic visualization were completed in R software.

Next, we used miRcode database to validate LINC00462 and find the downstream miRNAs. We used miRDB, miRTarBase, and TargetScan databases to find miRNAs targeting specific genes. Finally, we used the Cytoscape to structure the ceRNA network.

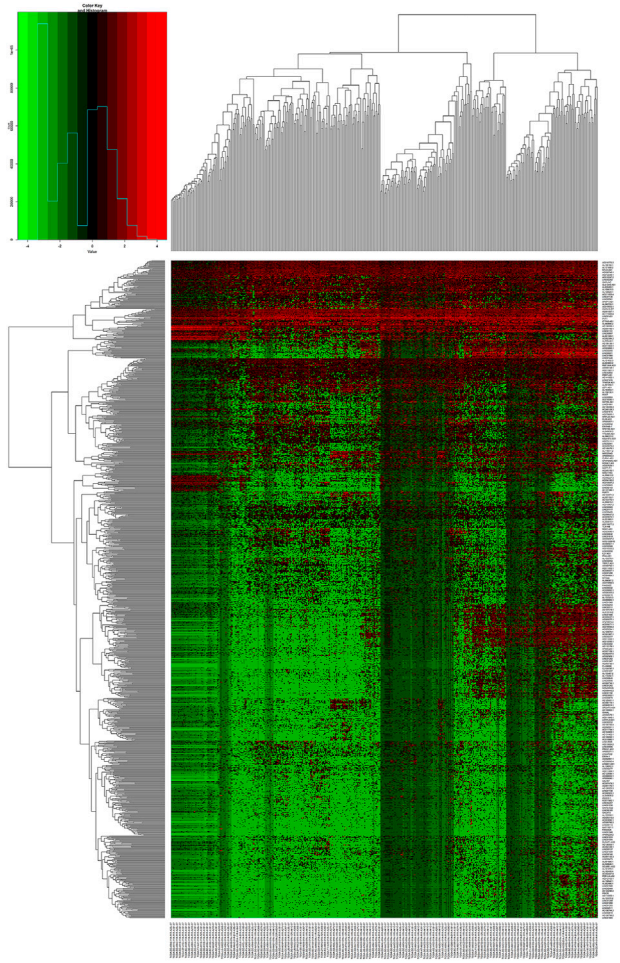

FIGURE 1 | A heat map showing the differential expression of lncRNAs.

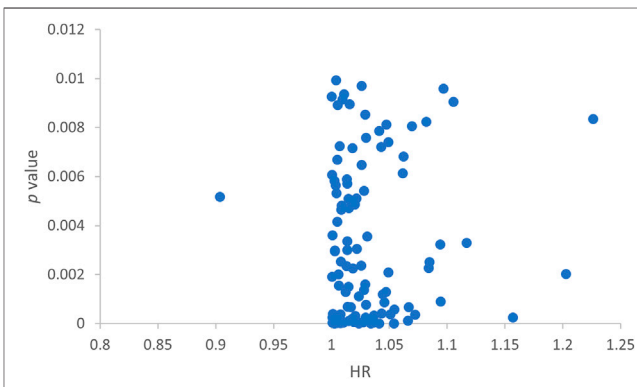

FIGURE 2 | Scatter plot showing lncRNAs screened by single-factor Cox analysis.

MATERIALS AND METHODS

Clinical Samples and Ethics Statement

The ethics committee of the Affiliated Hospital of Qingdao University approved this research. This study included 10 HCC patients (5 males and 5 females), who were diagnosed by pathology, between June 2018 and June 2019, at the Affiliated Hospital of Qingdao University (Shandong, China). The age range was 50–80 years. Tissues were sliced into small sections and stored at −80°C. Corresponding adjacent non-cancerous tissues (ANT) and cancerous tissues were simultaneously collected. The hospital's Institutional Review Board strictly adhered to the Declaration of Helsinki protocol for approving the study. Written informed consent was signed by each patient. The institutional approval number for human studies is QYFY ZWLL 26019.

Gene Expression Profiles of HCC Patients

The expression data of lncRNAs, miRNAs, and mRNAs, as well as clinical features were retrieved from TCGA (https://portal.gdc.cancer.gov/). We downloaded the annotation file of transcriptome from Ensembl online database (https://asia.ensembl.org/index.html) and used it to distinguish lncRNAs and miRNAs. There are not copyright issues. Thereafter, we selected differentially expressed genes for this

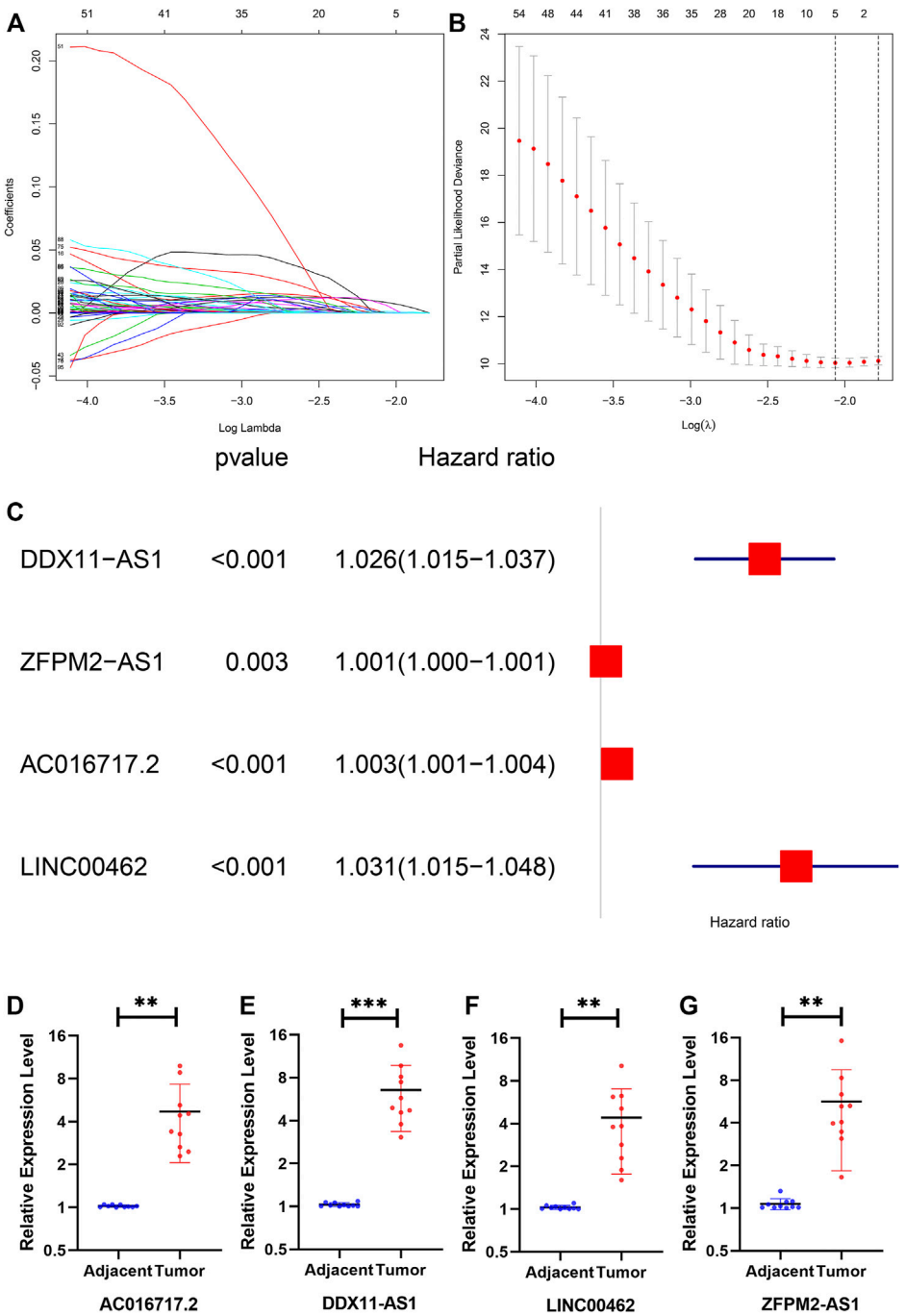

FIGURE 3 | (A) The lambda, the cvfit, **(B)** the forest **(C)** the expression of DDX11-AS1, ZFPM2- AS1, AC016717.2, and LINC00462 in tissues. The expression of all genes showed significant differences in 10 tissues.

study. The screening of genes was performed in the R software. We used edgeR package to identify differentially expressed genes.

Definition Of Prognostic Risk Model in the Training Dataset

We randomly divided 342 patients into the training dataset (172) and validation dataset (170). Cox regression analysis, and least absolute shrinkage and selection operator were used to screen prognosis related lncRNAs. Four lncRNAs were screened out in the training dataset. Finally, the following model was established to assess the prognostic risk. Risk score = coefficient_1 * Expression_1 + coefficient_2 * Expression_2 + coefficient_N * Expression_N. N is the above-selected lncRNAs, expression is the lncRNA expression in every HCC patient. Cox regression analysis was used to calculate the corresponding lncRNA coefficients in the training dataset. The

"survival", "caret", "glmnet", "survminer", and "survivalROC" packages were used in the analysis process.

RNA Extraction, Reverse Transcription, and Quantitative Real-Time PCR

We used RNAiso Plus (TaKaRa, Tokyo, Japan) to extract the total RNA from the tissues. The quality of RNA was detected by NanoDrop 2000 spectrophotometer (Thermo Fisher Scientific, Inc.). Next, reverse transcription was performed with T100™ thermal cycler (BIO-RAD, US) using PrimeScript™RT reagent kit and gDNA eraser (TaKaRa, Tokyo, Japan). Quantitative real-time PCR (qPCR) was performed in LightCycler® 96 (Roche, Switzerland) with TB Green®Premix Ex Taq™ II (Tli RNase H Plus) (TaKaRa, Tokyo, Japan). Primer sequences are listed in **Table 1**.

Statistical Analysis and the Formation of ceRNA Network

According to the median risk score, the patients were divided into the high-risk group and the low-risk group. All the analyses were performed using the R program and software package. The receiver operating characteristic (ROC) curve was used to test the predictive ability of the prognosis model composed of four lncRNAs (Mandrekar, 2010).

We used miRcode (http://www.mircode.org/) (Jeggari et al., 2012), miRDB (http://mirdb.org/) (Chen and Wang, 2020), miRTarBase (http://mirtarbase.mbc.nctu.edu.tw/index.html) (Chou et al., 2018), and TargetScan (http://www.targetscan.org) (Lewis et al., 2005) databases to predict the downstream genes. We used Cytoscape to visualize the ceRNA network.

RESULTS

Identification of Differentially Expressed lncRNAs

We downloaded the related data of 422 patients, 50 normal cases and 372 tumor cases from TCGA database. There were 1066 out of 6739 lncRNAs with logFC >2 and FDR <0.01 in the TCGA dataset, after removing lncRNAs with extremely similar gene expression between HCC and normal patients (**Figure 1**).

Identification of Prognostic lncRNAs From the Training Dataset

We randomly split 342 cancer patients. The training dataset included 172 patients and the test group had 170 patients. We further screened the predicting lncRNAs from the 1066 lncRNAs by univariate Cox analysis. Thereafter, 104 lncRNAs were selected that had an impact on the survival of patients (**Figure 2**).

Construction of the Prognostic Model and Checking the Expression of lncRNAs

The number of genes was reduced to 5 lncRNAs by least absolute shrinkage and selection operator (**Figure 3A**). Finally, four lncRNAs (DDX11-AS1, ZFPM2-AS1, AC016717.2, and LINC00462), which were closely related to patient survival, were selected by multivariate Cox analysis (**Figure 3B**). A prognostic model composed of the four lncRNAs was established as follows: Risk score = 0.0257 * DDX11-AS1 + 0.0008 * ZFPM2-AS1 + 0.0026 * AC016717.2 + 0.0306 * LINC00462. We verified the transcription levels of these four genes in 10 pairs of human tissue samples (**Figure 3C**).

The Model for Survival Prediction

Based on the median risk score, we divided the patients from the training dataset into the high-risk group (n = 86) and the low-risk group (n = 86) and compared the survival of the two risk groups by Kaplan–Meier survival analysis. The survival rate of the high-risk group was significantly lower than that of the low-risk group (**Figure 4A**). To confirm the predictive power of the prognostic model, we divided the patients in the test dataset into two risk groups according to the median risk score. The Kaplan-Meier curve showed that in the trial cohort, the lifespan of patients in the low-risk group was prominently longer than that in the high-risk group, which was similar to the results obtained from the training dataset (**Figure 4B**).

The survival status of HCC patients obtained from the training dataset and test dataset is depicted in the plot. The heat map shows the different expression patterns of the four prognosis-related lncRNAs in the low-risk and high-risk populations (**Figures 4C,D**). Similar to the training dataset, patients with high-risk scores tended to have higher levels of the four lncRNAs than patients with low-risk scores. According to the ROC (AUC) curve, the size of the AUC was related to the prognosis. The ROC curves at 1 year of the whole, training, and validation datasets are shown in **Figures 4E–G**.

Prognostic Model and Clinicopathological Features

The Chi square test was used to analyze the significance of clinicopathological features between high- and low-risk groups (**Figure 5A**). In addition, by analyzing the data of patients with different characteristics, we found that the risk score can significantly distinguish the prognostic differences in different age, gender, G stage, M0, N0, stage, and T group (**Figure 5B**), which significantly improves the prognostic value of our model.

Construction of the ceRNA Network with the Prognostic lncRNAs

Using the TCGA database, 1976 differentially expressed mRNAs were selected from 424 HCC patients (logFC > 2 or logFC < −2,FDR<0.01). From 50 normal samples and 376 tumor samples, 247 differentially expressed miRNAs were selected (logFC > 1 or logFC < −1, FDR < 0.01). We compared DDX11-AS1, ZFPM2-AS1, AC016717.2, and LINC00462 in the miRcode database to identify the downstream miRNAs, and only LINC00462 could be found in the miRcode database. The miRNAs found in the miRcode intersected with the differentially expressed miRNAs in TCGA. The miRDB, miRTarBase, and TargetScan data were combined to predict the downstream mRNAs with the miRNAs obtained in the previous step. The downstream target genes were obtained using the intersection of the differentially expressed

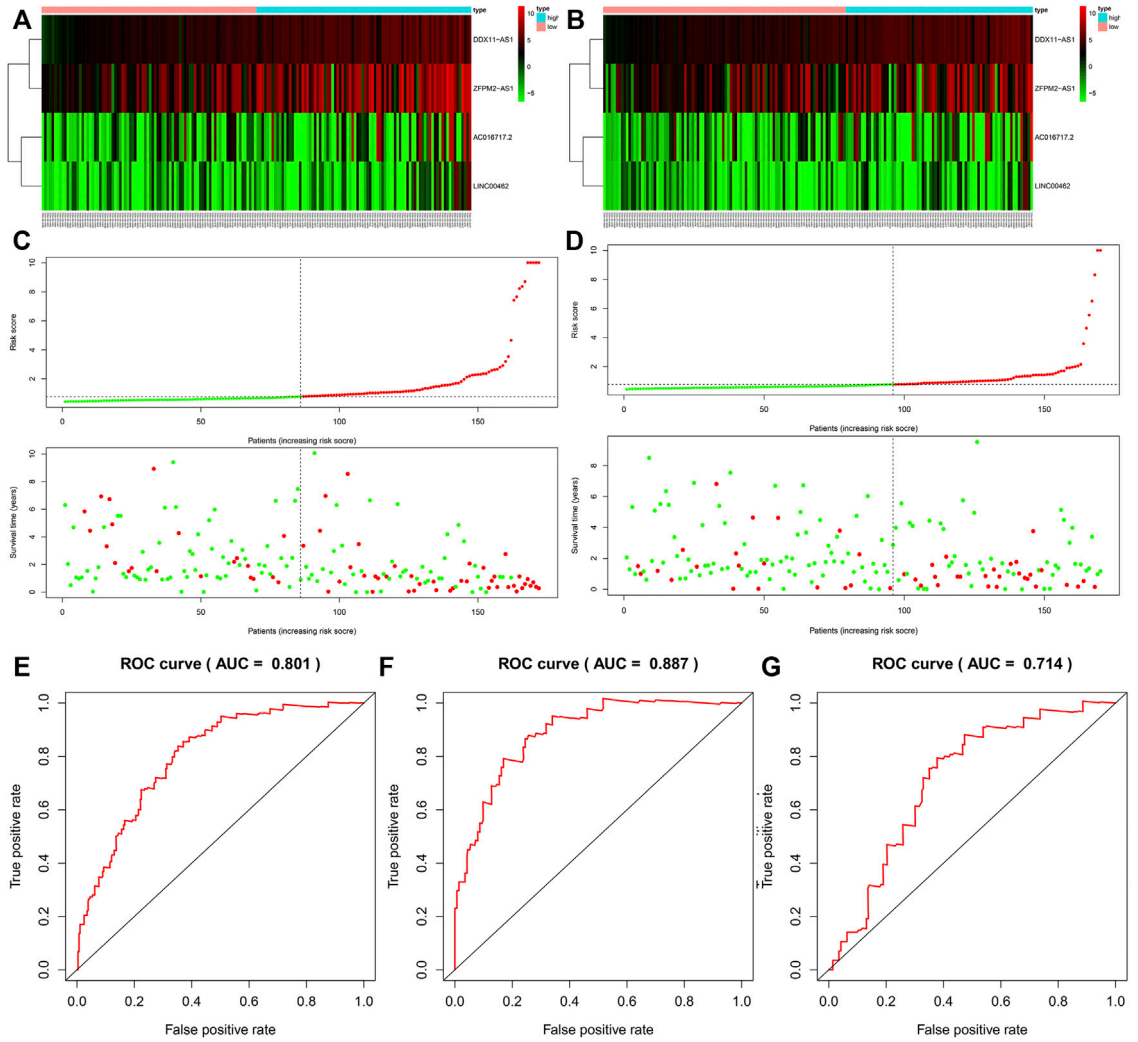

FIGURE 4 | The survival rate of the high-risk group and the low-risk group in the training group **(A)** and the test group **(B)**. The survival status of the training group **(C)** and the test group **(D)**. The ROC curve of the whole group **(E)**, training group **(F),** and the test group **(G)**.

mRNAs in the previous TCGA database and the predicted mRNAs in the three databases (**Figure 6**).

DISCUSSION

In recent years, with the gradual advancements in the study of lncRNAs, their function in the occurrence and development of HCC has become a research hotspot. Therefore, it is critical to understand the mechanism of action of lncRNAs and comprehensively analyze their clinical significance in patients with liver cancer. The purpose of this study was to establish lncRNA markers related to prognosis of HCC and explore their molecular mechanisms. This study was undertaken to provide a better understanding of the prognosis of patients with liver cancer and facilitate the discovery of biomarkers.

In this study, we downloaded related data of 422 patients from TCGA database and screened out 1066 lncRNAs. We randomly split 342 cancer patients. We further selected the 104 predictive lncRNAs from 1066 lncRNAs by univariate Cox analysis in the training dataset. Finally, four lncRNAs (DDX11-AS1, ZFPM2-AS1, AC016717.2, and LINC00462), which were closely related to patient survival, were selected by least absolute shrinkage and selection operator, and multivariate Cox analysis. A prognostic model or a risk score was constituted with the above lncRNAs. We divided patients from the training dataset into the high-risk group and the low-risk group. The survival of patients in the high-risk group was significantly less than those in the low-risk group. The survival of patients in the test dataset was similar to the training dataset. Furthermore, ROC curve analysis showed that the lncRNA risk score model had good prediction efficiency in HCC. The AUC value of our model is significantly higher than that of Wu et al. (2020) and Zhou et al. (2021). Finally, we used the miRcode, miRDB, miRTarBase, and TargetScan databases to find the downstream miRNAs and mRNAs, and create the ceRNA network.

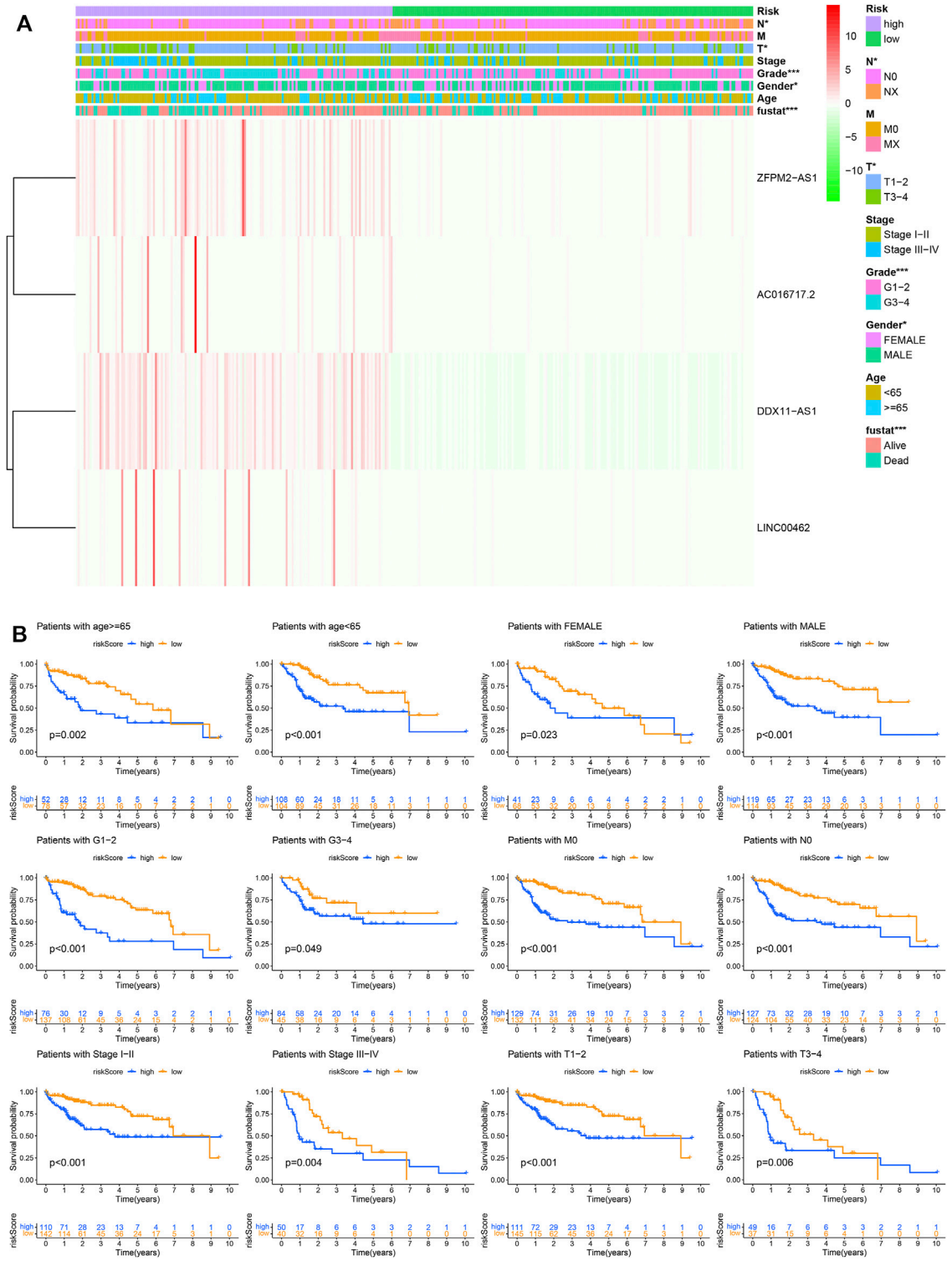

FIGURE 5 | The prognostic model and clinicopathological features. **(A)** The significance of clinicopathological features between high- and low-risk groups. **(B)** Prognostic differences in different groups.

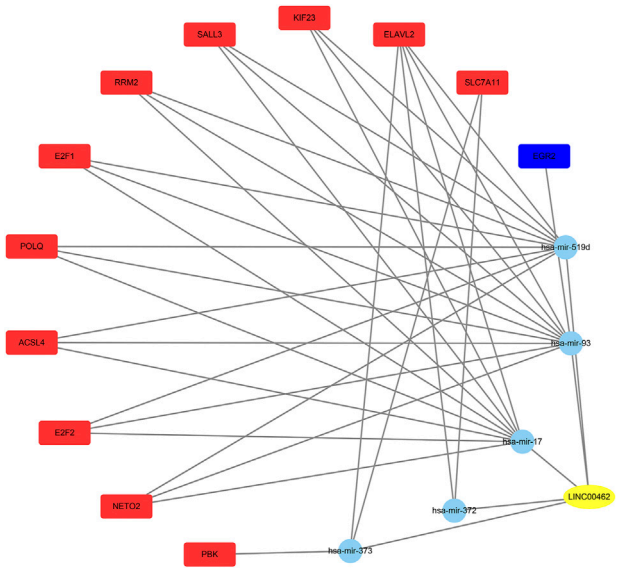

FIGURE 6 | The yellow oval is lncRNA, the blue circles represent miRNAs, the red rectangles represent the up-regulated mRNAs, and the blue rectangle represents the down-regulated mRNA.

DDX11-AS1 was identified as an oncogene in HCC. Silencing the expression of this gene reduced the proliferation, migration, and invasion ability of HCC cells, and the gene could promote the growth of tumors *in vivo* (Wan et al., 2020). DDX11-AS1 was also reported to be related to overall survival (Li et al., 2019). DDX11-AS1 displayed a cancer-promoting role by regulating the expression of related genes directly or indirectly in various malignant tumors, such as osteosarcoma, colorectal cancer, gastric cancer, non-small cell lung cancer, and bladder cancer (Feng et al., 2020). ZFPM2-AS1 regulates the expression of GDF10 through competitive binding to miRNA to promote cell proliferation, migration, invasion, and inhibit apoptosis in HCC (He et al., 2020). As an oncogenic gene, ZFPM2-AS1 plays a role in retinoblastoma (Lyv et al., 2020), breast cancer (Zhao et al., 2020), small cell lung cancer (Yan et al., 2020), cervical cancer (Dai et al., 2020), esophageal squamous cell carcinoma (Sun and Wu, 2020), and other tumors. AC016717.2 is located on chromosome 2 and the gene maps to 226, 563, 230–226, 568, 370 in GRCh37 coordinates. There are few studies on this lncRNA. LINC00462 can significantly increase the invasive ability of HCC cells (Gong et al., 2017). It can also promote pancreatic cancer (Zhou et al., 2018).

In summary, this was the first study to propose a prediction model based on four lncRNAs, in which the effects of DDX11-AS1, ZFPM2-AS1, and lncRNAs on the prognosis of patients with liver cancer have been confirmed. AC016717.2 and LINC00462 are new biomarkers in liver cancer. Although the lncRNAs selected by the predictive model showed good performance, this study only included internal validation results but no external data validation due to resource constraints. Hence, clear evidence with multi-center clinical data is required to validate the results of this study.

DATA AVAILABILITY STATEMENT

The original contributions presented in the study are included in the article/**Supplementary Material**. Further inquiries can be directed to the corresponding author.

ETHICS STATEMENT

The ethics committee of the Affiliated Hospital of Qingdao University approved this research. This study included 10 HCC patients (5 males and 5 females), who were diagnosed by pathology, between June 2018 and June 2019, at the Affiliated Hospital of Qingdao University (Shandong, China). The age range was 50–80 years. Tissues were sliced into small sections and stored at −80°C. Corresponding adjacent non-cancerous tissues (ANT) and cancerous tissues were simultaneously collected. The hospital's Institutional Review Board strictly adhered to the Declaration of Helsinki protocol for approving the study. Written informed consent was signed by each patient. The institutional approval number for human studies is QYFY ZWLL 26019.

AUTHOR CONTRIBUTIONS

H.Z. contributed to the study design, acquired and analyzed data, and wrote the manuscript. R.L. and L.S. contributed to statistical analysis and data acquisition. X.H. provided intellectual input. All authors read and approved the final manuscript.

SUPPLEMENTARY MATERIAL

The Supplementary Material for this article can be found online at: https://www.frontiersin.org/articles/10.3389/fmolb.2021.749313/full#supplementary-material

REFERENCES

Chen, Y., and Wang, X. (2020). miRDB: an Online Database for Prediction of Functional microRNA Targets. *Nucleic Acids Res.* 48 (D1), D127–D131. doi:10.1093/nar/gkz757

Chou, C.-H., Shrestha, S., Yang, C.-D., Chang, N.-W., Lin, Y.-L., Liao, K.-W., et al. (2018). miRTarBase Update 2018: a Resource for Experimentally Validated microRNA-Target Interactions. *Nucleic Acids Res.* 46 (D1), D296–D302. doi:10.1093/nar/gkx1067

Dai, J., Wei, R., Zhang, P., and Liu, P. (2020). Long Noncoding RNA ZFPM2-AS1 Enhances the Malignancy of Cervical Cancer by Functioning as a Molecular Sponge of microRNA-511-3p and Consequently Increasing FGFR2 Expression. *Cmar* 12, 567–580. doi:10.2147/cmar.s238373

Farazi, P. A., and DePinho, R. A. (2006). Hepatocellular Carcinoma Pathogenesis: from Genes to Environment. *Nat. Rev. Cancer* 6 (9), 674–687. doi:10.1038/nrc1934

Feng, Y., Wu, M., Hu, S., Peng, X., and Chen, F. (2020). LncRNA DDX11-AS1: a Novel Oncogene in Human Cancer. *Hum. Cel* 33 (4), 946–953. doi:10.1007/s13577-020-00409-8

Gil, N., and Ulitsky, I. (2020). Regulation of Gene Expression by Cis-Acting Long Non-coding RNAs. *Nat. Rev. Genet.* 21 (2), 102–117. doi:10.1038/s41576-019-0184-5

Gong, J., Qi, X., Zhang, Y., Yu, Y., Lin, X., Li, H., et al. (2017). Long Noncoding RNA Linc00462 Promotes Hepatocellular Carcinoma Progression. *Biomed. Pharmacother.* 93, 40–47. doi:10.1016/j.biopha.2017.06.004

He, H., Wang, Y., Ye, P., Yi, D., Cheng, Y., Tang, H., et al. (2020). Long Noncoding RNA ZFPM2-AS1 Acts as a miRNA Sponge and Promotes Cell Invasion through Regulation of miR-139/GDF10 in Hepatocellular Carcinoma. *J. Exp. Clin. Cancer Res.* 39 (1), 159. doi:10.1186/s13046-020-01664-1

Jeggari, A., Marks, D. S., and Larsson, E. (2012). miRcode: a Map of Putative microRNA Target Sites in the Long Non-coding Transcriptome. *Bioinformatics* 28 (15), 2062–2063. doi:10.1093/bioinformatics/bts344

Lewis, B. P., Burge, C. B., and Bartel, D. P. (2005). Conserved Seed Pairing, Often Flanked by Adenosines, Indicates that Thousands of Human Genes Are microRNA Targets. *Cell* 120 (1), 15–20. doi:10.1016/j.cell.2004.12.035

Li, Y., Zhuang, W., Huang, M., and Li, X. (2019). Long Noncoding RNA DDX11-AS1 Epigenetically Represses LATS2 by Interacting with EZH2 and DNMT1 in Hepatocellular Carcinoma. *Biochem. Biophysical Res. Commun.* 514 (4), 1051–1057. doi:10.1016/j.bbrc.2019.05.042

Lyv, X., Wu, F., Zhang, H., Lu, J., Wang, L., and Ma, Y. (2020). Long Noncoding RNA ZFPM2-AS1 Knockdown Restrains the Development of Retinoblastoma by Modulating the MicroRNA-515/HOXA1/Wnt/β-Catenin Axis. *Invest. Ophthalmol. Vis. Sci.* 61 (6), 41. doi:10.1167/iovs.61.6.41

Mandrekar, J. N. (2010). Receiver Operating Characteristic Curve in Diagnostic Test Assessment. *J. Thorac. Oncol.* 5 (9), 1315–1316. doi:10.1097/jto.0b013e3181ec173d

Sun, G., and Wu, C. (2020). ZFPM2-AS1 Facilitates Cell Growth in Esophageal Squamous Cell Carcinoma via Up-Regulating TRAF4. *Biosci. Rep.* 40 (4). doi:10.1042/BSR20194352

Wan, T., Zheng, J., Yao, R., Yang, S., Zheng, W., and Zhou, P. (2020). LncRNA DDX11-AS1 Accelerates Hepatocellular Carcinoma Progression via the miR-195-5p/MACC1 Pathway. *Ann. Hepatol.* 20, 100258. doi:10.1016/j.aohep.2020.09.003

Wu, H., Liu, T., Qi, J., Qin, C., and Zhu, Q. (2020). Four Autophagy-Related lncRNAs Predict the Prognosis of HCC through Coexpression and ceRNA Mechanism. *Biomed. Res. Int.* 2020, 3801748. doi:10.1155/2020/3801748

Yan, Z., Yang, Q., Xue, M., Wang, S., Hong, W., and Gao, X. (2020). YY1-induced lncRNA ZFPM2-AS1 Facilitates Cell Proliferation and Invasion in Small Cell Lung Cancer via Upregulating of TRAF4. *Cancer Cel Int* 20, 108. doi:10.1186/s12935-020-1157-7

Zhao, Y. F., Li, L., Li, H. J., Yang, F. R., Liu, Z. K., Hu, X. W., et al. (2020). LncRNA ZFPM2-AS1 Aggravates the Malignant Development of Breast Cancer via Upregulating JMJD6. *Eur. Rev. Med. Pharmacol. Sci.* 24 (21), 11139–11147. doi:10.26355/eurrev_202011_23601

Zhou, B., Guo, W., Sun, C., Zhang, B., and Zheng, F. (2018). Linc00462 Promotes Pancreatic Cancer Invasiveness through the miR-665/tgfbr1-Tgfbr2/smad2/3 Pathway. *Cell Death Dis* 9 (6), 706. doi:10.1038/s41419-018-0724-5

Zhou, X., Dou, M., Liu, Z., Jiao, D., Li, Z., Chen, J., et al. (2021). Screening Prognosis-Related lncRNAs Based on WGCNA to Establish a New Risk Score for Predicting Prognosis in Patients with Hepatocellular Carcinoma. *J. Immunol. Res.* 2021, 5518908. doi:10.1155/2021/5518908

Zhu, A. X., Duda, D. G., Sahani, D. V., and Jain, R. K. (2011). HCC and Angiogenesis: Possible Targets and Future Directions. *Nat. Rev. Clin. Oncol.* 8 (5), 292–301. doi:10.1038/nrclinonc.2011.30

Conflict of Interest: The authors declare that the research was conducted in the absence of any commercial or financial relationships that could be construed as a potential conflict of interest.

Publisher's Note: All claims expressed in this article are solely those of the authors and do not necessarily represent those of their affiliated organizations, or those of the publisher, the editors, and the reviewers. Any product that may be evaluated in this article, or claim that may be made by its manufacturer, is not guaranteed or endorsed by the publisher.

frontiers in Molecular Biosciences

ORIGINAL RESEARCH
published: 16 November 2021
doi: 10.3389/fmolb.2021.747650

Activity of PD-1 Inhibitor Combined With Anti-Angiogenic Therapy in Advanced Sarcoma: A Single-Center Retrospective Analysis

*Yang You[1], Xi Guo[1], Rongyuan Zhuang[1], Chenlu Zhang[1], Zhiming Wang[1], Feng Shen[1], Yan Wang[1], Wenshuai Liu[1], Yong Zhang[1], Weiqi Lu[1], Yingyong Hou[1], Jing Wang[2], Xuan Zhang[2], Minzhi Lu[1] and Yuhong Zhou[1]**

[1]Oncology Department, Zhongshan Hospital, Shanghai, China, [2]GenomiCare Biotechnology (Shanghai) Co., Ltd., Shanghai, China

OPEN ACCESS

Edited by:
Kui Wang,
Eastern Hepatobiliary Surgery Hospital, China

Reviewed by:
Yiping Zou,
Guangdong Provincial People's Hospital, China
Taicheng Zhou,
The Sixth Affiliated Hospital of Sun Yat-sen University, China

***Correspondence:**
Yuhong Zhou
zhou.yuhong@zs-hospital.sh.cn

Specialty section:
This article was submitted to Molecular Diagnostics and Therapeutics, a section of the journal Frontiers in Molecular Biosciences

Received: 26 July 2021
Accepted: 29 September 2021
Published: 16 November 2021

Citation:
You Y, Guo X, Zhuang R, Zhang C, Wang Z, Shen F, Wang Y, Liu W, Zhang Y, Lu W, Hou Y, Wang J, Zhang X, Lu M and Zhou Y (2021) Activity of PD-1 Inhibitor Combined With Anti-Angiogenic Therapy in Advanced Sarcoma: A Single-Center Retrospective Analysis. Front. Mol. Biosci. 8:747650. doi: 10.3389/fmolb.2021.747650

Background: Immune checkpoint inhibitors (ICIs) are employed to treat various cancers, including soft tissue sarcomas (STSs), and less than 20% of patients benefit from this treatment. Vascular endothelial growth factor (VEGF) promotes the immunosuppressive tumor microenvironment and contributes to ICI-resistant therapy. Anti-VEGF receptor tyrosine-kinase inhibitors (TKIs) combined with ICIs have shown antitumor activity in patients with alveolar soft-part sarcoma (ASPS). However, they have not been extensively studied to treat other STS subtypes, such as leiomyosarcoma (LMS), dedifferentiated liposarcoma (DDLPS), undifferentiated pleomorphic sarcoma (UPS), myxofibrosarcoma (MFS), and angiosarcoma (AS).

Methods: In this retrospective study, we collected data from 61 patients who were diagnosed with advanced STS based on imaging and histology, including LMS, DDLPS, and UPS. Among them, 41 patients were treated with ICIs combined with TKIs and 20 patients received ICI therapy. The endpoints of progression-free survival (PFS) and overall response rate (ORR) were analyzed in the two groups, and the overall response [partial response (PR), stable disease (SD), and progressive disease (PD)] of each patient was determined using RECIST 1.1 evaluation criteria.

Results: In total, 61 STS patients had the following subtypes: LMS (n = 20), DDLPS (n = 17), UPS (n = 8), ASPS (n = 7), MFS (n = 7), and AS (n = 2). The median PFS (mPFS) was significantly prolonged after ICI treatment in combination with TKIs (11.74 months, 95% CI 4.41–14.00) compared to ICI treatment alone (6.81 months, 95% CI 5.43–NA) (HR 0.5464, p = 0.043). The 12-month PFS rates of patients who received ICI–TKI treatment were increased from 20.26% (95% CI 0.08–0.53) to 42.90% (95% CI 0.27–0.68). In the combination therapy group, 12 patients (30%) achieved PR, 25 patients (62.5%) achieved SD, and 3 patients (7.5%) achieved PD for 3 months or longer. In the non-TKI-combination group, 2 patients (9.5%) achieved PR, 14 patients (66.7%) achieved SD, and 5 patients (23.8%) achieved PD within 3 months. The ORRs in the two groups were 30.0% (ICI–TKI combination) and 9.5% (ICI only), respectively. A notable ORR was observed in the ICI–TKI combination group, especially for subtypes

ASPS (66.7%), MFS (42.9%), and UPS (33.3%). The PD-L1 expression (n = 33) and tumor mutation burden (TMB, n = 27) were determined for each patient. However, our results showed no significant difference in PFS or response rates between the two groups.

Conclusion: This study suggests that ICI–TKI treatment has antitumor activity in patients with STS, particularly the ASPS and MFS subtypes. Moreover, effective biomarkers to predict clinical outcomes are urgently needed after combination therapy in the STS subtypes.

Keywords: sarcoma, immunotherapy, anti-angiogenesis, PD-1, biomarker

INTRODUCTION

Sarcoma represents a heterogeneous group of various soft tissue and bone tumors of mesenchymal origin that accounts for approximately 1% of adult malignancies and 15% of pediatric malignancies and is comprised of over 100 different subtypes (Fletcher et al., 2013). Although soft tissue sarcoma (STS) is a rare cancer, the global annual incidence of STS is 1.8–5.0/100,000 in people younger than 45 years (Siegel et al., 2021). Surgery (combined with chemotherapy and radiotherapy) remains the mainstay treatment for local STS, but up to 40% of patients experience tumor recurrence and inevitably progress to advanced disease (Judson et al., 2014). For advanced STS, anthracycline-based chemotherapy or other drug combinations have been widely used albeit with limited benefit, and with restricted success when utilized as second-line or systemic therapies (Savina et al., 2017). Therefore, more effective agents and therapeutic strategies need to be explored for STS treatment.

Immune checkpoint inhibitors (ICIs; anti-PD-1/PD-L1 and anti-CTLA4 antibodies) are a compelling new option for the treatment of various advanced cancers, including sarcomas. Previous studies have shown that the expression of PD-1/PD-L1 in sarcoma patients has a strong positive correlation with T cell infiltration and B cell activation (Kim et al., 2021; Petitprez et al., 2020). In the SARC028 and Alliance A0914401 clinical trials, anti-PD-1 agents (pembrolizumab and nivolumab) or those combined with an anti-CTLA agent (ipilimumab) have shown clinical benefits in advanced/metastatic sarcoma, but the overall response rate (ORR) in all cohorts was only 18 and 16%, respectively (D'Angelo et al., 2018; Tawbi et al., 2017). Most non-responders have a significant correlation with restricted infiltration of immune cells, such as T cells and macrophages, and PD-L1 expression levels. The immunosuppressive tumor microenvironment (TME) generated by the dysfunctional tumor immune system leads to resistance to immunotherapy (Rabinovich et al., 2007). It has been proved that angiogenesis contributed to the maintenance of immunosuppressive TME in renal cell carcinoma and melanoma and was associated with antitumor activity (Yang et al., 2018); however, its roles and related mechanisms for immunosuppressive actions in sarcoma remain unexplored.

Vascular endothelial growth factor (VEGF) is considered to be the main driver gene of angiogenesis, leading to tumor growth and metastasis, and it also contributes to suppression of the immunotherapy response (Fukumura et al., 2018). Therefore, the anti-VEGF receptor tyrosine-kinase inhibitors (TKIs) display anti-cancer activity against STS, including anlotinib, pazopanib, and regorafenib (Berry et al., 2017; Chi et al., 2018; Weiss et al., 2020). Notably, on the basis of the role of VEGF in the suppressive TME, immune checkpoint inhibitor–based therapies combined with TKIs have exhibited favorable outcomes in various types of cancers (Fukumura et al., 2018). According to a phase 3 trial, axitinib plus pembrolizumab exhibited anti-cancer activity in patients with ASPS (Wilky et al., 2019). However, the safety and efficiency of immunotherapy combined with TKIs in other sarcoma subtypes are still to be determined.

In this retrospective study, we collected data from 61 STS patients treated with ICIs or ICIs combined with TKIs. The aims were to determine the progression-free survival (PFS) and overall response rate (ORR) for five sarcoma subtypes and to correlate the patients' demographics and clinical data that may predict improved outcomes.

METHODS

Patients and Study Design

In this single-institution retrospective cohort study, we selected 61 STS patients diagnosed with STS. The subjects of this study were patients with sarcoma at any stage who received ICI (PD-1/PD-L1 inhibitor) or ICI–TKI treatment at Zhongshan Hospital Affiliated to Fudan University, China, from January 1, 2015, to April 10, 2021. The ICI agents were administered to patients with STS, including LMS, DDLPS, ASPS, UPS, MFS, and AS; the TKI agents include anlotinib, pazopanib, and regorafenib. The exclusion criteria for patients were 1) autoimmune disease, 2) rheumatic disease, or 3) active bleeding. By reviewing their electronic medical records, the treatment history, demographics, genetics, pathology, and radiology information were retrospectively collected. If ≥1% of various markers in the collected tumor tissues were stained positive, it was considered that the expression of PD-L1 in the tumor was positive. The study protocol was approved by the Ethics Committee of Zhongshan hospital (IRB protocol number B2020-338).

Immunohistochemistry (IHC)

The PD-L1 expression in each patient was determined by immunohistochemistry. The tumor tissue slides were baked at 63°C for 60 min and then boiled in 10 mM sodium citrate (pH

TABLE 1 | Baseline characteristics of patients with STS.

	ICIs (n = 21)	ICIs + TKIs (n = 40)	Total (n = 61)	*p*-Value
Gender	—	—	—	0.227
Female	12	22	1/20	—
Male	9	18	5%	—
Age (average, years)	48	48	4/17	—
Primary tumor location	—	—	—	0.377
Retroperitoneum	15	24	39	—
Heart	0	2	2	—
Uterus	2	5	7	—
Extremities	2	5	7	—
Others	2	4	6	—
Chemo treatment	—	—	—	0.485
Gemcitabine	5	14	19	—
Anthracyclines	5	10	15	—
Dacarbazine	2	2	4	—
Best response	—	—	—	0.071
PR	2	12	14	—
SD	14	25	39	—
PD	5	3	8	—
Immunotherapy	—	—	—	0.297
PD-1 inhibitor	21	38	58	—
PD-L1 inhibitor	0	2	2	—
PD-L1 status	—	—	—	0.114
Positive	8	8	16	—
Negative	4	13	17	—
FNCLCC	—	—	—	0.356
II	4	12	16	v
III	17	28	45	
Histological grade	—	—	—	0.262
Grade II	4	4	8	—
Grade III	9	22	31	—
Unknown	8	14	22	—

6.0) for 30 min to retrieve the antigen. Anti-PD-L1 polyclonal antibody was used as the primary antibody (Abcam, Cambridge, United Kingdom; rabbit SP142, 1:300; Dako IHC 22C3, 1:300) and goat anti-rabbit biotinylated IgG as the secondary antibody (Maxim, UltraSensitive^{TM} SP IHC Kit, KIT-9707). The slides were then counterstained with hematoxylin (Gene, GT100540), dehydrated, and mounted. Images were digitally scanned at ×20 magnification.

Statistical Analysis

A radiologist certified by the board of directors performed tumor measurements on the lesions found on the patient's CT or MRI imaging and evaluated the clinical response of the patients to ICI treatment according to Response Evaluation Criteria in Solid Tumors Version 1.1 (RECIST 1.1). In order to include patients in the PFS analysis, they were required to have a baseline scan within 3 weeks of the first ICI treatment. In addition, follow-up scans were required at least 9 weeks after the start of ICI treatment. The best tumor response was evaluated using the RECIST 1.1 standard and defined as the maximum reduction in the target tumor burden. Kaplan–Meier analysis was used to compare PFS rates between the two treatment groups. To perform PFS analysis on patients who were lost to follow-up or survived without PFS at the end of the study, the data were checked at the last tumor imaging. All statistical analyses were performed using GraphPad Prism (GraphPad Software, CA, United States).

RESULTS

Patient Demographics

Sixty-one patients were included in the study with various subtypes, including leiomyosarcoma (LMS, n = 20), dedifferentiated liposarcoma (DDLPS, n = 17), undifferentiated pleomorphic sarcoma (UPS, n = 8), ASPS (n = 7), myxofibrosarcoma (MFS, n = 7), and angiosarcoma (AS, n = 2). Among these patients, males accounted for 54.1%, the median age was 48.5 years, and all of them were Asians (**Supplementary Table S1**). Among them, 21 patients received ICI treatment only and 40 patients received ICIs combined with TKIs. The baseline characteristics between the two groups have no significant difference and are listed in **Table 1**. At the beginning of ICI treatment, 58 patients had metastatic disease (95.1%) and 3 patients had local disease (4.9%). The most common tumor sites were the retroperitoneum (n = 49), followed by the uterus (n = 7), heart (n = 2), paranasal sinus (n = 1), and mediastinum (n = 1). Most of the patients had already undergone chemotherapy and received a median of two cycles of conventional treatment (range 1–4) before ICI or ICI–TKI

TABLE 2 | Treatment strategies in STS subtypes.

	ICIs (n = 21)	ICIs + TKIs (n = 40)	Total (n = 60)	*p*-Value
LMS (n = 20)	0/5	1/15	1/20	0.62
	0%	6.7%	5%	—
DDLPS (n = 17)	0/6	4/11	4/17	0.09
	0%	36.3%	23.5%	
UPS (n = 8)	2/5	1/3	3/8	0.85
	40%	33.3%	37.5%	—
ASPS (n = 7)	0/4	2/3	2/7	0.05
	0%	66.7%	28.6%	—
MFS (n = 7)	0	3/7	3/7	—
	—	42.9%	42.9%	—
AS (n = 2)	0	1/2	1/2	—
	—	50%	50%	—

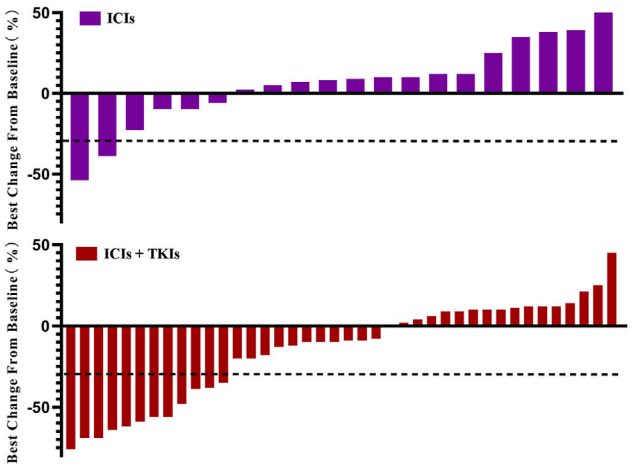

FIGURE 1 | Change of tumor burden from baseline. Patients who received immune checkpoint inhibitors (ICIs; n = 21) or ICIs combined with tyrosine-kinase inhibitors (TKIs; n = 40) are listed. Each bar represents one patient.

treatment. The main common reasons interrupting the treatment were progression of the disease or intolerable toxicity (**Supplementary Table S2**).

Efficacy

Of the 61 subjects, 21 received ICI treatment (group A) and 40 received ICI–TKI combination treatment (group B; **Table 2**). Patients' response to treatment was assessed be measuring the tumor size according to the RECIST 1.1 criteria (**Figure 1**). In group A, 2 patients achieved a partial response (PR), 14 achieved stable disease (SD), and 5 had progressive disease (PD). In group B, 12 patients achieved a partial response (PR), 25 achieved stable disease (SD), and 3 had progressive disease (PD). Thus, the ORR in groups A and B was 9.5 and 30.0%, respectively. Although no patients achieved complete response (CR), one DDLPS patient achieved pCR after surgery, one patient had a pathological response rate up to 86%, and three patients had a pathological PR [at least 30% reduction in the target tumor mutation burden (TMB)].

TABLE 3 | Clinical response rate of soft tissue sarcoma subtypes in the two groups.

	ICIs (n = 21)	ICIs + TKIs (n = 40)	Total (n = 61)	*p*-Value
PR	2/21	12/40	14/61	0.07
	9.5%	30.0%	23.0%	
SD	14/21	25/40	39/61	0.75
	66.7%	62.5%	63.9%	
PD	5/21	3/40	8/61	0.07
	23.8%	7.5%	13.1%	
mPFS	7 (2–19)	12 (2–NA)	9 (2–NA)	—

Considering the best response rate in less than 3 months, PR, SD, and PD accounted for 24.6, 60.7, and 14.8%, respectively (**Table 3**). Compared to ICI treatment alone, ICI–TKI treatment enhanced the ORR and DCR (CR + PR + SD) in the first 3 months (ORR 10 vs. 31.7%; DCR 80 vs. 87.9%; **Figure 2A**). Moreover, we found that seven patients received mono-immunotherapy, four ASPS (2 PR and 2 SD for best response), one LMS (SD for 3 months and PD for 6 months), one UPS (SD for 1 year), and one DDLPS (PD for 4 months). Regarding the different STS subtypes, there was a significant difference in the response between the two groups who received immune-based treatment. In general, UPS, ASPS, and MFS patients had the highest response rates, with DDLPS greatly fluctuating and LMS having a low response rate (**Figure 2B**). In addition, we also found that patients with ASPS were sensitive to ICI–TKI combination treatment. However, those with UPS appeared to benefit from ICIs instead of the combination treatment. All seven patients with MFS received ICI–TKI combination treatment, and they responded satisfactorily. DDLPS appeared to maintain SD, regardless of whether TKI treatment was used or not, with regression of the lesion not observed. Although LMS patients had the lowest response rate in both groups, the patients achieved rapid progress in the ICI treatment group compared to the combination treatment group (**Supplementary Figure S1**).

Progression-free survival (PFS) during treatment of the two groups was also assessed. Our results showed that the median PFS (mPFS) was significantly prolonged in the ICI–TKI group (11.74 months) compared to the ICI group (6.81 months; HR 0.55, 95% CI 0.2673–0.9791, $p = 0.043$; **Figure 3**). The 12-month PFS rate for patients who were given ICIs in combination with

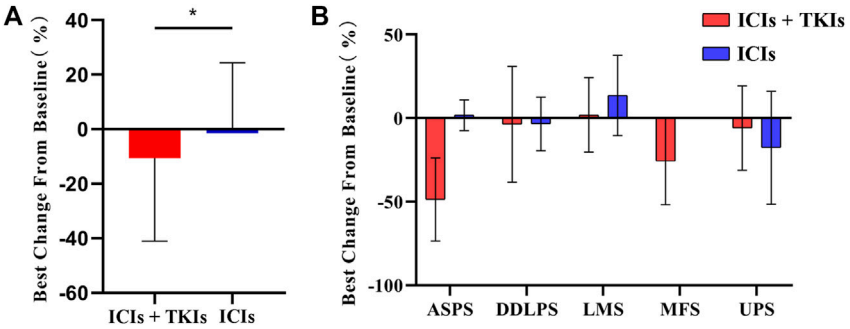

FIGURE 2 | Clinical response rate in soft tissue sarcoma (STS) subtypes: **(A)** tumor burden changes from baseline in the two groups; **(B)** changes of tumor burden in STS subtypes. ASPS, alveolar soft-part sarcoma; DDLPS, dedifferentiated liposarcoma; LMS, leiomyosarcoma; MFS, myxofibrosarcoma; UPS, undifferentiated pleomorphic sarcoma.

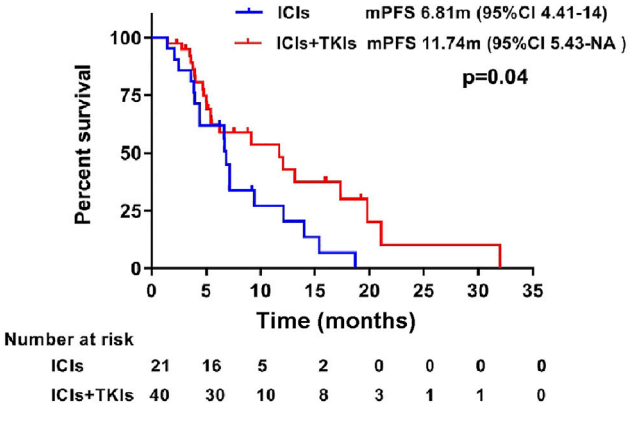

FIGURE 3 | Progression-free survival between treatment with immune checkpoint inhibitors (ICIs) and ICIs combined with tyrosine-kinase inhibitors (TKIs). Kaplan–Meier estimates showed a significant difference in progression-free survival in patients treated with ICIs and ICIs combined with TKIs.

TKIs was increased from 20.26% (95% CI 0.078–0.53) to 42.9% (95% CI 0.27–0.68).

In order to explore the correlation between TMB and treatment, we carried out next-generation sequencing in 27 patients who received ICI (8/27) or ICI–TKI (19/27) treatment. Our results showed no significant differences in the TMB value between the two groups (**Figure 4A**). Moreover, the patients were divided into two groups based on the TMB value (TMB-high and TMB-low). We also found that the PFS was not significantly different (**Figure 4B**). We supposed that the expression of PD-L1 could predict the clinical benefit of ICI–TKI treatment. Our results revealed that there was no difference in the rate of change of tumor (**Figure 4C**) and in the PFS (**Figure 4D**) in the two treated groups. Overall, our results demonstrated that both the TMB and the PD-L1 status were not satisfactory predictors to distinguish clinical outcomes.

Safety

Treatment-related adverse events, as graded by Common Terminology Criteria for Adverse Events (CTCAE) Version 4.0, included rash (14.8%), fever (16.4%), fatigue (26.2%), hypothyroidism (18%), hypertension (50.8%), elevated ALT/AST/ALP levels (41.0%), vitamin D deficiency (37.7%), hyperlipidemia (34.4%), anemia (23.0%), and dental ulcer (2/61, 3.3%). None grade 4 CTCAE occurred in either groups (**Supplementary Table S3**).

DISCUSSION

Emerging data suggest that immunotherapy has become a new therapeutic model in oncology. However, the results of clinical trials have shown that the majority of STS patients do not benefit from this treatment (total response rate <20%) (Monga et al., 2020). Tumor angiogenesis not only contributes to tumor growth and metastasis but also induces the immunosuppressive formation of TME (Yi et al., 2019). Therefore, the combination of immunotherapy and anti-angiogenic therapy has recently emerged as a novel treatment pattern (Fukumura et al., 2018; Wang et al., 2020; Zhang et al., 2019). Based on the single-arm clinical trial of NCT02636725, the anti-VEGF inhibitor (axitinib) plus anti-PD-1 antibody (pembrolizumab) had antitumor activity in ASPS patients (the mPFS was 12.4 months, the ORR was 54.5%, and the CBR was 72.7% at 3 months) (Wilky et al., 2019). However, data on the real-world clinical effectiveness of combination therapy in ASPS and other STS subtypes remain scarce.

Sixty-one eligible patients with various STS subtypes were included in this real-world study. Twenty-one patients received immunotherapy, and 40 patients received immunotherapy in combination with anti-angiogenesis inhibitors. Our results showed that combination therapy exerts a good therapeutic effect, providing evidence for the effectiveness of this treatment pattern in STS (**Figure 1**). Although the mixture of low- and high-grade sarcomas makes comparison difficult, we have made certain observations in this heterogeneous sarcoma and therapy combination.

First, patients with ASPS had the best response to immunotherapy, although with limited sample size (7 patients). Among them, about 71.4% exhibited a strong partial

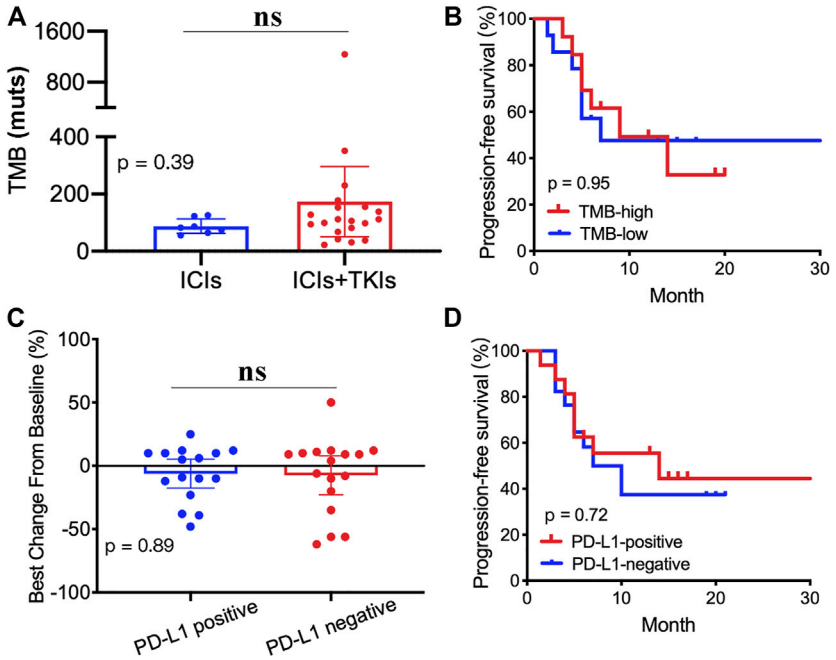

FIGURE 4 | Correlation between tumor mutation burden (TMB), PD-L1 expression, and clinical outcomes: **(A)** TMB value in the two groups; **(B)** Kaplan–Meier analyses based on the TMB value; **(C)** tumor mutation burden changes from baseline between PD-L1–positive and PD-L1–negative groups; **(D)** Kaplan–Meier analyses based on the PD-L1 status.

response (**Supplementary Figure S2**). Two of the patients who received combination therapy achieved SD for more than 3 months, far beyond than expected (Tawbi et al., 2017). In addition, we found that the response rate was higher in the combination therapy group than in the ICI therapy group (10 vs. 31.7%). These findings were consistent with the results of a prospective phase 2 clinical trial, where the patients with ASPS who received axitinib in combination with pembrolizumab exhibited significant improvements in mPFS, ORR, and CBR (Wilky et al., 2019). We also showed that the combination of immunotherapy and anti-vascular therapy has advantages for the treatment of ASPS subtypes, and we are looking forward to more data and mechanism research to further illustrate this point of view.

Previous studies have shown that LMS subtypes respond to immunotherapy, with an ORR of 45% (Tawbi et al., 2017). However, in our cohort, 37.5% (6/16) of LMS patients achieved PD and 50% (8/16) achieved SD. Monga et al. (2020) suggested that the TMB alteration of multiple lines of chemotherapy or radiation in the real world could lead to different response rates for immunotherapy treatment. We did not investigate TMB or PD-L1 status within the patients, which is a limitation in our study. Although LMS patients in our study did not benefit from either ICI or ICI–TKI treatment, we found that the patients achieved SD instead of PD in the combination therapy group (**Figure 2**). It is therefore important to investigate the efficacy and safety of combination therapy for LMS in future randomized clinical trials and to discover prognostic biomarkers that may assist in response prediction. In addition, we verified the effectiveness of PD-1 inhibitors for UPS, but in the process by boldly trying anti-vascular TKI combination. We found that the combination did not further improve the efficacy of these patients in terms of PFS and ORR. Our results suggest that UPS, as a complex and heterogeneous STS, requires further exploration of a more appropriate combination plan to screen patients who will benefit.

MFS is similar to UPS in the analysis of genotypes, and both were considered to be the same responding subtype to ICI for its TIL microenvironment (Pollack et al., 2017). Seven MFS patients in our cohort were given combination therapy as a leading exploration. Our results showed that the patients not only had a satisfactory ORR (42.9%) but also prolonged the PFS, and all patients achieved SD. Our center actively evaluated four patients: two received ICI–TKI two-drug combination therapy and two received ICI combined with chemotherapy and TKI three-drug combination therapy, and the results are encouraging. We found that the ORR reached 50% and CBR reached 100%. This result gives us great confidence to further perform the larger-scale, mechanism research of immunotherapy-combined anti-vascular targeted therapy in MFS.

Previous studies have demonstrated that PD-L1 expression is a prognostic factor for STS immunotherapy (Kim et al., 2021). However, we found that the status of PD-L1 did not predict the CBR of ICI–TKI treatment. Moreover, the TMB was not a satisfactory marker to predict clinical outcomes in STS patients who received immune-based therapies.

The tolerability of immunotherapy in sarcoma patients appears to be similar to that in other patients (Horvat et al., 2015). Rash, fever, and fatigue were the most common adverse events. Similar to other experiences with immunotherapeutic agents, certain unusual toxicities were observed, necessitating discontinuation of the drug and administration of steroids (D'Angelo et al., 2018).

CONCLUSION

In general, anti-angiogenesis inhibitors combined with PD-1 inhibitor therapy can enhance the mPFS (more than 5 months), ORR, and DCR in patients with STS. Our study showed that patients with ASPS and UPS are more sensitive to immunotherapy and that MFS is another promising subtype to benefit from ICI–TKI combination therapy. Although LMS does not significantly change the ORR of immunotherapy, we found that the mPFS of LMS patients who received immunotherapy was significantly prolonged.

DATA AVAILABILITY STATEMENT

The original contributions presented in the study are included in the article/**Supplementary Material**, and further inquiries can be directed to the corresponding author.

ETHICS STATEMENT

The studies involving human participants were reviewed and approved by the Ethics Committee of Zhongshan Hospital Affiliated to Fudan University. Written informed consent to participate in this study was provided by the participants' legal guardian/next of kin.

AUTHOR CONTRIBUTIONS

YY contributed to sorting, writing the article, and chart analysis. Gx, RZ, CZ, ZW, FS, YY, and YW contributed to data collection, and Gx, RZ, CZ, ZW, FS, and YW collated the article. ZY, WL, and WL contributed to specimen collection and genetic analysis. YH contributed to pathological diagnosis and immunohistochemical analysis. ML was responsible for statistical analysis. JW and XZ contributed to NGS analysis. YZ provided experimental design ideas and data analysis guidance.

SUPPLEMENTARY MATERIAL

The Supplementary Material for this article can be found online at: https://www.frontiersin.org/articles/10.3389/fmolb.2021.747650/full#supplementary-material

REFERENCES

Berry, V., Basson, L., Bogart, E., Mir, O., Blay, J.-Y., Italiano, A., et al. (2017). REGOSARC: Regorafenib versus Placebo in Doxorubicin-Refractory Soft-Tissue Sarcoma-A Quality-Adjusted Time without Symptoms of Progression or Toxicity Analysis. *Cancer* 123, 2294–2302. doi:10.1002/cncr.30661

Chi, Y., Fang, Z., Hong, X., Yao, Y., Sun, P., Wang, G., et al. (2018). Safety and Efficacy of Anlotinib, a Multikinase Angiogenesis Inhibitor, in Patients with Refractory Metastatic Soft-Tissue Sarcoma. *Clin. Cancer Res.* 24, 5233–5238. doi:10.1158/1078-0432.CCR-17-3766

D'Angelo, S. P., Mahoney, M. R., Van Tine, B. A., Atkins, J., Milhem, M. M., Jahagirdar, B. N., et al. (2018). A Non-comparative Multi-center Randomized Phase II Study of Nivolumab +/− Ipilimumab for Patients with Metastatic Sarcoma (Alliance A091401). *Lancet Oncol.* 19, 416–426. doi:10.1016/S1470-2045(18)30006-8

Fletcher, C., Bridge, J., Hogendoorn, P., and Mertens, F. (2013). *WHO Classification of Tumours of Soft Tissue and Bone*. 4th edition (Wold Health Organization, Lund University Publishtions).

Fukumura, D., Kloepper, J., Amoozgar, Z., Duda, D. G., and Jain, R. K. (2018). Enhancing Cancer Immunotherapy Using Antiangiogenics: Opportunities and Challenges. *Nat. Rev. Clin. Oncol.* 15, 325–340. doi:10.1038/nrclinonc.2018.29

Horvat, T. Z., Adel, N. G., Dang, T.-O., Momtaz, P., Postow, M. A., Callahan, M. K., et al. (2015). Immune-Related Adverse Events, Need for Systemic Immunosuppression, and Effects on Survival and Time to Treatment Failure in Patients with Melanoma Treated with Ipilimumab at Memorial Sloan Kettering Cancer Center. *J. Clin. Oncol.* 33, 3193–3198. doi:10.1200/JCO.2015.60.8448

Judson, I., Verweij, J., Gelderblom, H., Hartmann, J. T., Schöffski, P., Blay, J.-Y., et al. (2014). Doxorubicin Alone versus Intensified Doxorubicin Plus Ifosfamide for First-Line Treatment of Advanced or Metastatic Soft-Tissue Sarcoma: a Randomised Controlled Phase 3 Trial. *Lancet Oncol.* 15, 415–423. doi:10.1016/S1470-2045(14)70063-4

Kim, S. K., Kim, J. H., Kim, S. H., Lee, Y. H., Han, J. W., Baek, W., et al. (2021). PD-L1 Tumour Expression Is Predictive of Pazopanib Response in Soft Tissue Sarcoma. *BMC Cancer* 21, 336. doi:10.1186/s12885-021-08069-z

Monga, V., Skubitz, K. M., Maliske, S., Mott, S. L., Dietz, H., Hirbe, A. C., et al. (2020). A Retrospective Analysis of the Efficacy of Immunotherapy in Metastatic Soft-Tissue Sarcomas. *Cancers* 12, 1873. doi:10.3390/cancers12071873

Petitprez, F., de Reyniès, A., Keung, E. Z., Chen, T. W.-W., Sun, C.-M., Calderaro, J., et al. (2020). B Cells Are Associated with Survival and Immunotherapy Response in Sarcoma. *Nature* 577, 556–560. doi:10.1038/s41586-019-1906-8

Pollack, S. M., He, Q., Yearley, J. H., Emerson, R., Vignali, M., Zhang, Y., et al. (2017). T-cell Infiltration and Clonality Correlate with Programmed Cell Death Protein 1 and Programmed Death-Ligand 1 Expression in Patients with Soft Tissue Sarcomas. *Cancer* 123, 3291–3304. doi:10.1002/cncr.30726

Rabinovich, G. A., Gabrilovich, D., and Sotomayor, E. M. (2007). Immunosuppressive Strategies that Are Mediated by Tumor Cells. *Annu. Rev. Immunol.* 25, 267–296. doi:10.1146/annurev.immunol.25.022106.141609

Savina, M., Le Cesne, A., Blay, J.-Y., Ray-Coquard, I., Mir, O., Toulmonde, M., et al. (2017). Patterns of Care and Outcomes of Patients with METAstatic Soft Tissue SARComa in a Real-Life Setting: the METASARC Observational Study. *BMC Med.* 15, 78. doi:10.1186/s12916-017-0831-7

Siegel, R. L., Miller, K. D., Fuchs, H. E., and Jemal, A. (2021). Cancer Statistics, 2021. *CA A. Cancer J. Clin.* 71, 7–33. doi:10.3322/caac.21654

Tawbi, H. A., Burgess, M., Bolejack, V., Van Tine, B. A., Schuetze, S. M., Hu, J., et al. (2017). Pembrolizumab in Advanced Soft-Tissue Sarcoma and Bone Sarcoma (SARC028): a Multicentre, Two-Cohort, Single-Arm, Open-Label, Phase 2 Trial. *Lancet Oncol.* 18, 1493–1501. doi:10.1016/s1470-2045(17)30624-1

Wang, Q., Gao, J., Di, W., and Wu, X. (2020). Anti-angiogenesis Therapy Overcomes the Innate Resistance to PD-1/pd-L1 Blockade in VEGFA-Overexpressed Mouse Tumor Models. *Cancer Immunol. Immunother.* 69, 1781–1799. doi:10.1007/s00262-020-02576-x

Weiss, A. R., Chen, Y.-L., Scharschmidt, T. J., Chi, Y.-Y., Tian, J., Black, J. O., et al. (2020). Pathological Response in Children and Adults with Large Unresected Intermediate-Grade or High-Grade Soft Tissue Sarcoma Receiving Preoperative Chemoradiotherapy with or without Pazopanib (ARST1321): a Multicentre, Randomised, Open-Label, Phase 2 Trial. *Lancet Oncol.* 21, 1110–1122. doi:10.1016/S1470-2045(20)30325-9

Wilky, B. A., Trucco, M. M., Subhawong, T. K., Florou, V., Park, W., Kwon, D., et al. (2019). Axitinib Plus Pembrolizumab in Patients with Advanced Sarcomas Including Alveolar Soft-Part Sarcoma: a single-centre, Single-Arm, Phase 2 Trial. *Lancet Oncol.* 20, 837–848. doi:10.1016/S1470-2045(19)30153-6

Yang, J., Yan, J., and Liu, B. (2018). Targeting VEGF/VEGFR to Modulate Antitumor Immunity. *Front. Immunol.* 9, 978. doi:10.3389/fimmu.2018.00978

Yi, M., Jiao, D., Qin, S., Chu, Q., Wu, K., and Li, A. (2019). Synergistic Effect of Immune Checkpoint Blockade and Anti-angiogenesis in Cancer Treatment. *Mol. Cancer* 18, 60. doi:10.1186/s12943-019-0974-6

Zhang, G., Liu, C., Bai, H., Cao, G., Cui, R., and Zhang, Z. (2019). Combinatorial Therapy of Immune Checkpoint and Cancer Pathways Provides a Novel Perspective on Ovarian Cancer Treatment (Review). *Oncol. Lett.* 17, 2583. doi:10.3892/ol.2019.9902

Conflict of Interest: The authors JW and XZ were employed by the company GenomiCare Biotechnology (Shanghai) Co., Ltd.

The remaining authors declare that the research was conducted in the absence of any commercial or financial relationships that could be construed as a potential conflict of interest.

Publisher's Note: All claims expressed in this article are solely those of the authors and do not necessarily represent those of their affiliated organizations, or those of the publisher, the editors, and the reviewers. Any product that may be evaluated in this article, or claim that may be made by its manufacturer, is not guaranteed or endorsed by the publisher.

frontiers in Molecular Biosciences

ORIGINAL RESEARCH
published: 26 November 2021
doi: 10.3389/fmolb.2021.761163

Nomogram to Predict Tumor-Infiltrating Lymphocytes in Breast Cancer Patients

*Jikun Feng[1], Jianxia Li[2], Xinjian Huang[1], Jiarong Yi[1], Haoming Wu[1], Xuxiazi Zou[1], Wenjing Zhong[1] and Xi Wang[1]**

[1]Department of Breast Oncology, Sun Yat-Sen University Cancer Center, The State Key Laboratory of Oncology in South China, Collaborative Innovation Center for Cancer Medicine, Guangzhou, China, [2]Department of Medical Oncology, The Sixth Affiliated Hospital of Sun Yat-Sen University, Guangdong Provincial Key Laboratory of Colorectal and Pelvic Floor Diseases, Guangzhou, China

OPEN ACCESS

Edited by:
Yu Guo,
The First Affiliated Hospital of Sun Yat-sen University, China

Reviewed by:
Yizi Cong,
Yantai Yuhuangding Hospital, China
Yiping Zou,
Guangdong Provincial People's Hospital, China
Taicheng Zhou,
The Sixth Affiliated Hospital of Sun Yat-sen University, China

***Correspondence:**
Xi Wang
wangxi@sysucc.org.cn

Specialty section:
This article was submitted to Molecular Diagnostics and Therapeutics, a section of the journal Frontiers in Molecular Biosciences

Received: 19 August 2021
Accepted: 08 October 2021
Published: 26 November 2021

Citation:
Feng J, Li J, Huang X, Yi J, Wu H, Zou X, Zhong W and Wang X (2021) Nomogram to Predict Tumor-Infiltrating Lymphocytes in Breast Cancer Patients. Front. Mol. Biosci. 8:761163. doi: 10.3389/fmolb.2021.761163

Background: Tumor-infiltrating lymphocytes (TILs) play important roles in the prediction of prognosis and neoadjuvant therapy (NAT) efficacy in breast cancer (BRCA) patients, in this study, we identified clinicopathological factors related to BRCA TILs, then to construct and validate nomogram to predict high density of TILs.

Methods: A total of 826 patients diagnosed with BRCA in Sun Yat-Sen University cancer center were enrolled in nomogram cohort. TILs were assessed using hematoxylin-eosin (H&E) staining by two pathologists. Complete clinical data were collected for analysis. Then the enrolled patients were split into a training set and validation set at a ratio of 8:2. and the backward multivariate binary logistic regression model was used to establish nomogram for predicting BRCA TILs, which were further evaluated and validated using the C-index, receiver operating characteristic (ROC) curves and calibration curves. Then another independent NAT cohort of 106 patients was established for verifying this nomogram in NAT efficacy prediction.

Results: TILs were significantly correlated with body mass index (BMI), tumor differentiation, ER, PR, HER2 expression, Ki67, blood biochemical indicators including total bilirubin (TBIL), indirect bilirubin (IBIL), total protein (TP), Globulin (GLOB), inorganic phosphorus (IP), calcium (Ca). In which ER expression level [OR = 0.987, 95%CI (0.982–0.992), $p < 0.001$], IP [OR = 4.462, 95%CI (1.171~17.289), $p = 0.029$], IBIL [OR = 0.906, 95%CI (0.845–0.966), $p = 0.004$] and TP [OR = 1.053, 95%CI (1.010–1.098, $p = 0.016$)] were independent predictors of TILs. Then nomogram was established, for which calibration curves (C-index = 0.759) and ROC curve (AUC = 0.759, 95%CI 0.717–0.801) in training sets, calibration curves (C-index = 0.708) and ROC curve (AUC = 0.708, 95%CI 0.617–0.800) in validation sets demonstrated great evaluation efficiency. Besides, independent NAT cohort verified this nomogram can distinguish patients with greater NAT efficacy ($p = 0.041$).

Conclusion: The finds of clinicopathological factors associated with TILs could help clinicians to understand the tumor immunity of BRCA and improve treatment system for

patients, and the established nomogram with high evaluation efficiency may be used as a complement tool for distinguishing patients with better NAT efficacy.

Keywords: breast cancer, tumor-infiltrating lymphocytes (TILs), nomogram, neoadjuvant therapy (NAC), precise medicine

INTRODUCTION

According to the latest cancer statistics, in 2021, there would be about 284,200 newly diagnosed breast cancer (BRCA) patients in the United States, accounting for around 15% of all cancer diagnosis. In the female population, BRCA has the highest incidence rate (30%) and the second mortality rate (15%), and the incidence has steadily increased in the past 2 decades, therefore, BRCA is considered as a major threat to women's health (Siegel et al., 2021). Although the treatment methods of BRCA patients has been improved to a certain extent, there is still space for improvement in precise treatment and management. And in clinical practice, there is an urgent need for indicators to predict prognosis, treatment efficacy and guide selections of treatment options.

Tumor-infiltrating lymphocytes (TILs) refer to mononuclear immune cells infiltrating into the tumor tissue, which have been reported and studied in a variety of solid tumors, including BRCA, colon cancer, cervical cancer, melanoma, and lung cancer (Underwood, 1974). TILs in the breast tissue mainly consist of $CD8^+$ T cells, as well as helper ($CD4^+$) T cells, $CD19^+$ B cells and a very small amount of NK cells with different infiltration degrees (Chin et al., 1992; Whitford et al., 1992). TILs is a highly complicated system (Gajewski et al., 2013). Thus, we need to do furthering research to better understanding tumor immunity.

TILs are of great significance in neoadjuvant treatment (NAT) efficacy evaluation for BRCA patients. Studies have shown that TILs are associated with positive disease-free survival (DFS) in triple-negative breast cancer (TNBC) and HER2 + patients. While TILs are related to increased overall survival (OS) in TNBC and HR+ HER2-patients (Denkert et al., 2018a), and TILs can serve as an independent prognosis factor for TNBC patients (Pruneri et al., 2016a). Besides, the level of TILs is also related to tumor metastasis in BRCA, research indicate metastatic BRCA tended to have lower TILs (Zhu et al., 2019). What's more, TILs were also reported to be correlated with the efficacy of NAT. For TNBC and HR+ HER2-subtypes, patients with higher TILs are more likely to have pathological complete response (pCR) after neoadjuvant chemotherapy (Hamy et al., 2019). A possible explanation for this association was that chemotherapy, including cyclophosphamide, and gemcitabine, can indirectly stimulate TILs mediated adaptive immune response by reducing immunosuppressive factors (Denkert et al., 2018a). Therefore, chemotherapy, besides being tumoricidal, may additionally have an immunotherapeutic effect via stimulation of immune responses in TILs leading to complete clinical responses (Pruneri et al., 2016a). For HER2+ subtype, patients with higher TILs tended to benefit more from neoadjuvant targeted therapy in regard of pCR (Ignatiadis et al., 2019; De Angelis et al., 2020).And the same trend has also been observed in BRCA immunotherapy (Loi et al., 2021), However, beneficial effects of neoadjuvant endocrine-therapy were found in tumors with low TILs infiltration for HR + HER2-patients (Skriver et al., 2020a; Skriver et al., 2020b; Lundgren et al., 2020).

Overall, TILs in BRCA patients are of great clinical significance in NAT and prognosis evaluation. However, there are some limitations for traditional H and E staining. Firstly, for patients receiving NAT, tumor sample could only be obtained through pre-operative fine-needle aspiration biopsy, the sample size is small and local, which on the one hand cannot represent the whole tumor, due to the heterogeneous distribution of TILs in BRCA patients (Dieci et al., 2018), and will affect the accuracy of detection on the other hand. Therefore, a prediction model, based on accurate TILs data of NAT naive surgical resection specimens and baseline available indictors, has important clinical significance for evaluating the baseline level of TILs and the efficacy of NAT. Finally, the prediction model of TILs, can serve as a newly prognosis tool for BRCA patients, whose tumor samples cannot be obtained (et: samples from other hospitals could not be borrowed and used, or the tissue itself was too small for further staining) to perform H and E staining and morphological evaluation of TILs. Thus, for those two kinds of specific BRCA patients, traditional H and E staining has noteworthy deficiencies, so we need an prediction model with great accuracy.

Therefore, NAT naive surgical resection specimens were analyzed and clinical data was collected, aiming to explore associations of TILs with clinicopathological characteristics, and to propose nomogram model for predicting high TILs in BRCA patients.

MATERIALS AND METHODS

Nomogram Cohort Patients

From June 2020 to March 2021, a total number of 826 patients' data were collected in Sun Yat-Sen University Cancer Center. The diagnosis of invasive breast cancer was confirmed by postoperative pathology. The main inclusion criteria were: 1. 18–80 years of age; 2. eligibility for radical tumor resection after comprehensive evaluation. Exclusion criteria mainly were: 1) previous NAT, i.e., chemotherapy, radiotherapy, targeted therapy, or immunotherapy, etc; 2) secondary tumors or multifocal tumors; 3) HIV infection or other immune system diseases; 4) past use of immune agents or drugs and health care products that may affect immune function; 5) state of inflammation and infection within nearly 1 week. This study was approved by the Ethics Committee of Sun Yat-Sen University Cancer Center.

General Information and Examination Results

Patients' information was obtained from the breast cancer single disease research platform of Sun Yat-Sen University Cancer Center. Inclusion and exclusion criteria were described above. General patient information, histopathological findings and specific blood test results were assessed retrospectively. General patient information included age, gender, BMI, blood type, hypertension, and diabetes. Blood test results included blood routine, blood biochemical, hormone level, and tumor markers. All blood test results were obtained from the patients within 1 week before surgery. The histopathological data included postoperative paraffin pathological findings: pathological type and stage, TNM staging, degree of tumor differentiation, immunohistochemical staining results. ER positivity was defined as ER ≥ 1%. PR positivity was defined as PR ≥ 1%.

Tumor-Infiltrating Lymphocyte Assessment

Postoperative tumor paraffin specimens from 826 patients underwent H and E staining, and two pathologists independently calculated stromal TILs density percentages; the final values of TILs were obtained through unified discussion, with the measurement standard referring to "RECOMMENDATIONS BY AN INTERNATIONAL TILs–For the supplemental versions of WORKING GROUP 2014 and 2018",the standardized approach mainly including: 1) select tumor aera.2) define stromal area.3) scan at low magnification.4) determine type of inflammatory infiltrate.5) assess the percentage of stromal TILs (Salgado et al., 2015; Dieci et al., 2018). In this study, "10%" TILs was taken as the cut-off value; therefore, patients with >10% TILs were considered the high TILs group, and the remaining individuals constituted the low TILs group.

Construction and Validation of Nomogram

To improve the robustness and reliability of our prediction model, the nomogram cohort were split into a training set and validation set in a random manner without replacement at a ratio of 8:2. Training set was used to construct the predicted nomogram and perform internal validation. For training cohort, baseline predictors of TILs in BRCA patients were evaluated by the univariate and multivariate binary logistic regression model. Then variables with p value less than 0.05 were included in the backward multivariate binary logistic regression model (Erratum: Borderud et al., 2015) to further screen the optimal prediction model with the lowest Akaike information criterion (AIC). Finally, nomogram establishment was performed based on the optimal prediction model with the R software (version 4.0.1). Bootstrapping with 80 samples was applied for internal validation of the nomogram. The performance of nomogram was assessed by Harrell's concordance index (C-index). Calibration curves were implemented to validate the accuracy and reliability of the nomogram (Kramer and Zimmerman, 2007). In the end, model performance in predicting high TILs were quantified using the area under the curve (AUC) of the receiver operating characteristic (ROC) analysis in training set and validated in validation set, respectively. During the validation of the nomogram, the total points of each patient in the validation cohort were calculated according to the established nomogram, then ROC curve were derived using the total points as predicting parameter. All analyses and plots were performed using the following R packages: "rms", "calibrate", "pROC" and "nomogramEx".

Validation of Nomogram in NAT Cohort

In order to verify the clinical significance of TILs nomogram model, we included an independent cohort treated with NAT, to verify our nomogram model with the prediction of NAT pCR ratio. The main inclusion criteria were: 1) 18–80 years of age female patients; 2) Preoperative diagnosed as the early and intermediate stage breast cancer, and eligibility for NAT after comprehensive evaluation according to the latest NCCN BRCA guideline. Exclusion criteria mainly were: 1) previous anti-tumor therapy, i.e., surgery, chemotherapy, radiotherapy, targeted therapy, or immuno-therapy, etc; 2) secondary tumors or multifocal tumors; 3) HIV infection or other immune system diseases; 4) past use of immune agents or drugs and health care products that may affect immune function; 5) state of inflammation and infection within nearly 1 week; 6) Participated in any prospective drug clinical study. Then, a total of 106 patients' data were collected in Sun Yat-Sen University Cancer Center from December 2017 to March 2021.Total points of each patient in the NAT cohort were calculated according to the established nomogram. NAT efficacy was calculated with Pathological complete response (pCR), pCR defined as pathological Miller-payne grade5 together with no lymph nodes metastasis. Patients were divided into predicted high and low TILs groups according to the optimal cut-off points defined by ROC analysis in nomogram training set.

Statistical Analysis

Categorical variables were analyzed by the Chi-square test or Fisher's exact test. Continuous variables were analyzed by non-parametric tests. Associations of clinical and pathological variables with TILs were determined. Then, the optimal cutoff value of TILs was determined by ROC curve analysis, predicting low and high-immune cell groups and further stratifying the patients into the low and high-TILs groups. All statistical tests were two-sided, and $p < 0.05$ was considered significant. Statistical analysis was performed with Programming language R (version 4.0.1, http://www.R-project.org).

RESULTS

General Patient Characteristics and Histopathological Findings

A total of 826 patients were included in nomogram cohort according to the above criteria, H andE staining was performed in enrolled cases to assess the density of TILs, and the results were confirmed by two pathologists. As shown in

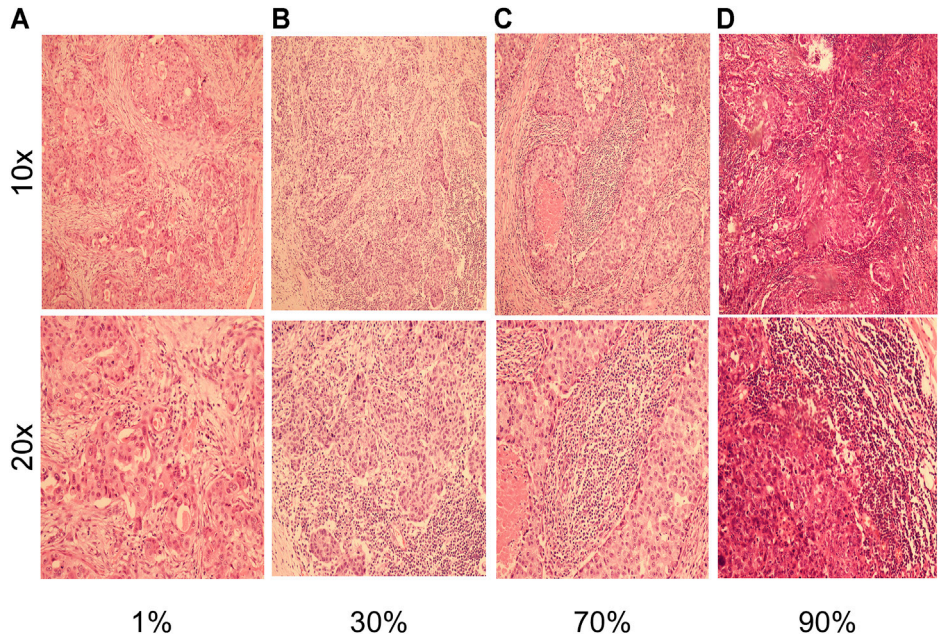

FIGURE 1 | H and E staining with of breast cancer tissues, shown at 10× magnification (inset at 100×) and 20× magnification (inset at ×200). **(A)** Representative images of H and E in a breast cancer patient with 1% TILs density at 10x and 20x magnifications. **(B)** Representative images of H and E in a breast cancer patient with 30% TILs density at 10x and 20x magnifications. **(C)** Representative images of H and E in a breast cancer patient with 70% TILs density at 10x and 20x magnifications. **(D)** Representative images of H and E in a breast cancer patient with 90% TILs density at 10x and 20x magnifications.

Figures 1H,E, staining showed various concentration gradients of TILs under a microscope at 100 and 200×, respectively, (**Figure 1**). The general information is shown in **Table.1**. Related factors were included for analysis, and the associations of these factors with TILs in tumor tissue samples were analyzed. It was found that tumor differentiation ($p < 0.001$), TNM staging ($p = 0.045$) and BMI ($p = 0.015$) were significantly correlated with TILs. In addition, age, gender, marital status, blood group, tumor location, tumor T and N stages, hypertension, and diabetes mellitus were not significantly correlated with tumor TILs.

Pathological Features

Pathological findings were collected to analyze the associations of these factors with TILs (**Table.2**). Comparative analysis indicated that positive status of ER (37 vs. 63%, $p < 0.001$), PR (38 vs. 62%, $p < 0.001$), AR (14 vs. 86%, $p < 0.001$) expression and peri-tumor nerve invasion (10 vs. 89%, $p = 0.009$) were correlated with lower TILs. Meanwhile, HER2 positive rate (60 vs. 40%, $p < 0.001$), Ki67 expression ($p < 0.001$), and peri-tumor vascular invasion(62 vs. 38%, $p = 0.039$) were positively correlated with high TILs.

Further analysis showed that even in HR + HER2-breast cancer, ER expression level (p = 4.6e-07) and PR (p = 0.00043) were negatively correlated with TILs, indicating that the association between TILs and HR is independent of molecular subtyping. Patients with TILs <30% showed increased ER and PR expression levels, especially ER levels (**Figures 2A,B**). Besides, in HR + HER2-patients (p = 1.6e-11) and HER2+, TNBC patients ($p = 0.0072$), the expression of Ki67 was positively correlated with TILs (**Figures 2C,D**).

Blood Specimen Analysis

In biochemical indicators, median levels of total bilirubin (TBIL) (10.7 vs. 10.2, $p = 0.033$) and indirect bilirubin (IBIL) (7.6 vs. 7.2, p = 0.018) were significantly higher in low TILs group. Conversely, median levels of total protein (TP) (72.67 vs. 73.18, p = 0.020), globulin (GLOB) (29.02 vs. 29.77, p = 0.019), calcium (Ca) (2.25 vs. 2.28, p = 0.011) and inorganic phosphorus (IP) (1.15 vs. 1.18, p = 0.006) were significantly higher in high TILs group. (**Table 3**).

However, we found no significant correlations between TILs and indicators of blood routine (**Supplementary Table S1**), tumor markers (CEA, CA153, CA125, CA199) (**Supplementary Table S3**) and hormone levels (**Supplementary Table S2**).

Nomogram for Evaluating Breast Cancer TILs

Various factors affecting BRCA TILs were included in the analysis. In order to establish a predicted model that can be used in baseline situation, we only include TILs associated factors that can be accurately detected at baseline biopsy tissue and blood samples, including ER expression level, PR expression level, Ki67 expression level, HER2 status, and significant blood indicators mentioned above (TP, GLOB, IP, Ca, TBIL, and IBLI).

We divided the nomogram cohort with complete parameter information mentioned above (n = 773) into training set and validation set in a random manner without replacement at a ratio of 8:2. Nomogram model construction was performed in training

TABLE 1 | Patient and general features.

	Low TILs (≤10%) *n* (%)	High TILs (>10%) *n* (%)	*p* Value
Age	—	—	0.192
≤40	84 (14)	39 (18)	—
>40	523 (86)	180 (82)	—
Sex	—	—	0.699
Female	604 (100)	219 (100)	—
Male	3 (0)	0	—
BMI	—	—	0.015
≥28	71 (12)	12 (5)	—
<28	536 (88)	207 (95)	—
Blood group	—	—	0.667
A	170 (28)	67 (31)	—
B	152 (25)	46 (21)	—
O	209 (34)	78 (26)	—
AB	42 (7)	16 (7)	—
Unknown	34	12	—
Blood Rh	—	—	1.000
+	571 (94)	206 (94)	—
-	2 (0)	1 (0)	—
Unknown	34	12	—
Location	—	—	1.000
Left side	304 (50)	109 (50)	—
Right side	303 (50)	110 (50)	—
Histology	—	—	0.648
Invasive Ductal	546 (90)	200 (91)	—
Others	61 (10)	19 (9)	—
Histological grade	—	—	<0.001
I	14 (2)	1 (0)	—
II	378 (62)	78 (37)	—
III	182 (30)	134 (61)	—
Unknown	33	6	—
N stage	—	—	0.106
N0	343 (57)	109 (50)	—
N1	155 (26)	73 (33)	—
N2	61 (10)	26 (12)	—
N3	38 (6)	10 (5)	—
Unknown	10	1	—
T stage	—	—	0.192
T1	420 (69)	145 (66)	—
T2	178 (29)	69 (32)	—
T3	5 (1)	5 (2)	—
T4	4 (1)	0	—
TNM	—	—	0.045
I	279 (46)	82 (37)	—
II	216 (36)	98 (45)	—
III	102 (17)	38 (17)	—
Unknown	10	1	—
Hypertension	—	—	0.803
No	569 (94)	207 (95)	—
Yes	38 (6)	12 (5)	—
Diabetes	—	—	0.618
No	578 (95)	211 (96)	—
Yes	29 (5)	8 (4)	—

*$p < 0.05$, *statistically significant.*
a Chi-square test; $p < 0.05$ *was considered statistically significant.*
Abbreviation: BMI, body mass index.

set ($n = 618$). In univariate logistic regression analysis, all of the baseline indicators showed significant correlation with TILs and were further enrolled in the backward multivariate logistic regression model (**Table.4**). It turned out that the model with IBIL, IP TP, histology grade, ER, and Ki67 as input variables has the lowest AIC. Therefore, factors of PR, HER2, TBIL, GLOB were excluded after backward multivariate binary logistic regression analysis and further nomogram construction. Finally, a nomogram model for BRCA (**Figure 3**) was further established with variates of IBIL, IP TP, histology grade, ER, and Ki67 (**Figure 3A**). Harrell' concordance indicators of the nomogram were assessed (c-index = 0.772), and calibration

TABLE 2 | correlations between Pathological features and TILs.

	Low TILs (≤10%) *n* (%)	High TILs (>10%) *n* (%)	*p* Value
ER	—	—	<0.001
–	81 (13)	81 (37)	—
+	526 (87)	138 (63)	—
PR	—	—	<0.001
–	93 (15)	84 (38)	—
+	514 (85)	135 (62)	—
AR	—	—	<0.001
–	25 (4)	31 (14)	—
+	582 (96)	188 (86)	—
HER2	—	—	<0.001
–	463 (76)	131 (60)	—
+	144 (24)	88 (40)	—
Ki67	—	—	<0.001
1–25%	293 (48)	45 (21)	—
26–50%	215 (35)	80 (37)	—
51–75%	76 (13)	63 (29)	—
76–99%	23 (4)	31 (14)	—
Molecular subtype	—	—	<0.001
HR + HER2(–)	440 (72)	100 (46)	—
HER2(+)	44 (24)	88 (40)	—
TNBC	25 (4)	31 (14)	—
Peri-tumor vascular invasion	—	—	0.039
+	183 (30)	83 (38)	—
–	424 (70)	135 (62)	—
Unknown	0	1	—
Peri-tumor nerve invasion	—	—	0.009
+	109 (18)	22 (10)	—
–	498 (82)	196 (89)	—
Unknown	0	1	—

*p < *0.05, statistically significant.*

aChi-square test; p < *0.05 was considered statistically significant.; Abbreviation: ER, estrogen receptor; PR, Progesterone receptor; AR, androgen receptor; HER2, Human epidermal growth factor receptor 2. HR + HER2-, ER+/PR+, HER2-,; HER2+, ER + -, PR + -, HER2+; TNBC, ER-, PR-, HER2-.*

curves showed good agreement between predicted and observed values (**Figure 3B**). In ROC curve analysis to evaluate the discrimination power of the TILs nomogram, the AUC was 0.759 (95%CI 0.717–0.801) in training set and 0.708 (95%CI 0.617–0.800) in validation set, respectively (**Figures 3C,D**). Univariate binary logistic analysis showed that large point value calculated using the nomogram model had a significant association with higher TILs (OR = 1.033 95%CI:1.026–1.04, p < 0.001).

In addition, we also found that ER expression level [OR = 0.987, 95%CI (0.982–0.992), p < 0.001], IP [OR = 4.462, 95%CI (1.171–17.289), p = 0.029] ,IBIL [OR = 0.906, 95%CI (0.845–0.966), p = 0.004], and TP [OR = 1.053, 95%CI (1.010–1.098, p = 0.016)] were independent predictors of TILs in BRCA patients. (**Table.4**).

Validation of Nomogram in NAT Patients

To further verify the prediction effect of this nomogram on NAT efficacy, another independent NAT cohort was collected for testing. A total of 106 patients were included, including 26 patients with pCR and 80 patients with non-PCR (**Table.5**), and scored those patients with this nomogram model. Patients were divided into the high TILs group and the low TILs group. 30% (24/80) of patients in the high TILs group achieved pCR, for which only 7.69% (2/26) in the low TILs group (p = 0.041) (**Figure 4A**). And in pCR group, patients tended to have higher nomogram points compared with non-pCR group (p = 0.022) (**Figure 4B**).

DISCUSSION

This study retrospectively analyzed factors affecting TILs in BRCA patients and established nomogram model with a large sample size and relatively complete and comprehensive clinical data. Through a series of statistical tests, a model with certain predictive efficacy was established and validated, and relevant factors affecting TILs were obtained. With considerable clinical significance, aiming to help clinicians understand the influencing factors of TILs and evaluate the TILs status of some specific BRCA patients. There is a nomogram model to predict TILs in ovarian cancer (Dai et al., 2021), while to our knowledge, this is the first nomogram model for predicting TILs in BRCA patients with a large sample size and explicit clinical significance.

Some influencing factors of TILs were obtained. HR + HER2- BRCA had the lowest density of TILs, significantly less than TNBC and HER2 + BRCA cases, corroborating withprevious findings (Stanton et al., 2016). In addition, based on a large sample size, this study firstly found that even in HR + HER2- BRCA, TILs were negatively correlated with ER and PR

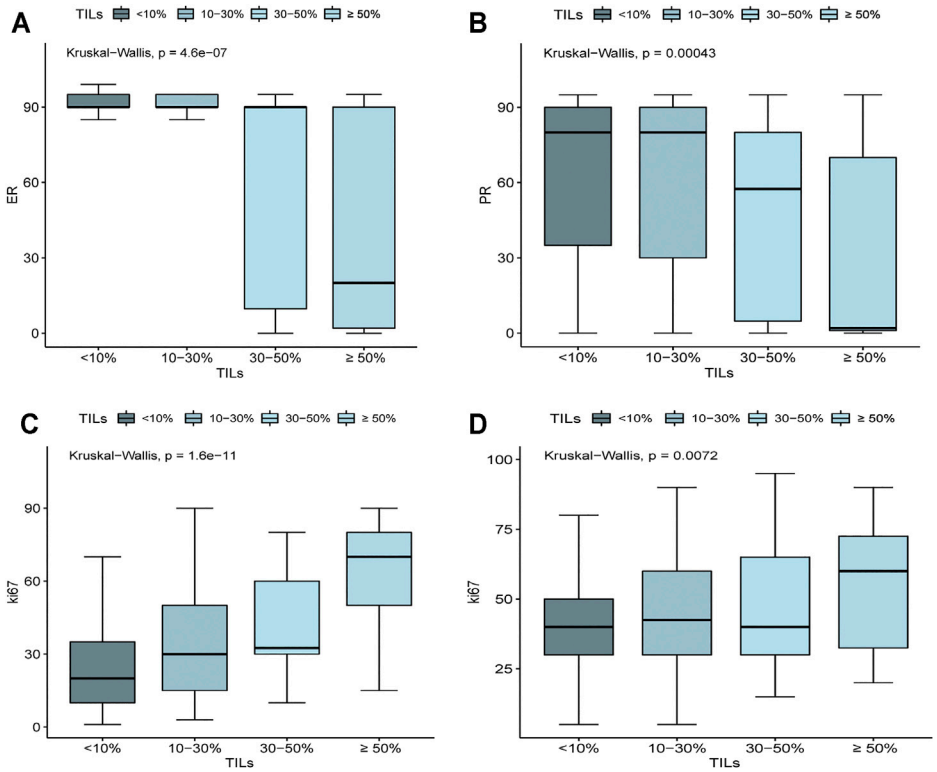

FIGURE 2 | Associations of ER, PR, and Ki67 expression level with the density of TILs. **(A)** In HR+ HER2– BRCA, ER expression was negatively correlated with TILs (p = 4.6e-07). **(B)** In HR+ HER2– BRCA, PR expression was negatively correlated with TILs (p = 0.00043). **(C)** In HR+ HER2– BRCA, ki67 expression was positively correlated with TILs (p = 1.6e-11). **(D)** In TNBC and HER2+ BRCA, ki67 expression was positively correlated with TILs (p = 0.0072).

expression, and positively associated with Ki67. In TNBC and HER2+ BRCA cases, there was a positive correlation between TILs and Ki67 expression. These findings indicated that molecular subtyping of BRCA alone is not enough to predict TILs, and detailed information has valuable significance to improve TILs evaluation.

Based on the postoperative pathological results of patients in this study, TILs were correlated with pathological grade, peri-tumor vascular invasion, molecular typing and other factors, which were in agreement with the conclusions of previous studies (Pruneri et al., 2016b; Criscitiello et al., 2020; Dülgar et al., 2020). In addition, this study innovatively found that BRCA peri-tumor nerve invasion was also negatively correlated with TILs, providing another influencing factor as a reference, although the specific mechanism still needs to be further explored.

Furthermore, this study firstly found significantly negative correlations between TBIL, IBIL, and IP with TILs, based on large sample size. To our knowledge, this is the first work to report an association between bile acid metabolism and BRCA TILs. Previous studies have suggested that bile acids, as tumor suppressants, can regulate the production and function of CD4, Th17, and Treg cells in peripheral blood, which impacts the body's tumor immunity (Hang et al., 2019; Campbell et al., 2020). Lithocholic acid (LAC) as a part of bile acid metabolism, which has been reported to inhibit the proliferation and invasion of BRCA cells and induce their death through lipid metabolism and other mechanisms (Krishnamurthy et al., 2008; Luu et al., 2018; Mikó et al., 2018). Besides, studies have shown that bile acids can affect the expression of chemokine CXCL16, and then affect the infiltration of natural killer T cells in liver cancer through intestines-liver axis, and then affect the biological behavior of tumor (Ma et al., 2018). While there is no such concept as intestines-liver axis in BRCA, and the specific mechanism behind this phenomenon remains unclear, our results may bridge a connection between bile acid metabolism, tumor immunity, and tumor biological behavior, providing clinical evidence for subsequent mechanism studies. As for IP, this study suggested a significant positive correlation with TILs. In the above multivariate logistic model, IP was the strongest independent predictor. According to previously reported data, IP increase can reduce the occurrence risk of HR- BRCA (Papadimitriou et al., 2021). Besides, some clinical BRCA treatment drugs, such as fulvestrant and bisphosphonates, may also affect IP metabolism (Robertson et al., 2016). Therefore, the relationship between IP and TILs deserves further investigation, as well as the role of IP in BRCA. Due to the limitations of retrospective study, a higher level of evidence can't be provided, which could only confirm the correlation between the two, but not for determining the causal relationships. Furthermore, during clinical treatment, especially during NAT, abnormal blood index as bile acid or blood biochemical caused by drug therapy (as

TABLE 3 | correlations between blood biochemistry and TILs.

	Low TILs (≤10%) N = 596 Median (Min-Max)	High TILs (>10%) N = 215 Median (Min-Max)	*p* Value
LDL.C	3.11 (1.09–6.33)	3.05 (0.90–5.43)	0.722
CHO	4.94 (2.65–8.36)	4.93 (2.05–8.62)	0.998
TBA	3.60 (0.20–137)	3.40 (0.40–51.60)	0.729
TBIL	10.7 (2.50–32.8)	10.2 (2.20–39.00)	0.033
TG	1.17 (0.38–8.51)	1.15 (0.31–8.19)	0.617
DBIL	3.10 (0.50–8.90)	2.90 (0.30–11.60)	0.148
ApoA1	1.48 (0.92–2.58)	1.49 (0.79–2.39)	0.953
ApoB	0.92 (0.40–1.86)	0.91 (0.37–1.63)	0.842
IBIL	7.60 (1.40–24.3)	7.20 (0.40–27.40)	0.018
HDL.C	1.40 (0.65–2.86)	1.37 (0.71–2.90)	0.832
LDH	158.40 (97.20–451.60)	159.40 (68.80–333.70)	0.471
UREA	4.60 (1.80–15.20)	4.60 (1.90–10.90)	0.583
UA	298.25 (94.00–609.40)	298.50 (137.10–551.00)	0.830
TP	72.67 (58.57–87.23)	73.18 (54.40–85.42)	0.020
GLOB	29.02 (20.00–42.23)	29.77 (21.30–39.38)	0.019
AG	1.50 (0.99–2.26)	1.47 (1.07–2.00)	0.110
ALB	43.45 (34.70–51.60)	43.70 (36.80–51.60)	0.403
ALP	67.30 (23.90–156.10)	67.70 (30.00–145.90)	0.382
IP	1.15 (0.77–1.75)	1.18 (0.43–1.92)	0.006
CRE	53.10 (28.80–337.80)	54.40 (36.20–117.10)	0.095
CK	65.00(19.00–578.00)	67.00 (15.00–415.00)	0.858
CHE	8,010(3,839–15,194)	8244 (4,179–15,287)	0.207
CYCS	0.82 (0.49–4.93)	0.83 (0.60–1.57)	0.374
Ca	2.25 (1.96–2.54)	2.28(1.51–2.57)	0.011
SAA	5.80 (0.50–104.60)	5.90 (0.10–380.64)	0.888
GLU	5.15 (3.98–19.05)	5.13 (4.20–11.50)	0.370
ALT	13.90 (2.90–623.40)	14.00 (1.00–70.90)	0.955
GGT	17.20 (4.60–159.90)	16.50 (6.00–857.70)	0.253
AS.AL	1.16(0.39–5.28)	1.18 (0.51–13.40)	0.421
AST	16.70 (9.20–283.10)	17.00 (9.80–66.50)	0.383

Abbreviation: LDL, very low density lipoprotein; CHO, cholesterol; TBA, total bile acid; TBIL, total bilirubin; TG, triglyceride; DBIL, direct bilirubin; ApoA1, Apolipoprotein A1; ApoB, Apolipoprotein B; IBIL, Indirect bilirubin; HDL.C, high density lipoprotein; LDH, low density lipoprotein; UREA; UA, uric acid; TP, total protein; GLOB, Globulin; AG, Anion gap; ALB, albumin; ALP, alkaline phosphatase; IP,inorganic phosphorus; CRE, creatinine; CK, Creatine kinase; CHE, cholinesterase; CYCS, Cystatin C; Ca,calcium; SAA, Serum amyloid A protein; Glu, glucose; ALT, Alanine aminotransferase; GGT, glutamyl transferase; AST, aspartate aminotransferase.

TABLE 4 | Correlative factors for TILs identified by univariate binary logistic regression and results of backward binary logistic multivariate logistic regression analysis.

	OR (95%CI) (univariate)	p	OR (95%CI) (multivariate)	p
BMI				
<28	1	–	—	—
≥28	0.955 (0.902–~1.009)	0.105	—	—
Tumor differentiation				
I	1	–	1	–
II	2.163 (0.409~39.914)	0.464	1.269 (0.231~23.705)	0.823
III	8.326 (1.584~153.353)	0.044	2.510 (0.437~47.607)	0.395
ER	0.981 (0.977~0.986)	<0.001	0.987 (0.982~0.992)	<0.001
PR	0.983 (0.978~0.987)	<0.001	—	—
HER2				
Negative	1	–	—	—
Positive	2.024 (1.386~2.951)	<0.001	—	—
Ki67	1.030 (1.022~1.038)	<0.001	1.010 (0.999~1.020)	0.080
TBIL	0.939 (0.897~0.981)	0.006	—	—
IBIL	0.916 (0.862~0.97)	0.003	0.906 (0.845~0.966)	0.004
IP	5.569 (1.65~19.271)	0.006	4.462 (1.171~17.289)	0.029
Ca	5.565 (0.932~34.63)	0.063	—	—
GLOB	1.060 (1.006~1.117)	0.028	—	—
TP	1.045 (1.006~1.085)	0.023	1.053 (1.01~1.098)	0.016

Abbreviation: BMI, body mass index; ER, estrogen receptor; PR, Progesterone receptor; AR, androgen receptor; HER2, Human epidermal growth factor receptor two; TBIL, total bilirubin; GLOB, Globulin; IP, inorganic phosphorus; TP, total protein; IBIL, Indirect bilirubin; Ca, calcium.

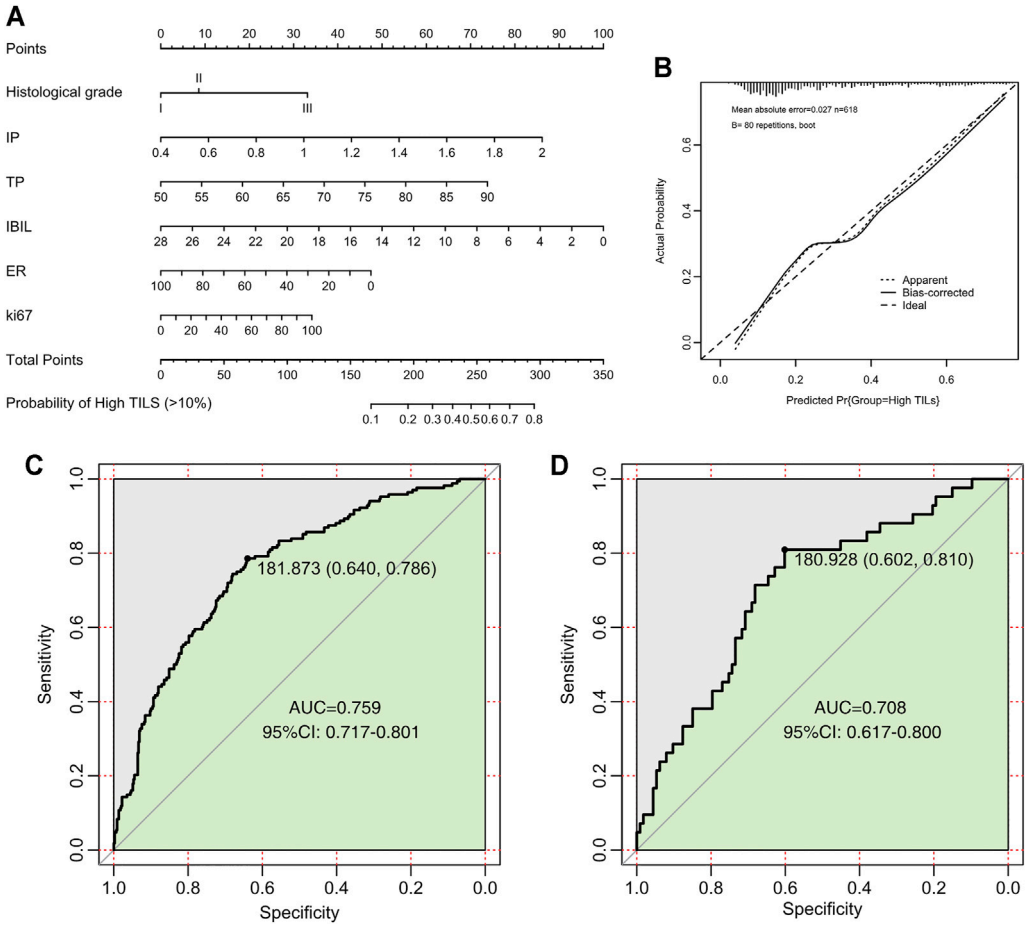

FIGURE 3 | Nomogram, calibration curves, and ROC curve analysis for predicting the density of TILs in patients with breast cancer. **(A)** Prediction nomogram for TILs in breast cancer patients. **(B)** Calibration curves for predicting the density of TILs. **(C)** ROC curves for the TILs prediction nomogram in the internal training set. **(D)** ROC curves for the TILs prediction nomogram in the validation set. All the points assigned on the top point scales for various factors were summed to generate a total point score. The total score was projected on the bottom scales to determine the probability of high-density TILs in an individual. The nomogram-predicted frequency of high TIL density was plotted on the *x*-axis, and the actual observed frequency of high T cell density was plotted on the *y*-axis. The AUC was calculated, and its 95% CI was estimated by bootstrapping. TILs, tumor-infiltrating lymphocytes; ROC, receiver operating characteristic; CI, confidence interval.

TABLE 5 | general infromation in independent validation cohort.

Variables	Numbers (*n* = 106)	Percent (%)
Age(years)		
>40	83	78.3
≤40	23	21.7
Molecular subtype		
HR + HER2(-)	46	43.4
HER2 (+)	49	46.2
TNBC	11	10.4
NAT efficacy		
pCR	26	24.5
Non-pCR	80	75.5
Nomogram prediction		
high TILs group	80	75.5
low TILs group	26	24.5

Abbreviation: ER, estrogen receptor; PR, Progesterone receptor; AR, androgen receptor; HER2, Human epidermal growth factor receptor 2. HR + HER2-, ER+/PR+, HER2-,:HER2+, ER + -, PR + -, HER2+; TNBC, ER-, PR-, HER2-. pCR: Pathological complete response, TILs: tumor-infiltrating lymphocytes.

neoadjuvant chemotherapy, targeted therapy and immune-checkpoint inhibitors) or other reasons, should be paid fully attention by clinicians, which may be related with TILs and furthering tumor immunity, or even prognosis and treatment efficacy.

In recent years, the correlation between body metabolism and tumor biological behaviors has become one of the research hotspots and attracted increasing attention. This study suggested that patients' BMI was correlated with BRCA TILs. Previous studies have reported that BMI in BRCA patients is related to tumor prognosis and sensitivity to chemotherapy: obesity increases the risk of BRCA recurrence and mortality by about 35–40% (Jiralerspong and Goodwin, 2016). Another retrospective study confirmed that BMI is associated with the efficacy of docetaxel chemotherapy in BRCA patients (Desmedt et al., 2020). Accordingly, *in vivo* experiments have confirmed that obesity can affect the function and number of $CD8^+$ immune cells through the related STAT3 pathway, metabolite GATM and

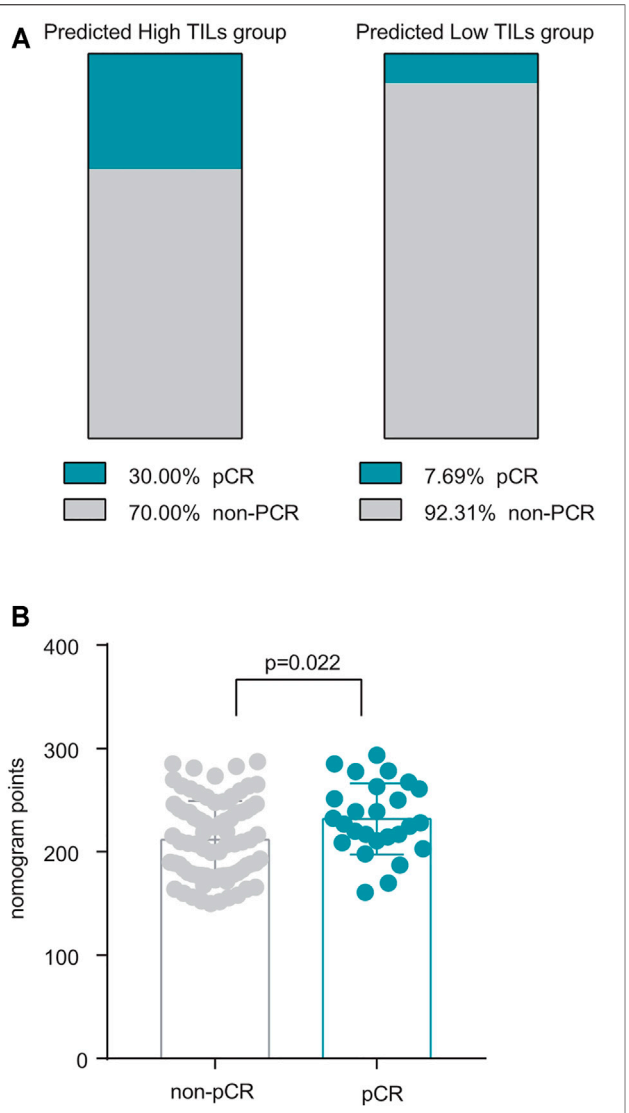

FIGURE 4 | Validation of nomogram in NAT patients. **(A)** The distribution of pCR patients in the high and low TILs groups predicted by this nomogram, pCR ratio in predicted high TILs group 30 vs. 7.69% in predicted low TILs group, $p = 0.041$ **(B)** Patients in the pCR group tended to have a higher nomogram score, $p = 0.022$.

ACSBG1 gene (Ringel et al., 2020; Zhang et al., 2020; Maguire et al., 2021). Meanwhile this study based on lager sample size, firstly demonstrated BMI as an independent influencing factor for BRCA TILs, which may further impact on the prognosis and treatment efficacy. Consequently, the relationships and mechanism between BMI, TILs, BRCA prognosis, and treatment efficacy are worthy of further investigation. While the present findings could help us to understand the correlation between BMI and BRCA, and promote the positive effect of weight control and physical exercise on the prognosis and treatment of BRCA patients.

Studies have shown that TILs can predict the prognosis of BRCA, and can serve as an independent prognosis factor for TNBC (Pruneri et al., 2016b; Denkert et al., 2018a). Thus, the nomogram could be of great significant in prognostic evaluation especially for patients whose pathological slides cannot be obtained for further immunohistochemical staining. In addition to prognosis evaluation, studies have shown that TILs can be used as a predictor of the efficacy of different neoadjuvant therapies, a meta-analysis based on a large sample size indicated that for BRCA of various subtypes, patients with TILs >10% (intermediate and high TILs) had high NAT pCR ratio than patients with TILs ≤ 10 (Low TILs) (Denkert et al., 2018b). Besides, with the application of neoadjuvant immune-checkpoint inhibitors (ICIs) in breast cancer, Loi, S, et al. found that TILs with 10% cut-off value can be used to screen specific benefit groups of ICIs (Loi et al., 2021). Therefore, for this Nomogram model, TILs = 10% was used as cut-off value and patients were divided into two groups: patients with TILs> 10% were defined as high TILs subgroup, while TILs ≤ 10% is low TILs subgroup. Patients in the High TILs group tended to have better NAT efficacy and ICIs efficacy. And our independent NAT cohort also verified this view.

For patients receiving NAT, the method of obtaining specimens for immunohistochemical examination was fine needle biopsy. Due to the heterogeneous distribution of BRCA TILs (Denkert et al., 2018a; Dieci et al., 2018), the accuracy of TILs evaluation from needle biopsy samples were much inferior to those from postoperative specimens, which may further affected the screening of patients benefiting from NAT. In this study, we proposed a nomogram predicted model for TILs, which only required parameters that can be accurately obtained from the baseline tissue. Therefore, this nomogram model could be helpful for the evaluation of NAT efficacy. And with consideration of side effects of various treatment methods available, we could make the preferable selection for BRCA NAT.

At present, clinical evaluation methods for the efficacy of BRCA chemotherapy mainly include Oncotype DX 21 gene testing (Wang et al., 2018) and MammaPrint 70 gene testing (Krop et al., 2017). It can help clinicians to screen out suitable patients with early and middle stage HR+ HER2− BRCA, who could benefit from chemotherapy. However, those methods are expensive, and require additional blood samples from patients. While our nomogram model is convenient, quick, and non-invasive, and it can be expected to be applied in the evaluation of much more kinds of neoadjuvant therapy for subtypes of BRCA patients.

In this study, postoperative specimens were collected retrospectively for TILs assay, and factors influencing TILs were analyzed, for which may have great clinical significance. Then a nomogram model was established using basic and widely available clinical information (BMI, tumor differentiation, ER, Ki67, IP, IBIL, GLOB), which can accurately estimate the actual TILs of patients, providing a tool for patients and clinicians to make estimation of prognosis and therapeutic efficacy, so as to achieve precise treatment in BRCA.

The limitations of this study mainly include: 1) This study was a retrospective study conducted by single center, which has inherent limitations. 2) We only validated this nomogram with NAT patients in cohort with small sample size, and other

items as prognosis and immunotherapy were not verified. 3) The correlation between some indicators such as bilirubin and TILs has been found, but the mechanism has not been further explored.

CONCLUSION

The findings of clinicopathological factors associated with TILs could help clinicians understand the tumor immunity of BRCA patients, serval factors including IBIL and IP as independent predictors of TILs have not been reported before, which may have great clinical significance. And the established nomogram with high evaluation efficiency may be used as a complement tool for distinguishing patients with better neoadjuvant therapeutic efficacy.

DATA AVAILABILITY STATEMENT

The original contributions presented in the study are included in the article/**Supplementary Material**, further inquiries can be directed to the corresponding author.

ETHICS STATEMENT

The studies involving human participants were reviewed and approved by Sun yat-sen university cancer center. The ethics committee waived the requirement of written informed consent for participation.

AUTHOR CONTRIBUTIONS

Conceptualization, JF and XW; Data curation, JF and XW; Formal analysis, JF; Funding acquisition, XW; Investigation, JF; Methodology, JF and JL; Project administration, JF and XW; Resources, JF and XW; Software, JF; Supervision, XW; Validation, JF, XH , JY, HW, WZ; Visualization, JF; Writing–original draft, JF; Writing–review and editing, JF and XW.

FUNDING

This research was funded by the National Natural Science Foundation of China (No. 81772826, No. 81972459).

ACKNOWLEDGMENTS

We would like to thank Dr.Lan in the Department of Pathology in Sun Yat-sen University cancer center, and thanks to the efforts of all the technical staff of the Single disease Research Platform.

SUPPLEMENTARY MATERIAL

The Supplementary Material for this article can be found online at: https://www.frontiersin.org/articles/10.3389/fmolb.2021.761163/full#supplementary-material

REFERENCES

Campbell, C., McKenney, P. T., Konstantinovsky, D., Isaeva, O. I., Schizas, M., Verter, J., et al. (2020). Bacterial Metabolism of Bile Acids Promotes Generation of Peripheral Regulatory T Cells. *Nature* 581 (7809), 475–479. doi:10.1038/s41586-020-2193-0

Chin, Y., Janseens, J., Vandepitte, J., Vandenbrande, J., Opdebeek, L., and Raus, J. (1992). Phenotypic Analysis of Tumor-Infiltrating Lymphocytes from Human Breast Cancer. *Anticancer Res.* 12 (5), 1463–1466. doi:10.1093/jnci/84.17.1368

Criscitiello, C., Vingiani, A., Maisonneuve, P., Viale, G., Viale, G., and Curigliano, G. (2020). Tumor-infiltrating Lymphocytes (TILs) in ER+/HER2− Breast Cancer. *Breast Cancer Res. Treat.* 183 (2), 347–354. doi:10.1007/s10549-020-05771-7

Dai, D., Liu, L., Huang, H., Chen, S., Chen, B., Cao, J., et al. (2021). Nomograms to Predict the Density of Tumor-Infiltrating Lymphocytes in Patients with High-Grade Serous Ovarian Cancer. *Front. Oncol.* 11, 590414. doi:10.3389/fonc.2021.590414

De Angelis, C., Nagi, C., Hoyt, C. C., Liu, L., Roman, K., Wang, C., et al. (2020). Evaluation of the Predictive Role of Tumor Immune Infiltrate in Patients with HER2-Positive Breast Cancer Treated with Neoadjuvant Anti-HER2 Therapy without Chemotherapy. *Clin. Cancer Res.* 26 (3), 738–745. doi:10.1158/1078-0432.ccr-19-1402

Denkert, C., von Minckwitz, G., Darb-Esfahani, S., Lederer, B., Heppner, B. I., Weber, K. E., et al. (2018). Tumour-infiltrating Lymphocytes and Prognosis in Different Subtypes of Breast Cancer: a Pooled Analysis of 3771 Patients Treated with Neoadjuvant Therapy. *Lancet Oncol.* 19 (1), 40–50. doi:10.1016/s1470-2045(17)30904-x

Denkert, C., von Minckwitz, G., Darb-Esfahani, S., Lederer, B., Heppner, B. I., Weber, K. E., et al. (2018). Tumour-infiltrating Lymphocytes and Prognosis in Different Subtypes of Breast Cancer: a Pooled Analysis of 3771 Patients Treated with Neoadjuvant Therapy. *Lancet Oncol.* 19 (1), 40–50. doi:10.1016/s1470-2045(17)30904-x

Desmedt, C., Fornili, M., Clatot, F., Demicheli, R., De Bortoli, D., Di Leo, A., et al. (2020). Differential Benefit of Adjuvant Docetaxel-Based Chemotherapy in Patients with Early Breast Cancer According to Baseline Body Mass Index. *Jco* 38 (25), 2883–2891. doi:10.1200/jco.19.01771

Dieci, M. V., Radosevic-Robin, N., Fineberg, S., van den Eynden, G., Ternes, N., Penault-Llorca, F., et al. (2018). Update on Tumor-Infiltrating Lymphocytes (TILs) in Breast Cancer, Including Recommendations to Assess TILs in Residual Disease after Neoadjuvant Therapy and in Carcinoma *In Situ*: A Report of the International Immuno-Oncology Biomarker Working Group on Breast Cancer. *Semin. Cancer Biol.* 52 (Pt 2), 16–25. doi:10.1016/j.semcancer.2017.10.003

Dülgar, O., İlvan, ˆ., Ilvan, S., and Turna, Z. H. (2020). Prognostic Factors and Tumor Infiltrating Lymphocytes in Triple Negative Breast Cancer. *Eur. J. Breast Health* 16 (4), 276–281. doi:10.5152/ejbh.2020.5305

Erratum: Borderud, S. P., Li, Y., Burkhalter, J. E., Sheffer, C. E., and Ostroff, J. S. (2015). Electronic Cigarette Use Among Patients with Cancer: Characteristics of Electronic Cigarette Users and Their Smoking Cessation Outcomes. *Cancer* 121 (5), 800–801. doi:10.1002/cncr.2881110.1002/cncr.29118

Gajewski, T. F., Schreiber, H., and Fu, Y.-X. (2013). Innate and Adaptive Immune Cells in the Tumor Microenvironment. *Nat. Immunol.* 14 (10), 1014–1022. doi:10.1038/ni.2703

Hamy, A.-S., Bonsang-Kitzis, H., De Croze, D., Laas, E., Darrigues, L., Topciu, L., et al. (2019). Interaction between Molecular Subtypes and Stromal Immune Infiltration before and after Treatment in Breast Cancer Patients Treated with Neoadjuvant Chemotherapy. *Clin. Cancer Res.* 25 (22), 6731–6741. doi:10.1158/1078-0432.ccr-18-3017

Hang, S., Paik, D., Yao, L., Kim, E., Trinath, J., Lu, J., et al. (2019). Bile Acid Metabolites Control TH17 and Treg Cell Differentiation. *Nature* 576 (7785), 143–148. doi:10.1038/s41586-019-1785-z

Ignatiadis, M., Van den Eynden, G., Roberto, S., Fornili, M., Bareche, Y., Desmedt, C., et al. (2019). Tumor-Infiltrating Lymphocytes in Patients Receiving Trastuzumab/Pertuzumab-Based Chemotherapy: A Tryphaena Substudy. *J. Natl. Cancer Inst.* 111 (1), 69–77. doi:10.1093/jnci/djy076

Jiralerspong, S., and Goodwin, P. J. (2016). Obesity and Breast Cancer Prognosis: Evidence, Challenges, and Opportunities. *Jco* 34 (35), 4203–4216. doi:10.1200/jco.2016.68.4480

Kramer, A. A., and Zimmerman, J. E. (2007). Assessing the Calibration of Mortality Benchmarks in Critical Care: The Hosmer-Lemeshow Test Revisited*. *Crit. Care Med.* 35 (9), 2052–2056. doi:10.1097/01.ccm.0000275267.64078.b0

Krishnamurthy, K., Wang, G., Rokhfeld, D., and Bieberich, E. (2008). Deoxycholate Promotes Survival of Breast Cancer Cells by Reducing the Level of Pro-apoptotic Ceramide. *Breast Cancer Res.* 10 (6), R106. doi:10.1186/bcr2211

Krop, I., Ismaila, N., Andre, F., Bast, R. C., Barlow, W., Collyar, D. E., et al. (2017). Use of Biomarkers to Guide Decisions on Adjuvant Systemic Therapy for Women with Early-Stage Invasive Breast Cancer: American Society of Clinical Oncology Clinical Practice Guideline Focused Update. *Jco* 35 (24), 2838–2847. doi:10.1200/jco.2017.74.0472

Loi, S., Michiels, S., Adams, S., Loibl, S., Budczies, J., Denkert, C., et al. (2021). The Journey of Tumor Infiltrating Lymphocytes (TIL) as a Biomarker in Breast Cancer: Clinical Utility in an Era of Checkpoint Inhibition. *Ann. Oncol.*32 (10), 1236–1244. official journal of the European Society for Medical Oncology. doi:10.1016/j.annonc.2021.07.007

Lundgren, C., Bendahl, P.-O., Ekholm, M., Fernö, M., Forsare, C., Krüger, U., et al. (2020). Tumour-infiltrating Lymphocytes as a Prognostic and Tamoxifen Predictive Marker in Premenopausal Breast Cancer: Data from a Randomised Trial with Long-Term Follow-Up. *Breast Cancer Res.* 22 (1), 140. doi:10.1186/s13058-020-01364-w

Luu, T. H., Bard, J.-M., Carbonnelle, D., Chaillou, C., Huvelin, J.-M., Bobin-Dubigeon, C., et al. (2018). Lithocholic Bile Acid Inhibits Lipogenesis and Induces Apoptosis in Breast Cancer Cells. *Cell Oncol.* 41 (1), 13–24. doi:10.1007/s13402-017-0353-5

Ma, C., Han, M., Heinrich, B., Fu, Q., Zhang, Q., Sandhu, M., et al. (2018). Gut Microbiome-Mediated Bile Acid Metabolism Regulates Liver Cancer via NKT Cells. *Science* 360 (6391). doi:10.1126/science.aan5931

Maguire, O. A., Ackerman, S. E., Szwed, S. K., Maganti, A. V., Marchildon, F., Huang, X., et al. (2021). Creatine-mediated Crosstalk between Adipocytes and Cancer Cells Regulates Obesity-Driven Breast Cancer. *Cel Metab.* 33 (3), 499–512.e6. doi:10.1016/j.cmet.2021.01.018

Mikó, E., Vida, A., Kovács, T., Ujlaki, G., Trencsényi, G., Márton, J., et al. (2018). Lithocholic Acid, a Bacterial Metabolite Reduces Breast Cancer Cell Proliferation and Aggressiveness. *Biochim. Biophys. Acta (Bba) - Bioenerg.* 1859 (9), 958–974. doi:10.1016/j.bbabio.2018.04.002

Papadimitriou, N., Dimou, N., Gill, D., Tzoulaki, I., Murphy, N., Riboli, E., et al. (2021). Genetically Predicted Circulating Concentrations of Micronutrients and Risk of Breast Cancer: A Mendelian Randomization Study. *Int. J. Cancer* 148 (3), 646–653. doi:10.1002/ijc.33246

Pruneri, G., Vingiani, A., Bagnardi, V., Rotmensz, N., De Rose, A., Palazzo, A., et al. (2016). Clinical Validity of Tumor-Infiltrating Lymphocytes Analysis in Patients with Triple-Negative Breast Cancer. *Ann. Oncol.* 27 (2), 249–256. doi:10.1093/annonc/mdv571

Pruneri, G., Vingiani, A., Bagnardi, V., Rotmensz, N., De Rose, A., Palazzo, A., et al. (2016). Clinical Validity of Tumor-Infiltrating Lymphocytes Analysis in Patients with Triple-Negative Breast Cancer. *Ann. Oncol.* 27 (2), 249–256. doi:10.1093/annonc/mdv571

Ringel, A. E., Drijvers, J. M., Baker, G. J., Catozzi, A., García-Cañaveras, J. C., Gassaway, B. M., et al. (2020). Obesity Shapes Metabolism in the Tumor Microenvironment to Suppress Anti-tumor Immunity. *Cell* 183 (7), 1848–1866.e26. doi:10.1016/j.cell.2020.11.009

Robertson, J. F. R., Bondarenko, I. M., Trishkina, E., Dvorkin, M., Panasci, L., Manikhas, A., et al. (2016). Fulvestrant 500 Mg versus Anastrozole 1 Mg for Hormone Receptor-Positive Advanced Breast Cancer (FALCON): an International, Randomised, Double-Blind, Phase 3 Trial. *The Lancet* 388 (10063), 2997–3005. doi:10.1016/s0140-6736(16)32389-3

Salgado, R., Denkert, C., Demaria, S., Sirtaine, N., Klauschen, F., and Pruneri, G. (2015). The Evaluation of Tumor-Infiltrating Lymphocytes (TILs) in Breast Cancer: Recommendations by an International TILs Working Group 2014. *Ann. Oncol. official J. Eur. Soc. Med. Oncol.* 26 (2), 259–271. doi:10.1093/annonc/mdu450

Siegel, R. L., Miller, K. D., Fuchs, H. E., and Jemal, A. (2021). Cancer Statistics, 2021. *CA A. Cancer J. Clin.* 71 (1), 7–33. doi:10.3322/caac.21654

Skriver, S. K., Jensen, M.-B., Knoop, A. S., Ejlertsen, B., and Laenkholm, A.-V. (2020). Tumour-infiltrating Lymphocytes and Response to Neoadjuvant Letrozole in Patients with Early Oestrogen Receptor-Positive Breast Cancer: Analysis from a Nationwide Phase II DBCG Trial. *Breast Cancer Res.* 22 (1), 46. doi:10.1186/s13058-020-01285-8

Skriver, S. K., Jensen, M.-B., Knoop, A. S., Ejlertsen, B., and Laenkholm, A.-V. (2020). Tumour-infiltrating Lymphocytes and Response to Neoadjuvant Letrozole in Patients with Early Oestrogen Receptor-Positive Breast Cancer: Analysis from a Nationwide Phase II DBCG Trial. *Breast Cancer Res.* 22 (1), 46. doi:10.1186/s13058-020-01285-8

Stanton, S. E., Adams, S., and Disis, M. L. (2016). Variation in the Incidence and Magnitude of Tumor-Infiltrating Lymphocytes in Breast Cancer Subtypes. *JAMA Oncol.* 2 (10), 1354–1360. doi:10.1001/jamaoncol.2016.1061

Underwood, J. C. (1974). Lymphoreticular Infiltration in Human Tumours: Prognostic and Biological Implications: a Review. *Br. J. Cancer* 30 (6), 538–548. doi:10.1038/bjc.1974.233

Wang, S.-Y., Dang, W., Richman, I., Mougalian, S. S., Evans, S. B., and Gross, C. P. (2018). Cost-Effectiveness Analyses of the 21-Gene Assay in Breast Cancer: Systematic Review and Critical Appraisal. *Jco* 36 (16), 1619–1627. doi:10.1200/jco.2017.76.5941

Whitford, P., George, W. D., and Campbell, A. M. (1992). Flow Cytometric Analysis of Tumour Infiltrating Lymphocyte Activation and Tumour Cell MHC Class I and II Expression in Breast Cancer Patients. *Cancer Lett.* 61 (2), 157–164. doi:10.1016/0304-3835(92)90174-t

Zhang, C., Yue, C., Herrmann, A., Song, J., Egelston, C., Wang, T., et al. (2020). STAT3 Activation-Induced Fatty Acid Oxidation in CD8+ T Effector Cells Is Critical for Obesity-Promoted Breast Tumor Growth. *Cel Metab.* 31 (1), 148–161.e5. doi:10.1016/j.cmet.2019.10.013

Zhu, L., Narloch, J. L., Onkar, S., Joy, M., Broadwater, G., Luedke, C., et al. (2019). Metastatic Breast Cancers Have Reduced Immune Cell Recruitment but Harbor Increased Macrophages Relative to Their Matched Primary Tumors. *J. Immunotherapy Cancer* 7 (1), 265. doi:10.1186/s40425-019-0755-1

Conflict of Interest: The authors declare that the research was conducted in the absence of any commercial or financial relationships that could be construed as a potential conflict of interest.

Publisher's Note: All claims expressed in this article are solely those of the authors and do not necessarily represent those of their affiliated organizations, or those of the publisher, the editors and the reviewers. Any product that may be evaluated in this article, or claim that may be made by its manufacturer, is not guaranteed or endorsed by the publisher.

frontiers in Molecular Biosciences

ORIGINAL RESEARCH
published: 14 January 2022
doi: 10.3389/fmolb.2021.784667

A Low Advanced Lung Cancer Inflammation Index Predicts a Poor Prognosis in Patients With Metastatic Non–Small Cell Lung Cancer

Ping Lu[1], Yifei Ma[2], Jindan Kai[3], Jun Wang[1], Zhucheng Yin[1], Hongli Xu[1], Xinying Li[4], Xin Liang[2], Shaozhong Wei[2]† and Xinjun Liang[1]*†*

[1]Department of Medical Oncology, Hubei Cancer Hospital, Wuhan, China, [2]Department of Gastrointestinal Oncology Surgery, Hubei Cancer Hospital, Wuhan, China, [3]Department of Thoracic Surgery, Hubei Cancer Hospital, Wuhan, China, [4]Department of Epidemiology and Biostatistics, The Ministry of Education Key Lab of Environment and Health, School of Public Health, Huazhong University of Science and Technology, Wuhan, China

OPEN ACCESS

Edited by:
Yu Guo,
The First Affiliated Hospital of Sun Yat-sen University, China

Reviewed by:
Shihai Liu,
The Affiliated Hospital of Qingdao University, China
Arianna Vignini,
Marche Polytechnic University, Italy

***Correspondence:**
Xinjun Liang
doctorlxj@163.com
Shaozhong Wei
weishaozhong@163.com

†These authors have contributed equally to this work and share senior authorship

Specialty section:
This article was submitted to Molecular Diagnostics and Therapeutics, a section of the journal Frontiers in Molecular Biosciences

Received: 28 September 2021
Accepted: 10 December 2021
Published: 14 January 2022

Citation:
Lu P, Ma Y, Kai J, Wang J, Yin Z, Xu H, Li X, Liang X, Wei S and Liang X (2022) A Low Advanced Lung Cancer Inflammation Index Predicts a Poor Prognosis in Patients With Metastatic Non–Small Cell Lung Cancer. Front. Mol. Biosci. 8:784667. doi: 10.3389/fmolb.2021.784667

Introduction: Inflammation plays a crucial role in cancers, and the advanced lung cancer inflammation index (ALI) is considered to be a potential factor reflecting systemic inflammation.

Objectives: This work aimed to explore the prognostic value of the ALI in metastatic non–small cell lung cancer (NSCLC) and classify patients according to risk and prognosis.

Methods: We screened 318 patients who were diagnosed with stage IV NSCLC in Hubei Cancer Hospital from July 2012 to December 2013. The formula for ALI is body mass index (BMI, kg/m^2) × serum albumin (Alb, g/dl)/neutrophil–lymphocyte ratio (NLR). Categorical variables were analyzed by the chi-square test or Fisher's exact test. The overall survival (OS) rates were analyzed by the Kaplan–Meier method and plotted with the R language. A multivariate Cox proportional hazard model was used to analyze the relationship between ALI and OS.

Results: According to the optimal cut-off value determined by X-tile software, patients were divided into two groups (the ALI <32.6 and ALI ≥32.6 groups), and the median OS times were 19.23 and 39.97 months, respectively ($p < 0.01$). A multivariable Cox regression model confirmed that ALI and chemotherapy were independent prognostic factors for OS in patients with NSCLC. OS in the high ALI group was better than that in the low ALI group (HR: 1.39; 95% CI: 1.03–1.89; $p = 0.03$).

Conclusions: Patients with a low ALI tend to have lower OS among those with metastatic NSCLC, and the ALI can serve as an effective prognostic factor for NSCLC patients.

Keywords: advanced lung cancer inflammation index, inflammation, prognosis, non–small cell lung cancer, overall survival

INTRODUCTION

Due to the lack of symptoms in the early stages of lung cancer, only 21% of patients are diagnosed when they are at stage I and 61% of them at advanced stages of lung cancer (Molina et al., 2008; Miller et al., 2019) Because early disease is typically asymp-tomatic, the majority of lung cancers (61%) are diagnosed at stage III or IV; only 21% of cases are diagnosed at stage I. In terms of prognosis, the 5-year survival rate for stage I lung cancer patients is 57%, while that for stage IV patients is significantly lower at 4%. The 5-year relative survival rate for non–small cell lung cancer (NSCLC) patients is 23%, while the 5-year relative survival rate for small-cell lung cancer (SCLC) patients is even lower at 6% (Miller et al., 2019). NSCLC is one of the main causes of cancer-related deaths, and the prognosis of patients with NSCLC is extremely poor. The 5-year overall survival rate of patients with NSCLC at stage IV was less than 5% over the past 10 years (Arbour and Riely, 2019).

Precision medicine is committed to identifying and classifying individual patients to make the best treatment decisions (Vargas and Harris, 2016). Many demographic characteristics and clinicopathological indicators are recognized as prognostic factors for NSCLC patients, and the pathological stage of the tumor is a vital predictor of overall survival (OS). Various combinations of T (primary tumor), N (regional lymph nodes), and M (distant metastasis classification) stages distinguish cancer patients with different survival characteristics (Eberhardt et al., 2015). It has also been confirmed that some demographic characteristics are of great value in predicting the survival time of NSCLC; these include sex, age (Wang et al., 2019), chronic obstructive pulmonary disease (COPD) status (Loganathan et al., 2006; Ytterstad et al., 2016), and smoking status (de Groot and Munden, 2012). Various inflammatory factors, such as the Glasgow prognostic score (GPS) (Sandfeld-Paulsen et al., 2019; Imai et al., 2021), systemic immune-inflammation index (SII) (Tong et al., 2017; Zheng et al., 2021), NLR (Diem et al., 2017; Bongiovanni et al., 2021), and Aarhus composite biomarker score (ACBS) (Sandfeld-Paulsen et al., 2019), have been validated as prognostic markers in lung cancer.

Chronic inflammation can be triggered by the tumor microenvironment (Balkwill and Mantovani, 2001) and plays a vital role in the occurrence, development, and escape of tumors (Perwez Hussain and Harris, 2007). This may be mediated by the excessive secretion of proinflammatory cytokines and other immunosuppressive factors, resulting in damage to DNA (Ikwegbue et al., 2019) and crosstalk in signal transduction pathways. In addition, the susceptibility and severity of cancer may be related to inflammatory cytokines, and the development of cancer is inhibited when inflammatory cytokine expression is lacking or suppressed (Balkwill and Mantovani, 2001). Moreover, inflammation can contribute to cancer-related clinical symptoms, such as anorexia, cachexia, and pain, which seriously affect the quality of life of patients (Batista et al., 2012). There is growing evidence that inflammatory markers can predict the prognosis of patients with various cancers, such as lung cancer (Sarraf et al., 2009), liver cancer (Aleksandrova et al., 2014), and colorectal cancer (Al-Shaer, 2004). Jafri and his colleagues found that the advanced lung cancer inflammation index (ALI), an inflammatory index, can evaluate inflammation and predict survival time in patients with advanced NSCLC and that low ALI is considered to be a risk factor for poor OS (Jafri et al., 2013). ALI is a powerful prognostic biomarker for both NSCLC (Jafri et al., 2013) and SCLC (He et al., 2015) patients. It has been confirmed that low ALI is also associated with a poor prognosis in patients with esophageal cancer (Feng et al., 2014; Tan et al., 2021), diffuse large B-cell lymphoma (Park et al., 2017), HPV-negative head and neck squamous cell carcinoma (Gaudioso et al., 2021), melanoma (Cheng et al., 2021), and colorectal cancer (Pian et al., 2021). Our study aims to evaluate the prognostic value of ALI in patients with metastatic NSCLC. The results are consistent with Jafri and colleagues' finding that the ALI can be used as a valuable prognostic indicator for NSCLC patients.

TABLE 1 | Baseline characteristics and median OS.

Variable	N (%)	Median OS, Months (95% CI)	P
Age			
<65	221 (69.5)	30.60 (21.16–40.04)	0.23
≥65	97 (30.5)	20.93 (12.78–29.10)	—
Gender			
Male	211 (66.4)	22.27 (13.50–31.04)	0.47
Female	107 (33.6)	32.40 (21.60–43.20)	—
Smoking Status			
Never	154 (48.4)	28.13 (19.90–36.38)	0.95
Current or ever	164 (51.6)	22.27 (12.1–32.35)	—
Drinking Status			
Never	240 (75.5)	26.37 (18.00–34.73)	0.80
Current or ever	78 (24.5)	26.2 (12.93–39.50)	—
Location			
Left	186 (58.5)	28.83 (18.98–38.70)	0.38
Right	132 (41.5)	21.00 (11.74–30.13)	—
Family history of cancer			
Yes	60 (81.1)	29.4 (17.09–41.71)	0.40
No	258 (18.9)	25.23 (17.11–33.36)	—
COPD			
Yes	16 (5)	16.90 (3.64–30.16)	0.35
No	302 (95)	26.37 (18.94–33.79)	—
Tuberculosis			
Yes	18 (5.7)	14.67 (7.46–21.87)	0.44
No	300 (94.3)	26.97 (19.95–33.99)	—
Chemotherapy			
Yes	232 (73)	32.40 (25.61–39.20)	0.003
No	86 (27)	14.83 (9.96–19.71)	—
Radiotherapy			
Yes	40 (12.6)	18.4 (11.90–24.91)	0.23
No	278 (87.4)	28.13 (19.66–36.61)	—
LDH			
<274.4	237 (74.5)	31.53 (24.75–38.32)	0.013
≥274.4	81 (25.5)	16.60 (12.81–20.39)	—
ALI			
<32.6	191 (60.0)	19.23 (13.39–25.09)	0.003
≥32.6	127 (40.0)	39.97 (33.51–46.43)	—

MATERIALS AND METHODS

Study Design

The study is a cross-sectional survey of cancer patients, a total of 318 of whom were pathologically diagnosed with stage IV NSCLC at Hubei Cancer Hospital (HBCH) between July 2012 and December 2013. We selected patients on the basis of the

following inclusion criteria: 1) age >18 years, 2) pathological diagnosis of NSCLC, and 3) metastatic pathologic stage IV according to the American Joint Committee on Cancer (AJCC) Staging Manual (Seventh Edition). The exclusion criteria were as follows: 1) second primary cancer at NSCLC diagnosis, 2) a history of malignancy or hematologic disease, 3) blood test results and clinical symptoms and signs indicating severe infection status, and 4) missing follow-up data. Of the 351 eligible patients, we excluded 33 based on missing data on variables of interest. Finally, 318 patients were analyzed further.

Demographic and Clinical Variables

Related inflammatory indicators, including serum albumin (Alb), neutrophil count, lymphocyte count, and lactate dehydrogenase (LDH) were collected. Furthermore, demographic baseline and clinicopathological characteristics, including age, gender, smoking and drinking status, cancer location, family history, treatment of cancer, and history of lung-related diseases, were obtained through medical records. Body mass index (BMI) was derived using its established derivation formula: body weight (kg)/height squared (m^2). The neutrophil–lymphocyte ratio (NLR) was calculated as follows: peripheral blood absolute neutrophil count divided by absolute lymphocyte count. The formula for the ALI was BMI ×Alb/NLR, where the unit of BMI is kg/m (Molina et al., 2008), and the unit of Alb is g/dl.

Follow-Up

In this study, we defined OS as the period spanning from the date of pathological diagnosis of NSCLC to the date of the final follow-up (i.e., December 31, 2013) or the date of censoring the patient as alive or dead. The follow-up started from the diagnosis in Hubei Cancer Hospital in December 2013 and continued until the end of the follow-up period or the loss of follow-up. During this period, patients underwent routine reexaminations, such as blood laboratory tests and imaging tests.

Statistical Analysis

The optimal cut-off values of ALI and LDH were determined through X-tile and used to convert these factors into categorical variables. The chi-square test and Fisher's exact test were used to analyze the relationships among the categorical variables. The OS rate was analyzed by the Kaplan–Meier method, and the survival differences were assessed for statistical significance using the log-rank test. The median survival time and 95% confidence interval (CI) were reported for each group. Furthermore, survival curves including 95% CIs were generated using R language. The influence of variables on OS was analyzed by multivariate Cox proportional hazard regression, and variables that reached statistical significance ($p < 0.05$) and were associated with ALI were included in the multivariable analysis. Moreover, the hazard ratio (HR) was estimated. All tests were bilateral, and $p < 0.05$ was considered the threshold for statistical significance. Statistical analyses were performed by SPSS 25.0 software.

TABLE 2 | Basic characteristics according to the level of ALI.

Variable	ALI <32.6	ALI ≥32.6	P
Age			
≥65	134 (70.2)	87 (68.5)	0.75
≥65	57 (29.8)	40 (31.5)	—
Gender			
Male	135 (70.7)	76 (59.8)	0.045
Female	56 (29.3)	51 (40.2)	—
Smoking Status			
Never	90 (47.1)	64 (50.4)	0.57
Current or ever	101 (52.9)	63 (49.6)	—
Drinking Status			
Never	147 (77.0)	93 (73.2)	0.45
Current or ever	44 (23.0)	34 (26.8)	—
Location			
Left	118 (61.8)	68 (53.5)	0.14
Right	73 (38.2)	59 (46.5)	—
Family history of cancer			
Yes	37 (19.4)	23 (18.1)	0.78
No	154 (80.6)	104 (81.9)	—
COPD			
Yes	8 (4.2)	8 (6.3)	0.40
No	183 (95.8)	119 (93.7)	—
Tuberculosis			
Yes	14 (7.3)	4 (3.1)	0.11
No	177 (92.7)	123 (96.9)	—
Chemotherapy			
Yes	132 (69.1)	100 (78.7)	0.06
No	59 (30.9)	27 (21.3)	—
Radiotherapy			
Yes	25 (13.1)	15 (11.8)	0.74
No	166 (86.9)	112 (88.2)	—
LDH			
<274.4	127 (66.5)	110 (86.6)	<0.001
≥274.4	64 (33.5)	17 (13.4)	—

RESULTS

Baseline Characteristics

The demographic and clinical variables of the patients who were pathologically diagnosed with NSCLC are shown in **Table 1**. The majority of patients (n = 221) were younger than 65 years old, and 66.4% of patients were male. A history of cigarette smoking and alcohol consumption was reported by 164 (51.6%) and 78 (24.5%) patients, respectively. In total, 16 (5%) patients had a history of COPD, and 18 (5.7%) had a history of tuberculosis. Regarding treatment, 73% (n = 232) of patients accepted chemotherapy, and 12.6% of patients (n = 40) were treated with radiotherapy. The level of LDH in 74.5% of the patients was lower than 274.4, and the ALI level of most patients was low, ALI <32.6. The median survival time and 95% confidence interval of patients in different groups were obtained by univariate survival analysis. Among them, patients who received chemotherapy tended to have a longer survival time ($p = 0.003$). The difference in survival time between patients with different levels of LDH and ALI was considered to be statistically significant; furthermore, patients with low levels of LDH ($p = 0.013$) and a high ALI ($p = 0.003$) had longer survival times.

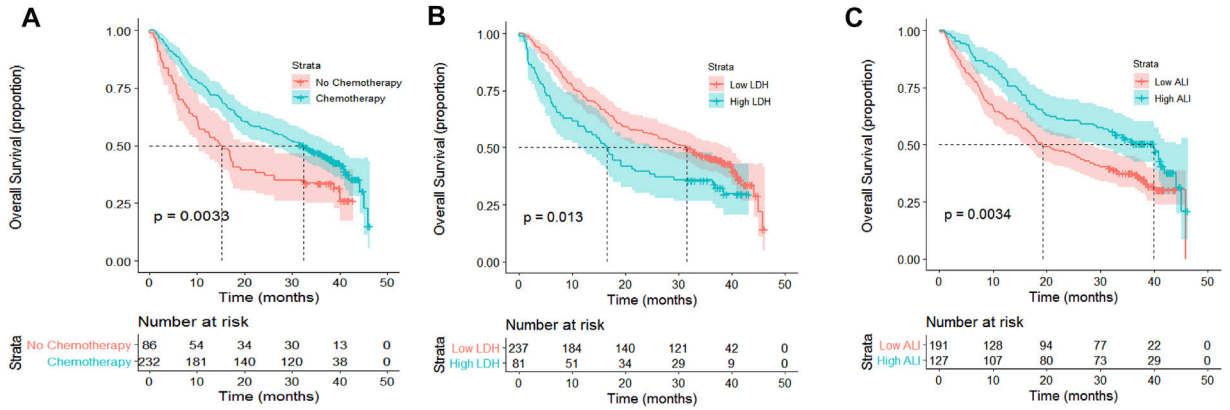

FIGURE 1 | Kaplan–Meier curves for OS and risk tables according to chemotherapy, LDH, and ALI level. **(A)** OS stratification according to chemotherapy. No chemotherapy was significantly associated with poor OS (p = 0.003). **(B)** OS stratification according to LDH. High LDH was significantly associated with poor OS (p = 0.013). **(C)** OS stratification according to ALI. Low ALI was significantly associated with poor OS (p = 0.003).

TABLE 3 | Multivariable Cox regression model (adjusted for gender, chemotherapy, LDH, and ALI).

Variables	Hazard Ratio	95% CI	p
Gender			
Male	—	—	—
Female	0.90	0.67–1.22	0.50
Chemotherapy			
No	—	—	—
Yes	0.67	0.49–0.91	0.01
LDH			
<274.4	—	—	—
≥274.4	1.33	0.96–1.83	0.08
ALI			
≥32.6	—	—	—
<32.6	1.39	1.03–1.89	0.03

Relationship Between Baseline Characteristic Variables and Advanced Lung Cancer Inflammation Index Analysed by Chi-Square Test or Fisher's Exact Test

According to X-tile software, the optimal cut-off value of ALI was determined to be 32.6. Then, all patients were divided into two groups: ALI<32.6 (n = 191) and ALI ≥32.6 (n = 127). The optimal cut-off value of LDH was determined to be 274.4. The relationship between demographic and clinical variables and ALI was analyzed by the chi-square test or Fisher's exact test, as shown in **Table 2**. The results indicated that gender (p = 0.045) and LDH (p < 0.001) were significantly associated with ALI.

Univariate Survival Analysis and Survival Curves

Some factors were recognized as associated with poor OS according to the results of univariate survival analysis (**Figure 1**), including no chemotherapy (p = 0.003; Figure A), high LDH (p = 0.013; Figure B), and low ALI (p = 0.003; Figure C). According to the Kaplan–Meier survival curve, the median survival times in the no chemotherapy and chemotherapy groups were 14.83 months (95% CI: 9.96–19.71 months) and 32.40 months (95% CI: 25.61–39.20 months), respectively, signifying a marked difference, as revealed by the log-rank test (p = 0.003). Moreover, the high LDH group had a shorter median OS period than the low LDH group (16.60 vs 31.53 months, p = 0.013). The OS of patients with a high ALI (≥32.6) was longer than that of patients with a low ALI (<32.6) (39.97 vs 19.23 months, respectively).

Multivariate Cox Regression Model

A multivariate Cox proportional hazard model was used to analyze the influence of variables on OS and estimated its HR with 95% CI. Gender, chemotherapy, LDH, and ALI were included in the multivariate Cox regression model (**Table 3**). Chemotherapy (p = 0.01) and ALI (p = 0.03) were independent prognostic factors in terms of OS. Furthermore, the risk of death in patients with low ALI was 1.39 times higher than that in patients with high ALI (HR: 1.39; 95% CI: 1.03–1.89; p = 0.03).

DISCUSSION

Inflammation is an automatic defense response against pathogens, and inflammatory cytokines contribute to reactive oxygen species production, DNA damage, cell proliferation, and tumor-related angiogenesis in the tumor microenvironment. Inflammation contributes to the occurrence, development, and immune escape of tumors and even affects the treatment response.

The NLR and C-reactive protein (CRP) level have been proven to be prognostic factors for NSCLC and other tumors, including hepatocellular carcinoma (Liao et al., 2018), colorectal cancer (Tsai et al., 2016), and esophageal cancer (Otowa et al., 2019). It has been reported that patients with NSCLC whose NLR returned to normal after one cycle of systematic treatment had a better prognosis than those whose NLR was still not in the normal range (Cedrés et al.,

2012). However, in a study of advanced renal cell carcinoma, it was found that the remission rate of NLR after treatment was not related to the survival rate (Keizman et al., 2012). An increase in neutrophil count or a decrease in lymphocyte count can lead to an increase in the NLR. Neutrophils can produce cytokines and inhibit lymphocyte-mediated immune activity, thus affecting the prognosis of tumor patients.

Another study confirmed that hypoalbuminemia is related to a poor prognosis in NSCLC patients who are treated with erlotinib (Fiala et al., 2016). The correlation between hypoalbuminemia and shorter survival after tumor resection is statistically significant and has been confirmed in resectable colon cancer. It is well known that Alb is one of the indicators for assessing nutritional status. In addition, albumin is an acute phase protein that can indicate inflammatory activity; it can bind to other laboratory indicators, such as C-reactive protein, lymphocytes, and globulins, and its predictive value has been evaluated.

Moreover, as a nutritional status assessment indicator, BMI is also associated with the prognosis of cancer patients. Both underweight and morbidly obese statuses are associated with poor survival in NSCLC and SCLC (Shepshelovich et al., 2019). Similarly, Masaaki et al. explained that both low BMI and high BMI are related to an increased risk of poor survival in breast cancer (Kawai et al., 2012). For thyroid cancer, patients who have a high BMI might have a higher risk of suffering from cancer (Son et al., 2018; Abdel-Rahman, 2019).

As a metric reflecting BMI, Alb, and NLR, ALI provides a more comprehensive assessment of inflammation than these indicators alone. A low ALI value means higher systemic inflammatory activity and plays an important role in the prognosis of patients. A high ALI suggests low activity systemic inflammation in cancer patients, which may result from moderately increased BMI, increased albumin, and decreased NLR. These factors can be involved in the inhibition of tumor occurrence, invasion, and metastasis, promoting a good prognosis. Conversely, a low ALI is usually associated with a poor prognosis. In the univariate survival analysis, there was a significant correlation between a low ALI and poor OS (p = 0.003). In the multivariate Cox regression analysis, we adjusted for gender, chemotherapy, and LDH, and the results proved that a low ALI is an independent risk factor for OS in NSCLC patients. (HR = 1.39; p = 0.03). Therefore, we proposed that ALI can serve as an effective prognostic factor for NSCLC patients.

CONCLUSION

Our study confirms that the difference in survival time of metastatic NSCLC patients with different ALI statuses is statistically significant, and tumor patients with a low ALI have lower OS. Due to the clinical feasibility of assessing the ALI, it can be used to help distinguish patients with different prognoses.

DATA AVAILABILITY STATEMENT

The datasets used and/or analyzed during this study are available from the corresponding authors upon reasonable request.

ETHICS STATEMENT

The studies involving human participants were reviewed and approved by the Ethical Committee of the Hubei Cancer Hospital. The patients/participants provided their written informed consent to participate in this study.

AUTHOR CONTRIBUTIONS

All authors made a significant contribution to the work reported in one or more of the following aspects: conception, study design, execution, acquisition of data, analysis and interpretation, or in all these areas. All authors took part in drafting, revising, or critically reviewing the article; gave final approval of the version to be published; have agreed on the journal to which the article has been submitted; and agree to be accountable for all aspects of the work.

FUNDING

This work was financially supported by the National Natural Sciences Foundation of China (grant numbers: 81772499, 81572287), Health Commission of Hubei Province scientific research project (grant numbers: WJ2021Z001), Applied Basic Research Program of Wuhan Science and Technology Bureau (grant numbers: 2020020601012250), Chinese Society of Clinical Oncology (grant numbers: CSCO: Y-HS2019-39, Y-QL2019-0351), and Cancer Research Program of National Cancer Center (No.NCC201817B052).

ACKNOWLEDGMENTS

The authors would like to thank all participants who volunteered to provide data and samples in this study.

REFERENCES

Abdel-Rahman, O. (2019). Prediagnostic BMI and Thyroid Cancer Incidence in the PLCO Trial. *Future Oncol.* 15 (30), 3451–3456. doi:10.2217/fon-2019-0292

Al-Shaer, M. H. (2004). C-reactive Protein and Risk of colon Cancer. *JAMA* 291 (23), 2819. author reply 2819. doi:10.1001/jama.291.23.2819-a

Aleksandrova, K., Boeing, H., Nöthlings, U., Jenab, M., Fedirko, V., Kaaks, R., et al. (2014). Inflammatory and Metabolic Biomarkers and Risk of Liver and Biliary Tract Cancer. *Hepatology* 60 (3), 858–871. doi:10.1002/hep.27016

Arbour, K. C., and Riely, G. J. (2019). Systemic Therapy for Locally Advanced and Metastatic Non-small Cell Lung Cancer: A Review. *JAMA* 322 (8), 764–774. doi:10.1001/jama.2019.11058

Balkwill, F., and Mantovani, A. (2001). Inflammation and Cancer: Back to Virchow? *The Lancet* 357 (9255), 539–545. doi:10.1016/s0140-6736(00)04046-0

Batista, M. L., Jr., Peres, S. B., McDonald, M. E., Alcantara, P. S. M., Olivan, M., Otoch, J. P., et al. (2012). Adipose Tissue Inflammation and Cancer Cachexia: Possible Role of Nuclear Transcription Factors. *Cytokine* 57 (1), 9–16. doi:10.1016/j.cyto.2011.10.008

Bongiovanni, A., Foca, F., Menis, J., Stucci, S. L., Artioli, F., Guadalupi, V., et al. (2021). Immune Checkpoint Inhibitors with or without Bone-Targeted Therapy in NSCLC Patients with Bone Metastases and Prognostic Significance of Neutrophil-To-Lymphocyte Ratio. *Front. Immunol.* 12, 697298. doi:10.3389/fimmu.2021.697298

Cedrés, S., Torrejon, D., Martínez, A., Martinez, P., Navarro, A., Zamora, E., et al. (2012). Neutrophil to Lymphocyte Ratio (NLR) as an Indicator of Poor Prognosis in Stage IV Non-small Cell Lung Cancer. *Clin. Transl Oncol.* 14 (11), 864–869. doi:10.1007/s12094-012-0872-5

Cheng, X., Dong, Y., and Lou, F. (2021). The Predictive Significance of the Advanced Lung Cancer Inflammation Index (ALI) in Patients with Melanoma Treated with Immunotherapy as Second-Line Therapy. *Cmar* Vol. 13, 173–180. doi:10.2147/cmar.s286453

de Groot, P., and Munden, R. F. (2012). Lung Cancer Epidemiology, Risk Factors, and Prevention. *Radiologic Clin. North America* 50 (5), 863–876. doi:10.1016/j.rcl.2012.06.006

Diem, S., Schmid, S., Krapf, M., Flatz, L., Born, D., Jochum, W., et al. (2017). Neutrophil-to-Lymphocyte Ratio (NLR) and Platelet-To-Lymphocyte Ratio (PLR) as Prognostic Markers in Patients with Non-small Cell Lung Cancer (NSCLC) Treated with Nivolumab. *Lung Cancer* 111, 176–181. doi:10.1016/j.lungcan.2017.07.024

Eberhardt, W. E., Mitchell, A., Crowley, J., Kondo, H., Kim, Y. T., Turrisi, A., et al. (2015). The IASLC Lung Cancer Staging Project: Proposals for the Revision of the M Descriptors in the Forthcoming Eighth Edition of the TNM Classification of Lung Cancer. *J. Thorac. Oncol.* 10 (11), 1515–1522. doi:10.1097/JTO.0000000000000673

Feng, J., Huang, Y., and Chen, Q. (2014). A New Inflammation index Is Useful for Patients with Esophageal Squamous Cell Carcinoma. *Ott* 7, 1811–1815. doi:10.2147/ott.s68084

Fiala, O., Pesek, M., Finek, J., Racek, J., Minarik, M., Benesova, L., et al. (2016). Serum Albumin Is a strong Predictor of Survival in Patients with Advanced-Stage Non-small Cell Lung Cancer Treated with Erlotinib. *Neoplasma* 63 (3), 471–476. doi:10.4149/318_151001N512

Gaudioso, P., Borsetto, D., Tirelli, G., Tofanelli, M., Cragnolini, F., Menegaldo, A., et al. (2021). Advanced Lung Cancer Inflammation index and its Prognostic Value in HPV-Negative Head and Neck Squamous Cell Carcinoma: a Multicentre Study. *Support Care Cancer* 29 (8), 4683–4691. doi:10.1007/s00520-020-05979-9

He, X., Zhou, T., Yang, Y., Hong, S., Zhan, J., Hu, Z., et al. (2015). Advanced Lung Cancer Inflammation Index, a New Prognostic Score, Predicts Outcome in Patients with Small-Cell Lung Cancer. *Clin. Lung Cancer* 16 (6), e165–e171. doi:10.1016/j.cllc.2015.03.005

Ikwegbue, P. C., Masamba, P., Mbatha, L. S., Oyinloye, B. E., and Kappo, A. P. (2019). Interplay between Heat Shock Proteins, Inflammation and Cancer: a Potential Cancer Therapeutic Target. *Am. J. Cancer Res.* 9 (2), 242–249.

Imai, H., Kishikawa, T., Minemura, H., Yamada, Y., Ibe, T., Yamaguchi, O., et al. (2021). Pretreatment Glasgow Prognostic Score Predicts Survival Among Patients with High PD-L1 Expression Administered First-line Pembrolizumab Monotherapy for Non-small Cell Lung Cancer. *Cancer Med.* 10 (20), 6971–6984. doi:10.1002/cam4.4220

Jafri, S. H., Shi, R., and Mills, G. (2013). Advance Lung Cancer Inflammation index (ALI) at Diagnosis Is a Prognostic Marker in Patients with Metastatic Non-small Cell Lung Cancer (NSCLC): a Retrospective Review. *BMC cancer* 13, 158. doi:10.1186/1471-2407-13-158

Kawai, M., Minami, Y., Nishino, Y., Fukamachi, K., Ohuchi, N., and Kakugawa, Y. (2012). Body Mass index and Survival after Breast Cancer Diagnosis in Japanese Women. *BMC Cancer* 12, 149. doi:10.1186/1471-2407-12-149

Keizman, D., Ish-Shalom, M., Huang, P., Eisenberger, M. A., Pili, R., Hammers, H., et al. (2012). The Association of Pre-treatment Neutrophil to Lymphocyte Ratio with Response Rate, Progression Free Survival and Overall Survival of Patients Treated with Sunitinib for Metastatic Renal Cell Carcinoma. *Eur. J. Cancer* 48 (2), 202–208. doi:10.1016/j.ejca.2011.09.001

Liao, M., Chen, P., Liao, Y., Li, J., Yao, W., Sun, T., et al. (2018). Preoperative High-Sensitivity C-Reactive Protein to Lymphocyte Ratio index Plays a Vital Role in the Prognosis of Hepatocellular Carcinoma after Surgical Resection. *Ott* Vol. 11, 5591–5600. doi:10.2147/ott.s167857

Loganathan, R. S., Stover, D. E., Shi, W., and Venkatraman, E. (2006). Prevalence of COPD in Women Compared to Men Around the Time of Diagnosis of Primary Lung Cancer. *Chest* 129 (5), 1305–1312. doi:10.1378/chest.129.5.1305

Miller, K. D., Nogueira, L., Mariotto, A. B., Rowland, J. H., Yabroff, K. R., Alfano, C. M., et al. (2019). Cancer Treatment and Survivorship Statistics, 2019. *CA A. Cancer J. Clin.* 69 (5), 363–385. doi:10.3322/caac.21565

Molina, J. R., Yang, P., Cassivi, S. D., Schild, S. E., and Adjei, A. A. (2008). Non-small Cell Lung Cancer: Epidemiology, Risk Factors, Treatment, and Survivorship. *Mayo Clinic Proc.* 83 (5), 584–594. doi:10.1016/s0025-6196(11)60735-0

Otowa, Y., Nakamura, T., Yamazaki, Y., Takiguchi, G., Nakagawa, A., Yamamoto, M., et al. (2019). Meaning of C-Reactive Protein Around Esophagectomy for cStage III Esophageal Cancer. *Surg. Today* 49 (1), 90–95. doi:10.1007/s00595-018-1706-z

Park, Y. H., Yi, H. G., Lee, M. H., Kim, C. S., and Lim, J. H. (2017). Prognostic Value of the Pretreatment Advanced Lung Cancer Inflammation Index (ALI) in Diffuse Large B Cell Lymphoma Patients Treated with R-CHOP Chemotherapy. *Acta Haematol.* 137 (2), 76–85. doi:10.1159/000452991

Perwez Hussain, S., and Harris, C. C. (2007). Inflammation and Cancer: an Ancient Link with Novel Potentials. *Int. J. Cancer* 121 (11), 2373–2380. doi:10.1002/ijc.23173

Pian, G., Hong, S. Y., and Oh, S. Y. (2021). Prognostic Value of Advanced Lung Cancer Inflammation index in Patients with Colorectal Cancer Liver Metastases Undergoing Surgery. *Tumori*, 300891620983465. doi:10.1177/0300891620983465

Sandfeld-Paulsen, B., Meldgaard, P., Sorensen, B. S., Safwat, A., and Aggerholm-Pedersen, N. (2019). The Prognostic Role of Inflammation-Scores on Overall Survival in Lung Cancer Patients. *Acta Oncologica* 58 (3), 371–376. doi:10.1080/0284186x.2018.1546057

Sarraf, K. M., Belcher, E., Raevsky, E., Nicholson, A. G., Goldstraw, P., and Lim, E. (2009). Neutrophil/lymphocyte Ratio and its Association with Survival after Complete Resection in Non-small Cell Lung Cancer. *J. Thorac. Cardiovasc. Surg.* 137 (2), 425–428. doi:10.1016/j.jtcvs.2008.05.046

Shepshelovich, D., Xu, W., Lu, L., Fares, A., Yang, P., Christiani, D., et al. (2019). Body Mass Index (BMI), BMI Change, and Overall Survival in Patients with SCLC and NSCLC: A Pooled Analysis of the International Lung Cancer Consortium. *J. Thorac. Oncol.* 14 (9), 1594–1607. doi:10.1016/j.jtho.2019.05.031

Son, H., Lee, H., Kang, K., and Lee, I. (2018). The Risk of Thyroid Cancer and Obesity: A Nationwide Population-Based Study Using the Korea National Health Insurance Corporation Cohort Database. *Surg. Oncol.* 27 (2), 166–171. doi:10.1016/j.suronc.2018.03.001

Tan, X., Peng, H., Gu, P., Chen, M., and Wang, Y. (2021). Prognostic Significance of the L3 Skeletal Muscle Index and Advanced Lung Cancer Inflammation Index in Elderly Patients with Esophageal Cancer. *Cmar* Vol. 13, 3133–3143. doi:10.2147/cmar.s304996

Tong, Y.-S., Tan, J., Zhou, X.-L., Song, Y.-Q., and Song, Y.-J. (2017). Systemic Immune-Inflammation index Predicting Chemoradiation Resistance and Poor Outcome in Patients with Stage III Non-small Cell Lung Cancer. *J. Transl Med.* 15 (1), 221. doi:10.1186/s12967-017-1326-1

Tsai, P. L., Su, W. J., Leung, W. H., Lai, C. T., and Liu, C. K. (2016). Neutrophil-lymphocyte Ratio and CEA Level as Prognostic and Predictive Factors in Colorectal Cancer: A Systematic Review and Meta-Analysis. *J. Cancer Res. Ther.* 12 (2), 582–589. doi:10.4103/0973-1482.144356

Vargas, A. J., and Harris, C. C. (2016). Biomarker Development in the Precision Medicine Era: Lung Cancer as a Case Study. *Nat. Rev. Cancer* 16 (8), 525–537. doi:10.1038/nrc.2016.56

Wang, H., Hou, J., Zhang, G., Zhang, M., Li, P., Yan, X., et al. (2019). Clinical Characteristics and Prognostic Analysis of Multiple Primary Malignant Neoplasms in Patients with Lung Cancer. *Cancer Gene Ther.* 26 (11-12), 419–426. doi:10.1038/s41417-019-0084-z

Ytterstad, E., Moe, P., and Hjalmarsen, A. (2016). COPD in Primary Lung Cancer Patients: Prevalence and Mortality. *Int. J. Chron. Obstruct Pulmon Dis.* 11, 625–636. doi:10.2147/copd.s101183

Zheng, K., Liu, X., Ji, W., Lu, J., Cui, J., and Li, W. (2021). The Efficacy of Different Inflammatory Markers for the Prognosis of Patients with Malignant Tumors. *Jir* Vol. 14, 5769–5785. doi:10.2147/jir.s334941

Conflict of Interest: The authors declare that the research was conducted in the absence of any commercial or financial relationships that could be construed as a potential conflict of interest.

Publisher's Note: All claims expressed in this article are solely those of the authors and do not necessarily represent those of their affiliated organizations, or those of the publisher, the editors, and the reviewers. Any product that may be evaluated in this article, or claim that may be made by its manufacturer, is not guaranteed or endorsed by the publisher.

frontiers in Molecular Biosciences

ORIGINAL RESEARCH
published: 17 January 2022
doi: 10.3389/fmolb.2021.799651

Prognostic Value and Immunological Role of KIFC1 in Hepatocellular Carcinoma

Dan Li[1†], Tao Yu[2†], Jingjing Han[3], Xu Xu[4], Jie Wu[1], Wei Song[1], Gang Liu[1], Hua Zhu[5] and Zhi Zeng[6*]*

[1]Department of Pharmacy, Renmin Hospital of Wuhan University, Wuhan, China, [2]Department of Oncology, Integrated Traditional Chinese and Western Medicine, The Central Hospital of Wuhan, Tongji Medical College, Huazhong University of Science and Technology, Wuhan, China, [3]Department of Infection Control, Renmin Hospital of Wuhan University, Wuhan, China, [4]Department of Geriatrics, Renmin Hospital of Wuhan University, Wuhan, China, [5]Department of Neurosurgery, Renmin Hospital of Wuhan University, Wuhan, China, [6]Department of Pathology, Renmin Hospital of Wuhan University, Wuhan, China

OPEN ACCESS

Edited by:
Bing Han,
The Affiliated Hospital of Qingdao University, China

Reviewed by:
Luigi Alfano,
G. Pascale National Cancer Institute Foundation (IRCCS), Italy
Amy Paschall,
University of Georgia, United States

***Correspondence:**
Hua Zhu
zhuhuawhu@163.com
Zhi Zeng
zhizeng@whu.edu.cn

[†]These authors have contributed equally to this work

Specialty section:
This article was submitted to Molecular Diagnostics and Therapeutics, a section of the journal Frontiers in Molecular Biosciences

Received: *21 October 2021*
Accepted: *06 December 2021*
Published: *17 January 2022*

Citation:
Li D, Yu T, Han J, Xu X, Wu J, Song W, Liu G, Zhu H and Zeng Z (2022) Prognostic Value and Immunological Role of KIFC1 in Hepatocellular Carcinoma. Front. Mol. Biosci. 8:799651. doi: 10.3389/fmolb.2021.799651

As one of the members of the kinesin family, the role and potential mechanism of kinesin family member C1 (KIFC1) in the development of liver hepatocellular carcinoma (LIHC), especially in the immune infiltration, have not been fully elucidated. In this study, multiple databases and immunohistochemistry were employed to analyze the role and molecular mechanism including the immune infiltration of KIFC1 in LIHC. Generally, KIFC1 mRNA expression was overexpressed in LIHC tissues than normal tissues, and its protein was also highly expressed in the LIHC. KIFC1 mRNA expression was correlated with tumor grade and TNM staging, which was negatively correlated with overall survival and disease-free survival. Moreover, univariable and multivariate Cox analysis revealed that upregulated KIFC1 mRNA is an independent prognostic factor for LIHC. The KIFC1 promoter methylation level was negatively associated with KIFC1 mRNA expression and advanced stages and grade in LIHC. The different methylation sites of KIFC1 had a different effect on the prognosis of LIHC. Specifically, the KIFC1 mRNA expression level showed intense correlation with tumor immunity, such as tumor-infiltrating immune cells and immune scores as well as multiple immune-related genes. Moreover, KIFC1 co-expressed with some immune checkpoints and related to the responses to immune checkpoint blockade (ICB) and chemotherapies. Significant GO analysis showed that genes correlated with KIFC1 served as catalytic activity, acting on DNA, tubulin binding, histone binding, ATPase activity, and protein serine/threonine kinase activity. KEGG pathway analysis showed that these genes related to KIFC1 are mainly enriched in signal pathways such as cell cycle, spliceosome, pyrimidine metabolism, and RNA transport. Conclusively, KIFC1 was upregulated and displayed a prognostic value in LIHC. Moreover, KIFC1 may be involved in the LIHC progression partially through immune evasion and serve as a predictor of ICB therapies and chemotherapies.

Keywords: KIFC1, liver hepatocellular carcinoma, prognosis biomarker, immune infiltration, ICB, immunotherapy

INTRODUCTION

Primary liver cancer is one of the top 10 lethal tumors worldwide. China accounts for 55% of new liver cancer cases and related deaths every year (Torre et al., 2012). Liver hepatocellular carcinoma (LIHC) accounts for approximately 90% of primary liver cancer. An early diagnosis of LIHC is difficult because of its insipid onset and inconspicuous early symptoms. In clinical practice, patients often come to the hospital for treatment and diagnosis when they have symptoms in the late stage. At this time, the 5-year survival rate of patients with advanced LIHC is less than 5% due to the loss of active treatment opportunities or high recurrence and metastasis after treatment (Ziogas and Tsoulfas, 2017). At present, the development and clinical application of various targeted drugs for LIHC such as sorafenib extend the survival of patients to a certain degree (Hu et al., 2021). However, for another part of patients with advanced LIHC, targeted drugs did not show satisfactory efficacy. The total life expectancy is less than 1 year. Hence, it is necessary to develop novel and valuable biomarkers to help us for the accurate and early diagnosis of LIHC and find effective targets to further improve the therapeutic effect of liver cancer (Huang et al., 2017).

Studies have shown that abnormal expression of kinesin family genes plays a vital role in the occurrence and development of a variety of human cancers (Li et al., 2017; Li et al., 2020a). As a motor protein, it plays an important role in intracellular transport and cell division. Kinesin family member C1 (KIFC1) is a microtubule-dependent molecular kinesin with ATP activity and participates in a variety of cellular events, such as mitosis, meiosis, and macromolecular transport. A meta-analysis showed that high expression of KIFC1 can be used as a predictor for patients with non-small cell lung cancer, ovarian cancer, breast cancer, and LIHC. In addition, high levels of KIFC1 are associated with lymphatic metastasis (Sun et al., 2019). Therefore, KIFC1 may be a rational target for tumor therapy, which is worthy of further study. Previous studies have shown that KIFC1 can facilitate the occurrence of liver cancer. The possible mechanism is that TCF-4 activates KIFC1 and then upregulates the transcriptional activity of HMGA1 (Teng et al., 2019). KIFC1 is related to worse prognosis in patients with LIHC (Li et al., 2017), and the key mechanism is that KIFC1 not only can regulate the proliferation of HCC cells, but it can also reduce the apoptosis of HCC-LM3 and SMMC-7721 cell lines. Mechanistically, the apoptosis-related protein, B-cell lymphoma-2 (Bcl-2), was downregulated, whereas Bcl-2-associated X (Bax) and p53 protein were upregulated, and the expression levels of phosphorylated phosphoinositide 3-kinase (p-PI3K) and phosphorylated AKT were decreased significantly when KIFC1 was silenced (Fu et al., 2018). In addition, KIFC1 can promote invasion and metastasis through the signal pathway involving endothelial mesenchymal transition (Han et al., 2019). This process is carried out in a microtubule-dependent manner.

Although the incidence of cancer was increased partially by multiple genetic mutations, the impact of the tumor microenvironment (TME) on tumor progression or immune response did not attract enough attention (Li et al., 2019; Zhu et al., 2021). Recently, cytokine and immune checkpoint blockade (ICB) therapy have become treatment strategies for various types of cancers (Long et al., 2017; Zhang et al., 2021). As a consequence, biomarkers that predict response in immune and stromal cells may help determine which patients will benefit most from ICB treatment. Besides the reported mechanism, the potential mechanisms about KIFC1 in the TME involved in the formation and progression of LIHC have not been elucidated; few studies have addressed the relationship between KIFC1 expression and immune cell infiltration in LIHC. Whether KIFC1 can provide guidance for immunotherapy as well as chemotherapy in LIHC has not been studied.

Therefore, multiple bioinformatics methods and clinical samples were used to comprehensively evaluate the relationship between KIFC1 expression and clinicopathological features as well as the prognosis of LIHC. In addition, the relationship between KIFC1 gene promoter methylation and prognosis were analyzed. The correlation of KIFC1 with tumor immune cell infiltration, immune checkpoints, immune-related genes, and responses to ICB and drugs was detected. The results provide novel insights on the function of KIFC1 and new goals for the diagnosis and prognosis of LIHC.

METHODS

HCCDB Database Analysis

The HCCDB database (http://lifeome.net/database/hccdb/home.html) includes the liver cancer gene expression profile data in GEO, TCGA-LIHC, and ICGC LIRI-JP (Lian et al., 2018). A total of 3,917 samples were divided into 15 data sets. We use HCCDB to analyze the KIFC1 expression difference between hepatocellular carcinoma tissues and normal liver tissues.

GEO and TCGA Analysis

Four LIHC datasets were enrolled in this study including GSE14520, GSE57957, GSE36376, and TCGA. Among the GEO datasets, GSE14520 included 217 paired non-cancerous and LIHC samples, while there are 36 paired tumor and adjacent non-cancerous liver samples in GSE57957; in addition, there are 193 normal tissues and 240 LIHC tissues in GSE36376. Likewise, the TCGA database contained 159 normal liver tissues and 371 primary liver tumor samples. In this study, we used different datasets from multiple databases to investigate the KIFC1 expression difference to make sure that the results are authentic.

Association Between DNA Methylation of KIFC1 and Prognosis of LIHC

The URL of the UALCAN database is http://ualcan.path.uab.edu, which can query and analyze the expression difference of genes between tumor and normal samples (Chandrashekar et al., 2017). We can also compare the expression differences and promoter methylation levels among different tumor subgroups and different clinical characteristics groups. In addition, it can also be used to analyze the impact of a gene on the prognosis of a

tumor. We used this database to analyze KIFC1 expression and its promoter methylation levels in normal and cancerous tissues according to the individual cancer stage and grade of patients. The results are shown in the box chart. The association between the KIFC1 methylation value and expression level was assessed by the MethHC (http://methhc.mbc.nctu.edu.tw/php/index.php) tool. The MethSurv data set (https://biit.cs.ut.ee/methsurv/) was used to assess the DNA methylation and the association between KIFC1 methylation and the prognosis of LIHC.

Exploring the Association of Survival With KIFC1 in LIHC

We performed univariate and multivariate Cox regression analyses to determine the appropriate terms for building nomograms. A forest was applied to display the *p*-value, HR, and 95% CI for each variable by using the "forestplot" R package through R software. A nomogram was created according to the results of the multivariate Cox proportional hazards analysis to predict the total recurrence rate in 1, 3, and 5 years. The "rms" R package was used to evaluate the risk of recurrence for individual patients by the points associated with each risk factor.

We extracted survival information for each sample in TCGA. Indicators such as OS, disease-specific survival (DSS), disease-free survival (DFS), and progression-free survival (PFS) were used to elucidate the relationship between KIFC1 and the prognosis of LIHC patients. Kaplan–Meier (KM) and log-rank tests were used for the survival analysis of LIHC ($p < 0.05$), and survival curves were analyzed by the "survminer" and "survivor" R packages.

GEPIA Analysis

Gene Expression Profiling Interactive Analysis (GEPIA) is a newly developed interactive web server. Its website is http://gepia.cancer-pku.cn/index.html. This database provides online analysis based on data from TCGA and GTeX projects (Tang et al., 2017). In our study, we used the given TCGA expression dataset to assess the difference of KIFC1 between LIHC and normal liver tissues and to confirm the results of gene expression analysis in the HCCDB database and GEO database. In addition, we used GEPIA to analyze the prognostic significance of KIFC1 mRNA expression in LIHC and draw the survival curve with log rank *p*-value.

LinkedOmics Analysis

LinkedOmics is a public website on http://www.linkedomics.org/login.php, which contains 32 TCGA cancer types of multiple omics data, including federation generated from the Clinical Proteomics Tumor Analysis Consortium (Vasaikar et al., 2018). We applied this online tool to identify and analyze KIFC1 co-expression genes in hepatocellular carcinoma cohort from TCGA, which contains 371 samples. The data from Linkfinder are signed and sorted; after that, GO analyses, including molecular function (MF), biological process (BP), cellular component (CC), and KEGG analysis, are performed by the gene set enrichment analysis (GSEA) method.

Association Between KIFC1 and Immune Infiltration, Immune-Related Genes, Immune Checkpoints, and Immune Checkpoint Blockade Responses

The TIMER database is an online tool that is used to evaluate the immune infiltration of various types of cancers to explore the immunological, clinical, and genomic characteristics of cancer. Its website is https://cistrome.shinyapps.io/timer (Li et al., 2020b). The ESTIMATE algorithm was applied to calculate immune and stromal scores for each sample (Yoshihara et al., 2013). In this study, we firstly investigated the expression of KIFC1 in different cancers using TIMER. The correlation between the expression of KIFC1 and the abundance of tumor-infiltrating immune cells and the corresponding cellular genetic markers was also analyzed. The results are presented in box diagrams and tables.

We further investigated the correlation of KIFC1 with immune cell infiltration by the CIBERSORT algorithm using the R packages "ggplot2," "ggpubr," and "ggExtra." In addition, co-expression analyses between KIFC1 and immune-related genes or immune checkpoints were performed using the R packages "limma," "reshape2," "RColorBrewer," "ggplot2," "pheatmap," and "immuneeconv." The TIDE algorithm was used to predict potential ICB responses (Zhu et al., 1950; Jiang et al., 2018).

The Human Protein Atlas Project

The Human Protein Atlas Project (HPAP) (https://www.proteinatlas.org/) is a dataset for analyzing the expression of different proteins. It contains 16,975 unique proteins from different kinds of human tissues and cells. We used it to evaluate the KIFC1 expression in protein levels in LIHC and normal liver tissues.

Clinical Tissue Samples and Data Collection

A total of 36 patients with LIHC who did not receive radiotherapy or chemotherapy before surgery (26 men and 10 women; age range, 23–73 years) were included in the present study. The LIHC tissues and their matched non-cancerous liver tissues were formalin-fixed and paraffin-embedded to compare the KIFC1 protein expression difference for validation.

Immunohistochemistry

IHC staining procedures were performed according to a standard protocol that was described in detail in our previous study (Zeng et al., 2020). The paraffin sections were placed in xylene for 15 min twice for dewaxing and rehydrated in gradient alcohol for 5 min. The sections were treated with 3% H_2O_2 and then antigen retrieval by a citric acid buffer (pH 6.0). Then, the sections were blocked with 5% bovine serum albumin for 20 min and incubated with a rabbit anti-human KIFC1 antibody solution (1:100; Proteintech, Manchester, United Kingdom) at 4°C overnight (16–18 h). Then sections were incubated with horseradish peroxidase-labeled polymer with secondary antibody [UltraSensitiveTM SP (Mouse/Rabbit) IHC Kit-9710; Maixin Bio, Fuzhou, China] at room temperature for 15 min each. After washing with PBS for three times, the reaction products

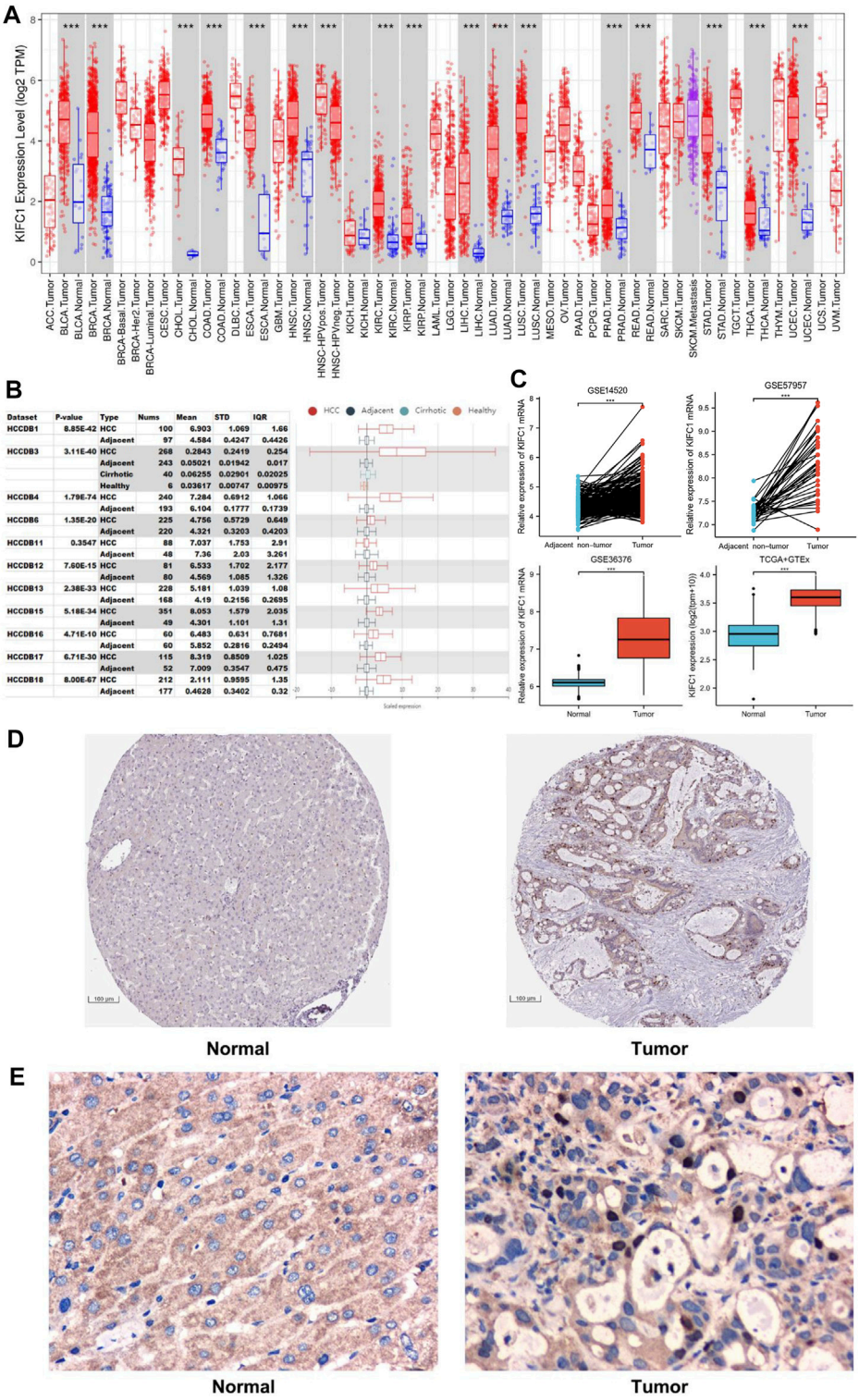

FIGURE 1 | The expression level of KIFC1 in LIHC from different databases. **(A)** KIFC1 expression levels in different tumor types in TIMER. **(B)** KIFC1 expression in tumor tissues and the adjacent normal tissues in HCCDB. **(C)** KIFC1 mRNA expression difference in LIHC and adjacent non-cancerous or normal liver tissues from GSE14520, GSE57957, GSE36376. and TCGA. **(D)** IHC profile of KIFC1 protein expression in normal and LIHC tissues from HPA database. **(E)** Typical IHC staining of KIFC1 protein expression in normal and LIHC tissues from clinical samples. The *p*-value was calculated using Student's t-test. $^{*}p < 0.05$, $^{**}p < 0.01$, $^{***}p < 0.001$.

were stained with 3,3′-diaminobenzidine and lightly counterstained with hematoxylin. The sections with PBS instead of the primary antibody served as negative control. The total staining score was used to evaluate the protein expression of KIFC1 in normal and tumor tissues. The total staining score is the multiplication of the score of staining intensity and staining range. In this study, regardless of staining intensity, the staining score was regarded as positive if the proportion of positive cells is greater than 5%.

Correlation of KIFC1 With Drug Sensitivity

We collected LIHC-related RNA sequences and clinicopathological and survival data while keeping samples with recorded clinical information from TGCA. We predicted the chemotherapeutic response for samples of cancers that had a correlation of KIFC1 with OS according to the available pharmacogenomics database [the Genomics of Drug Sensitivity in Cancer (GDSC), https://www.cancerrxgene.org/]. The prediction of the half-maximum inhibitory concentration (IC50) of the samples was achieved by ridge regression and the prediction accuracy through R package "pRRophetic." All parameters were set by the default values with the removal of the batch effect of the "combat" and tissue type of "allSoldTumours," and duplicate gene expression was summarized as the mean value.

Statistical Analysis

Statistical analyses were conducted using R software (version 4.0.2). The analysis results of HCCDB database showed the *p*-value. The analysis of KIFC1 expression in TIMER and GEO databases showed *p*-value. The survival curve generated by GEPIA analysis showed *p*-value. The difference of KIFC1 and its methylation levels in different clinical feature groups was analyzed by the UALCAN database, and the correlation of the prognosis of LIHC with KIFC1 methylation was analyzed by the MethSurv database and the *p*-value was given. T-test was used to estimate the significance of gene expression level between groups. Univariate and multivariate Cox regression analyses were conducted to analyze the effect of KIFC1 on the prognosis of LIHC. Forest was used to show the *p*-value, HR, and 95% CI of each variable. Spearman correlation analysis was used for genetic correlation, and $p < 0.05$ was considered statistically significant.

RESULTS

Expression of KIFC1 in LIHC

Firstly, in order to more accurately understand the expression of KIFC1 between LIHC and normal liver tissue, we used three different kinds of databases for confirmation. The data from TCGA were analyzed using the TIMER online tool. The results indicated that the mRNA expression of KIFC1 in LIHC was higher than in normal tissues ($p < 0.001$) (**Figure 1A**). Secondly, 11 LIHC cohorts from the specialized liver cancer database HCCDB were analyzed, and the same trends were obtained (**Figure 1B**). Thirdly, from analyzing the KIFC1 mRNA expression from GSE14520, GSE57957, GSE36376, and TCGA, it indicated that the KIFC1 mRNA expression was markedly higher in LIHC compared with its adjacent non-cancerous tissues or normal liver tissues ($p < 0.001$) (**Figure 1C**). Besides, the IHC profile from HPA database showed a higher expression in LIHC tissues (**Figure 1D**). Moreover, the protein expression analysis from our clinical samples with IHC also indicated that KIFC1 was located and highly expressed near the nucleus of liver cancer cells, which was statistically different from that in normal liver tissues (8/36 vs. 1/36, chi-square test, $p < 0.05$) (**Supplementary Figure S1**). However, no significant difference was observed in cytoplasm (**Figure 1E**).

The Expression of KIFC1 Is Associated With Patients' Survival in LIHC

The survival data of KIFC1 expression in LIHC patients were analyzed. Kaplan–Meier survival curves were used to evaluate the relationship between the KIFC1 expression and survival outcomes. The cut-off value of the high and low KIFC1 expression group was set as the median. The results showed that patients with higher KIFC1 mRNA expression had shorter OS ($p = 3.12e-05$) (**Figure 2A**), DSS ($p = 0.00001$) (**Figure 2B**), DFS ($p = 0.00121$) (**Figure 2C**), and PFS ($p = 1.14e-05$) (**Figure 2D**). Consequently, the expression of KIFC1 mRNA in LIHC is associated with survival. The result from GEPIA is also consistent with our results (**Supplementary Figure S2**).

Prognostic Potential of KIFC1 in LIHC

For further subgroup analysis, the correlation of KIFC1 mRNA expression with multiple clinicopathological features was performed in the UALCAN database, which includes 371 LIHC samples. It revealed that the transcription level of KIFC1 was markedly higher compared with normal liver tissue in different subgroups according to age, tumor stage, and grade ($p < 0.001$). Moreover, KIFC1 expression was positively related to the first three stages and grades of LIHC (**Figures 3A–C**), excluding stage IV and grade IV. Furthermore, univariate and multivariate Cox regression analyses illustrated that KIFC1 expression ($p < 0.001$) and pTNM-stage ($p < 0.05$) were important independent factors to the prognosis of LIHC (**Figures 3D,E**). We further constructed a nomogram that combined only two independent prognostic factors (including KIFC1 and pTNM-stage) to provide a quantitative guideline for clinicians to predict the probability of 1-, 3-, and 5-year OS in LIHC patients (**Figure 3F**). Each patient is given a total score through adding each prognostic parameter point, with a higher total score meaning a worse outcome for that patient. In addition, the calibration curves showed that the nomogram performed well in estimating 1-, 3-, and 5-year OS (**Figure 3G**). Therefore, KIFC1 may be a potential diagnostic marker for LIHC.

Relationship Between KIFC1 Methylation and KIFC1 Expression, Prognosis of LIHC

DNA methylation significantly affects gene expression in cancer. MethHC analysis showed that the KIFC1 mRNA was negatively correlated with its promoter methylation level ($r = -0.3$, FDR = 2.5e-09) (**Figure 4A**). Moreover, the methylation level of the KIFC1 promoter in liver cancer is downregulated

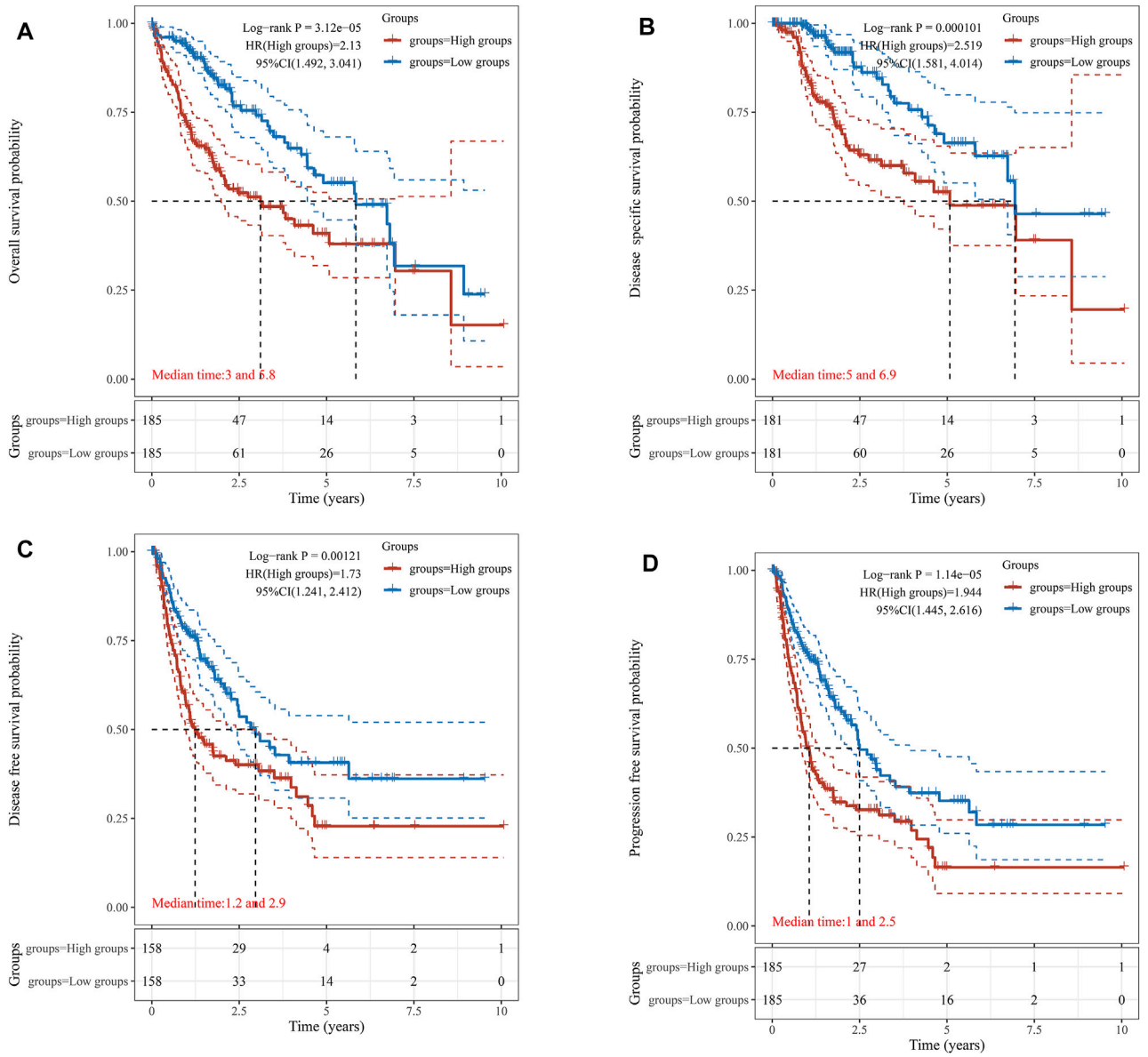

FIGURE 2 | Association of KIFC1 expression with patient survival curve. **(A)** Overall survival curve. **(B)** Disease-specific survival. **(C)** Disease-free survival. **(D)** Progression-free survival.

than normal and was negatively correlated with the individual cancer grade and stage of the LIHC patient (**Figures 4B–D**). In addition, using the MethSurv tool, we found that the LIHC patients with high methylation values of cg08709879 were associated with poor OS (p = 0.00069) (**Figure 4E**). The other methylation sites that had a significant association with the prognosis of LIHC were also presented in **Figure 4E**.

Relationship Between KIFC1 and Immune Cell Infiltration in LIHC

To further explore how the KIFC1 gene affects tumor progression, TIMER was employed to analyze the correlation of KIFC1 expression with the level of immune invasion. The results indicated that KIFC1 copy number variation was related to the infiltration levels of B cells, CD8+ T cells, macrophages, neutrophils, and dendritic cells (**Figure 5A**). Specifically, the expression of KIFC1 was notably associated with tumor purity (r = 0.215, p = 5.37e-05) and the level of major infiltrating immune cell as B cells, CD8+ T cells, CD4+ T cells, macrophages, neutrophils, and dendritic cells (**Figure 5B**). In order to evaluate whether KIFC1 expression will affect the tumor immunity, the patients were divided into high and low KIFC1 expression groups, and the immune score was calculated; results indicated that KIFC1 expression was associated with immune and stromal scores (**Figures 5C–E**).

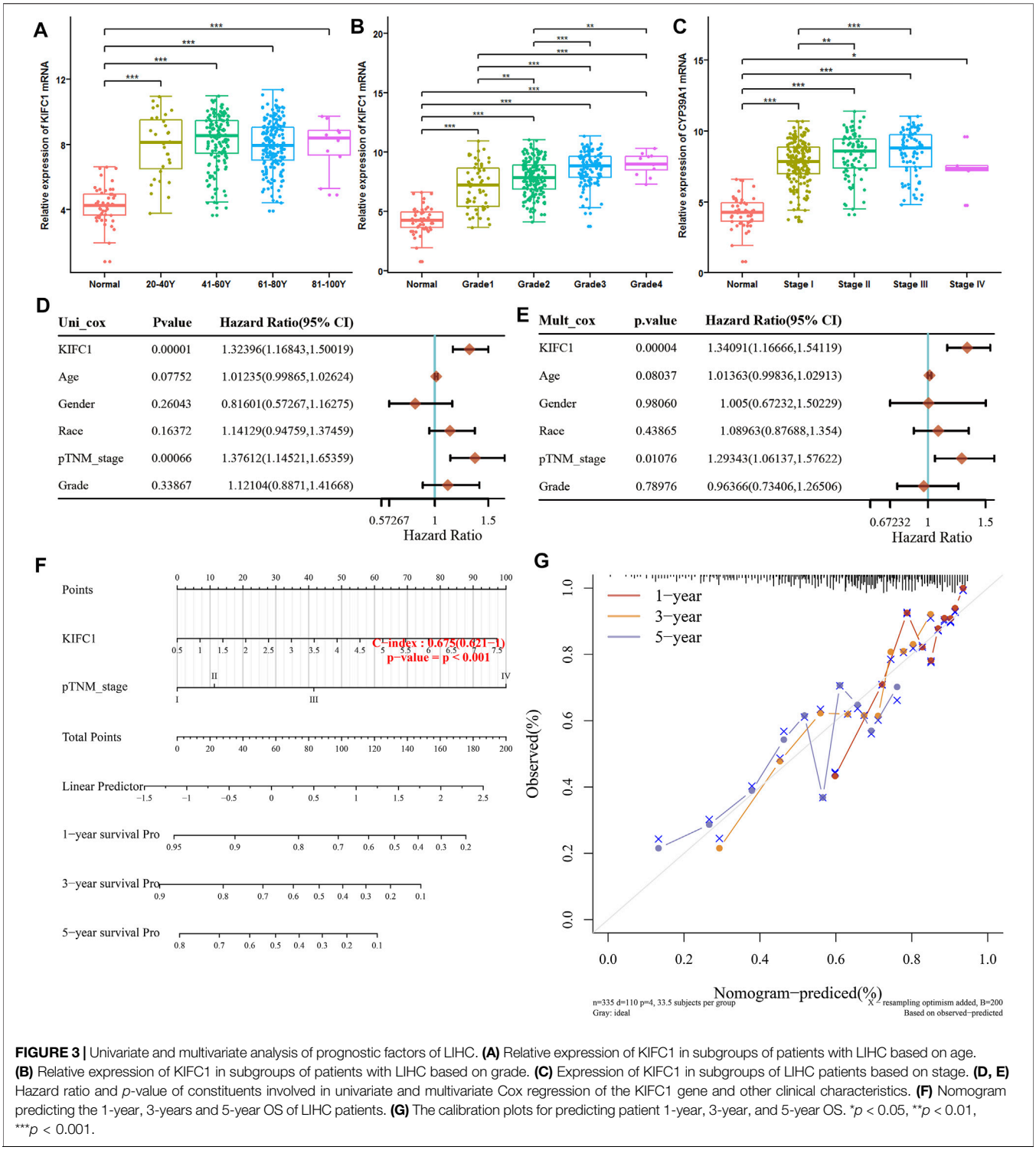

FIGURE 3 | Univariate and multivariate analysis of prognostic factors of LIHC. **(A)** Relative expression of KIFC1 in subgroups of patients with LIHC based on age. **(B)** Relative expression of KIFC1 in subgroups of patients with LIHC based on grade. **(C)** Expression of KIFC1 in subgroups of LIHC patients based on stage. **(D, E)** Hazard ratio and *p*-value of constituents involved in univariate and multivariate Cox regression of the KIFC1 gene and other clinical characteristics. **(F)** Nomogram predicting the 1-year, 3-years and 5-year OS of LIHC patients. **(G)** The calibration plots for predicting patient 1-year, 3-year, and 5-year OS. **p* < 0.05, ***p* < 0.01, ****p* < 0.001.

We further used the CIBERSORT algorithm to investigate the tumor-infiltrating immune cells, we found that the expression of KIFC1 was negatively correlated with the infiltration of naïve B cells, M2 macrophages, resting mast cells, resting natural killer (NK) cells, and resting memory CD4+ T cells (**Figure 5F**). However, the results indicated that KIFC1 expression was positively associated with the infiltration of resting dendritic cells, M0 macrophages, follicular helper T cells, activated memory CD4+ T cells, and regulatory T cells (**Figure 5F**). In addition, we discovered that in immune cells, KIFC1 was highly expressed in Tregs (**Figure 5G**). The variation in transcript expression was

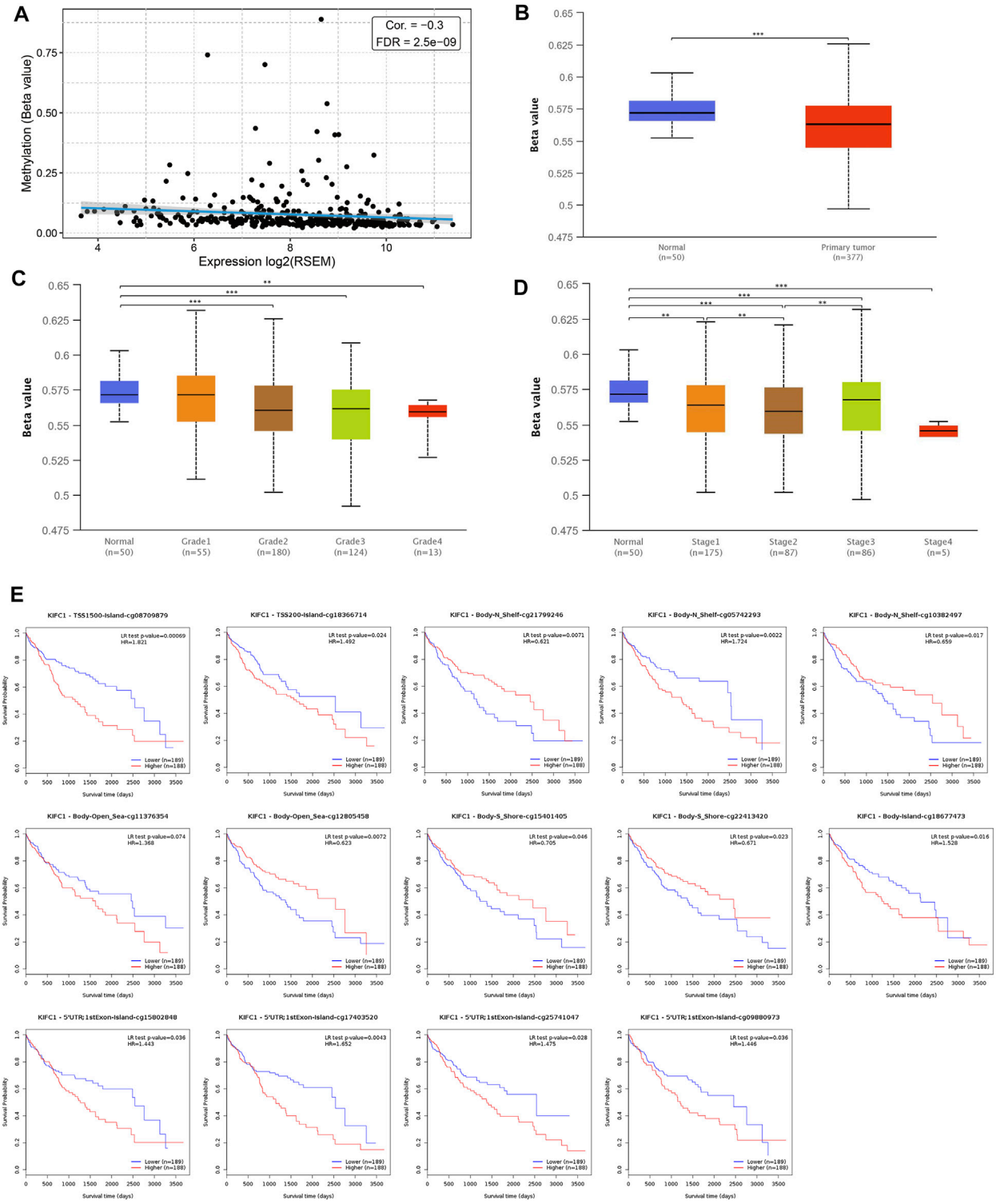

FIGURE 4 | Association of KIFC1 methylation level and its expression in LIHC. **(A)** Correlation between KIFC1 methylation and its expression level. **(B)** The promoter methylation level of KIFC1 in LIHC and normal tissues. **(C, D)** The correlation between promoter methylation level of KIHC1 with different grade and tumor stages. **(E)** The impact of different methylation sites of KIFC1 on OS of LIHC patients analyzed by MethSurv webtool. The *p*-value was calculated using Student's t-test. $*p < 0.05$, $**p < 0.01$, $***p < 0.001$.

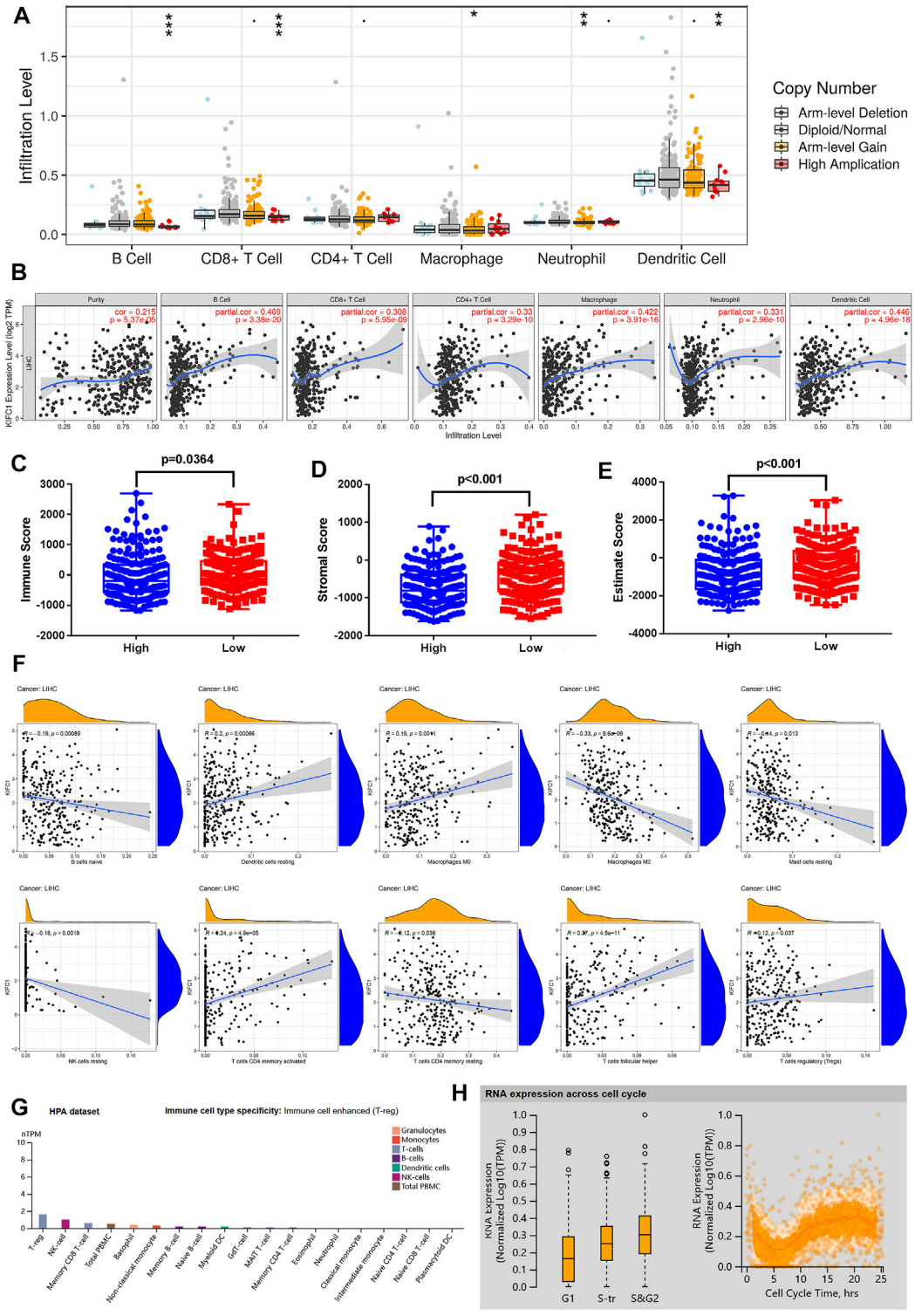

FIGURE 5 | KIFC1 expression was associated with immune infiltration level in LIHC. **(A)** The immune infiltration cells in LIHC. **(B)** KIFC1 expression level is related to the degree of immune infiltration in LIHC from TIMER. Correlation of KIFC1 with immune **(C)**, stromal **(D)**, and estimate **(E)** scores. **(F)** Association between LIFC1 and immune infiltration levels analyzed by CIBERSORT algorithm. The *p*-value was calculated using Student's t-test. $^{*}p < 0.05$, $^{**}p < 0.01$, $^{***}p < 0.001$. **(G)** Different mRNA expression levels of KIFC1 in immune cells. **(H)** Association between KIFC1 expression and cell cycle.

TABLE 1 | Correlation between KIFC1 and immune cell markers for LIHC.

Description	Gene markers	Cor	*p*-Value	*P* Star
CD8+ T cell	CD8A	0.203398	8.22E-05	**
	CD8B	0.200194	0.000103	**
T cell (general)	CD3D	0.262876	3.09E-07	**
	CD3E	0.175419	0.000701	**
B cell	CD19	0.286148	2.01E-08	**
	CD79A	0.154896	0.002776	**
Monocyte	CD86	0.265267	2.40E-07	**
	CD115 (CSF1R)	0.132829	0.010477	*
TAM	CCL2	0.039289	0.450371	
	CD68	0.197832	0.000129	**
M1				
Macrophage	INOS (NOS2)	−0.0387	0.457349	
	IRF5	0.434875	0	**
	COX2 (PTGS2)	0.041373	0.426875	
M2				
Macrophage	CD163	0.04255	0.413647	
	VSIG4	0.053858	0.300694	
	MS4A4A	0.050356	0.333247	
	CD66b			
Neutrophils	(CEACAM8)	0.154884	0.002778	**
	CD11b (ITGAM)	0.252297	9.28E-07	**
	CCR7	0.043555	0.402704	
Natural killer cell	KIR2DL1	−0.00925	0.859044	
	KIR2DL3	0.122901	0.017873	*
	KIR2DL4	0.215475	2.84E-05	**
	KIR3DL1	0.050247	0.334464	
	KIR3DL2	0.171911	0.000885	**
	KIR3DL3	0.094199	0.069939	
	KIR2DS4	0.044908	0.388409	
Dendritic cell	HLA-DPB1	0.169081	0.001094	**
	HLA-DQB1	0.162709	0.001684	**
	HLA-DRA	0.152419	0.003278	**
	HLA-DPA1	0.112032	0.03102	*
	BDCA-1 (CD1C)	0.118305	0.022664	*
	BDCA-4 (NRP1)	0.200391	0.000105	**
	CD11c (ITGAX)	0.279898	4.78E-08	**
Th1	T-bet (TBX21)	0.063403	0.222987	
	STAT4	0.233002	6.11E-06	**
	STAT1	0.364553	5.76E-13	**
	IFN-γ (IFNG)	0.275613	6.83E-08	**
	TNF-α (TNF)	0.222424	1.53E-05	**
Th2	GATA3	0.152103	0.003344	**
	STAT6	0.132692	0.010557	*
	STAT5A	0.274166	9.09E-08	**
	IL13	0.121788	0.018944	*
Tfh	BCL6	0.169588	0.001056	**
	IL21	0.192633	0.000189	**
Th17	STAT3	0.087206	0.093487	
	IL17A	0.084484	0.104228	
Treg	FOXP3	0.137818	0.007895	**
	CCR8	0.339772	1.77E-11	**
	STAT5B	0.302215	3.41E-09	**
	TGFβ (TGFB1)	0.268872	1.62E-07	**
T-cell exhaustion	PD-1 (PDCD1)	0.329187	7.96E-11	**
	CTLA4	0.316216	4.64E-10	**
	LAG3	0.318865	4.10E-10	**
	TIM-3 (HAVCR2)	0.264626	2.57E-07	**
	GZMB	0.102434	0.048696	*

Cor, R-value of Spearman's correlation; TAM, tumor-associated macrophage
*p < *0.05*; **p < *0.01*.

correlated to the cell cycle. The KIFC1 RNA expression peak phase was G2 (**Figure 5H**), indicating that KIFC1 had a role in the cell cycle profile. This suggests that KIFC1 plays a critical role in regulating immune cell infiltration in LIHC.

Correlation Analysis Between KIFC1 Expression and Immune Cell Markers, Immune-Related Genes

In order to further confirm the correlation of KIFC1 with immune-infiltrating cells, we focus next on the relationship between KIFC1 and various immune cell marker genes. In addition to the six types of immune cells as shown in **Figure 5**, it is worth mentioning that T cells with various functions are also included, such as Th1 cells, Th2 cells, Tfh cells, Th17 cells, Tregs, and depleted T cells. It indicated that KIFC1 expression was notably related to the immune markers of most immune T cells in LIHC, especially with Th1, Th2, Treg, and T-cell exhaustion markers (**Table 1**). Interestingly, we found no correlation between KIFC1 and the M2 macrophage marker and Th17 marker in LIHC. Thus, we could further confirm the specific association with immune infiltrating cells in the LIHC microenvironment.

We further assessed the co-expression of KIFC1 with MHC, immunosuppressive, immune activation, chemokine, and chemokine receptor genes. The results demonstrated that KIFC1 was co-expressed with several MHC genes, especially TAP1 (**Figure 6A**). KIFC1 was positively co-expressed with almost all immunosuppressive genes except KIR2DL1, KDR, CSF1R, and CD160 (**Figure 6B**). KIFC1 also had a significant correlation with immune activation genes, particularly MICB and CD276 (**Figure 6C**). For chemokine and chemokine receptor genes, KIFC1 had a high correlation with XCL1 and CCR10 (**Figures 6D,E**).

Correlation of KIFC1 With the Sensitivity of ICB and Chemotherapies

We further predicted the association between KIFC1 expression and ICB response. Firstly, we evaluated the expression of immune checkpoints (including SIGLEC15, PDCD1, CTLA4, TIGIT, PDCD1LG2, CD274, HAVCR2, and LAG3) in LIHC and normal tissues. We found that these immune checkpoints, except CD274, were all highly expressed in LIHC (**Figures 6F,G**). Moreover, we found that KIFC1 was positively co-expressed with these immune checkpoints, except SIGLEC15 (**Table 2**). Additionally, LIHC patients with high KIFC1 expression had a high TIDE score, indicating that these patients may had a better response to ICB therapy (**Figure 6H**). We also assessed the relationship between KIFC1 and the chemotherapeutic drug that is usually used in LIHC, we found that KIFC1 was negatively related to the IC50 of doxorubicin, sorafenib,

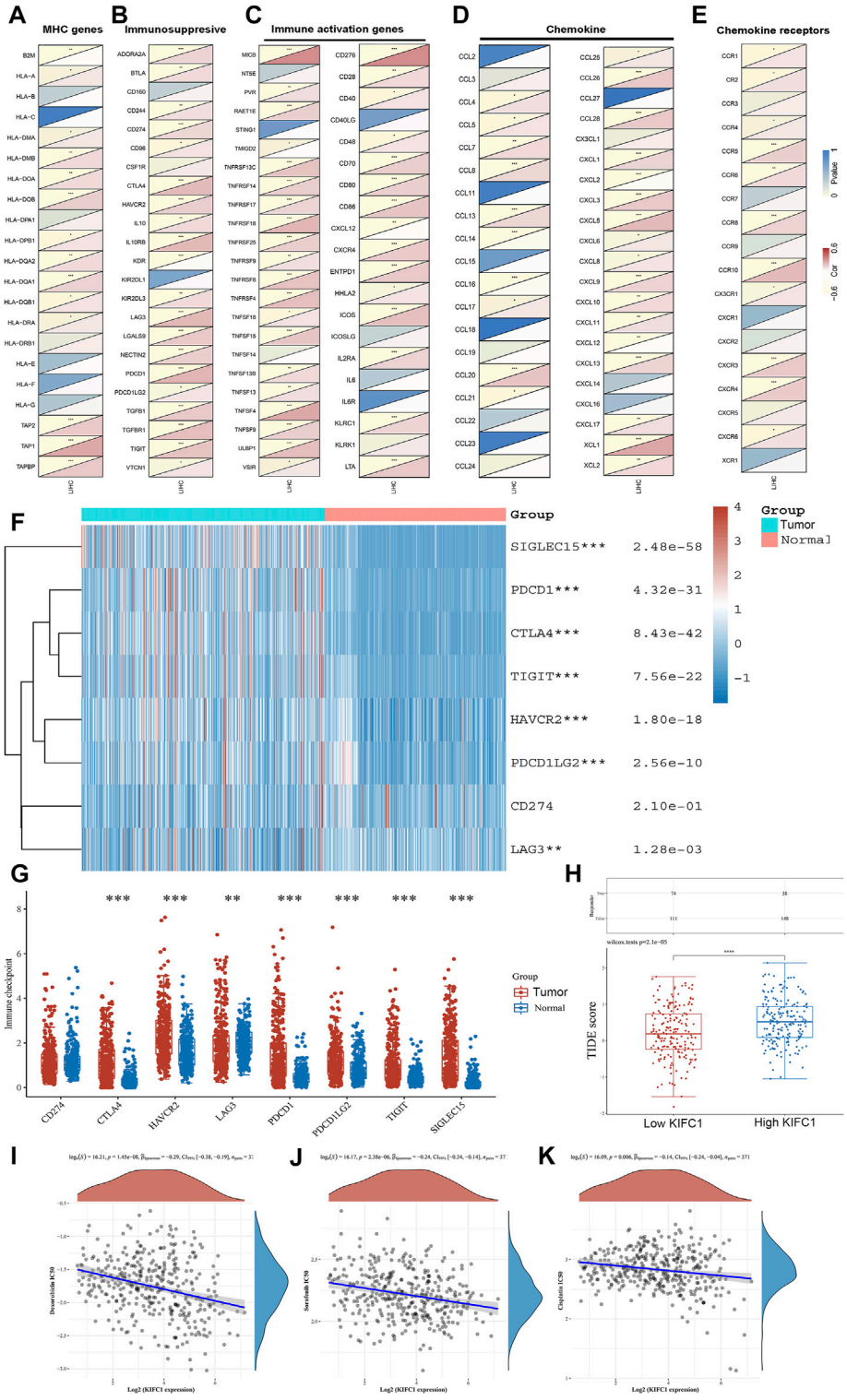

FIGURE 6 | Co-expression of KIFC1 with **(A)** MHC, **(B)** immunosuppressive, **(C)** immune activation, **(D)** chemokine, and **(E)** chemokine receptor genes. **(F, G)** Different expressions of immune checkpoints in LIHC and normal patients. **(H)** Different responses to ICB therapy in low and high KIFC1 expressions. **(I–K)** Correlations between KIFC1 and the IC50 of chemotherapy drugs. $^{*}p < 0.05$, $^{**}p < 0.01$, $^{***}p < 0.001$.

TABLE 2 | Correlation of KIFC1 with immune checkpoints in LIHC.

Genes	Cor	*p*-value
TIGIT	0.267	1.548e-07
CD274	0.171	0.0009
HAVCR2	0.217	2.408e-05
PDCD1LG2	0.116	0.024
SIGLEC15	0.070	0.175
LAG3	0.302	2.427e-09
CTLA4	0.296	5.405e-09
PDCD1	0.324	1.456e-10

and cisplatin (**Figures 6I–K**). KIFC1 may be a predictor of ICB and chemotherapies.

Enrichment Analysis of KIFC1 Neighborhood Genes in LIHC

In order to study the functional network of KIFC1 neighborhood genes in LIHC, we first identified KIFC1 neighborhood genes with LinkedOmics. The results are shown in a volcanic plot (**Figure 7A**). In addition, the top 50 negatively and positively significant related genes were shown in the heat map, respectively (**Figures 7B,C**). Significant GO term analysis by GSEA indicated that genes correlated with KIFC1 were located mainly in the chromosomal region, microtubule, protein–DNA complex, nuclear chromatin, and spliceosome complex, where they were involved in chromosome segregation, mitotic cell cycle phase transition, the regulation of chromosome organization, and DNA recombination. These related genes also served as catalytic activity, acting on DNA, tubulin binding, histone binding, ATPase activity, and protein serine/threonine kinase activity (**Figures 8A–C**). KEGG pathway analysis demonstrated that these genes related to KIFC1 were mainly enriched in signal pathways such as cell cycle, spliceosome, pyrimidine metabolism, and RNA transport (**Figure 8D**).

DISCUSSION

Due to the characteristics of delayed diagnosis and high recurrence of liver cancer, there are still some patients in clinic with unsatisfactory treatment effect and poor prognosis; therefore, it is important to explore novel genes related to the occurrence and development of LIHC and find markers with higher specificity and sensitivity, especially the other molecular mechanism targets such as immune infiltration, to improve the therapy of LIHC. This study aims to explore the diagnostic value of KIFC1 gene in LIHC and its influence on tumor immune invasion. As a member of the kinesin superfamily, the main function of KIFC1 is to act as a motor protein affecting microtubule dynamics and function, including spindle formation and the regulation of centrosome amplification (Xiao et al., 2017). The overexpression of KIFC1 has been reported to lead to the formation of monopolar spindles in tumor cells. This promotes the process of the division and proliferation of tumor cells (Mittal et al., 2016). Several studies have verified that KIFC1 expression is related with poor prognosis in multiple tumors, such as non-small cell lung cancer, renal cell carcinoma, and breast cancer, and it does happen primarily by affecting the proliferation of tumor cells (Liu et al., 2016; Li et al., 2018). Taken together, we can infer that KIFC1 may be involved in tumor formation and development by further affecting cell proliferation through its effect on microtubules.

In our study, we found that KIFC1 was differentially expressed in various types of cancers compared with its corresponding normal tissues such as BLCA, BRCA, CHOL, COAD, ESCA, LIHC, LUAD, LUSC, PRAD, READ, STAD, THCA, UCEC, HNSC, KIRC, and KIRP. Then, KIFC1 expression was further validated in liver cancer, and it indicated that patients with higher KIFC1 expression had worse prognosis. An IHC analysis of tissues from the HPA database and clinical samples indicated that there was a higher expression of KIFC1 protein in LIHC tissues than in normal tissues. Additionally, we also found that KIFC1 gene expression was correlated with tumor stage and clinical grade. In addition, patients with high expression of KIFC1 have a worse prognosis. Furthermore, univariate and multivariate Cox regression analyses revealed that KIFC1 expression was an independent prognosis factor of LIHC. Therefore, KIFC1 has a

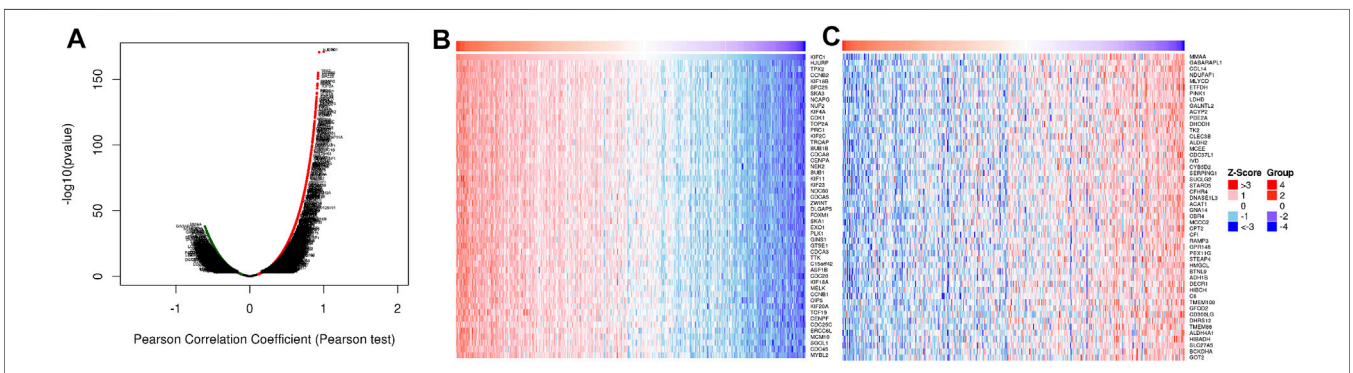

FIGURE 7 | Genes differentially expressed in association with KIFC1 in LIHC. **(A)** Volcano plot. **(B, C)** Heat maps of the top 50 genes positively and negatively correlated with KIFC1.

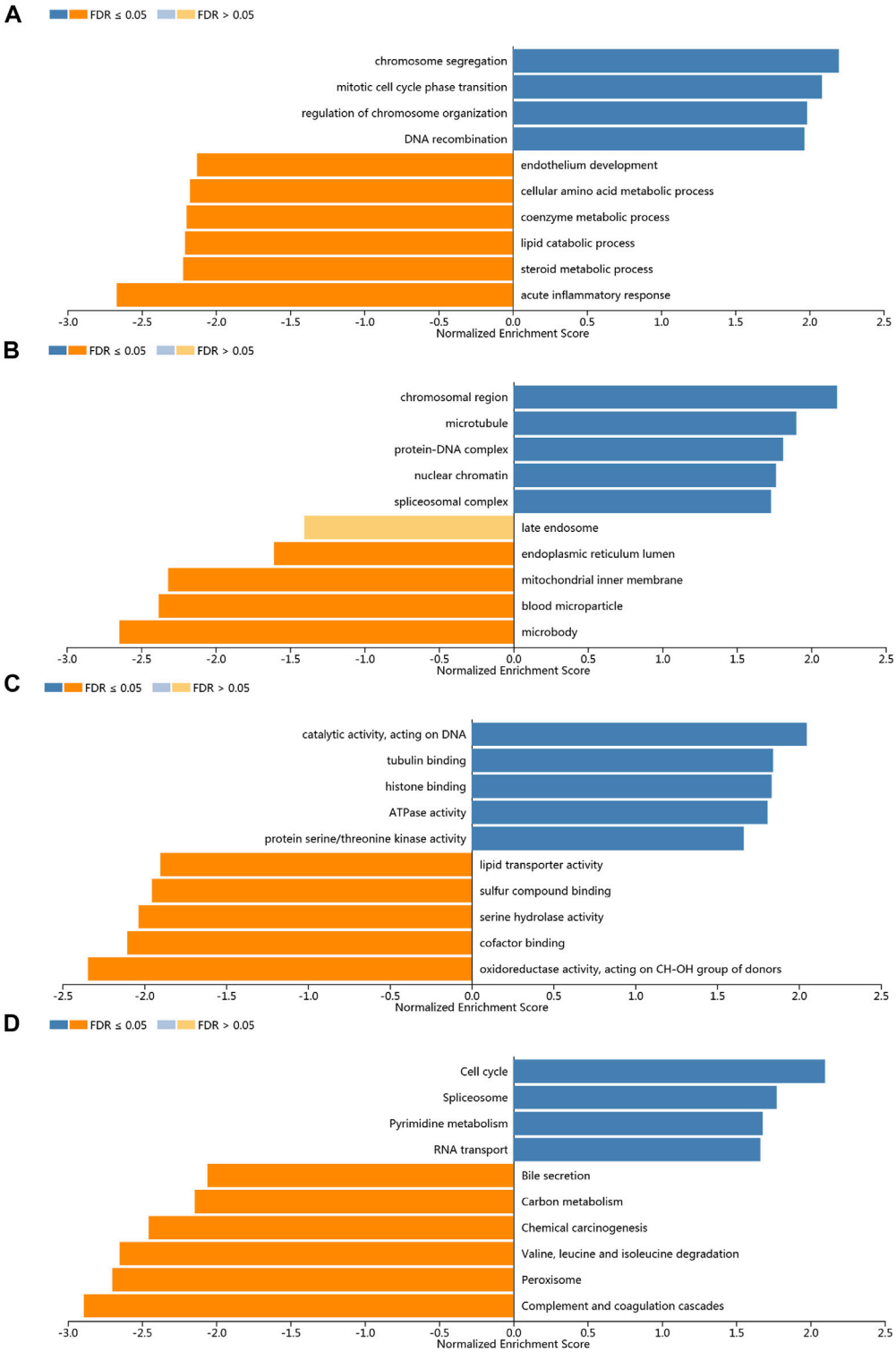

FIGURE 8 | Enrichment analysis of the genes altered in the KIFC1 neighborhood in LIHC. **(A)** Biological processes. **(B)** Cellular components. **(C)** Molecular functions. **(D)** KEGG pathway analysis.

potential diagnostic value in LIHC. Interestingly, in this study, KIFC1 protein was highly expressed in the nucleus of LIHC cells; however, there was no significant difference in the cytoplasm between LIHC and normal liver tissues. It was found in a previous study that KIFC1 plays a potential function in nuclear formation and the nuclear localization sequence on N-terminal domain, which is critical for the translocation of KIFC1 into the nucleus (Wei et al., 2019) as it reported that KIFC1 showed specific transport characteristics during the cell cycle, which is involved in regulating DNA synthesis in S phase and chromatin maintenance in mitosis (Wei and Yang, 2019). These all indicated that KIFC1 may play its function by transporting into the nucleus. In addition, it is consistent with a previous study that high expression of KIFC1 in the nucleus was correlated with worse OS, which could serve as an independent biomarker for African-American triple-negative breast cancer (Ogden et al., 2017). In our study, the differential expression of KIFC1 also mainly exists in the nucleus instead of cytoplasm, and the higher expression in the nucleus contributed to the progression of LIHC.

It has been reported that abnormal DNA molecular changes are the initiator of tumors, which appear in the early stage of tumors and accompany with the whole process of tumor development and are closely related to the prognosis of tumors (Cabel et al., 2017). DNA methylation, copy number variation, gene mutation, and microsatellite sequence changes are all important components of tumor epigenetics. However, DNA methylation is more prevalent in almost all tumors than the latter three, which can directly regulate gene expression (Schübeler, 2015). Therefore, the relationship between methylation and the prognosis of liver cancer can be explored. Abnormal methylated genes may serve as markers for the early diagnosis and prognostic evaluation of LIHC (Liu et al., 2020a). In this study, we used UALCAN to analyze the promoter methylation of the KIFC1 gene in liver cancer and its relationship with clinical characteristics. The results showed that KIFC1 was hypomethylated in LIHC tissues regardless of stage. Although KIFC1 methylation was not significantly different among different stages or grades, it showed a gradual decreasing trend with the increase of stages. This result partly explains that the increased expression of KIFC1 is regulated by methylation. Likewise, it was found in a previous study that targeted genes NEFH and SMPD3 were hypermethylated in paired LIHC samples than in the normal samples, which were lower expressed in LIHC samples; thereby, they could serve as tumor suppressor genes in LIHC (Revill et al., 2013). Similarly, it was reported that NAT1 mRNA was reduced in colorectal carcinoma compared with normal tissues, while the methylation of the promoter region of NAT1 was higher in colorectal carcinoma than that in normal tissues (Shi et al., 2019). We also found that the different methylation sites of the KIFC1 gene had a different effect on the prognosis of LIHC patients as shown in **Figure 4E**. These all suggested that DNA methylation affects the expression of targeted genes and then affects the tumor cell behavior.

Next, we analyzed the KIFC1-related pathway in LIHC to understand its carcinogenic mechanism. Based on GO and KEGG analyses, we observed that the functional network of KIFC1 in LIHC was related to the chromosome segregation, mitotic cell cycle phase transition, the regulation of chromosome organization, and DNA recombination. They also served as catalytic activity, acting on DNA, tubulin binding, histone binding, ATPase activity, and protein serine/threonine kinase activity. KEGG pathway analysis indicated that KIFC1-related genes were enriched in cell cycle, spliceosome, pyrimidine metabolism, and RNA transport. All these results suggested that KIFC1 regulates cell cycle by affecting mitosis, mainly by affecting chromatin tissue regulation and tubulin binding. It is consistent with previous studies that KIFC1 can affect microtubules (Ma et al., 2017).

To further evaluate the potential immune mechanisms of KIFC1 in LIHC, we secondly analyzed KIFC1-related immune infiltration levels. The results demonstrate that the KIFC1 expression level is strongly positive correlated with the infiltration level of B cells, CD8+ T cells, macrophages, neutrophils, and dendritic cells in LIHC. In addition, the expression of KIFC1 was negatively correlated with the infiltration of naïve B cells, M2 macrophages, resting mast cells, resting NK cells, and resting memory CD4+ T cells but positively correlated with the infiltration of resting dendritic cells, M0 macrophages, activated memory CD4+ T cells, follicular helper T cells, and regulatory T cells. After analyzing the correlation between KIFC1 expression and immune cell marker genes, the results revealed that the function of KIFC1 in regulating different immune infiltrating cells is different. Likewise, immune score evaluation indicated that KIFC1 expression was significantly correlated with immune and stromal score, which suggested that KIFC1 level was linked to the level of immune infiltration.

Studies have shown that T-cell infiltration in tumor tissue as a protective factor can inhibit tumor invasion and metastasis. Patients with higher levels of T-cell infiltration often have a better prognosis (Oh et al., 2020; van der Leun et al., 2020). In this study, there was a positive correlation between KIFC1 and T-cell marker genes (CD3D and CD3E). Hence, we hypothesized that patients with high KIFC1 expression may have a better prognosis, but the opposite was true. Firstly, it is known that tumor-associated macrophages (TAMs) are the most plentiful immune cells in TME. CD68 is the most reliable marker of macrophages, and IRF5 of M1 macrophages, both of which are positively correlated with KIFC1. This indicates that KIFC1 may play a part in regulating the polarization of TAM. Researchers have found that TAM can promote tumor cells' growth and metastasis through a variety of pathways (Batoon and McCauley, 2021; Kong et al., 2021). This could partly explain why KIFC1 can promote LIHC progress. Secondly, it is well known that Treg cells can inhibit the function of T cells and are an important factor in maintaining the immune tolerance of the body. However, in tumors, Treg cells become accomplices of cancer cells to help them escape the immune surveillance of the body, leading to tumor progression and metastasis (Liu et al., 2020b). Moreover, in immune cells, the mRNA expression of LIFC1 was the highest in Tregs. FOXP3, CCR8, STAT5b, and TGFB1 are genetic markers of Treg cells. T-cell depletion is the main factor that causes the immune dysfunction in tumor patients, of which, tumor cells and TME can induce the expression of PD1 on activated T cells and activate relevant signaling pathways, leading to T-cell depletion

(Wang et al., 2020). PD-1, CTLA4, LAG3, HAVCR2, and GZMB are T-cell depletion markers, and all of these marker genes are positively correlated with KIFC1 expression in LIHC in this study. Thus, the high expression of KIFC1 may be a factor involved in the T-cell depletion process. This is the second reason why KIFC1 promotes LIHC progression through the immune pathway. Most importantly, we investigated the correlation of KIFC1 and immune checkpoints, including SIGLEC15, TIGIT, CTLA4, CD274, HAVCR2, LAG3, PDCD1, and PDCD1LG2, which were associated with the response to ICB (Marwitz et al., 2017; Nebhan and Johnson, 2020). These immune checkpoints except CD274 were all highly expressed in LIHC. Moreover, we found that KIFC1 was positively co-expressed with these immune checkpoints, except SIGLEC15. As high expression of immune checkpoints was associated with T-cell exhaustion and worse prognosis, this also partly explained the cancer-promoting effect of KIFC1. Additionally, LIHC patients with high KIFC1 expression may had a better response to ICB therapy, indicating that LIHC patients with high KIFC1 expression were more suitable for ICB therapy. Interestingly, KIFC1 was negatively related to the IC50 of doxorubicin, sorafenib, and cisplatin. These results indicated that KIFC1 may be a predictor of ICB and chemotherapeutics; for example, LIHC patients with high KIFC1 expression may have a better response to ICB, doxorubicin, sorafenib, and cisplatin therapy. These findings provided new ideas for the precise treatment of LIHC patients.

Taken together, the effect of KIFC1 on immune cell infiltration has both positive and negative effects on tumor patients. The inhibitory and promotive effects on the tumor are coexisting. The negative side accounts for a greater proportion and therefore appears to promote tumor progression. The limitation is that we do not yet understand the mechanism involved in this process by which KIFC1 influences immune cell infiltration. However, it is clear that KIFC1 is involved in the recruitment and regulation of immune infiltrating cell in LIHC. In this study, our study differs from previous literature in that we found the differential expression of KIFC1 in the location of nucleus that contributes to the occurrence and development of LIHC, and hypomethylation may explain the higher expression of KIFC1 in LIHC. Most importantly, KIFC1 expression may affect the immune microenvironment and then indirectly affects the prognosis of LIHC and serves as a predictor of ICB therapies and chemotherapeutics. However, the limitation of this study is that a large number of samples were needed to verify our results, and more clinical samples will be collected to enrich the data in the future. Moreover, the underlying immune mechanisms should be explored and KIFC1 as biomarkers to predict the immune response rate in real-world LIHC patients should be conducted.

CONCLUSION

Conclusively, the increased expression of KIFC1 in LIHC was associated with increased levels of different immune cells infiltration level with a worse prognosis. The lower level of promoter methylation may be the reason for the increased expression of the KIFC1 gene in LIHC cells. KIFC1 alters the clinical outcomes of patients with LIHC by affecting immune cells in the TME, and it may be used as an independent predictor of ICB therapies and chemotherapeutics.

DATA AVAILABILITY STATEMENT

The datasets presented in this study can be found in online repositories. The names of the repository/repositories and accession number(s) can be found in the article/ **Supplementary Material**.

ETHICS STATEMENT

The studies involving human participants were reviewed and approved by Ethics Committee of Renmin Hospital of Wuhan University. The patients/participants provided their written informed consent to participate in this study.

AUTHOR CONTRIBUTIONS

DL, TY, and ZZ conceived and designed the project, ZZ, XX, and JW acquired the data, WS, HZ, and JH analyzed and interpreted the data, DL and TY wrote the paper, DL, GL, HZ, and TY revised the manuscript.

FUNDING

This study was supported by the National Natural Science Foundation of China (Grant No. 81803789 to DL, No. 81704023 to TY, and No. 81602535 to ZZ), Wu Jieping Medical Foundation (Grant No. 320.6750) and the guidance funding of Renmin Hospital of Wuhan University (Grant No. RMYD2018M79).

ACKNOWLEDGMENTS

Thanks to Professor Gu Lijuan for her valuable suggestions on the revision of the manuscript.

SUPPLEMENTARY MATERIAL

The Supplementary Material for this article can be found online at: https://www.frontiersin.org/articles/10.3389/fmolb.2021.799651/full#supplementary-material

Supplementary Figure S1 | Protein expression analysis from our clinical samples with IHC (8/36 vs. 1/36, chi-square test, $p < 0.05$).

Supplementary Figure S2 | Association of KIFC1 expression with patient survival curve. **(A)** Overall survival curve. **(B)** Disease-free survival.

REFERENCES

Batoon, L., and McCauley, L. K. (2021). Cross Talk between Macrophages and Cancer Cells in the Bone Metastatic Environment. *Front. Endocrinol.* 12, 763846. doi:10.3389/fendo.2021.763846

Cabel, L., Riva, F., Servois, V., Livartowski, A., Daniel, C., Rampanou, A., et al. (2017). Circulating Tumor DNA Changes for Early Monitoring of Anti-PD1 Immunotherapy: a Proof-Of-Concept Study. *Ann. Oncol.* 28 (8), 1996–2001. doi:10.1093/annonc/mdx212

Chandrashekar, D. S., Bashel, B., Balasubramanya, S. A. H., Creighton, C. J., Ponce-Rodriguez, I., Chakravarthi, B. V. S. K., et al. (2017). UALCAN: A Portal for Facilitating Tumor Subgroup Gene Expression and Survival Analyses. *Neoplasia* 19 (8), 649–658. doi:10.1016/j.neo.2017.05.002

Fu, X., Zhu, Y., Zheng, B., Zou, Y., Wang, C., Wu, P., et al. (2018). KIFC1, a Novel Potential Prognostic Factor and Therapeutic Target in Hepatocellular Carcinoma. *Int. J. Oncol.* 52 (6), 1912–1922. doi:10.3892/ijo.2018.4348

Han, J., Wang, F., Lan, Y., Wang, J., Nie, C., Liang, Y., et al. (2019). KIFC1 Regulated by miR-532-3p Promotes Epithelial-To-Mesenchymal Transition and Metastasis of Hepatocellular Carcinoma via Gankyrin/AKT Signaling. *Oncogene* 38 (3), 406–420. doi:10.1038/s41388-018-0440-8

Hu, X., Zhu, H., Shen, Y., Zhang, X., He, X., and Xu, X. (2021). The Role of Non-coding RNAs in the Sorafenib Resistance of Hepatocellular Carcinoma. *Front. Oncol.* 11, 696705. doi:10.3389/fonc.2021.696705

Huang, A., Zhao, X., Yang, X.-R., Li, F.-Q., Zhou, X.-L., Wu, K., et al. (2017). Circumventing Intratumoral Heterogeneity to Identify Potential Therapeutic Targets in Hepatocellular Carcinoma. *J. Hepatol.* 67 (2), 293–301. doi:10.1016/j.jhep.2017.03.005

Jiang, P., Gu, S., Pan, D., Fu, J., Sahu, A., Hu, X., et al. (2018). Signatures of T Cell Dysfunction and Exclusion Predict Cancer Immunotherapy Response. *Nat. Med.* 24 (10), 1550–1558. doi:10.1038/s41591-018-0136-1

Kong, X., Bu, J., Chen, J., Ni, B., Fu, B., Zhou, F., et al. (2021). PIGF and Flt-1 on the Surface of Macrophages Induces the Production of TGF-B1 by Polarized Tumor-Associated Macrophages to Promote Lung Cancer Angiogenesis. *Eur. J. Pharmacol.* 912, 174550. doi:10.1016/j.ejphar.2021.174550

Li, F., Kitajima, S., Kohno, S., Yoshida, A., Tange, S., Sasaki, S., et al. (2019). Retinoblastoma Inactivation Induces a Protumoral Microenvironment via Enhanced CCL2 Secretion. *Cancer Res.* 79 (15), 3903–3915. doi:10.1158/0008-5472.Can-18-3604

Li, G., Chen, J., Li, S., Zhou, S., Cao, S., Lou, Y., et al. (2017). Kinesin Superfamily Protein Expression and its Association with Progression and Prognosis in Hepatocellular Carcinoma. *J. Can. Res. Ther.* 13 (4), 651–659. doi:10.4103/jcrt.JCRT_491_17

Li, G., Chong, T., Yang, J., Li, H., and Chen, H. (2018). Kinesin Motor Protein KIFC1 Is a Target Protein of miR-338-3p and Is Associated with Poor Prognosis and Progression of Renal Cell Carcinoma. *Oncol. Res.* 27 (1), 125–137. doi:10.3727/096504018x15213115046567

Li, Q., Qiu, J., Yang, H., Sun, G., Hu, Y., Zhu, D., et al. (2020). Kinesin Family Member 15 Promotes Cancer Stem Cell Phenotype and Malignancy via Reactive Oxygen Species Imbalance in Hepatocellular Carcinoma. *Cancer Lett.* 482, 112–125. doi:10.1016/j.canlet.2019.11.008

Li, T., Fu, J., Zeng, Z., Cohen, D., Li, J., Chen, Q., et al. (2020). TIMER2.0 for Analysis of Tumor-Infiltrating Immune Cells. *Nucleic Acids Res.* 48 (W1), W509–w514. doi:10.1093/nar/gkaa407

Lian, Q., Wang, S., Zhang, G., Wang, D., Luo, G., Tang, J., et al. (2018). HCCDB: A Database of Hepatocellular Carcinoma Expression Atlas. *Genomics, Proteomics & Bioinformatics* 16 (4), 269–275. doi:10.1016/j.gpb.2018.07.003

Liu, A., Wu, Q., Peng, D., Ares, I., Anadón, A., Lopez-Torres, B., et al. (2020). A Novel Strategy for the Diagnosis, Prognosis, Treatment, and Chemoresistance of Hepatocellular Carcinoma: DNA Methylation. *Med. Res. Rev.* 40 (5), 1973–2018. doi:10.1002/med.21696

Liu, X., Xu, Q., Li, Z., and Xiong, B. (2020). Integrated Analysis Identifies AQP9 Correlates with Immune Infiltration and Acts as a Prognosticator in Multiple Cancers. *Sci. Rep.* 10 (1), 20795. doi:10.1038/s41598-020-77657-z

Liu, Y., Zhan, P., Zhou, Z., Xing, Z., Zhu, S., Ma, C., et al. (2016). The Overexpression of KIFC1 Was Associated with the Proliferation and Prognosis of Non-small Cell Lung Cancer. *J. Thorac. Dis.* 8 (10), 2911–2923. doi:10.21037/jtd.2016.10.67

Long, J., Lin, J., Wang, A., Wu, L., Zheng, Y., Yang, X., et al. (2017). PD-1/PD-L Blockade in Gastrointestinal Cancers: Lessons Learned and the Road toward Precision Immunotherapy. *J. Hematol. Oncol.* 10 (1), 146. doi:10.1186/s13045-017-0511-2

Ma, D.-D., Bi, L., and Yang, W.-X. (2017). KIFC1 Is Essential for Acrosome Formation and Nuclear Shaping during Spermiogenesis in the Lobster *Procambarus clarkii*. *Oncotarget* 8 (22), 36082–36098. doi:10.18632/oncotarget.16429

Marwitz, S., Scheufele, S., Perner, S., Reck, M., Ammerpohl, O., and Goldmann, T. (2017). Epigenetic Modifications of the Immune-Checkpoint Genes CTLA4 and PDCD1 in Non-small Cell Lung Cancer Results in Increased Expression. *Clin. Epigenet* 9, 51. doi:10.1186/s13148-017-0354-2

Mittal, K., Choi, D. H., Klimov, S., Pawar, S., Kaur, R., Mitra, A. K., et al. (2016). A Centrosome Clustering Protein, KIFC1, Predicts Aggressive Disease Course in Serous Ovarian Adenocarcinomas. *J. Ovarian Res.* 9, 17. doi:10.1186/s13048-016-0224-0

Nebhan, C. A., and Johnson, D. B. (2020). Predictive Biomarkers of Response to Immune Checkpoint Inhibitors in Melanoma. *Expert Rev. Anticancer Ther.* 20 (2), 137–145. doi:10.1080/14737140.2020.1724539

Ogden, A., Garlapati, C., Li, X., Turaga, R. C., Oprea-Ilies, G., Wright, N., et al. (2017). Multi-institutional Study of Nuclear KIFC1 as a Biomarker of Poor Prognosis in African American Women with Triple-Negative Breast Cancer. *Sci. Rep.* 7, 42289. doi:10.1038/srep42289

Oh, D. Y., Kwek, S. S., Raju, S. S., Li, T., McCarthy, E., Chow, E., et al. (2020). Intratumoral CD4+ T Cells Mediate Anti-tumor Cytotoxicity in Human Bladder Cancer. *Cell* 181 (7), 1612–1625. doi:10.1016/j.cell.2020.05.017

Revill, K., Wang, T., Lachenmayer, A., Kojima, K., Harrington, A., Li, J., et al. (2013). Genome-wide Methylation Analysis and Epigenetic Unmasking Identify Tumor Suppressor Genes in Hepatocellular Carcinoma. *Gastroenterology* 145 (6), 1424e1–143525. doi:10.1053/j.gastro.2013.08.055

Schübeler, D. (2015). Function and Information Content of DNA Methylation. *Nature* 517 (7534), 321–326. doi:10.1038/nature14192

Shi, C., Xie, L.-y., Tang, Y.-p., Long, L., Li, J.-l., Hu, B.-l., et al. (2019). Hypermethylation of N-Acetyltransferase 1 Is a Prognostic Biomarker in Colon Adenocarcinoma. *Front. Genet.* 10, 1097. doi:10.3389/fgene.2019.01097

Sun, Y., Zhang, Y., Lang, Z., Huang, J., and Zou, Z. (2019). Prognostic and Clinicopathological Significance of Kinesin Family Member C1 in Various Cancers. *Medicine (Baltimore)* 98 (40), e17346. doi:10.1097/md.0000000000017346

Tang, Z., Li, C., Kang, B., Gao, G., Li, C., and Zhang, Z. (2017). GEPIA: a Web Server for Cancer and normal Gene Expression Profiling and Interactive Analyses. *Nucleic Acids Res.* 45 (W1), W98–w102. doi:10.1093/nar/gkx247

Teng, K., Wei, S., Zhang, C., Chen, J., Chen, J., Xiao, K., et al. (2019). KIFC1 Is Activated by TCF-4 and Promotes Hepatocellular Carcinoma Pathogenesis by Regulating HMGA1 Transcriptional Activity. *J. Exp. Clin. Cancer Res.* 38 (1), 329. doi:10.1186/s13046-019-1331-8

Torre, L. A., Bray, F., Siegel, R. L., Ferlay, J., Lortet-Tieulent, J., and Jemal, A. (2012). Global Cancer Statistics, 2012. *CA: A Cancer J. Clinicians* 65 (2), 87–108. doi:10.3322/caac.21262

van der Leun, A. M., Thommen, D. S., and Schumacher, T. N. (2020). CD8+ T Cell States in Human Cancer: Insights from Single-Cell Analysis. *Nat. Rev. Cancer* 20 (4), 218–232. doi:10.1038/s41568-019-0235-4

Vasaikar, S. V., Straub, P., Wang, J., and Zhang, B. (2018). LinkedOmics: Analyzing Multi-Omics Data within and across 32 Cancer Types. *Nucleic Acids Res.* 46 (D1), D956–d963. doi:10.1093/nar/gkx1090

Wang, J., Zhao, X., Wang, Y., Ren, F., Sun, D., Yan, Y., et al. (2020). circRNA-002178 Act as a ceRNA to Promote PDL1/PD1 Expression in Lung Adenocarcinoma. *Cell Death Dis* 11 (1), 32. doi:10.1038/s41419-020-2230-9

Wei, Y.-L., Yang, T., Kovacs, T., and Yang, W.-X. (2019). C-terminal Kinesin Motor Es-KIFC1 Regulates Nuclear Formation during Spermiogenesis in Chinese Mitten Crab Eriocheir Sinensis. *Gene* 719, 144074. doi:10.1016/j.gene.2019.144074

Wei, Y.-L., and Yang, W.-X. (2019). Kinesin-14 Motor Protein KIFC1 Participates in DNA Synthesis and Chromatin Maintenance. *Cel Death Dis* 10 (6), 402. doi:10.1038/s41419-019-1619-9

Xiao, Y.-X., Shen, H.-Q., She, Z.-Y., Sheng, L., Chen, Q.-Q., Chu, Y.-L., et al. (2017). C-terminal Kinesin Motor KIFC1 Participates in Facilitating Proper Cell

Division of Human Seminoma. *Oncotarget* 8 (37), 61373–61384. doi:10.18632/oncotarget.18139

Yoshihara, K., Shahmoradgoli, M., Martínez, E., Vegesna, R., Kim, H., Torres-Garcia, W., et al. (2013). Inferring Tumour Purity and Stromal and Immune Cell Admixture from Expression Data. *Nat. Commun.* 4, 2612. doi:10.1038/ncomms3612

Zeng, Z., Zhang, X., Li, D., Li, J., Yuan, J., Gu, L., et al. (2020). Expression, Location, Clinical Implication, and Bioinformatics Analysis of RNASET2 in Gastric Adenocarcinoma. *Front. Oncol.* 10, 836. doi:10.3389/fonc.2020.00836

Zhang, Z., Wu, H.-X., Lin, W.-H., Wang, Z.-X., Yang, L.-P., Zeng, Z.-L., et al. (2021). EPHA7 Mutation as a Predictive Biomarker for Immune Checkpoint Inhibitors in Multiple Cancers. *BMC Med.* 19 (1), 26. doi:10.1186/s12916-020-01899-x

Zhu, H., Hu, X., Gu, L., Jian, Z., Li, L., Hu, S., et al. (1950). TUBA1C Is a Prognostic Marker in Low-Grade Glioma and Correlates with Immune Cell Infiltration in the Tumor Microenvironment. *Front. Genet.* 12, 202112. doi:10.3389/fgene.2021.759953

Zhu, H., Hu, X., Ye, Y., Jian, Z., Zhong, Y., Gu, L., et al. (2021). Pan-Cancer Analysis of PIMREG as a Biomarker for the Prognostic and Immunological Role. *Front. Genet.* 12, 687778. doi:10.3389/fgene.2021.687778

Ziogas, I. A., and Tsoulfas, G. (2017). Advances and Challenges in Laparoscopic Surgery in the Management of Hepatocellular Carcinoma. *Wjgs* 9 (12), 233–245. doi:10.4240/wjgs.v9.i12.233

Conflict of Interest: The authors declare that the research was conducted in the absence of any commercial or financial relationships that could be construed as a potential conflict of interest.

Publisher's Note: All claims expressed in this article are solely those of the authors and do not necessarily represent those of their affiliated organizations, or those of the publisher, the editors and the reviewers. Any product that may be evaluated in this article, or claim that may be made by its manufacturer, is not guaranteed or endorsed by the publisher.

frontiers in Molecular Biosciences

ORIGINAL RESEARCH
published: 18 January 2022
doi: 10.3389/fmolb.2021.800679

Somatic Mutation Profiles Revealed by Next Generation Sequencing (NGS) in 39 Chinese Hepatocellular Carcinoma Patients

Lixin Ke[1†], Jianming Shen[1†], Jikun Feng[2†], Jialin Chen[1], Shunli Shen[1], Shaoqiang Li[1], Ming Kuang[1], Lijian Liang[1], Cuncun Lu[3], Dongming Li[1], Qiang He[1]*, Baogang Peng[1]* and Yunpeng Hua[1]**

[1]Hepatobiliary and Pancreatic Center, The First Affiliated Hospital, Sun Yat-sen University, Guangzhou, China, [2]Sun Yat-sen University Cancer Center, Guangzhou, China, [3]Institute of Basic Research in Clinical Medicine, China Academy of Chinese Medical Sciences, Beijing, China

The features and significance of somatic mutation profiles in hepatocellular carcinoma (HCC) have not been completely elucidated to date. In this study, 39 tumor specimens from HCC patients were collected for gene variation analysis by next-generation sequencing (NGS), and a correlation analysis between mutated genes and clinical characteristics was also conducted. The results were compared with genome data from cBioPortal database. Our study found that T > G/A > C transversions (Tv) and C > T/G > A transitions (Ti) were dominant. The sequence variations of TP53, MUC16, MUC12, MUC4 and others, and the copy number variations (CNVs) of FGF3, TERT, and SOX2 were found to be more frequent in our cohort than in cBioPortal datasets, and they were highly enriched in pathways in cancer and participated in complex biological regulatory processes. The TP53 mutation was the key mutation (76.9%, 30/39), and the most common amino acid alteration and mutation types were p.R249S (23.5%) and missense mutation (82.3%) in the TP53 variation. Furthermore, TP53 had more co-mutations with MUC17, NBPF10, and AHNAK2. However, there were no significant differences in clinical characteristics between HCC patients with mutant TP53 and wild-type TP53, and the overall survival rate between treatment *via* precision medication guided by NGS and that *via* empirical medication (logrank $p = 0.181$). Therefore, the role of NGS in the guidance of personalized targeted therapy, solely based on NGS, may be limited. Multi-center, large sample, prospective studies are needed to further verify these results.

Keywords: hepatocellular carcinoma, next generation sequencing, TP53, targeted therapy, SNV, CNV, INDEL

OPEN ACCESS

Edited by:
Miroslaw Kornek, Medizinische Fakultät, Universität Bonn, Germany

Reviewed by:
Vinay Kumar Mittal, ThermoFisher Scientific, United States
Ammar Husami, Cincinnati Children's Hospital Medical Center, United States

***Correspondence:**
Yunpeng Hua
hyp0427@163.com
Baogang Peng
pengbg@mail.sysu.edu.cn
Qiang He
lheqiang@hotmail.com
Dongming Li
dongmingli@medmail.com.cn

†These authors have contributed equally to this work and share first authorship

Specialty section:
This article was submitted to Molecular Diagnostics and Therapeutics, a section of the journal Frontiers in Molecular Biosciences

Received: *23 October 2021*
Accepted: *07 December 2021*
Published: *18 January 2022*

Citation:
Ke L, Shen J, Feng J, Chen J, Shen S, Li S, Kuang M, Liang L, Lu C, Li D, He Q, Peng B and Hua Y (2022) Somatic Mutation Profiles Revealed by Next Generation Sequencing (NGS) in 39 Chinese Hepatocellular Carcinoma Patients. Front. Mol. Biosci. 8:800679. doi: 10.3389/fmolb.2021.800679

INTRODUCTION

Hepatocellular carcinoma (HCC) is now the fourth most common cause of cancer-related deaths worldwide. Approximately 78,000 patients died from HCC in 2018 (Bray et al., 2018; Forner et al., 2018). Recent next-generation sequencing (NGS)-based studies have uncovered the genetic landscape of HCC (Totoki et al., 2014; Schulze et al., 2015; Cancer Genome Atlas Research, 2017), including driver mutations in TP53, CTNNB1, TERT promoter, and other key gene loci.

However, how genetic alterations drive the occurrence and development of HCC remains largely unknown.

As a high-throughput sequencing technique, NGS can perform multiple typological analyses on thousands of genes. The main purpose of NGS is to find the main driver gene in patients with advanced cancer and carry out targeted therapy, as well as to try to discover the molecular mutation target of drug resistance (Deng et al., 2019). An increasing number of clinical studies have shown that the analysis of comprehensive characterization of genome changes has clinical benefits for cancer patients (Takeda et al., 2015; Staaf et al., 2019). However, there are still many unknown pathogenic variants waiting to be discovered. Identification of these alterations in cancer patients is the first step toward providing therapeutic targets.

Herein, we characterized differences of the genomic profiles between HCC patients in our cohort and HCC patients in the cBio Cancer Genomics Portal (cBioPortal, http://cBioPortal.org) database using six datasets (MSK, Clin Cancer Res 2018; INSERM, Nat Genet 2015; MSK, PLOS One 2018; AMC, Hepatology 2014; RIKEN, Nat Genet 2012; TCGA, Firehose Legacy) (Gao et al., 2013). We also explored the correlations between high-frequency mutated genes and clinical characteristics of patients, and compared the efficacy between precision medication guided by NGS and empirical medication.

METHODS

Patients and Tissue Acquisition

A total of 39 HCC samples were collected for targeted panel or whole-exome sequencing between 2014 and 2019 at the First Affiliated Hospital of Sun Yat-sen University. After obtaining the approval of the Ethics Committee, written informed consent was obtained from all patients. The study inclusion criteria were as follows: 1) age at diagnosis was more than 18 years; 2) HCC samples were confirmed by pathological diagnosis; 3) patients underwent hepatectomy as treatment. The exclusion criteria included the following: 1) patients having other types of malignant tumors in addition to HCC; 2) severe organ damage, autoimmune diseases, and mental illness. In addition, patients were grouped according to the Barcelona Clinic Liver Cancer (BCLC) staging system (Forner et al., 2018). Tumor pathological grade was based on the Edmondson-Steiner Grading System (Edmondson and Steiner, 1954).

Tumor samples were collected immediately following surgical resection, and then stored in pre-cold RPMI-1640 medium with 5% FBS and 1 × Penicillin/Streptomycin, or in Histidine-Tryptophan-Ketoglutarate tissue preservation solution if the estimated shipping time was longer than 1 h. Formalin-fixed paraffin-embedded (FFPE) sections of surgical tumor samples were also sent for analysis when fresh tumor samples were unavailable. Samples were anonymized for further analysis.

After discharge, patients were seen in the clinic monthly for the first 6 months, and then every 3 months, as described in our previous study (Ke et al., 2020). Telephonic follow-up was also conducted every 6 months. The diagnosis of tumor recurrence was made based on clinical examination, laboratory data, and radiological examinations (such as MRI, CT, and positron emission tomography [PET] scan).

Targeted Panel Sequencing, Whole-Exome Sequencing and cBioPortal Database Analysis

The panel of targeted deep sequencing comprised 4,557 exons of 365 tumor-associated genes, and 45 introns from 25 genes where frequent gene fusions could be captured in cancer (**Supplementary Figure S1**). All targeted panel sequencing assays were performed at the 3D Med Clinical Laboratory Co., Ltd. (Shanghai). The detailed method used to perform targeted deep sequencing has been described elsewhere (Feng et al., 2020). All whole-exome sequencing assays were performed at the GenomiCare Medical Laboratory Co., Ltd. (Shanghai). The process of whole-exome sequencing included the following: 1) exome capture, library construction, and sequencing; 2) sequence mapping and somatic variant detection; and 3) detection of copy-number alterations, which have been described in detail elsewhere (Tan et al., 2016; Yang et al., 2019).

We further used the online analysis tool of the cBioPortal database to explore the differences of mutation profiles between our cohort and cBioPortal datasets. The correlations between the high-frequency mutation gene and clinical characteristics were also analyzed.

Statistical Analysis

Statistical analyses for clinical data and mutation profiles were performed using SPSS Statistical software, version 25.0 (IBM, Chicago, Illinois, United States) and Excel 2019. Unordered categorical variables were analyzed by Fisher's exact or Chi-Square test, and ordinal or continuous variables were analyzed by non-parametric Mann–Whitney U test. Correlations were analyzed to identify clinical characteristics related to mutation profiles. Mutation frequency of gene = the number of patients with gene mutation/total number of patients ×100%. Overall survival (OS) was defined as the time from the date of surgery until death or last follow-up, and disease-free survival (DFS) was defined as the time from the date of surgery to initial tumor recurrence, metastasis, or death. The last follow-up was conducted in August 2021. The survival analysis was conducted using the Kaplan–Meier method and compared *via* log-rank test. A two-sided value of $p < 0.05$ was considered to be statistically significant.

RESULTS

Clinical Characteristics of Patients

In the present study, we enrolled 39 HCC patients with a median age of 47 years (range, 26–70 years) at diagnosis from May 2014 to December 2019 for targeted panel or whole exome sequencing. These patients consisted of 36 males and 3 females; 5 patients had cirrhosis and 29 were HBsAg positive. There were 24 patients (61.5%), 6 patients (15.4%), 8 patients (20.5%), and 1 patient (2.6%) with Edmondson-Steiner grade II, II-II, III, and IV, respectively. Tumor extrahepatic metastasis occurred in seven patients (17.9%, 7/39). According to BCLC staging system, the

TABLE 1 | The clinical characteristics of HCC patients.

Variables	Cases (%)
Age, year	
<60	30 (76.9%)
≥60	9 (23.1%)
Sex	
Male	36 (92.3%)
Female	3 (7.7%)
Liver cirrhosis	
no	34 (87.2%)
yes	5 (12.8%)
HBsAg	
Negative	10 (25.6%)
Positive	29 (74.4%)
HBV-DNA, IU/ml	
<100	21 (53.8%)
≥100	18 (46.2%)
Tumor size, cm	
<5 cm	10 (25.6%)
≥5cm, <10 cm	12 (30.8%)
≥10 cm	17 (43.6%)
Tumor number	
single	20 (51.3%)
multiple	19 (48.7%)
Extrahepatic metastasis	
no	32 (82.1%)
yes	7 (17.9%)
PVTT	
no	26 (66.7%)
yes	13 (33.3%)
MVI	
no	22 (56.4%)
yes	17 (43.6%)
AFP, ng/ml	
<200	17 (43.6%)
≥200	22 (56.4%)
BCLC stage	
A	16 (41.0%)
B	9 (23.1%)
C	14 (35.9%)
Edmondson-Steiner grade	
II	24 (61.5%)
II-III	6 (15.4%)
III	8 (20.5%)
IV	1 (2.6%)

HBV: Hepatitis B virus; PVTT: portal vein tumor thrombus; MVI: microvascular invasion; AFP: alpha fetoprotein; BCLC: barcelona clinic liver cancer.

number of stage A, B, and C patients was 16 (41.0%), 9 (23.1%), and 14 (35.9%), respectively. Portal vein tumor thrombus (PVTT) and microvascular invasion (MVI) were observed in 13 (33.3%) and 17 (43.6%) patients, respectively. The clinical characteristics of HCC patients are shown in **Table 1**. Detailed information is shown in **Supplementary Table S1**.

Overview of Somatic Mutations in HCC Patients

Mutation Identification of Targeted Panel Sequencing

In all, 17 patients underwent targeted sequencing and 117 somatic mutations were identified. Of these, 62.4% (73/117) were single nucleotide variants (SNVs), 32.5% (38/117) were copy number variants (CNVs), and 5.1% (6/117) were insertions/deletion variants (INDELs). Among SNVs, 87.7% (64/73) were missense mutations, 8.2% (6/73) were nonsense mutations, and 4.1% (3/73) were intron variants. With regard to mutation taster prediction, 56 gene variants (47.9%) were deleterious and 61 (52.1%) were unknown (**Supplementary Table S2**). The commonly mutated genes were TP53 (12.0%, 14/117), TSC2 (1.7%, 2/117), RB1 (1.7%, 2/117), EGF (1.7%, 2/117), CTNNB1 (1.7%, 2/117), BRCA2 (1.7%, 2/117), NTRK3 (1.7%, 2/117), LRP1B (1.7%, 2/117), AXIN1 (1.7%, 2/117), IRS2 (1.7%, 2/117), MCL1 (1.7%, 2/117), and MYC (1.7%, 2/117) (**Table 2**).

Somatic Mutations Profiles in HCC Determined *via* Whole-Exome Sequencing

In all, 22 patients underwent whole-exome sequencing. We mapped the sequence reads to the human reference genome and identified a total of 3,383 somatic SNVs, 468 INDELs, and 31 CNVs (**Supplementary Table S3**). There were a median of 6.42 (range: 3.03–9.10) somatic mutations per mega-base pair (Mb), 0.085% microsatellite instability (MSI) (range: 0.00–33.00%), 1.4% CNV (range: 0.16–19.56%), and 19.37% objective response rate (ORR) (range: 11.27–23.15%) of immunotherapy expectation (**Supplementary Table S4**).

T > G/A > C transversion (Tv) and C > T/G > A transition (Ti) patterns were dominant, C > A/G > T Tv and T > C/A > G Ti were moderate, and the proportion of T > A/A > T Tv and C > G/G > C Tv was the lowest in 22 HCC patients (**Figure 1A**). In addition, a relatively high ratio of Ti/Tv (median: 0.67; range: 0.24–1.35) was found (**Figure 1B**). With regard to INDELs, 67.9% (318/468) deletions, 20.3% (95/468) frameshift insertions, and 11.8% (55/468) duplications were observed (**Figure 1C**).

In total, 30 genes, including TP53 (77.3%, 17/22), MUC16 (50.0%, 11/22), MUC12 (45.5%, 10/22), MUC4 (45.5%, 10/22), ALPP (36.4%, 8/22), MUC17 (36.4%, 8/22), FRG1 (27.3%, 6/22), MUC3A (27.3%, 6/22), MUC5B (27.3%, 6/22), TPSAB1 (27.3%, 6/22), TTN (27.3%, 6/22), BIRC5 (27.3%, 6/22), MUC6 (27.3%, 6/22), C11orf80 (22.7%, 5/22), OR8U1 (22.7%, 5/22), TDG (22.7%, 5/22), ZNF701 (22.7%, 5/22), AHNAK2 (22.7%, 5/22), BCLAF1 (22.7%, 5/22), PAK2 (22.7%, 5/22), POU4F1 (22.7%, 5/22), DNHD1 (22.7%, 5/22), CYB561D1 (22.7%, 5/22), TAS2R30 (22.7%, 5/22), TNRC6B (22.7%, 5/22), HMCN1 (22.7%, 5/22), HRCT1 (22.7%, 5/22), PRKCSH (22.7%, 5/22), NBPF10 (22.7%, 5/22) and BCAS4 (22.7%, 5/22), were found to be mutated in at least 20% (5/22) HCC patients by whole-exome sequencing (**Figure 2A**) and details regarding the top four genes are listed in **Supplementary Table S5**. We also identified 27 amplified segments, which harbored several known oncogenes such as FGF3, SOX2, and TERT, *etc.* (**Figure 2B**); and four lost segments, which harbored tumor suppressors including BRCA1, BRCA2, APC, and B2M (**Supplementary Table S4**).

To understand the biological characteristics of the mutated genes, we performed enrichment analysis, which included Gene Ontology (GO) function and Kyoto Encyclopedia of Genes and Genomes (KEGG) pathway analysis. KEGG items revealed that mutated genes were highly enriched in multiple cancer pathways (**Figure 3A**). With regard to HCC, the cancer we focused on, its enrichment ratio was

TABLE 2 | Summary of frequent gene variation in HCC detected by targeted sequencing.

Gene	Cases	Variant type	Amino acid or nucleotide alteration	Mutation frequency/copy number	Mutation type	Mutation taster prediction
TP53	1	SNV	p.V157F	47.70%	missense	deleterious
TP53	2	SNV	p.R249S	0.44%	missense	deleterious
TP53	3	SNV	p.E258*	25.40%	nonsense	deleterious
TP53	3	SNV	p.F270V	2.00%	missense	deleterious
TP53	4	SNV	p.E258K	40.30%	missense	deleterious
TP53	5	SNV	p.R158L	75.30%	missense	deleterious
TP53	7	SNV	c.673-2A > T	54.90%	intron_variant	deleterious
TP53	10	SNV	p.R249S	no available	missense	deleterious
TP53	11	SNV	p.R249S	no available	missense	deleterious
TP53	13	SNV	p.R249S	no available	missense	deleterious
TP53	14	SNV	p.L194R	no available	missense	deleterious
TP53	17	INDEL	p.Q136Hfs*34	no available	frameshift mutation	deleterious
TP53	9	SNV	p.V157F	32.00%	missense	deleterious
TP53	6	SNV	p.R174W	no available	missense	unknown
TSC2	2	SNV	p.E1490G	no available	missense	unknown
TSC2	14	INDEL	exon5-exon16 dup	no available	—	unknown
RB1	1	SNV	p.T168A	no available	missense	unknown
RB1	8	INDEL	p.S393Rfs*8	74.90%	frameshift mutation	deleterious
EGF	8	SNV	p.G392R	no available	missense	deleterious
EGF	9	SNV	p.P644S	no available	missense	deleterious
CTNNB1	4	SNV	p.D32N	8.70%	missense	deleterious
CTNNB1	5	SNV	p.S37F	23.60%	missense	deleterious
BRCA2	2	SNV	p.D1898G	no available	missense	deleterious
BRCA2	7	SNV	p.S767C	no available	missense	deleterious
NTRK3	4	SNV	p.V289E	no available	missense	deleterious
NTRK3	16	SNV	p.V550I	no available	missense	unknown
LRP1B	6	SNV	p.D1096N	no available	missense	unknown
LRP1B	7	SNV	p.Y1865N	no available	missense	unknown
AXIN1	6	INDEL	p.H662Mfs*43	21.30%	frameshift mutation	deleterious
AXIN1	12	SNV	p.W444*	66.50%	nonsense	deleterious
IRS2	5	CNV	—	copy number gain (3)	—	deleterious
IRS2	16	CNV	—	copy number gain (3)	—	deleterious
MCL1	8	CNV	—	copy number gain (10)	—	deleterious
MCL1	10	CNV	—	copy number gain	—	deleterious
MYC	11	CNV	—	copy number gain	—	deleterious
MYC	13	CNV	—	copy number gain	—	deleterious

Mutation taster prediction: prediction of the pathogenicity risk of gene variants.

11.59% (q = 0.002). GO items demonstrated that mutated genes were mainly involved in glycoprotein metabolic and biosynthetic processes in biological processes (**Figure 3B**); extracellular matrix and Golgi lumen in cellular components (**Figure 3C**); and extracellular matrix structural constituents and phosphatase binding in molecular functions (**Figure 3D**). **Figure 3E** shows that some variant genes were related to complex cancer pathways. These genes were mainly involved in the JAK/STAT, PT3K/AKT, WNT, and MAPK/ERK pathways, and could influence each other (e.g., in terms of activation, inhibition, and phosphorylation), which could lead to cell evading apoptosis, cell proliferation, sustained angiogenesis, *etc.* and in turn affect the occurrence and development of cancers.

Variant Types of Key Mutations and Recommendations of Precision Medicine

By targeted panel and whole-exome sequencing, we identified 3,999 somatic variations among 86.4% (3,456/3,999) SNVs, 11.9% (474/3,999) INDELs, and 1.7% (69/3,999) CNVs in 39 HCC patients. It was worth noting that the variation rate of TP53 was the highest by both targeted and whole-exome sequencing (76.5%, 13/17 and 77.3%, 17/22, respectively). The mutation types and mutation taster prediction of TP53 are listed in **Table 3**. p.R249S was the most common amino acid alteration (23.5%), and 82.3% (28/34) of TP53 variations were missense mutations. Except for p.R174W in case 6, all remaining TP53 variations were deleterious. Furthermore, TP53 was frequently mutated with MUC17 (15.4%, 6/39), NBPF10 (12.8%, 5/39), and AHNAK2 (12.8%, 5/39).

According to the data obtained from targeted panel and whole-exome sequencing reports, 59.0% (23/39) patients had at least one clinically actionable somatic mutation for which clinical treatments could be prescribed using precision medicine (**Supplementary Tables S2, S4**).

The Differences of Genomic Profiles Compared With cBioPortal Datasets

Because 30 mutated genes and 3 amplified genes variated in at least 20% HCC patients, we further used cBioPortal database to

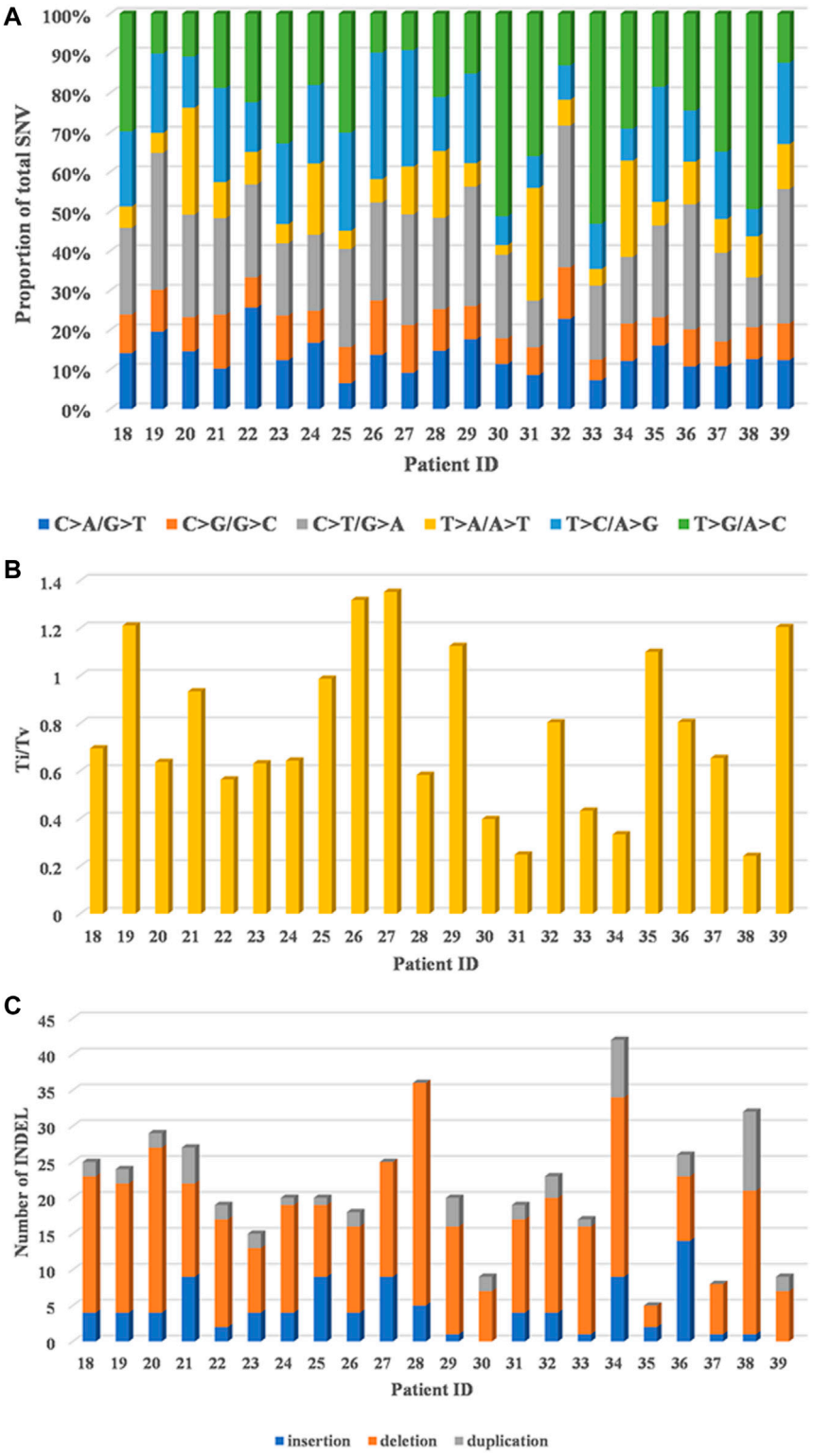

FIGURE 1 | Genomic alterations in 22 HCC patients by whole-exome sequencing. **(A)** Distribution of six substitution patterns. **(B)** The ratio of transition to transversion (Ti/Tv). **(C)** The number of different types of INDELs.

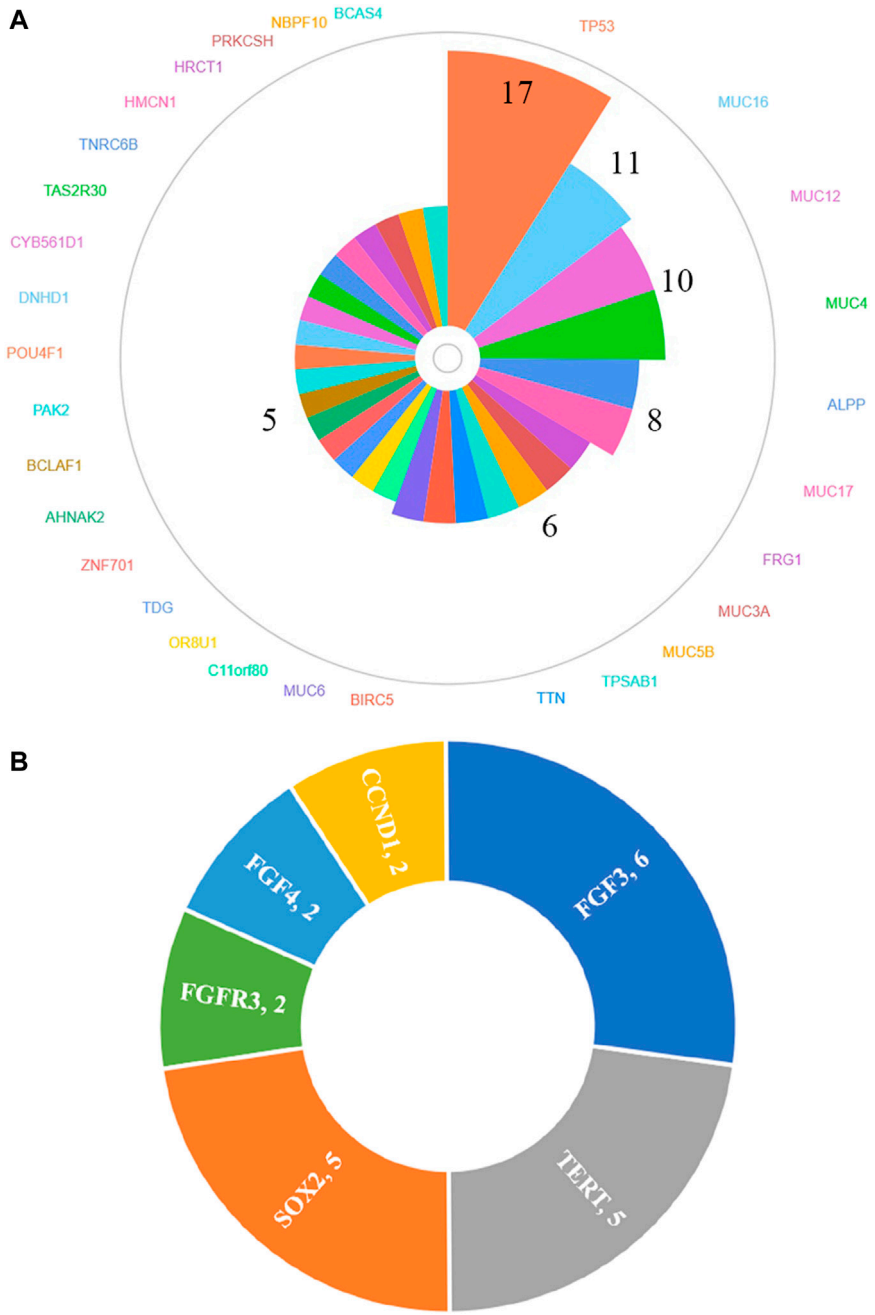

FIGURE 2 | Genes of high-frequency sequence variants **(A)** and CNV **(B)** detected by whole-exome sequencing.

explore the differences between our cohort and other cohorts. Mutated and amplified genes mentioned above were found in 594 cases and 71 cases, respectively. The common gene variation frequencies were as follows: TP53 (29%), TTN (23%), MUC16 (14%), HMCN1 (7%), MUC4 (6%), and AHNAK2 (5%). The gene variation frequencies for all other genes were less than 5% (**Supplementary Figure S2**). We found that except for TTN (15% vs. 23%), the mutation frequencies of most commonly mutated genes in our cohort all higher than those in cBioPortal: TP53 (77.3% vs. 29.0%), MUC16 (50.0% vs. 14.0%), MUC12 (45.5% vs. 1.8%), MUC4 (45.5% vs. 6.0%), ALPP (36.4% vs. 0.7%), MUC17 (36.4% vs. 4.0%), FRG1 (27.3% vs. 0.3%), MUC3A (27.3% vs. 0.1%), MUC5B (27.3% vs. 3.0%), TPSAB1 (27.3%, 0.2%), BIRC5 (27.3% vs. 0.1%), MUC6 (27.3% vs. 1.9%), C11orf80 (22.7% vs. 0.3%), OR8U1 (22.7% vs. 0.3%), TDG (22.7% vs. 0.6%), ZNF701 (22.7% vs. 0.7%), AHNAK2 (22.7% vs. 5%), BCLAF1 (22.7% vs. 2.1%), PAK2 (22.7% vs. 0.6%), POU4F1 (22.7% vs.

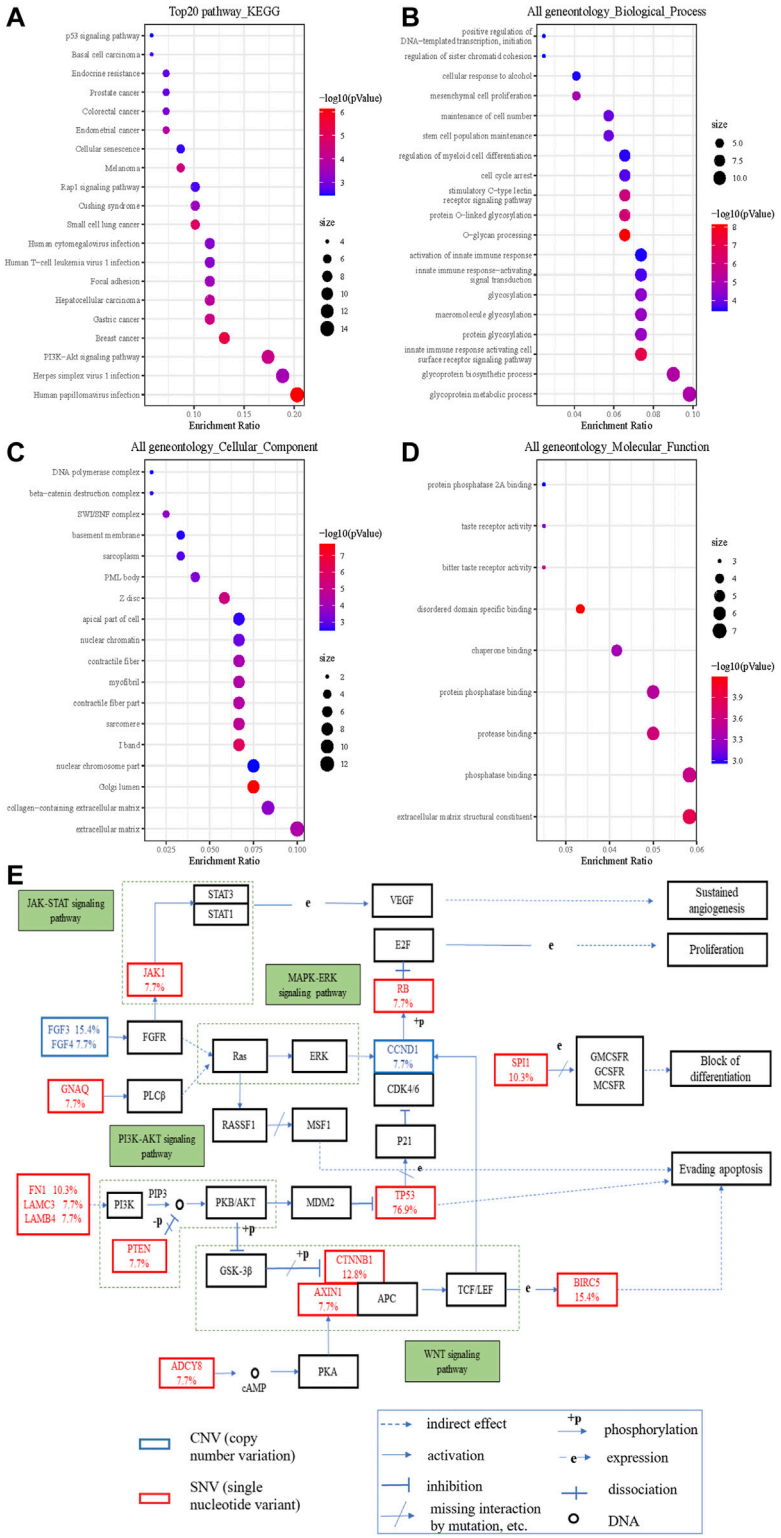

FIGURE 3 | The significantly enriched GO annotations and the KEGG pathways of somatic cell variants in HCC cases. **(A)** KEGG pathway analysis; **(B)** biological processes; **(C)** cellular components; **(D)** molecular functions; **(E)** KEGG pathway annotations of the cancer related pathway, with red lettering denoting SNVs and blue lettering denoting CNVs. The number represents the frequency of variations.

TABLE 3 | The variant types and mutation taster prediction of TP53.

Type		n (%)
Amino acid or nucleotide alteration		
	p.R249S	8 (23.5%)
	p.V157F	2 (5.9%)
	p.C176Y	1 (2.9%)
	p.C176W	1 (2.9%)
	p.R249W	1 (2.9%)
	p.H179Y	1 (2.9%)
	p.G226fs	1 (2.9%)
	p.H178P	1 (2.9%)
	p.R337L	1 (2.9%)
	p.S215G	1 (2.9%)
	p.R273C	1 (2.9%)
	p.R337C	1 (2.9%)
	p.R273H	1 (2.9%)
	p.G105S	1 (2.9%)
	p.P151S	1 (2.9%)
	p.R213*	1 (2.9%)
	p.G105V	1 (2.9%)
	p.E258*	1 (2.9%)
	p.F270V	1 (2.9%)
	p.E258K	1 (2.9%)
	p.R158L	1 (2.9%)
	c.673-2A > T	1 (2.9%)
	p.L194R	1 (2.9%)
	p.Q136Hfs*34	1 (2.9%)
	p.G245D	1 (2.9%)
	p.R174W	1 (2.9%)
Mutation type		
	missense	28 (82.3%)
	frameshift	2 (5.9%)
	nonsense	2 (5.9%)
	other	2 (5.9%)
Mutation taster prediction		
	deleterious	33 (97.1%)
	unknown	1 (2.9%)

0.6%), DNHD1 (22.7% vs. 2.4%), CYB561D1 (22.7% vs. 0.1%), TAS2R30 (22.7% vs. 0.3%), TNRC6B (22.7% vs. 1.4%), HMCN1 (22.7% vs. 7%), HRCT1 (22.7% vs. 0.1%), PRKCSH (22.7% vs. 0.5%), NBPF10 (22.7% vs. 2.2%) and BCAS4 (22.7% vs. 0.1%). As for CNVs, the FGF3 amplification rate of 15.4% (6/39), TERT amplification rate of 12.8% (5/39), and SOX2 amplification rate of 12.8% (5/39) in our cohort (**Figure 2B**) were also significantly higher than those found in the cBioPortal datasets (5.0, 4.0, and 1.1%, respectively, **Supplementary Figure S3**).

We further used cBioPortal to analyze the variated types of top 4 mutated genes in our cohort. We found 209 missense mutations, 93 truncating mutations, and 5 in-frame mutations in TP53; 136 missense mutations, 15 truncating mutations, and 1 in-frame mutation in MUC16; 15 missense mutations and 2 truncating mutations in MUC12; and 50 missense mutations, 2 truncating mutations, and 2 in-frame mutations in MUC4 (**Supplementary Figure S4**, **Supplementary Table S6**). This was similar to our results shown in **Supplementary Table S5** indicating that the top 4 mutated genes were dominated by missense and truncating mutations.

Correlation Analyses Between Gene Mutation and Clinical Characteristics

We used cBioPortal HCC cohorts to analyze the correlations between TP53 mutation and clinical characteristics (**Supplementary Table S7**) and found that only neoplasm histologic grade (q = 0.008) and race category (q = 0.003) had a significant association with TP53 mutation. With regard to OS and DFS, the survival differences between the TP53 mutation group and the wild-type group were significant in the cBioPortal dataset (OS: logrank p = 0.018; DFS: logrank p = 0.005) (**Supplementary Figure S5**). However, the results were different from our study which showed that there were no significant differences in survival outcomes (OS, logrank p = 0.084; DFS, logrank p = 0.201) as well as other clinical characteristics between the TP53 mutation group and the wild-type group. Cirrhosis tended to occur in FGF3 and MUC4 mutation groups (p = 0.019 and 0.011, respectively) (**Table 4**).

No significant statistical differences were observed between precision medication guided by NGS and empirical medication (logrank p = 0.181), especially between targeted therapy based on recommended drugs and clinical experience (logrank p = 0.376) (**Figure 4**). However, immunotherapy combined with targeted therapy seemed to result in a longer OS rate, even if there was no statistical difference.

DISCUSSION

In this study, we used NGS to detect multi-gene variations in HCC patients, analyzed the correlations with clinical characteristics, and compared our findings with those of the cBioPortal database.

First, we described the overall situation of somatic mutations. C > A/G > T Tv and T > C/A > G Ti were moderate in our study, and were shared by other HCC cohorts (Totoki et al., 2014; Schulze et al., 2015; Fujimoto et al., 2016). T > G/A > C Tv and C> T/G > A Ti patterns were dominant, but the proportion of T > A/A > T Tv and C > G/G > C Tv was the lowest, implying that T > G/A > C Tv and C > T/G > A Ti may have contributed to hypermutations in our cohort, but these results were different from two previous studies (where T > A/A > T Tv was dominant) (Gao et al., 2019; Zhou et al., 2019) and the Cancer Genome Atlas (TCGA) dataset (where T > G/A > C Tv showed the lowest occurrence) (**Supplementary Figure S6**), which may be the reason of the complexity of the genome, individual differences and small sample size. In addition, a relatively high ratio of Ti/Tv was found, in agreement with the results of previous HCC sequencing studies (Guichard et al., 2012; Huang et al., 2012) and other cancers studies (Moore et al., 2003; Hainaut and Pfeifer, 2016). Therefore, a high ratio of Ti/Tv in our study may have contributed to the biochemical structure of nucleotides and the chemical characteristics of complementary base pairing (Taylor et al., 2006; Massey, 2015; Stoltzfus and Norris, 2016), which could help researchers gain a deeper understanding of the patterns and strengths of molecular system development and HCC evolution.

TABLE 4 | Correlations among FGF3 mutation, MUC4 mutation and cirrhosis.

		FGF3		*p* value	MUC4		*p* value
		Wild type	Mutation		Wild type	Mutation	
Cirrhosis	no	31 (91.2%)	3 (8.8%)	0.019	28 (82.4%)	6 (17.6%)	0.011
	yes	2 (40.0%)	3 (60.0%)		1 (20.0%)	4 (80.0%)	

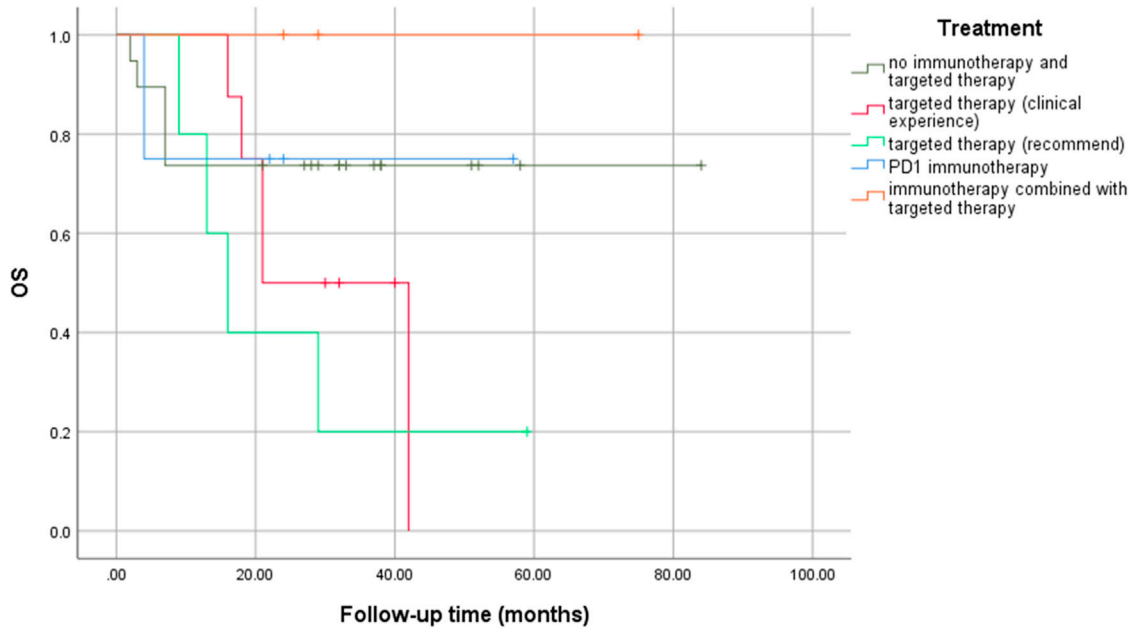

FIGURE 4 | Comparisons of OS rates in different treatment groups.

Second, we analyzed the main somatic gene variations and found that most of high-frequency mutations in our cohort were relatively low-frequency mutations in cBioPortal datasets. The top 4 mutated genes (TP53, MUC16, MUC12, and MUC4) were dominated by missense mutations, which was similar to the cBioPortal data. Further, TP53 mutations were the most frequent mutation in both our cohort (p.R249S was the most common amino acid alteration) and cBioPortal datasets, even if there was a significant difference in the mutation rate (76.9% vs 29.0%, respectively). In addition, the most common changes in CNV were FGF3, TERT, and SOX2, and their variant rates were all higher than those reported in cBioPortal-HCC patients (15.4% vs. 5.0%; 12.8% vs. 4.0%; 12.8% vs. 1.1%, respectively). We speculated that because of ethnic and individual differences, the genetic profile characteristics of HCC patients in China may be different from those in other countries (three datasets from the United States, one dataset from Europe, one dataset from Korea, the other dataset from Japan in cBioPortal database). Accordingly, large cohort studies are needed to verify these results.

We further explored whether mutant genes were related to clinical characteristics. TP53 mutation had significant correlations with histological grade, race category, OS, and DFS in cBioPortal database. However, our results suggested that there were little correlations between gene variations and clinical characteristics except that cirrhosis tended to occur in FGF3 and MUC4 mutation groups. We further found that the effect of treatments guided by NGS may be limited. There may be several reasons for this difference. First, individual differences, racial disparities, and sample sizes could have affected the results. Next, gene mutations (e.g., nonsense mutation) may not affect the protein expressions, which play a significant role in performing life functions. Further, co-occurring genetic alterations could alter the biological characteristics of tumors and affect the prognosis of patients (Deng et al., 2019), meaning that different genetic mutations may affect each other. Furthermore, enrichment analysis showed that the mutated genes were involved in complex cancer signaling pathways (e.g., PI3K/AKT, WNT, and JAK/STAT pathways), biological processes (e.g., glycoprotein metabolic process, protein glycosylation, and activation of innate immune response), cellular components (e.g., extracellular matrix, Golgi lumen, and nuclear chromosome part), and molecular functions (e.g., extracellular matrix structural constituent, phosphatase binding, and protease binding). When targeted drugs act on HCC cells, tumor cells can change the expression of related proteins, adjust

the connection of signal pathways, and change the microenvironment to evade targeted drug attacks. When a pathway is inhibited by targeted drugs, HCC cells can strengthen the signal transduction of other pathways by compensation, thereby re-promoting its own proliferation and invasion, leading to the failure of targeted therapy (Mir et al., 2017). Some targeted drugs can inhibit the angiogenesis of HCC tissues, but a continuous anti-angiogenesis effect can cause tumor starvation and hypoxia, promoting the proliferation of resistant HCC cells that adapt to hypoxia and lack of nutrients (Mendez-Blanco et al., 2018). Thus, intervention of a signaling pathway alone may be ineffective, and the negative feedback may result in the development of drug resistance. Accordingly, the use of several molecularly targeted agents in combination is an appealing way to counteract resistance. Finally, insignificant statistical differences may also be caused by the relatively small sample size. Multi-center, large sample, prospective studies are needed to further verify these results.

No therapeutic targets in many patients suggested that HCC is not completely caused by mutations, or that there are no approved drugs targeting these mutations. Moreover, targeted drugs may be invalid. SHIVA, a randomized trial conducted in France, found that there were no differences between NGS-guided treatment and conventional treatment in terms of PFS and OS (Le Tourneau et al., 2015). In addition, tumor mutation burden (TMB) can also fail to predict immune checkpoint blockade response (McGrail et al., 2018; McGrail et al., 2021). Therefore, the out-of-range use of NGS for targeted drugs should be focused on.

Further, the results of gene sequencing may vary considerably. For instance, different institutions may provide different results for gene sequencing, which may result from discrepancies in sequencing principles, sequencing systems, and bioinformatics algorithms, *etc.* Problems in the gene sequencing process (such as hardware, software, samples, and quality control) can also lead to false negatives or false positives (Xuan et al., 2013; Bean et al., 2020). Moreover, the different understandings of genes or treatments with potential clinical benefits may lead to different interpretations of the same test results (Rehm et al., 2013). Most institutions only rely on public databases to interpret data and recommend targeted drugs, but they fail to conduct individualized analysis based on patient-specific conditions. Therefore, some treatments, which are based on clinical experience rather than gene sequencing, may also be effective. This phenomenon can explain why precision medication guided by NGS was not superior to empirical medication in terms of OS rate in our study. It is worth discussing whether better the results can be obtained with more gene sequencing. If gene sequencing can only help a small number of patients, the incremental cost will be high when it is promoted. In addition, the results of gene sequencing could be useless for treatment if they are not sufficiently correlated with important clinical data (such as tumor size, family history, and drug use). Therapies only based on some gene signaling pathway theories and little literature evidence alone will hardly have any positive effects.

Therefore, gene sequencing may not be translated into improved patient outcomes and the detection of therapeutic gene mutations could be far from having a true clinical benefit. Some studies have reported that patients achieved good curative effects by implementing targeted therapy based on gene sequencing, but the sample size, methodology, and research design were not rigorous and the effective rate was also not mentioned in these studies (Yu et al., 2018; Sun et al., 2020). The effective rate of even programmed death 1 (PD-1) treatment was only 17%–20% (El-Khoueiry et al., 2017; Zhu et al., 2018; Lee et al., 2020). Nevertheless, targeted therapy-combined immunotherapy could improve efficacy, not only in our results but also in other studies (Finn et al., 2020; Xu et al., 2021). Therefore, different patients should choose different gene sequencing based on individual differences and genetic polymorphisms. Molecular biology experts, pathologists, oncologists, bioinformatics experts, and immunology experts should work together to find the best-matched therapeutic drugs and conduct cutting-edge clinical trials for each mutation site so as to provide a comprehensive interpretation of the genetic sequencing report for cancer patients. At the same time, researchers should perform reasonable clinical research, strictly define the outcome of clinical benefit, and prospectively evaluate the efficacy of targeted drugs under the guidance of gene sequencing.

Our study has several strengths. First, we described the somatic mutations profiles and identified the high-frequency variated genes in 39 Chinese HCC patients. Second, similarities and differences were revealed between our HCC cohort and cBioPortal-HCC patients with regard to genomic profiling, especially those genes that were relatively low-frequency in the cBioPortal database but commonly mutated in our cohort. Third, the correlations between gene mutation and clinical characteristics were also analyzed, and its limited values for guiding the clinical work were indicated. However, there are several limitations to our study. First, the sample size of the group was small. Accordingly, large umbrella trials of personalized precision therapy are needed to confirm our findings. Second, we did not perform multiple sequencing methods (such as transcriptomics, proteomics, and metabolomics), cell- and animal-based experiments to further verify the results. Third, the combination of the two sequencing methods may be confusing. For the reason of timeliness, we initially used targeted panel sequencing, and later adopted whole-exome sequencing for a larger genome screen. We wanted to expand the sample size so that the data can be fully utilized. In addition, samples are also being accumulated in our center to further verify our research results. Despite these limitations, this study reflected real-world clinical practice as it related to personalized targeted therapy guided by NGS in patients.

In conclusion, the characteristic somatic mutation profiles in 39 Chinese HCC patients were described in this study. Further, we conclude that the role of NGS in guiding treatment may be limited.

DATA AVAILABILITY STATEMENT

The data presented in the study are included in the article/**Supplementary Material** and deposited in the NCBI repository, accession number PRJNA787229.

ETHICS STATEMENT

The studies involving human participants were reviewed and approved by Ethics Committee of the First Affiliated Hospital of Sun Yat-sen University. The patients/participants provided their written informed consent to participate in this study.

AUTHOR CONTRIBUTIONS

1) Conception and design: YH, BP, LK; 2) Administrative support: YH, QH, DL; 3) Provision of study materials or patients: YH, LL, MK, SL; 4) Collection and assembly of data: LK, JS, JF, JC, SS; 5) Data analysis and interpretation: LK, JS, JF, CL; 6) Manuscript writing: All authors; 7) Final approval of manuscript: All authors.

SUPPLEMENTARY MATERIAL

The Supplementary Material for this article can be found online at: https://www.frontiersin.org/articles/10.3389/fmolb.2021.800679/full#supplementary-material

REFERENCES

Bean, L., Funke, B., Carlston, C. M., Gannon, J. L., Kantarci, S., Krock, B. L., et al. (2020). Diagnostic Gene Sequencing Panels: from Design to Report-A Technical Standard of the American College of Medical Genetics and Genomics (ACMG). *Genet. Med.* 22 (3), 453–461. doi:10.1038/s41436-019-0666-z

Bray, F., Ferlay, J., Soerjomataram, I., Siegel, R. L., Torre, L. A., and Jemal, A. (2018). Global Cancer Statistics 2018: GLOBOCAN Estimates of Incidence and Mortality Worldwide for 36 Cancers in 185 Countries. *CA: A Cancer J. Clinicians* 68 (6), 394–424. doi:10.3322/caac.21492

Cancer Genome Atlas Research Network (2017). Electronic address, w.b.e., and Cancer Genome Atlas Research, NComprehensive and Integrative Genomic Characterization of Hepatocellular Carcinoma. *Cell* 169 (7), 1327–1341. doi:10.1016/j.cell.2017.05.046

Deng, L.-L., Gao, G., Deng, H.-B., Wang, F., Wang, Z.-H., and Yang, Y. (2019). Co-occurring Genetic Alterations Predict Distant Metastasis and Poor Efficacy of First-Line EGFR-TKIs in EGFR-Mutant NSCLC. *J. Cancer Res. Clin. Oncol.* 145 (10), 2613–2624. doi:10.1007/s00432-019-03001-2

Edmondson, H. A., and Steiner, P. E. (1954). Primary Carcinoma of the liver.A Study of 100 Cases Among 48,900 Necropsies. *Cancer* 7 (3), 462–503. doi:10.1002/1097-0142(195405)7:3<462:aid-cncr2820070308>3.0.co;2-e

El-Khoueiry, A. B., Sangro, B., Yau, T., Crocenzi, T. S., Kudo, M., Hsu, C., et al. (2017). Nivolumab in Patients with Advanced Hepatocellular Carcinoma (CheckMate 040): an Open-Label, Non-comparative, Phase 1/2 Dose Escalation and Expansion Trial. *The Lancet* 389 (10088), 2492–2502. doi:10.1016/S0140-6736(17)31046-2

Feng, F., Cheng, Q., Zhang, D., Li, B., Qin, H., Xu, C., et al. (2020). Targeted Deep Sequencing Contributes to Guiding Personalized Targeted Therapy for Advanced Biliary Tract Cancer Patients with Non-radical R-esection: A R-eal-world S-tudy. *Oncol. Rep.* 43 (4), 1089–1102. doi:10.3892/or.2020.7491

Finn, R. S., Qin, S., Ikeda, M., Galle, P. R., Ducreux, M., Kim, T.-Y., et al. (2020). Atezolizumab Plus Bevacizumab in Unresectable Hepatocellular Carcinoma. *N. Engl. J. Med.* 382 (20), 1894–1905. doi:10.1056/NEJMoa1915745

Forner, A., Reig, M., and Bruix, J. (2018). Hepatocellular Carcinoma. *The Lancet* 391 (10127), 1301–1314. doi:10.1016/S0140-6736(18)30010-2

Fujimoto, A., Furuta, M., Totoki, Y., Tsunoda, T., Kato, M., Shiraishi, Y., et al. (2016). Whole-genome Mutational Landscape and Characterization of Noncoding and Structural Mutations in Liver Cancer. *Nat. Genet.* 48 (5), 500–509. doi:10.1038/ng.3547

Gao, J., Aksoy, B. A., Dogrusoz, U., Dresdner, G., Gross, B., Sumer, S. O., et al. (2013). Integrative Analysis of Complex Cancer Genomics and Clinical Profiles Using the cBioPortal. *Sci. Signal.* 6 (269), l1. doi:10.1126/scisignal.2004088

Gao, Q., Zhu, H., Dong, L., Shi, W., Chen, R., Song, Z., et al. (2019). Integrated Proteogenomic Characterization of HBV-Related Hepatocellular Carcinoma. *Cell* 179 (5), 1240. doi:10.1016/j.cell.2019.10.038

Guichard, C., Amaddeo, G., Imbeaud, S., Ladeiro, Y., Pelletier, L., Maad, I. B., et al. (2012). Integrated Analysis of Somatic Mutations and Focal Copy-Number Changes Identifies Key Genes and Pathways in Hepatocellular Carcinoma. *Nat. Genet.* 44 (6), 694–698. doi:10.1038/ng.2256

Hainaut, P., and Pfeifer, G. P. (2016). SomaticTP53Mutations in the Era of Genome Sequencing. *Cold Spring Harb Perspect. Med.* 6 (11), a026179. doi:10.1101/cshperspect.a026179

Huang, J., Deng, Q., Wang, Q., Li, K.-Y., Dai, J.-H., Li, N., et al. (2012). Exome Sequencing of Hepatitis B Virus-Associated Hepatocellular Carcinoma. *Nat. Genet.* 44 (10), 1117–1121. doi:10.1038/ng.2391

Ke, L., Shen, R., Fan, W., Hu, W., Shen, S., Li, S., et al. (2020). The Role of Associating Liver Partition and portal Vein Ligation for Staged Hepatectomy in Unresectable Hepatitis B Virus-Related Hepatocellular Carcinoma. *Ann. Transl Med.* 8 (21), 1402. doi:10.21037/atm-20-2420

Le Tourneau, C., Delord, J.-P., Gonçalves, A., Gavoille, C., Dubot, C., Isambert, N., et al. (2015). Molecularly Targeted Therapy Based on Tumour Molecular Profiling versus Conventional Therapy for Advanced Cancer (SHIVA): a Multicentre, Open-Label, Proof-Of-Concept, Randomised, Controlled Phase 2 Trial. *Lancet Oncol.* 16 (13), 1324–1334. doi:10.1016/S1470-2045(15)00188-6

Lee, M. S., Ryoo, B.-Y., Hsu, C.-H., Numata, K., Stein, S., Verret, W., et al. (2020). Atezolizumab with or without Bevacizumab in Unresectable Hepatocellular Carcinoma (GO30140): an Open-Label, Multicentre, Phase 1b Study. *Lancet Oncol.* 21 (6), 808–820. doi:10.1016/S1470-2045(20)30156-X

Massey, S. (2015). Genetic Code Evolution Reveals the Neutral Emergence of Mutational Robustness, and Information as an Evolutionary Constraint. *Life* 5 (2), 1301–1332. doi:10.3390/life5021301

McGrail, D. J., Federico, L., Li, Y., Dai, H., Lu, Y., Mills, G. B., et al. (2018). Multi-omics Analysis Reveals Neoantigen-independent Immune Cell Infiltration in Copy-Number Driven Cancers. *Nat. Commun.* 9 (1), 1317. doi:10.1038/s41467-018-03730-x

McGrail, D. J., Pilié, P. G., Rashid, N. U., Voorwerk, L., Slagter, M., Kok, M., et al. (2021). High Tumor Mutation burden Fails to Predict Immune Checkpoint Blockade Response across All Cancer Types. *Ann. Oncol.* 32 (5), 661–672. doi:10.1016/j.annonc.2021.02.006

Méndez-Blanco, C., Fondevila, F., García-Palomo, A., González-Gallego, J., and Mauriz, J. L. (2018). Sorafenib Resistance in Hepatocarcinoma: Role of Hypoxia-Inducible Factors. *Exp. Mol. Med.* 50 (10), 1–9. doi:10.1038/s12276-018-0159-1

Mir, N., Jayachandran, A., Dhungel, B., Shrestha, R., and Steel, J. C. (2017). Epithelial-to-Mesenchymal Transition: A Mediator of Sorafenib Resistance in Advanced Hepatocellular Carcinoma. *Ccdt* 17 (8), 698–706. doi:10.2174/1568009617666170427104356

Moore, P. S., Beghelli, S., Zamboni, G., and Scarpa, A. (2003). Genetic Abnormalities in Pancreatic Cancer. *Mol. Cancer* 2, 7. doi:10.1186/1476-4598-2-7

Rehm, H. L., Bale, S. J., Bayrak-Toydemir, P., Berg, J. S., Brown, K. K., Deignan, J. L., et al. (2013). ACMG Clinical Laboratory Standards for Next-Generation Sequencing. *Genet. Med.* 15 (9), 733–747. doi:10.1038/gim.2013.92

Schulze, K., Imbeaud, S., Letouzé, E., Alexandrov, L. B., Calderaro, J., Rebouissou, S., et al. (2015). Exome Sequencing of Hepatocellular Carcinomas Identifies

New Mutational Signatures and Potential Therapeutic Targets. *Nat. Genet.* 47 (5), 505–511. doi:10.1038/ng.3252

Staaf, J., Glodzik, D., Bosch, A., Vallon-Christersson, J., Reuterswärd, C., Häkkinen, J., et al. (2019). Whole-genome Sequencing of Triple-Negative Breast Cancers in a Population-Based Clinical Study. *Nat. Med.* 25 (10), 1526–1533. doi:10.1038/s41591-019-0582-4

Stoltzfus, A., and Norris, R. W. (2016). On the Causes of Evolutionary Transition: Transversion Bias. *Mol. Biol. Evol.* 33 (3), 595–602. doi:10.1093/molbev/msv274

Sun, H.-C., Zhu, X.-D., Zhou, J., Gao, Q., Shi, Y.-H., Ding, Z.-B., et al. (2020). Adjuvant Apatinib Treatment after Resection of Hepatocellular Carcinoma with portal Vein Tumor Thrombosis: a Phase II Trial. *Ann. Transl Med.* 8 (20), 1301. doi:10.21037/atm-20-6181

Takeda, M., Sakai, K., Terashima, M., Kaneda, H., Hayashi, H., Tanaka, K., et al. (2015). Clinical Application of Amplicon-Based Next-Generation Sequencing to Therapeutic Decision Making in Lung Cancer. *Ann. Oncol.* 26 (12), 2477–2482. doi:10.1093/annonc/mdv475

Tan, Q., Li, F., Wang, G., Xia, W., Li, Z., Niu, X., et al. (2016). Identification of FGF19 as a Prognostic Marker and Potential Driver Gene of Lung Squamous Cell Carcinomas in Chinese Smoking Patients. *Oncotarget* 7 (14), 18394–18402. doi:10.18632/oncotarget.7817

Taylor, J., Tyekucheva, S., Zody, M., Chiaromonte, F., and Makova, K. D. (2006). Strong and Weak Male Mutation Bias at Different Sites in the Primate Genomes: Insights from the Human-Chimpanzee Comparison. *Mol. Biol. Evol.* 23 (3), 565–573. doi:10.1093/molbev/msj060

Totoki, Y., Tatsuno, K., Covington, K. R., Ueda, H., Creighton, C. J., Kato, M., et al. (2014). Trans-ancestry Mutational Landscape of Hepatocellular Carcinoma Genomes. *Nat. Genet.* 46 (12), 1267–1273. doi:10.1038/ng.3126

Xu, J., Shen, J., Gu, S., Zhang, Y., Wu, L., Wu, J., et al. (2021). Camrelizumab in Combination with Apatinib in Patients with Advanced Hepatocellular Carcinoma (RESCUE): A Nonrandomized, Open-Label, Phase II Trial. *Clin. Cancer Res.* 27 (4), 1003–1011. doi:10.1158/1078-0432.CCR-20-2571

Xuan, J., Yu, Y., Qing, T., Guo, L., and Shi, L. (2013). Next-generation Sequencing in the Clinic: Promises and Challenges. *Cancer Lett.* 340 (2), 284–295. doi:10.1016/j.canlet.2012.11.025

Yang, B., Li, J., Li, F., Zhou, H., Shi, W., Shi, H., et al. (2019). Comprehensive Analysis of Age-related Somatic Mutation Profiles in Chinese Young Lung Adenocarcinoma Patients. *Cancer Med.* 8 (4), 1350–1358. doi:10.1002/cam4.1839

Yu, W.-C., Zhang, K.-Z., Chen, S.-G., and Liu, W.-F. (2018). Efficacy and Safety of Apatinib in Patients with Intermediate/advanced Hepatocellular Carcinoma. *Medicine (Baltimore)* 97 (3), e9704. doi:10.1097/MD.0000000000009704

Zhou, S.-L., Zhou, Z.-J., Hu, Z.-Q., Song, C.-L., Luo, Y.-J., Luo, C.-B., et al. (2019). Genomic Sequencing Identifies WNK2 as a Driver in Hepatocellular Carcinoma and a Risk Factor for Early Recurrence. *J. Hepatol.* 71 (6), 1152–1163. doi:10.1016/j.jhep.2019.07.014

Zhu, A. X., Finn, R. S., Edeline, J., Cattan, S., Ogasawara, S., Palmer, D., et al. (2018). Pembrolizumab in Patients with Advanced Hepatocellular Carcinoma Previously Treated with Sorafenib (KEYNOTE-224): a Non-randomised, Open-Label Phase 2 Trial. *Lancet Oncol.* 19 (7), 940–952. doi:10.1016/S1470-2045(18)30351-6

Conflict of Interest: The authors declare that the research was conducted in the absence of any commercial or financial relationships that could be construed as a potential conflict of interest.

Publisher's Note: All claims expressed in this article are solely those of the authors and do not necessarily represent those of their affiliated organizations, or those of the publisher, the editors, and the reviewers. Any product that may be evaluated in this article, or claim that may be made by its manufacturer, is not guaranteed or endorsed by the publisher.

frontiers in Molecular Biosciences

ORIGINAL RESEARCH
published: 24 January 2022
doi: 10.3389/fmolb.2022.814058

High Expression of Long Non-Coding RNA TMCO1-AS1 is Associated With Poor Prognosis of Hepatocellular Carcinoma

Xuelian Huang[1,2†], Sicong Zhu[1,3†], Kelin Zhang[3], Wenliang Tan[1,4], Yajin Chen[4] and Changzhen Shang[4*]*

[1]Guangdong Provincial Key Laboratory of Malignant Tumor Epigenetics and Gene Regulation, Sun Yat-sen Memorial Hospital, Sun Yat-sen University, Guangzhou, China, [2]Department of Anesthesiology, Sun Yat-sen Memorial Hospital, Sun Yat-sen University, Guangzhou, China, [3]Department of Surgical Intensive Care Unit, Sun Yat-sen Memorial Hospital, Sun Yat-sen University, Guangzhou, China, [4]Department of Hepatobiliary Surgery, Sun Yat-sen Memorial Hospital, Sun Yat-sen University, Guangzhou, China

OPEN ACCESS

Edited by:
Yu Guo,
The First Affiliated Hospital of Sun Yat-sen University, China

Reviewed by:
Zhanzhong Ma,
Yuebei People's Hospital, China
De-Hua Wu,
Southern Medical University, China

***Correspondence:**
Yajin Chen
cyj0509@126.com
Changzhen Shang
shangcz_sysu@163.com

[†]These authors have contributed equally to this work

Specialty section:
This article was submitted to Molecular Diagnostics and Therapeutics, a section of the journal Frontiers in Molecular Biosciences

Received: 12 November 2021
Accepted: 07 January 2022
Published: 24 January 2022

Citation:
Huang X, Zhu S, Zhang K, Tan W, Chen Y and Shang C (2022) High Expression of Long Non-Coding RNA TMCO1-AS1 is Associated With Poor Prognosis of Hepatocellular Carcinoma. Front. Mol. Biosci. 9:814058. doi: 10.3389/fmolb.2022.814058

Background: The molecular pathways along with the clinical significance of long non-coding RNAs (lncRNAs) in hepatocellular carcinoma (HCC) remain uncertain. Our study sought to identify and characterize lncRNAs associated with HCC.

Methods: LncRNA TMCO1-AS1 was identified by differential expression analysis, receiver operating characteristic (ROC) analysis, and univariate analysis using RNA sequencing and clinical information of HCC from the public database. Then clinical correlations and survival analysis were conducted to further appraise the prognostic significance of lncRNA TMCO1-AS1 in HCC. Hepatoma and adjoining normal tissues from 66 patients who received surgical operation at our center were used to verify the results of the bioinformatics analysis. A survival prognostic model was established combining TMCO1-AS1 expression and other clinical characteristics.

Results: Bioinformatics analysis showed the aberrant high expression of TMCO1-AS1 in HCC tissue. TMCO1-AS1 expression was positively correlated with alpha-fetoprotein (AFP) level, vascular invasion, tumor stage, as well as tumor differentiation. Moreover, survival analysis found a significant inverse association between the expression of TMCO1-AS1 and the survival of patients with HCC. Cox analysis indicated that TMCO1-AS1 was an independent factor for HCC prognosis. Analysis of the HCC tissues from patients at our center provided results similar to those of the bioinformatics analysis. Risk models for overall survival (OS) and recurrence-free survival (RFS) incorporating TMCO1-AS1 exhibited better sensitivity and specificity than using clinical characteristics alone.

Conclusion: High TMCO1-AS1 expression is significantly correlated with the unfavorable poor prognosis of HCC, indicating its potential of being a novel prognostic marker for HCC.

Keywords: long non-coding RNA, hepatocellular carcinoma, TMCO1-AS1, TCGA, prognosis

INTRODUCTION

Hepatocellular carcinoma (HCC) is generally acknowledged to be amongst the most prevalent digestive malignant tumors on a global scale. Recently, remarkable advancements have been achieved in the treatment of HCC patients, including local and systemic treatments, which have prolonged the survival of patients with HCC (Dhir et al., 2016; Reig et al., 2018). However, HCC is characterized by high invasiveness, metastasis, and frequent recurrence making the prognosis of patients with HCC far from satisfactory (Siegel et al., 2018). As such, identification of novel indicators or biomarkers of HCC may assist in the treatment of patients and help understand the underlying mechanisms of HCC.

Long non-coding RNA (lncRNA) are comprised of RNA transcripts whose length exceed 200 nucleotides but lack identifiable open reading frames. Growing studies have confirmed that lncRNAs participate in the proliferation, differentiation, apoptosis, and metastasis of many human cancers (Gibb et al., 2011; Bhan et al., 2017). In addition, the current relative study reveals that lncRNAs could act as tumor suppressor genes or oncogenes, thus exerting extensive and complicated roles in the regulation of the occurrence and progression of tumors (Maruyama and Suzuki, 2012). With advances in microarray technology and high-throughput RNA sequencing, numbers of dysregulated and expressed lncRNAs that participate in various processes of HCC have been identified (Da Sacco et al., 2012; Klingenberg et al., 2017). For example, lncRNA HOTTIP is shown to be implicated in the tumorigenesis and metastasis of HCC, and its overexpression predicts a poor outcome (Quagliata et al., 2014; Tsang et al., 2015). The lncRNA MATAL1, which is abnormally upregulated in HCC tissues, promotes the progression of HCC by suppressing ZEB1 expression *via* regulating miR-143-3p (Chen et al., 2017). MEG3 was the first lncRNA identified to function as a tumor suppressor gene; it interacts with P53 to inhibit tumor proliferation and its expression in HCC is low (Braconi et al., 2011). However, although many lncRNAs have been identified the biological functions of most remain unknown.

In this study, a novel lncRNA TMCO1-AS1 with aberrant expression in HCC was identified through bioinformatics analysis. The value of TMCO1-AS1 in HCC diagnosis and prognosis was evaluated by analyzing the gene expression matrix of The Cancer Genome Atlas (TCGA), and TMCO1-AS1 expression was demonstrated to be negatively correlated with survival of HCC patients. Furthermore, the data of HCC patients treated at our center was used to confirm the results of the bioinformatics analysis, and a prognostic model was built to improve the accuracy of prognosis prediction of HCC patients. Overall, our data indicate that lncRNA TMCO1-AS1 could serve as a promising novel prognostic marker for HCC.

MATERIALS AND METHODS

Data Sources

The gene expression matrix (TPM format) of liver cancer was acquired by data download from TCGA (https://cancergenome.nih.gov/) using the R programming language (r-project.org). RNA sequencing (RNA-seq) data of 377 hepatoma tissues as well as 50 adjoining normal tissues from 377 patients were obtained and normalized into $\log_2$(TPM+1). In addition, the clinical data of the 377 patients were acquired as well. Patients with incomplete clinical and survival data were excluded. At last, a total of 314 patients with 364 tissue samples (314 hepatoma tissues and 50 adjoining normal tissues) were incorporated in the present research.

Differential Expression Analysis

RNA-seq data were compared between 50 pairs of hepatoma tissues and corresponding adjacent tissues to identify the differentially expressed lncRNAs (DElncRNAs) using the "limma" package of R. False discovery rated (FDR) method was utilized for the purpose of adjusting the p values for several tests. The fold-change (FC) values of each lncRNA were calculated. A lncRNA was considered to have a significant differential expression when $\log_2|FC| > 1.0$ and $p < .05$.

Evaluation of the Prognostic and Diagnostic Significance of Differentially Expressed lncRNAs for Hepatocellular Carcinoma

The expression profiles of the DElncRNAs were acquired, and in combination with survival prognostic information, their prognostic values were evaluated. Univariate regression was used to investigate if the expression levels of DElncRNAs were closely related to overall survival (OS) and recurrence-free survival (RFS). Receiver operating characteristic (ROC) analysis was conducted to evaluate the sensitivity and specificity of the DElncRNAs in diagnosing HCC. The following were the parameters that determine the area under the ROC curve (AUC): .5–.7, poor evidence for diagnosis; >.7–.9, moderate evidence for diagnosis; >.9–1.0, high-quality diagnostic evidence; >.7–.9, moderate-quality diagnostic evidence; .5–.7, poor -quality diagnostic evidence.

Establishment of a Prognostic Model for Hepatocellular Carcinoma Survival

A risk model for anticipating the outcome of patients with HCC was constructed by combining DElncRNA expressions and patient clinicopathological characteristics. The necessary minimum number of clinicopathological characteristics were used to establish the model through least absolute shrinkage and selection operator) (LASSO) regression analysis, and the regression coefficients of each prognostic factor were calculated. Clinical characteristics scores were defined as 1 or 0 in accordance with different clinicopathological features. Utilizing equation as follows, we successfully calculated the risk score: Risk score = Exp $\times C_{DElncRNA} + S_1 \times C_1 + S_2 \times C_2 + \ldots + S_N \times C_N$ ("Exp" means the expression quantity of the DElncRNA, "C" denotes the regression coefficient calculated by Lasso analysis, and "S" refers to the clinical characteristics scores). The median risk score was defined as a cutoff, and the patients were stratified into 2 groups with different risk levels. The comparison of OS and RFS was made

between the grouped patients to evaluate the predictive ability of the models.

Tissue Sample Collection

Hepatoma and corresponding adjacent normal tissues were acquired from 66 HCC patients who received surgical interventions at Sun Yat-sen Memorial Hospital, Sun Yat-sen University (Guangzhou, China) from 2015 to 2018. All patients had given informed consent for the collection of tissue samples for research purposes. Hepatocellular carcinoma was diagnosed for each patient by pathological examination of the operation samples. Preoperatively, none of the patients underwent any type of treatment before surgery (e.g., received radiotherapy, chemotherapy, immunotherapy). Normal tissues that were adjoining to the malignant tumor were obtained at a distance of 2.0 cm. Liquid nitrogen was used to preserve all of the samples from the surgery. At least 2 years of follow-up was required for each patient.

Isolation of RNA and Quantitative Reverse Transcription-Polymerase Chain Reaction

Trizol (Takera, Japan) was utilized for the purpose of performing the isolation of the total RNA. Reverse transcription was conducted using A PrimeScript RT reagent Kit (Takara, Japan) was utilized for reverse-transcribing the isolated RNA, whereas SYBR Premix Ex Taq (Takara, Japan) was employed in cDNA amplification. PCR was performed on a CFX96 system (BIO-RAD, USA) at the temperature for 30 s at 95°C, followed by 40 cycles at 95°C for 5 s and 60°C for 20 s. Internal controls were implemented using GAPDH. The relative expression of TMCO1-AS1 was determined utilizing the $2^{-\Delta\Delta CT}$ method. The primers had the following sequences: TMCO1-AS1 forward: 5′-GTTTAGCTTGGGTTTGCCGT -3′, reverse: 5′- AGCGGCCCA CAACTAACTC -3′; GAPDH forward: 5′- CCAGAACATCAT CCCTGCCT -3′, reverse: 5′- CCTGCTTCACCACCTTCTTG -3′.

Statistical Analysis

Continuous variables were compared by one-way analysis of variance (ANOVA) or two-sided Student's t-test, as deemed necessary, whereas comparisons of categorical variables were performed by Chi-square test. The log-rank test, as well as the landmark analysis, were employed to contrast Kaplan–Meier curves. Univariable and multivariable analyses were conducted based on the Cox regression method. We conducted the receiver operating characteristic (ROC) analysis to examine the prediction capacity of the lncRNAs. All statistical analyses were implemented using SPSS (IBM Corporation). The volcano plot and heatmap were charted and analyzed utilizing ImageGP (http://www.ehbio.com/ImageGP/index.php). Differential expression analysis was performed using the "limma" package of R. LASSO analysis was conducted using the "glmnet" R package, and time-dependent ROC curves were drawn with the "survivalROC" R package. Statistical significance was judged to have been attained when $p < .05$.

RESULTS

The Cancer Genome Atlas Database Analysis of lncRNAs Differentially Expressed Between Hepatocellular Carcinoma and Adjacent Tissue

With the criteria of $\log_2|FC| > 1.0$ and $p < .05$, 1,304 DElncRNAs were identified with 1,111 upregulated and 193 downregulated. **Figure 1A** showed the volcano plot of the DElncRNAs which was plotted based on differential expression analysis. The expression profiles of the top 100 DElncRNAs (81 up-regulated and 19 downregulate; **Supplementary Table S1**) were illustrated using a heatmap (**Figure 1B**). Based on DElncRNA patterns, tumor tissue could be distinguished from normal tissue.

Diagnostic and Prognostic Value of Differentially Expressed lncRNAs

Univariate analysis was performed for OS and RFS to determine whether a DElncRNA was substantially correlated with HCC patients' prognosis. With $p < .05$, 31 DElncRNAs were detected to be significantly correlated to OS, and 35 DElncRNAs were significantly correlated to RFS (**Supplementary Table S2**). Among them, there was a significant difference of OS and RFS associated with 15 DElncRNAs (DUXAP8, DDX11-AS1, TMCO1-AS1, ZNF252P-AS1, AC091057.1, TM4SF19-AS1, HCG25, RP11-98G7.1, SNHG4, AC012313.8, TMCC1-AS1, ZFPM2-AS1, AL357079.1, LINC02709, and AC099850.4), suggesting they have remarkable prognostic value for HCC patients.

ROC analysis was performed on the 15 DElncRNAs to detect whether the DElncRNA could serve as a biomarker to distinguish HCC tissue from adjacent normal tissue. Of the 15 DElncRNAs, 5 (DDX11-AS1, TMCO1-AS1, ZNF252P-AS1, HCG25, and TMCC1-AS1) exhibited an AUC > .9 (**Figure 1C**). These results indicate that the 5 DElncRNAs, which are all up-regulated in HCC, have marked diagnostic potential for HCC.

For further study, we selected lncRNA TMCO1-AS1 which has not been reported to be associated with HCC before.

Expression and Clinical Correlation of TMCO1-AS1 in Hepatocellular Carcinoma

The expression of TMCO1-AS1 between 314 hepatoma tissues and 50 adjoining normal tissues from TCGA was compared. **Figure 2A** illustrates that TMCO1-AS1 expression in HCC tissues was obviously elevated in contrast with that in adjacent tissues ($p < .0001$). Median expression of TMCO1-AS1 was defined as a threshold point to classify the 314 HCC patients into low- and high-expression groups, and patient clinical data of the two groups were analyzed. Correlation analysis demonstrated that TMCO1-AS1 expression was considerably related to alpha-fetoprotein (AFP) level ($p = .0029$), vascular invasion ($p = .0014$), TNM stage ($p = .0182$) and tumor differentiation ($p = .0016$) (**Table 1**). The expression of TMCO1-AS1 in patients whose levels of AFP were >400 μg/L was substantially higher in contrast

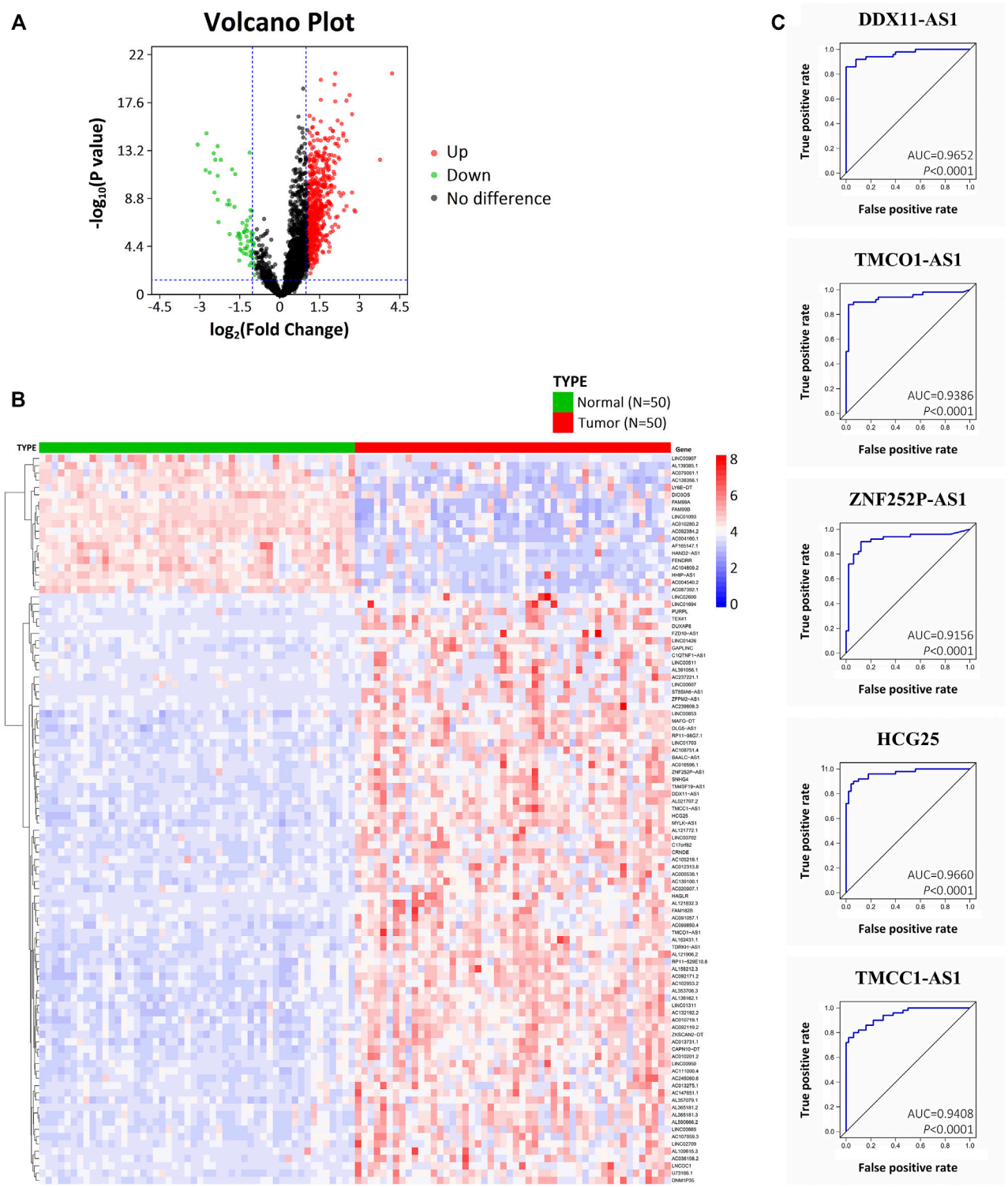

FIGURE 1 | Differentially expressed lncRNAs in HCC based on bioinformatics analysis of TCGA. **(A)** Volcano plot illustrating the DElncRNAs between HCC tissues and adjacent normal tissues. **(B)** Heatmap showing the hierarchical clustering of the top 100 DElncRNAs. **(C)** ROC curves of five DElncRNAs (DDX11-AS1, TMCO1-AS1, ZNF252P-AS1, HCG25, TMCC1-AS1) with an AUC > .9.

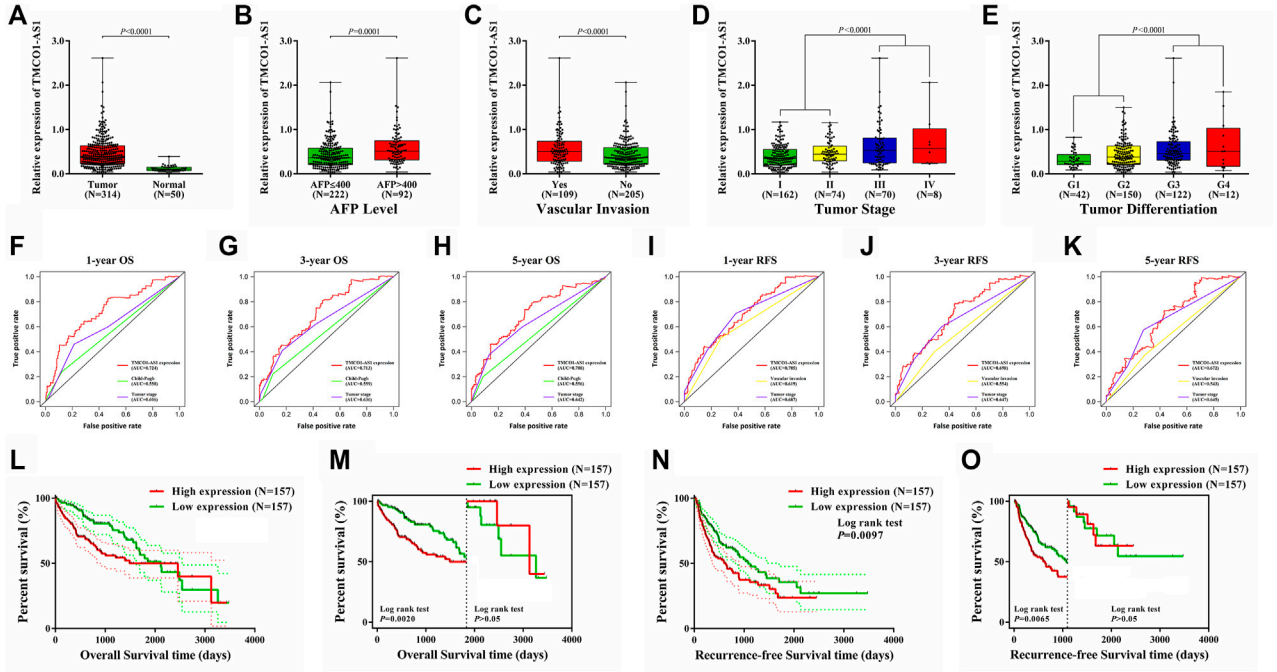

FIGURE 2 | Dysregulation of TMCO1-AS1 in HCC and its prognostic significance for HCC using data of patients from TCGA. **(A)** The expression levels of TMCO1-AS1 in HCC and adjacent normal tissues. **(B)** TMCO1-AS1 expression in patients with high (AFP >400 μg/L) and low (AFP ≤400 μg/L) serum AFP levels. **(C)** TMCO1-AS1 expression in patients with and without vascular invasion. **(D)** TMCO1-AS1 expression in patients with different tumor stages. **(E)** TMCO1-AS1 expression in patients with different degrees of tumor differentiation. **(F–H)** Time-dependent ROC curves of the relations of clinical characteristics and 1-/3-/5-year OS. **(I–K)** Time-dependent ROC curves of the relations of clinical characteristics and 1-/3-/5-year RFS. **(L)** Kaplan-Meier curves for OS of HCC patients from TCGA with high and low TMCO1-AS1 expression. **(M)** Landmark analysis discriminating between OS before and after 5 years of follow-up. **(N)** Kaplan-Meier curves for RFS of HCC patients from TCGA with high and low TMCO1-AS1 expression. **(O)** Landmark analysis discriminating between RFS before and after 3 years of follow-up.

with patients whose levels of AFP were ≤400 μg/L (**Figure 2B**). Patients with vascular invasion had greater expression of TMCO1-AS1 than in HCC tissues compared to those without vascular invasion (**Figure 2C**). High expression of TMCO1-AS1 in HCC tissues was positively related to an advanced stage and poor differentiation (**Figures 2D,E**). However, TMCO1-AS1 expression had no associations with other features, for example, age, sex, race, virus hepatitis, alcoholic hepatitis, Child-Pugh classification, and cirrhosis (all, $p > .05$).

Relations Between TMCO1-AS1 Expression and Hepatocellular Carcinoma Prognosis Using The Cancer Genome Atlas

Cox analysis was conducted to appraise the value of TMCO1-AS1 for HCC prognosis. Univariate regression analysis showed that hepatitis virus infection ($p = .0351$), Child-Pugh score ($p = .0153$), tumor stage ($p < .0001$) and the levels of TMCO1-AS1 expression ($p = .0079$) were considerably correlated with OS. Moreover, vascular invasion ($p = .0013$), tumor stage ($p < .0001$) and TMCO1-AS1 expression ($p = .0103$) were significantly associated with RFS (**Supplementary Table S3**). Multivariate regression analysis indicated that TMCO1-AS1 independently acted as a predictive marker of HCC prognosis (**Supplementary Table S4**).

Time-dependent ROC analysis was performed to compare the prediction values of the prognostic parameters determined through the Cox analysis. The time-dependent ROC curves of 1-year OS for TMCO1-AS1 expression, Child-Pugh score, and tumor stage are shown in **Figure 2F**. The AUC for TMCO1-AS1 expression was .724, and the AUC for tumor stage and Child-Pugh score were .606 and .558. The AUC of 3-year OS for TMCO1-AS1, tumor stage and Child-Pugh score were .713, .636, and .559, respectively (**Figure 2G**). The AUC of 5-year OS was .708, which was larger than that for Child-Pugh score and tumor stage (**Figure 2H**). Thus, of the three factors TMCO1-AS1 exhibited the best ability to predict OS of patients with HCC. Similarly, the time-dependent ROC curves of 1-year RFS for TMCO1-AS1 expression, tumor stage and vascular invasion are displayed in **Figure 2I**. The AUC for TMCO1-AS1 expression was .705, and that for tumor stage and vascular invasion were .687 and .619, respectively. The AUC of 3-/5-year RFS for TMCO1-AS1 was larger than that for tumor stage and vascular invasion (**Figures 2J,K**). Thus, of the three factors TMCO1-AS1 exhibited the best ability to predict RFS of HCC patients.

Kaplan-Meier curves were drawn to analyze OS and RFS between HCC patients exhibiting low and high TMCO1-AS1 expression. In patients exhibiting elevated TMCO1-AS1 expression, the median OS time was 1,490 days, whereas in patients having low TMCO1-AS1 expression, their median OS

TABLE 1 | Relationship between the expression levels of TMCO1-AS1 and clinicopathological characteristics in 314 HCC patients from TCGA.

Clinicopathological characteristics		TMCO1-AS1 expression		χ^2	*p* value
		Low (*N* = 157)	High (*N* = 157)		
Age (years)	≤60	70	75	.320	.5714
	>60	87	82		
Gender	Male	111	95	3.613	.0573
	Female	46	62		
Race	Yellow	69	68	.099	.9519
	White	80	82		
	Black	8	7		
AFP (μg/L)	≤400	123	99	8.855	.0029[a]
	>400	34	58		
Hepatitis virus infection	Yes	70	83	2.154	.1422
	No	87	74		
Alcoholic hepatitis	Yes	56	46	1.452	.2282
	No	101	111		
Child-Pugh	A	138	132	.952	.6213
	B	16	21		
	C	3	4		
Cirrhosis	Yes	57	64	.659	.4170
	No	100	93		
Vascular invasion	Yes	41	68	10.244	.0014[a]
	No	116	89		
Tumor stage	I	95	67	10.045	.0182[a]
	II	30	44		
	III	29	41		
	IV	3	5		
Tumor differentiation	G1	31	11	15.334	.0016[a]
	G2	78	72		
	G3	43	67		
	G4	5	7		

[a]p < .05.

time was 2,116 days (**Figure 2L**). **Figure 2M** showed a landmark analysis of OS before and after 5 years of follow-up. Within 5 years, patients in the high TMCO1-AS1 expression group exhibited obviously shortened OS time as opposed to patients in the low TMCO1-AS1 expression group ($p = .0020$). While after 5 years, no statistical differences were discovered between the OS of the two groups ($p > .05$). Patients having elevated TMCO1-AS1 expression had significantly shorter median RFS time compared to those with low TMCO1-AS1 expression (**Figure 2N**). Landmark analysis revealed the discrimination between tumor recurring before and after 3 years of follow-up, and a significant difference of RFS within 3 years was detected between patients exhibited low and high expression of TMCO1-AS1 (**Figure 2O**). Survival analysis showed that TMCO1-AS1 had a certain value in the prediction of HCC prognosis, especially for the early-term survival.

We especially carried out a subgroup analysis to thoroughly examine the prognostic significance of TMCO1-AS1 for HCC patients with different clinical characteristics. In accordance with the clinical characteristics including serum AFP level, tumor stage, liver cirrhosis and hepatitis virus infection, the patients with HCC obtained from TCGA were classified into various groups. Kaplan-Meier analysis indicated there was a statistical difference in OS and RFS of the patients classified under the group having the level of AFP as ≤400 μg/L (**Figure 3A**) in contrast with those having AFP > 400 μg/L (**Figure 3B**). In addition, statistical differences in OS and RFS were found between patients with and without cirrhosis (**Figures 3C,D**), patients with early-stage or advanced-stage disease (**Figures 3E,F**), and those with and without viral hepatitis (**Figures 3G,H**).

Correlation of Clinical Variables and Survival Analyses of Patients at Our Center

The expression of TMCO1-AS1 was detected in 66 paired samples of hepatoma and adjoining normal tissues from patients at our center that received surgery. **Figure 4A** depicted that the levels of TMCO1-AS1 expression were significantly increased in 74% of HCC tissues (49/66) in contrast with the matching adjoining normal tissues.

Correlation analysis using data from the patients treated at our center showed that serum AFP level ($p < .0001$), vascular invasion ($p = .0367$), tumor stage ($p = .0267$), and differentiation ($p = .0138$) were significantly associated with TMCO1-AS1 expression (**Table 2**). Furthermore, patients having an elevated AFP level and vascular invasion had a high expression level of TMCO1-AS1 in tumor tissue (**Figures 4B,C**). And TMCO1-AS1 was overexpressed in tumor tissue of patients with advanced tumor stage and attenuated tumor differentiation (**Figures 4D,E**). All patients from our center were followed up for more than

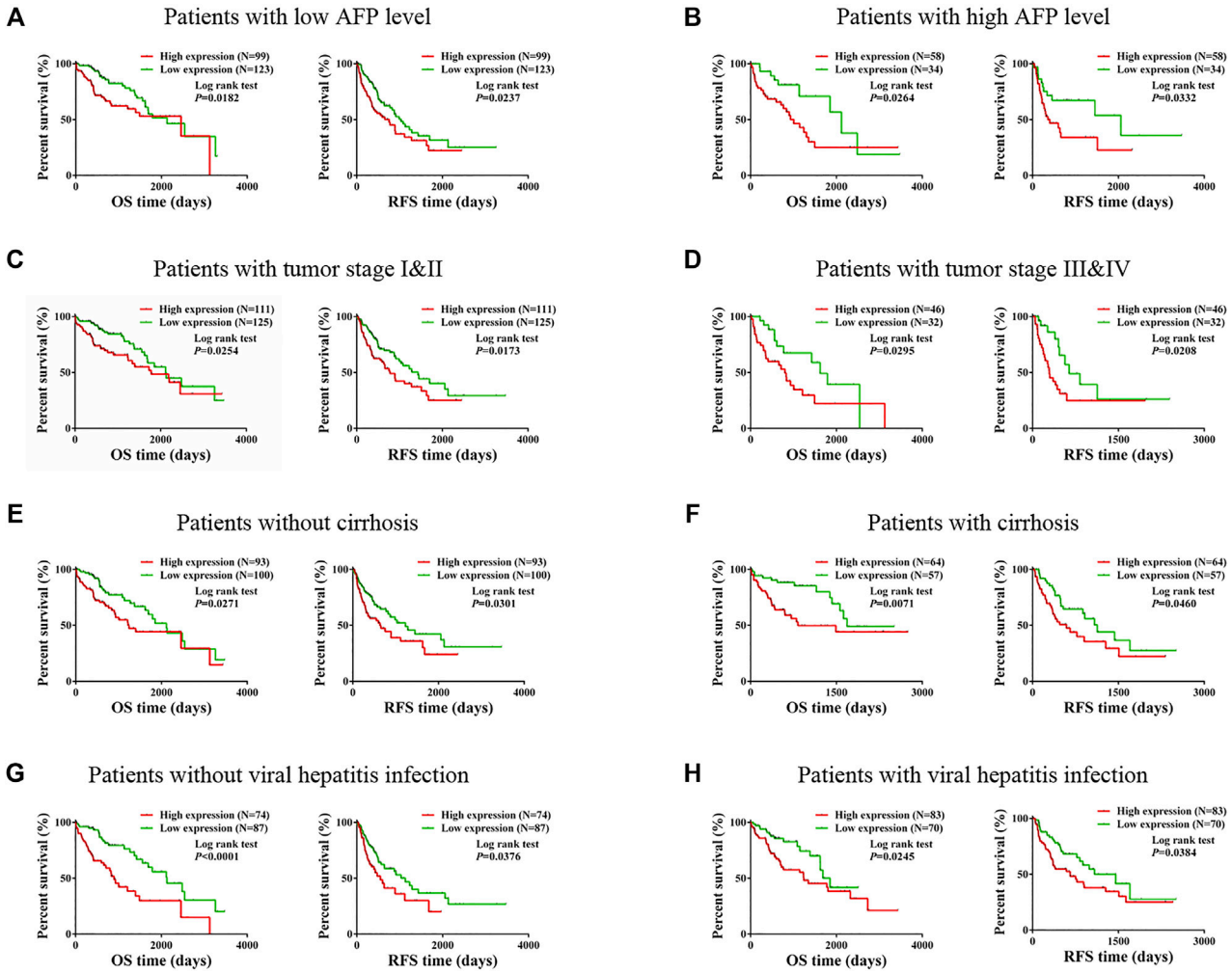

FIGURE 3 | Prognostic value of TMCO1-AS1 expression in HCC patients with different characteristics. **(A)** Survival curves for OS and RFS of patients with AFP ≤400 μg/L. **(B)** Survival curves for OS and RFS of patients with AFP >400 μg/L. **(C)** Survival curves for OS and RFS of patients with tumor stage I-II. **(D)** Survival curves for OS and RFS of patients with tumor stage III-IV. **(E)** Survival curves for OS and RFS of patients without cirrhosis. **(F)** Survival curves for OS and RFS of patients with cirrhosis. **(G)** Survival curves for OS and RFS of patients without viral hepatitis infection. **(H)** Survival curves for OS and RFS of patients with viral hepatitis infection.

2 years. Kaplan-Meier analysis illustrated that OS and RFS of patients exhibiting elevated TMCO1-AS1 expression were obviously shortened as opposed to that of patients exhibiting low TMCO1-AS1 expression, which were in line with the findings from bioinformatics in TCGA (**Figures 4F,G**).

Construction of Risk Score System for Hepatocellular Carcinoma

Data of 314 HCC patients from TCGA were used to build a model for predicting OS and RFS. The clinical characteristics score of 1 was assigned to the features of age >60 years, male, Child-Pugh class B/C, liver cirrhosis, serum AFP >400 μg/L, vascular invasion, tumor stage III–IV, and tumor grade 3–4. The score of 0 was assigned to age ≤60 years, female, Child-Pugh class A, no cirrhosis, serum AFP ≤400 μg/L, no vascular invasion, tumor stage I–II, and tumor grade 1–2. Using Lasso analysis, risk prognostic models were established for OS and RFS by combining the expression of TMCO1-AS1 and three clinical characteristics. The risk scores of all patients from TCGA were calculated using the following formula: Risk score = $.9066 \times \mathrm{Exp}_{\mathrm{TMCO1\text{-}AS1}} + .1207 \times \mathrm{S}_{\mathrm{AFP}} + .2787 \times \mathrm{S}_{\mathrm{Child}} + .0882 \times \mathrm{S}_{\mathrm{Cirrhosis}} + .6105 \times \mathrm{S}_{\mathrm{Stage}}$ (S is the score [0 or 1] of the subscripted variable and Exp is the expression of the lncRNA). Patients were classified into low- and high-risk groups according to their median value risk scores. As shown in **Figure 5A**, TMCO1-AS1 expression exhibited a positively association with the risk score. Moreover, the OS and RFS of the high-risk group patients were poorer in contrast with that of the low-risk group patients. Based on the risk model, a larger proportion of patients with high serum AFP, Child-Pugh class B/C, liver cirrhosis, and advanced tumor stage were defined as high-risk (**Figure 5B**). Kaplan-Meier analysis demonstrated that the median OS of high-risk patients (1,397 days) was substantially shortened in contrast with that

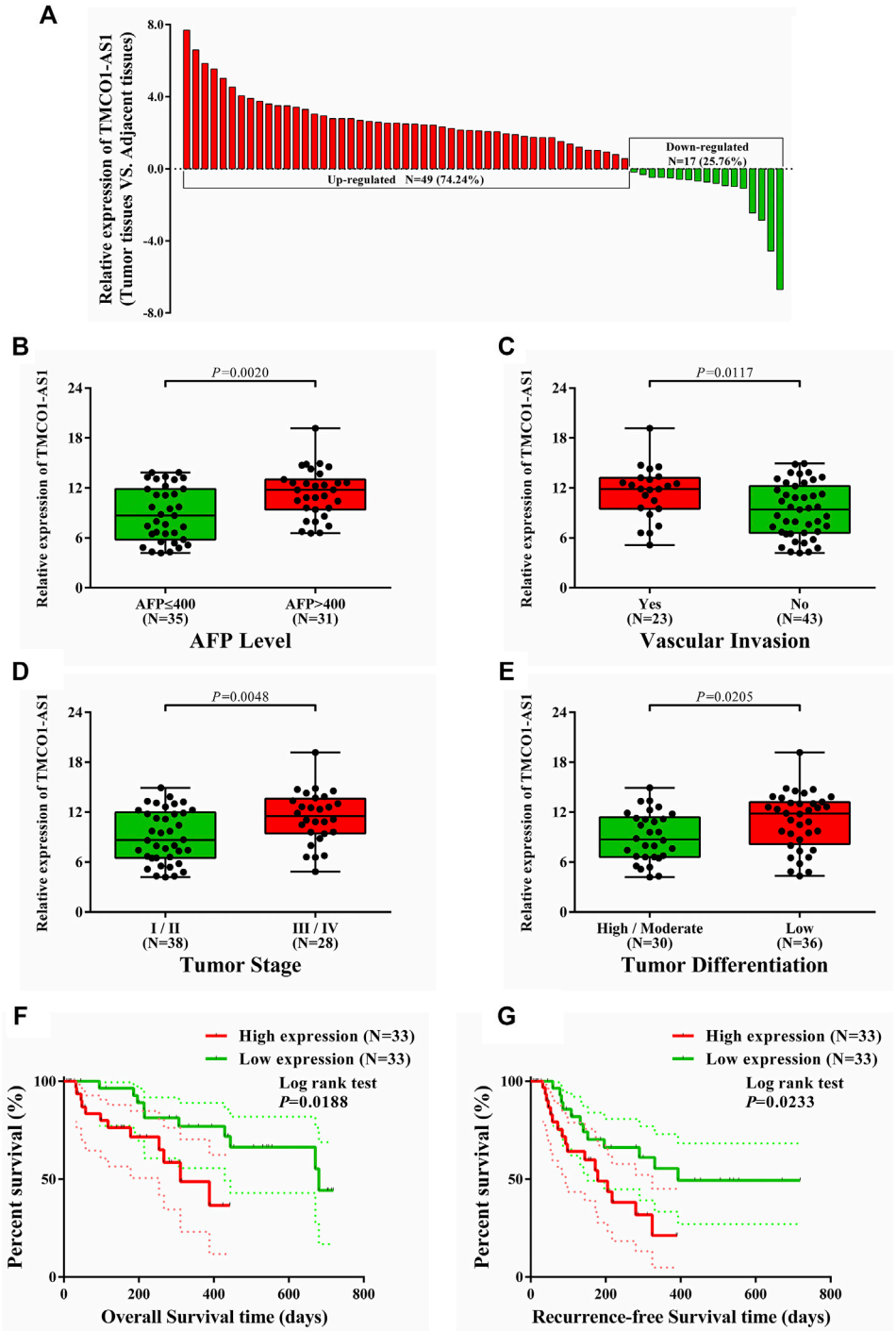

FIGURE 4 | Relations between TMCO1-AS1 expression and clinical characteristics of HCC patients treated at our center. **(A)** Relative expression of TMCO1-AS1 in 66 HCC and adjacent normal tissues. **(B)** TMCO1-AS1 expression in patients with high and low serum AFP levels. **(C)** TMCO1-AS1 expression in patients with and without vascular invasion. **(D)** TMCO1-AS1 expression in patients with different tumor stages. **(E)** TMCO1-AS1 expression in patients with different degrees of tumor differentiation. **(F)** Kaplan-Meier curves for OS of patients with high and low TMCO1-AS1 expression. **(G)** Kaplan-Meier curves for RFS of patients with high and low TMCO1-AS1 expression.

of low-risk patients (2,486 days) (**Figures 5C,D**). The time-dependent AUC of the risk model' OS for 1-/3-/5-year was .815, .801, and .788, respectively, which was larger than the 1-/3-/5-year AUC for TMCO1-AS1 expression, Child-Pugh class, and tumor stage. Comparable findings were observed when RFS was analyzed; the high-risk group patients exhibited considerably

TABLE 2 | Relationship between the expression levels of TMCO1-AS1 and clinicopathological characteristics in 66 HCC patients from our center.

Clinicopathological characteristics		TMCO1-AS1 expression		χ^2	*p* value
		Low (*N* = 33)	High (*N* = 33)		
Age(years)	≤60	20	22	.262	.6088
	>60	13	11		
Gender	Male	28	29	.129	.7198
	Female	5	4		
AFP (μg/L)	≤400	22	13	4.927	.0264[a]
	>400	11	20		
Hepatitis virus infection	Yes	27	26	.096	.7569
	No	6	7		
Alcoholic hepatitis	Yes	13	10	.601	.4383
	No	20	23		
Child-Pugh	A	32	31	.349	.5546
	B/C	1	2		
Cirrhosis	Yes	17	16	.061	.8055
	No	16	17		
Tumor size (cm)	≤5	9	12	.629	.4279
	>5	24	21		
Vascular invasion	Yes	7	16	5.405	.0201[a]
	No	26	17		
Tumor stage	I/II	24	14	6.203	.0128[a]
	III/IV	9	19		
Tumor differentiation	High/Moderate	19	11	3.911	.0480[a]
	Low	14	22		

[a]p < .05.

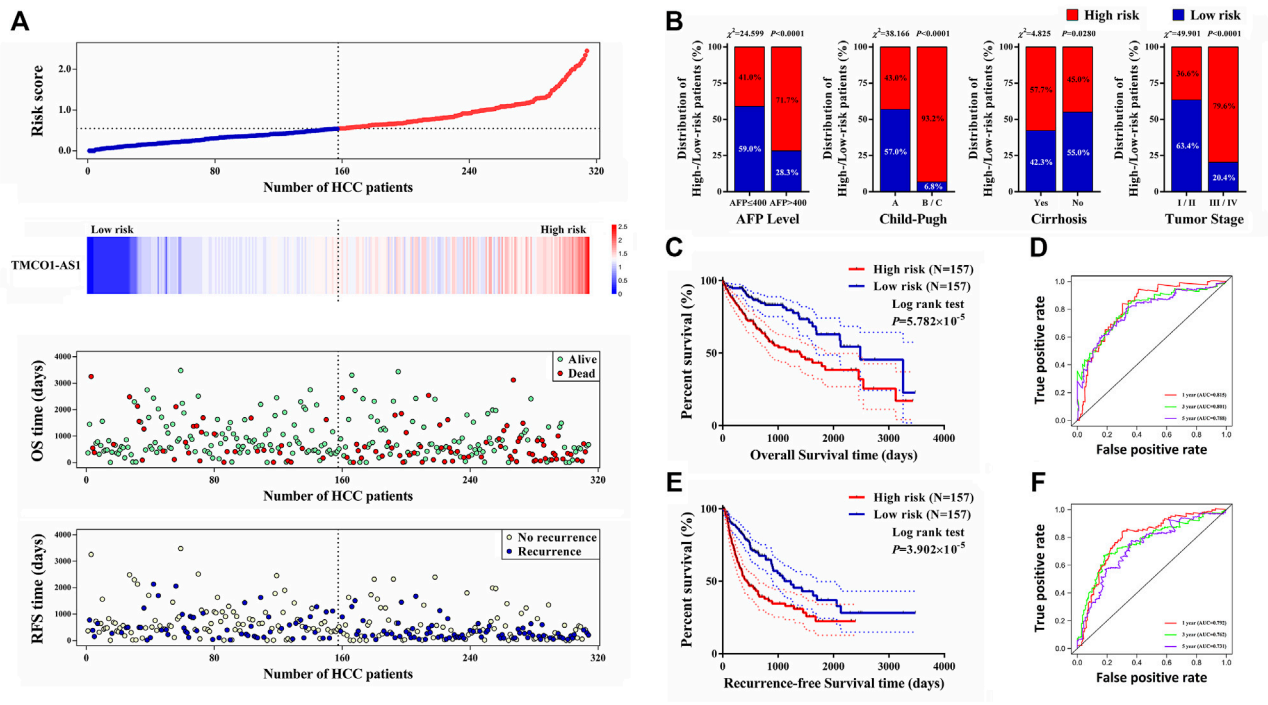

FIGURE 5 | A prognostic model for OS and RFS of HCC patients from TCGA. **(A)** Risk score distribution, TMCO1-AS1 expression, and OS and RFS of patients in the high- and low-risk group. **(B)** Comparison of the distributions of patients with different characteristics in the high- and low-risk groups. **(C)** Kaplan-Meier OS curves for patients in the high- and low-risk groups. **(D)** Time-dependence ROC curves of the risk score for OS. **(E)** Kaplan-Meier RFS curves for patients in the high- and low-risk groups. **(F)** Time-dependence ROC curves of the risk score for RFS.

shortened RFS in contrast with the low-risk group patients (**Figure 5E**). The AUC 1-/3-/5-year RFS for the risk score was .792, .762, and .731, suggesting a good predictive value of the model (**Figure 5F**). For both OS and RFS, the risk model exhibited better sensitivity and specificity for the prediction than any single clinical feature. The clinical data and expression profiles of 66 HCC patients from our center was utilized to further verify the prediction ability of the risk model in HCC prognosis, and the results were similar to those obtained by analyzing data from TCGA (**Supplementary Figure S1**).

DISCUSSION

Hepatocellular carcinoma is the seventh most frequent malignant tumor and has been ranked as the third major contributor to cancer-associated fatalities globally (Bray et al., 2018). Although recent developments of locoregional and molecular targeted therapies have been reported to provide a survival benefit, surgery is still a curative option (Kudo, 2018; Raoul et al., 2018; Raoul et al., 2019). However, because of a lack of obvious symptoms a considerable proportion of patients received their diagnosis at an advanced stage resulting in a poor prognosis (Fan, 2012). Moreover, the postoperative recurrence rate of patients who undergo liver resection is as high as 70% (Llovet et al., 2005). Thus, early diagnosis and prognostic markers are important in the treatment of HCC, as is timely following-up after surgery.

Alpha-fetoprotein is a traditional cancer biomarker that is used to monitor HCC treatment and recurrence; however, 35–45% of HCC patients have low serum AFP levels (<20 μg/L) (Sherman et al., 1995; Cedrone et al., 2000; Trevisani et al., 2001). Conventional prognostic systems such as Barcelona Clinic Liver Cancer (BCLC) stage and TNM classification are valuable in the prediction of HCC patients' survival status (Imai et al., 2014; Lee et al., 2014). However, HCC patients with the same BCLC stage or TNM classification may have different outcomes, illustrating the limitations of these systems for patients with HCC.

Tumorigenesis is commonly the result of the abnormal expression of a specific gene of genomes. Currently, lncRNAs are an active area of research because their expression is frequently dysregulated in cancers and their biological function may be oncogenic and tumor suppressor activity. Thus, the possibility that lncRNAs can serve as diagnostic and prognostic biomarkers has attracted increasing attention (Wang and Tran, 2013). A growing number of lncRNAs are demonstrated to play major parts in the process of HCC tumorigenesis. For instance, the plasma level of lncRNA HULC (highly upregulated in liver cancer) has been reported to be useful for HCC diagnosis and prognosis (Xie et al., 2013). Urothelial carcinoma associated-1 (UCA1) has an indispensable proliferation-related role in HCC *via* the Hippo signaling pathway, and it has been shown to be useful for predicting the prognosis (Qin et al., 2018). A lncRNA down-regulated in liver cancer stem cells (lncDILC) has been shown to interfere with NF-κB-mediated IL-6 expression *via* inhibiting STAT3 signaling, and thus has prognostic value for patients with HCC (Wang et al., 2016).

Bioinformatics analysis is an accurate and effective method to explore the functionality of genes in certain diseases, especially in malignancies. Increasing numbers of lncRNAs with an aberrant expression that are involved in HCC development and progression are being identified. In our study, DElncRNAs were distinguished and screened by differential expression analysis using the expression profiles of HCC tissues from TCGA. Subsequently, we identified five DElncRNAs with significant diagnostic and prognostic value in HCC. Among the five DElncRNAs, four have recently been shown to perform a function in the onset and progression of HCC. The lncRNA DDX11-AS1 suppresses the LATS2 protein *via* interacting with EZH2 and DNMT1 in HCC cells and may function as an oncogene, and the expression of DDX11-AS1 is correlated with a poor HCC prognosis (Li et al., 2019). The lncRNA ZNF252P-AS1 has been shown to be significantly associated with patients' OS with hepatitis B virus (HBV)-related HCC (Zhao et al., 2020). The lncRNA HCG25 is aberrantly expressed in HCC tissue, and has a significant diagnostic value for HCC (Shi et al., 2018). Prior studies have reported that TMCC1-AS1 is related to autophagy, and its expression is negatively correlated with HCC prognosis (Cui et al., 2017; Zhao et al., 2018; Deng et al., 2020).

TMCO1-AS1, also referred to as RP11-466F5.8 or ENSG00000224358, is antisense RNA located on chromosome 1 with a length of 2,148 bp. In our study, we identified this novel lncRNA, which has not been previously reported associated with HCC, *via* bioinformatics analysis. TMCO1-AS1 was found to be significantly overexpressed in HCC tissues, ROC analysis showed an excellent prognostic value for HCC, and survival analysis revealed that TMCO1-AS1 expression was inversely correlated with OS and RFS of HCC patients. TMCO1-AS1 was shown to independently serve as a risk factor for HCC, and it had a better prognostic value than other clinical features such as Child-Pugh class, cirrhosis, vascular invasion, and tumor stage.

In this study, we also developed a novel risk model for predicting OS and RFS using TMCO1-AS1 expression and other clinical characteristics. OS and RFS differed considerably between the low- and high-risk group patients, and the prognostic value for OS and RFS was verified by time-dependent ROC analysis. Moreover, the prediction ability of the constructed risk model was shown to be better than that of other clinical features, and thus may serve as a novel method for establishing the prognosis for the patients with HCC. Notably, TMCO1-AS1 expression was positively related to the HCC risk score. Overall, our findings indicated that TMCO1-AS1 is involved in the occurrence and progression of HCC and influences patients' prognosis. However, the exact biological function and molecular mechanism of TMCO1-AS1 require further study.

CONCLUSION

In summary, we identified a novel lncRNA, TMCO1-AS1, in HCC. High expression of TMCO1-AS1 in HCC tissues was correlated with poorer OS and RFS. Thus, the lncRNA

TMCO1-AS1 could serve as a valuable prognostic marker for HCC patients.

DATA AVAILABILITY STATEMENT

The original contributions presented in the study are included in the article/**Supplementary Material**, further inquiries can be directed to the corresponding authors.

ETHICS STATEMENT

The studies involving human participants were reviewed and approved by the Ethics Committee of Sun Yat-sen Memorial Hospital, Sun Yat-sen University. The patients/participants provided their written informed consent to participate in this study.

AUTHOR CONTRIBUTIONS

CS and YC conceived and designed the experiments; XH and SZ performed the experiments and wrote the manuscript; KZ and WT contributed data analysis and revised the manuscript. All authors read and approved the final manuscript.

FUNDING

This work was supported by grants from the National Natural Science Foundation of China (No. 82072714; No. 81972263) and Guangdong Provincial Clinical Research Center for Digestive Disease (No. 2020B1111170004).

ACKNOWLEDGMENTS

We acknowledge TCGA database for providing the platforms and contributors for uploading their meaningful datasets.

SUPPLEMENTARY MATERIAL

The Supplementary Material for this article can be found online at: https://www.frontiersin.org/articles/10.3389/fmolb.2022.814058/full#supplementary-material

Supplementary Figure 1 | A prognostic model for OS and RFS of HCC patients from our center. **(A)** Risk score distribution, TMCO1-AS1 expression, and OS and RFS of patients in the high- and low-risk group. **(B)** Comparison of the distributions of patients with different characteristics in the high- and low-risk groups. **(C)** Kaplan-Meier OS curves for patients in the high- and low-risk groups. **(D)** Kaplan-Meier RFS curves for patients in the high- and low-risk groups.

REFERENCES

Bhan, A., Soleimani, M., and Mandal, S. S. (2017). Long Noncoding RNA and Cancer: A New Paradigm. *Cancer Res.* 77 (15), 3965–3981. doi:10.1158/0008-5472.can-16-2634

Braconi, C., Kogure, T., Valeri, N., Huang, N., Nuovo, G., Costinean, S., et al. (2011). microRNA-29 Can Regulate Expression of the Long Non-coding RNA Gene MEG3 in Hepatocellular Cancer. *Oncogene* 30 (47), 4750–4756. doi:10.1038/onc.2011.193

Bray, F., Ferlay, J., Soerjomataram, I., Siegel, R. L., Torre, L. A., and Jemal, A. (2018). Global Cancer Statistics 2018: GLOBOCAN Estimates of Incidence and Mortality Worldwide for 36 Cancers in 185 Countries. *CA: A Cancer J. Clinicians* 68 (6), 394–424. doi:10.3322/caac.21492

Cedrone, A., Covino, M., Caturelli, E., Pompili, M., Lorenzelli, G., Villani, M. R., et al. (2000). Utility of Alpha-Fetoprotein (AFP) in the Screening of Patients with Virus-Related Chronic Liver Disease: Does Different Viral Etiology Influence AFP Levels in HCC? A Study in 350 Western Patients. *Hepatogastroenterology* 47 (36), 1654–1658.

Chen, L., Yao, H., Wang, K., and Liu, X. (2017). Long Non-Coding RNA MALAT1 Regulates ZEB1 Expression by Sponging miR-143-3p and Promotes Hepatocellular Carcinoma Progression. *J. Cel. Biochem.* 118 (12), 4836–4843. doi:10.1002/jcb.26158

Cui, H., Zhang, Y., Zhang, Q., Chen, W., Zhao, H., and Liang, J. (2017). A Comprehensive Genome-Wide Analysis of Long Noncoding RNA Expression Profile in Hepatocellular Carcinoma. *Cancer Med.* 6 (12), 2932–2941. doi:10.1002/cam4.1180

Da Sacco, L., Baldassarre, A., and Masotti, A. (2012). Bioinformatics Tools and Novel Challenges in Long Non-Coding RNAs (lncRNAs) Functional Analysis. *Int. J. Mol. Sci.* 13 (1), 97–114. doi:10.3390/ijms13010097

Deng, B., Yang, M., Wang, M., and Liu, Z. (2020). Development and Validation of 9-Long Non-Coding RNA Signature to Predicting Survival in Hepatocellular Carcinoma. *Medicine (Baltimore)* 99 (21), e20422. doi:10.1097/md.0000000000020422

Dhir, M., Melin, A. A., Douaiher, J., Lin, C., Zhen, W., Hussain, S. M., et al. (2016). A Review and Update of Treatment Options and Controversies in the Management of Hepatocellular Carcinoma. *Ann. Surg.* 263 (6), 1112–1125. doi:10.1097/sla.0000000000001556

Fan, S. T. (2012). Hepatocellular Carcinoma-Resection or Transplant? *Nat. Rev. Gastroenterol. Hepatol.* 9 (12), 732–737. doi:10.1038/nrgastro.2012.158

Gibb, E. A., Brown, C. J., and Lam, W. L. (2011). The Functional Role of Long Non-Coding RNA in Human Carcinomas. *Mol. Cancer* 10, 38. doi:10.1186/1476-4598-10-38

Imai, K., Beppu, T., Yamao, T., Okabe, H., Hayashi, H., Nitta, H., et al. (2014). Clinicopathological and Prognostic Significance of Preoperative Serum Zinc Status in Patients with Hepatocellular Carcinoma after Initial Hepatectomy. *Ann. Surg. Oncol.* 21 (12), 3817–3826. doi:10.1245/s10434-014-3786-3

Klingenberg, M., Matsuda, A., Diederichs, S., and Patel, T. (2017). Non-Coding RNA in Hepatocellular Carcinoma: Mechanisms, Biomarkers and Therapeutic Targets. *J. Hepatol.* 67 (3), 603–618. doi:10.1016/j.jhep.2017.04.009

Kudo, M. (2018). Systemic Therapy for Hepatocellular Carcinoma: Latest Advances. *Cancers* 10 (11), 412. doi:10.3390/cancers10110412

Lee, S. D., Park, S.-J., Han, S.-S., Kim, S. H., Kim, Y.-K., Lee, S.-A., et al. (2014). Clinicopathological Features and Prognosis of Combined Hepatocellular Carcinoma and Cholangiocarcinoma after Surgery. *Hepatobiliary Pancreat. Dis. Int.* 13 (6), 594–601. doi:10.1016/s1499-3872(14)60275-7

Li, Y., Zhuang, W., Huang, M., and Li, X. (2019). Long Noncoding RNA DDX11-AS1 Epigenetically Represses LATS2 by Interacting with EZH2 and DNMT1 in Hepatocellular Carcinoma. *Biochem. Biophysical Res. Commun.* 514 (4), 1051–1057. doi:10.1016/j.bbrc.2019.05.042

Llovet, J. M., Schwartz, M., and Mazzaferro, V. (2005). Resection and Liver Transplantation for Hepatocellular Carcinoma. *Semin. Liver Dis.* 25 (2), 181–200. doi:10.1055/s-2005-871198

Maruyama, R., and Suzuki, H. (2012). Long Noncoding RNA Involvement in Cancer. *BMB Rep.* 45 (11), 604–611. doi:10.5483/bmbrep.2012.45.11.227

Qin, L.-T., Tang, R.-X., Lin, P., Li, Q., Yang, H., Luo, D.-Z., et al. (2018). Biological Function of UCA1 in Hepatocellular Carcinoma and its Clinical Significance: Investigation with *In Vitro* and Meta-Analysis. *Pathol. - Res. Pract.* 214 (9), 1260–1272. doi:10.1016/j.prp.2018.03.025

Quagliata, L., Matter, M. S., Piscuoglio, S., Arabi, L., Ruiz, C., Procino, A., et al. (2014). Long Noncoding RNA HOTTIP/HOXA13 Expression Is Associated with Disease Progression and Predicts Outcome in Hepatocellular Carcinoma Patients. *Hepatology* 59 (3), 911–923. doi:10.1002/hep.26740

Raoul, J.-L., Forner, A., Bolondi, L., Cheung, T. T., Kloeckner, R., and de Baere, T. (2019). Updated Use of TACE for Hepatocellular Carcinoma Treatment: How and when to Use it Based on Clinical Evidence. *Cancer Treat. Rev.* 72, 28–36. doi:10.1016/j.ctrv.2018.11.002

Raoul, J.-L., Kudo, M., Finn, R. S., Edeline, J., Reig, M., and Galle, P. R. (2018). Systemic Therapy for Intermediate and Advanced Hepatocellular Carcinoma: Sorafenib and beyond. *Cancer Treat. Rev.* 68, 16–24. doi:10.1016/j.ctrv.2018.05.006

Reig, M., da Fonseca, L. G., and Faivre, S. (2018). New Trials and Results in Systemic Treatment of HCC. *J. Hepatol.* 69 (2), 525–533. doi:10.1016/j.jhep.2018.03.028

Sherman, M., Peltekian, K. M., and Lee, C. (1995). Screening for Hepatocellular Carcinoma in Chronic Carriers of Hepatitis B Virus: Incidence and Prevalence of Hepatocellular Carcinoma in a North American Urban Population. *Hepatology* 22 (2), 432–438. doi:10.1002/hep.1840220210

Shi, B., Zhang, X., Chao, L., Zheng, Y., Tan, Y., Wang, L., et al. (2018). Comprehensive Analysis of Key Genes, microRNAs and Long Non-coding RNAs in Hepatocellular Carcinoma. *FEBS Open Bio* 8 (9), 1424–1436. doi:10.1002/2211-5463.12483

Siegel, R. L., Miller, K. D., and Jemal, A. (2018). Cancer Statistics, 2018. *CA: A Cancer J. Clinicians* 68 (1), 7–30. doi:10.3322/caac.21442

Trevisani, F., D'Intino, P. E., Morselli-Labate, A. M., Mazzella, G., Accogli, E., Caraceni, P., et al. (2001). Serum α-Fetoprotein for Diagnosis of Hepatocellular Carcinoma in Patients with Chronic Liver Disease: Influence of HBsAg and Anti-HCV Status. *J. Hepatol.* 34 (4), 570–575. doi:10.1016/s0168-8278(00)00053-2

Tsang, F. H. C., Au, S. L. K., Wei, L., Fan, D. N. Y., Lee, J. M. F., Wong, C. C. L., et al. (2015). Long Non-Coding RNA HOTTIP Is Frequently Up-Regulated in Hepatocellular Carcinoma and Is Targeted by Tumour Suppressive miR-125b. *Liver Int.* 35 (5), 1597–1606. doi:10.1111/liv.12746

Wang, S., and Tran, E. (2013). Unexpected Functions of lncRNAs in Gene Regulation. *Communicative Integr. Biol.* 6 (6), e27610. doi:10.4161/cib.27610

Wang, X., Sun, W., Shen, W., Xia, M., Chen, C., Xiang, D., et al. (2016). Long Non-Coding RNA DILC Regulates Liver Cancer Stem Cells via IL-6/STAT3 axis. *J. Hepatol.* 64 (6), 1283–1294. doi:10.1016/j.jhep.2016.01.019

Xie, H., Ma, H., and Zhou, D. (2013). Plasma HULC as a Promising Novel Biomarker for the Detection of Hepatocellular Carcinoma. *Biomed. Res. Int.* 2013, 136106. doi:10.1155/2013/136106

Zhao, Q.-J., Zhang, J., Xu, L., and Liu, F.-F. (2018). Identification of a Five-Long Non-coding RNA Signature to Improve the Prognosis Prediction for Patients with Hepatocellular Carcinoma. *World J. Gastroenterol.* 24 (30), 3426–3439. doi:10.3748/wjg.v24.i30.3426

Zhao, X., Bai, Z., Li, C., Sheng, C., and Li, H. (2020). Identification of a Novel Eight-lncRNA Prognostic Signature for HBV-HCC and Analysis of Their Functions Based on Coexpression and ceRNA Networks. *Biomed. Res. Int.* 2020, 8765461. doi:10.1155/2020/8765461

Conflict of Interest: The authors declare that the research was conducted in the absence of any commercial or financial relationships that could be construed as a potential conflict of interest.

Publisher's Note: All claims expressed in this article are solely those of the authors and do not necessarily represent those of their affiliated organizations, or those of the publisher, the editors and the reviewers. Any product that may be evaluated in this article, or claim that may be made by its manufacturer, is not guaranteed or endorsed by the publisher.

frontiers in Molecular Biosciences

ORIGINAL RESEARCH
published: 04 February 2022
doi: 10.3389/fmolb.2021.810251

Case Report: One-Year Delay in the Effect of Conversion Surgery Therapy for Advanced Hepatocellular Carcinoma After Systemic Therapy

Qing-Yu Xie†, Hai-Yan Liu†, Ze-Yi Guo, Yan-Ping Wu, Guo-Lin He, Lei Cai, Ming-Xin Pan and Shun-Jun Fu**

Department of Hepatobiliary Surgery II, General Surgery Center, Guangdong Provincial Research Center for Artificial Organ and Tissue Engineering, Guangzhou Clinical Research and Transformation Center for Artificial Liver, Institute of Regenerative Medicine, Zhujiang Hospital, Southern Medical University, Guangzhou, China

OPEN ACCESS

Edited by:
Bing Han,
The Affiliated Hospital of Qingdao University, China

Reviewed by:
Daiwei Wan,
The First Affiliated Hospital of Soochow University, China
Qiao Fei,
Medical University of South Carolina, United States

***Correspondence:**
Ming-Xin Pan
pmxwxy@sohu.com
Shun-Jun Fu
fsj103@163.com

†These authors have contributed equally to this work

Specialty section:
This article was submitted to Molecular Diagnostics and Therapeutics, a section of the journal Frontiers in Molecular Biosciences

Received: *06 November 2021*
Accepted: *13 December 2021*
Published: *04 February 2022*

Citation:
Xie Q-Y, Liu H-Y, Guo Z-Y, Wu Y-P, He G-L, Cai L, Pan M-X and Fu S-J (2022) Case Report: One-Year Delay in the Effect of Conversion Surgery Therapy for Advanced Hepatocellular Carcinoma After Systemic Therapy. Front. Mol. Biosci. 8:810251. doi: 10.3389/fmolb.2021.810251

Hepatocellular carcinoma (HCC) is the sixth most commonly diagnosed malignancy and the third leading cause of cancer-related deaths worldwide. A 58-year-old man visited his local hospital due to abdominal discomfort and was diagnosed with lung metastasis. After admission to our hospital in April 2020, he received two cycles of transcatheter arterial embolization (TAE), hepatic arterial infusion chemotherapy (HAIC-Folfox), sorafenib, and camrelizumab every 3 weeks. Due to the end of HAIC treatment, he underwent drug-eluting transcatheter arterial chemoembolization (dTACE) once, sorafenib, and camrelizumab. However, because of worsening liver function, we interrupted TACE and only gave sorafenib and camrelizumab in August 2020. Although he received systemic therapy, the tumors still rapidly progressed and we considered the possibility of tumor resistance. Subsequently, regorafenib was given. In September, the patient underwent conventional TACE (cTACE) once, regorafenib, and camrelizumab. After half a year of comprehensive treatment, the treatment effect was not satisfactory, and he returned to the local hospital to received regorafenib every day and camrelizumab once every 3 weeks. The patient found that the tumor and lung metastasis had shrunk significantly after 1 year of the initial diagnosis, then he was admitted to our hospital and received surgery treatment, and now he has survived disease-free for 6 months.

Keywords: hepatocellular carcinoma, conversion therapy, camrelizumab, portal vein thrombosis (PVTT), operation

INTRODUCTION

Hepatocellular carcinoma (HCC) is the sixth most commonly diagnosed malignancy and the third leading cause of cancer-related deaths worldwide (Sung et al., 2021). In China, HCC is the fourth most commonly diagnosed and the second leading cause of cancer-related deaths (Chen et al., 2016). As we all know, the best treatment for HCC is radical surgical resection. Unfortunately, most patients with HCC are diagnosed at an advanced stage. In recent years, a new treatment called "conversion surgery therapy" has been reported that converts unresectable gastrointestinal cancer to resectable gastrointestinal cancer, which has improved the prognosis of patients (Sato et al., 2017).

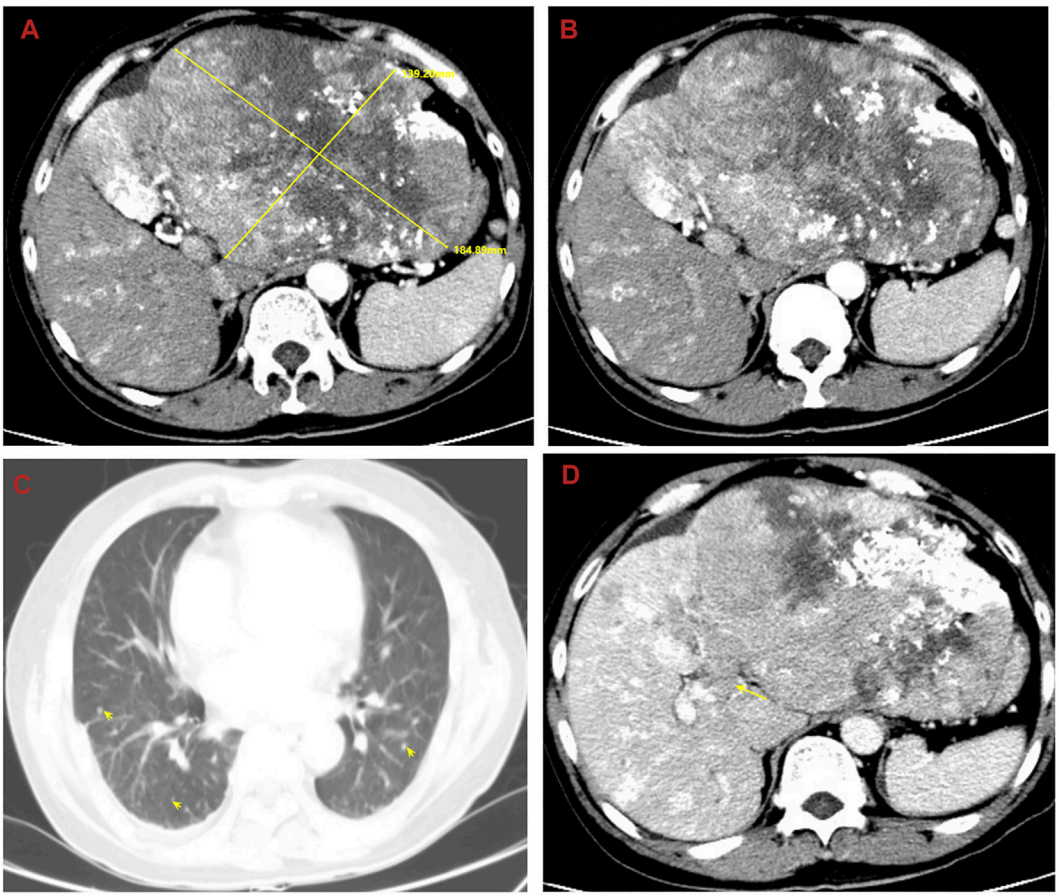

FIGURE 1 | Abdominal computed tomography (CT) shows the tumor in the left lobe of the liver considered to be HCC with multiple metastases in the right lobe of the liver, and with tumor thrombosis in the left portal vein and lung metastases. **(A)** The huge tumor in the left lobe of the liver; **(B)** the multiple metastases in the right lobe of the liver; **(C)** the lung metastases; **(D)** the tumor thrombosis in the left portal vein.

We herein report a case of advanced HCC that received conversion therapy up to a year before it took effect, and finally performed a successful operation.

MATERIALS AND METHODS

We retrospectively reported and analyzed a case that pathologically confirmed primary HCC at Zhujiang Hospital. The clinical data including clinical symptoms, signs, pathological diagnosis, radiological findings, laboratory analyses, treatments, and outcome were obtained from the hospital's electronic medical records. Pathological diagnosis including immunohistochemistry (IHC) was independently reviewed by two pathologists. The patient's family approved the anonymous use of the patient's data, which was in accordance with the Helsinki Declaration.

RESULTS

Case Report

A 58-year-old male patient complained abdominal discomfort for 2 months. He went to his local hospital and was diagnosed with HCC and Barcelona Clinic Liver Cancer (BCLC) stage C in March 2020. Then, transcatheter arterial chemoembolization (TACE) was performed.

In order to seek further diagnosis and treatment, he went to our hospital and was admitted in April 2020. He had a history of hepatitis B. On admission, physical examination showed tenderness over the right upper region area with a 5 cm palpable abdominal mass below the xiphoid process. Laboratory data were recorded as follows: alanine aminotransferase (ALT): 36 IU/L, aspartate transaminase (AST): 81 IU/L, albumin (ALB): 22.7 g/L, total bilirubin (TBIL): 9.7 μmol/L, prothrombin time (PT): 11.5 s, and HBV-DNA: 6.83×10^2 IU/ml. Among the tumor markers, alpha fetoprotein (AFP) was significantly elevated (1,649.0 μg/L), carbohydrate antigen 125 (CA125) was sightly increased (113.0 kU/L), and carcinoembryonic antigen (CEA) and carbohydrate antigen 199 (CA199) were normal. The cirrhosis was classified as Child-Pugh 7 and ALBI grade 3. The enhanced CT revealed small nodules in the middle and lower lobes of the lungs that were considered lung metastases, the tumor in the left lobe of the liver was considered HCC with multiple metastases in the right lobe of the liver, and tumor thrombosis was present in

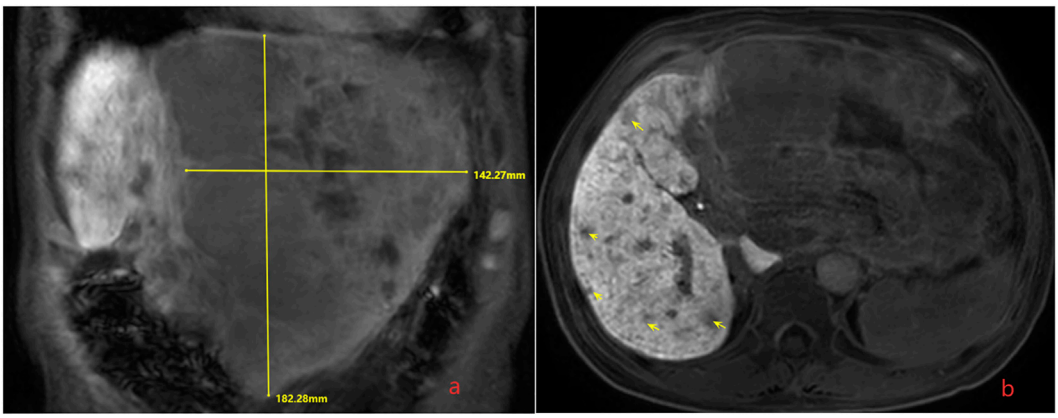

FIGURE 2 | Magnetic resonance imaging (MRI) shows the tumor in the left lobe of the liver with multiple metastases in the liver, and with tumor thrombosis in the left portal vein. **(A)** The huge tumor in the left lobe of the liver; **(B)** the multiple metastases in the right lobe of the liver.

the left portal vein (**Figure 1**). The magnetic resonance imaging (MRI) showed the tumor in the left lobe of the liver with multiple metastases in the right lobe of the liver, and with tumor thrombosis in the left portal vein (**Figure 2**).

1. After MDT discussion, HCC with BCLC stage C and portal vein tumor thrombus (PVTT) classified VP3 and Cheng's type II was diagnosed, and we believe that radical surgical resection was impossible due to the low residual liver volume and lung metastases. He finally received conversion therapy. The procedure details are as follows: The patient received two cycles of transcatheter arterial embolization (TAE), hepatic arterial infusion chemotherapy (HAIC-Folfox) (the HAIC scheme was as follows: We selectively placed a microcatheter into the feeding arteries of the tumor. Then, the microcatheter was connected to the artery infusion pump to perform the following treatment: Day 1: oxaliplatin 85 mg/m^2, leucovorin 400 mg/m^2, and 5-fluorouracil 400 mg/m^2 via intra-arterial infusion; day 2–3: 5-fluorouracil 2,400 mg/m^2 via continuous intra-arterial infusion. After HAIC was completed, the catheter was removed, and compression was performed to achieve hemostasis. The patient was treated every 3 weeks) (He et al., 2019), sorafenib (at a dose of 400 mg twice daily), and camrelizumab (200 mg intravenously every 3 weeks). At the end of HAIC treatment, we were disappointed to find that the tumor had rapidly progressed based on the modified Response Evaluation Criteria in Solid Tumors (mRECIST). Then, the patient received drug-eluting TACE (dTACE) once, sorafenib, and camrelizumab in July 2020. A month later, his liver function deteriorated (ALT: 33 IU/L, AST: 329 IU/L, ALB: 24.9 g/L, TBIL: 16.6 μmol/L, PT: 13.4 s, massive ascites), and the cirrhosis was classified as Child-Pugh 9 and ALBI grade 3. We had to interrupt TACE and only gave sorafenib and camrelizumab. Although he received systemic therapy, the tumors still rapidly progressed and we considered the possibility of tumor resistance. Among the tumor markers, AFP was significantly elevated (12,913.0 μg/L). Then, regorafenib (at a dose of 160 mg daily) was given. In September 2020, the patient received conventional TACE (cTACE) once, regorafenib, and camrelizumab. So far, he had received conversion therapy for half a year, and the treatment effect was not satisfactory. He returned to the local hospital to receive regorafenib every day and camrelizumab once every 3 weeks.

Until a year after his initial diagnosis, the patient found that the tumor and lung metastases had shrunk significantly in the local hospital. Then, he was admitted to our hospital again. On admission, physical examination showed no positive signs. Laboratory data were recorded as follows: ALT: 19 IU/L, AST: 27 IU/L, ALB: 34.2 g/L, TBIL: 8.4 μmol/L, and PT: 11.1 s. AFP was negative (8.1 μg/L). The cirrhosis was classified as Child-Pugh 5 and ALBI grade 2. The enhanced CT revealed there were multiple small nodules in both lungs, which were significantly reduced and shrunken compared to the previous CT. The tumor in the left lobe of the liver was significantly reduced, with local enhancement, and lipiodol deposition was seen. Multiple nodules in the right lobe of the liver had shrunk. And tumor thrombus had formed in the left and right branches of the portal vein (**Figure 3**). Based on these results, we judged that the patient had partial response (PR) and could be treated with radical surgery, according to the response evaluation in the mRECIST criteria. Then he received left hepatectomy, cholecystectomy, and portal vein incision and embolectomy. The pathological examination showed necrosis of a massive HCC with no tumor cells observed on the resection margins, and without metastasis in lymph nodes. The pathological diagnosis showed that the portal vein tumor thrombus had necrotic tissue (**Figure 4**). In the patient's postoperative maintenance therapy, the patient was given lenvatinib 8 mg orally once a day, and camrelizumab 200 mg intravenously once every 3 weeks. There was no clinical evidence of recurrence at 6 months after the resection. The AFP levels remained within the normal limits (**Figure 5**).

DISCUSSION

With the development of diagnosis and treatment of HCC, overall survival time has been prolonged. As we all known,

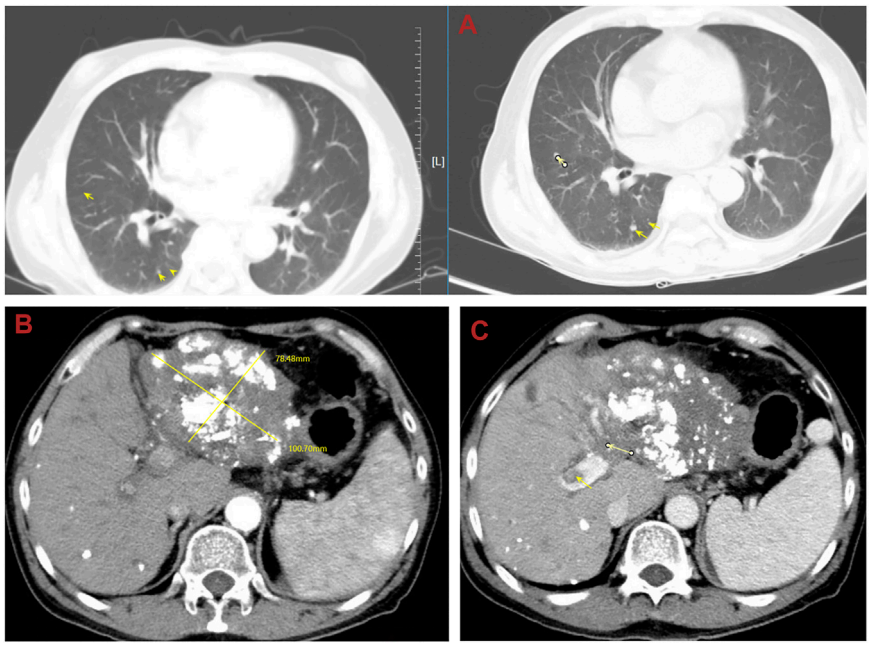

FIGURE 3 | Abdominal computed tomography (CT) shows that multiple small nodules in both lungs were significantly reduced and shrunken and the tumor in the liver was significantly reduced. **(A)** The lung metastases was reduced and shrunken; **(B)** the tumor in the left lobe of the liver shrunk; **(C)** the tumor thrombosis in the left portal vein.

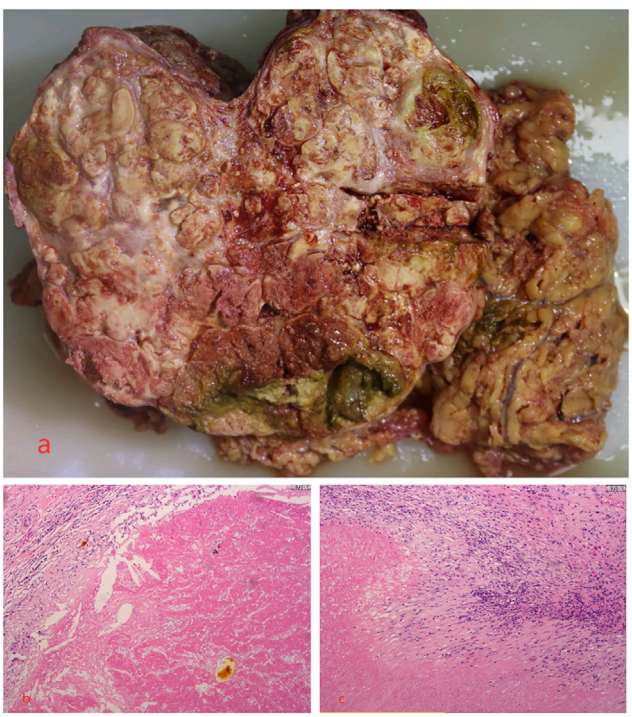

FIGURE 4 | Microscopic examination of the tumor revealed necrosis of the massive HCC with no tumor cells observed on the resection margins, and the portal vein tumor thrombus had necrotic tissue. **(A)** Necrosis of massive HCC; **(B,C)** the pathological examination.

surgical resection is the best treatment for liver cancer patients, which can lead to a 60%–70% chance of 5-year survival (Llovet et al., 2003). However, in China, even in the Asia-Pacific region, most patients were found to be at an advanced stage, and more aggressive approaches (systemic therapy, local therapy, targeted therapy, and immunotherapy) were preformed. The prognosis of patients from the Asia-Pacific region is still worse than those from North America or Europe (Cheng et al., 2009). The prognosis for advanced HCC (unresectable or metastatic) remains poor, with a median overall survival of 4.2 months for those without treatment (Cheng et al., 2009). As for HCC with Okuda stage II, the median survival time was 2.7 months (Yeung et al., 2005). Our case reported that the patient with lung metastasis and PVTT successfully underwent radical surgery after conversion therapy. It may provide an alternative treatment method for advanced HCC patients.

For HCC with PVTT, some studies recommend that an aggressive approach may lead to improved survival, and the patients who underwent radical surgery had the best survival, followed by HAIC and cTACE (Takizawa et al., 2007; Lin et al., 2011). When radical surgery cannot be performed, HAIC and cTACE are often used as the first-line treatment, especially in eastern countries (Korean Liver Cancer Study Group, 2014; Kudo et al., 2015; Omata et al., 2017). Liu BJ et al. found that cTACE combined with HAIC (cTACE-HAIC) would achieve longer overall survival (OS) than cTACE alone (median OS 9 vs. 5 months). For HCC patients with PVTT (Vp3-Vp4), the median OS was significantly different between the cTACE-HAIC group (10 months) and cTACE group (4 months) (Liu

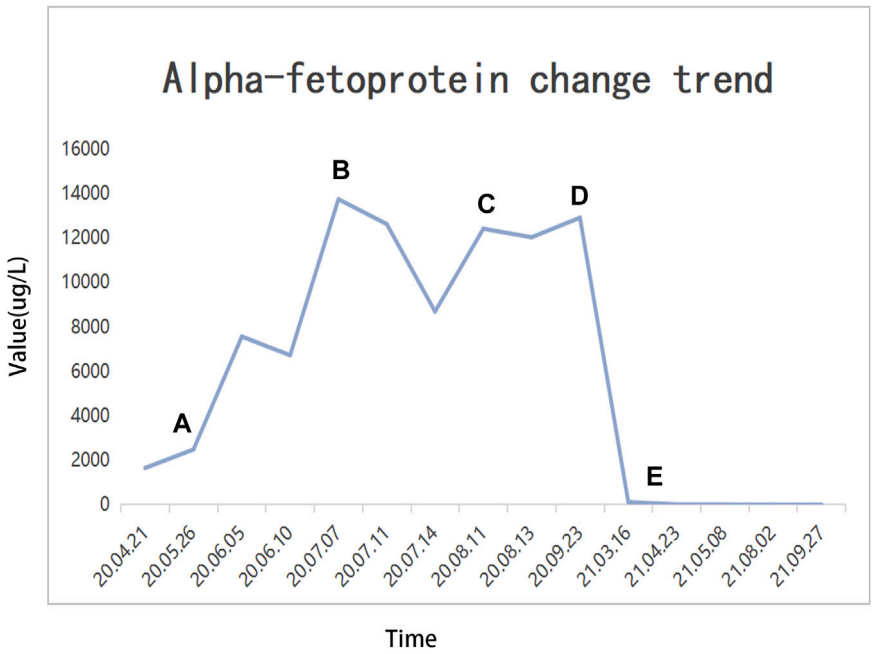

FIGURE 5 | Alpha fetoprotein (AFP) change trend and treatment options. **(A)** TAE + HAIC + sorafenib + camrelizumab; **(B)** dTACE + sorafenib + camrelizumab; **(C)** sorafenib-regorafenib + camrelizumab; **(D)** cTACE + regorafenib + camrelizumab; **(E)** radical surgical resection.

et al., 2021). A retrospective study that compared cTACE-HAIC and cTACE in the treatment of 83 patients with potentially resectable liver cancer by Yuan YF et al. demonstrated that the surgical conversion rate (48.8% vs 9.5%), mRECIST-objective response rate (ORR) (65.9% vs 16.7%), and progression-free survival (PFS) (HR = 0.38, 95%CI: 0.20–0.70) were better in patients in the cTACE-HAIC group than in the cTACE group (Chen et al., 2021).

When sorafenib, a small molecule that inhibits tumor cell proliferation and tumor angiogenesis, is widely used clinically, the survival time of patients with advanced HCC is prolonged (Wilhelm et al., 2004). A multicenter, phase III, double-blind, placebo-controlled trial of sorafenib conducted by Llovet JM et al. reported that median OS in the sorafenib group was significantly longer than the placebo group (10.7 vs. 7.9 months) (Llovet et al., 2008). A phase III randomized, double-blind, placebo-controlled trial in the Asia-Pacific region found that median OS was 6.5 months in patients treated with sorafenib, compared with 4.2 months for those who received placebo (Cheng et al., 2009). Therefore, sorafenib was recommended to be used with caution in patients classified as Child-Pugh A (Omata et al., 2017). Although sorafenib has improved the survival rate of the patients with advanced HCC, it still cannot disguise the disappointing prognosis. So, regorafenib, a novel multi-kinase inhibitor, came into being, which has more potent inhibitory activities against multiple angiogenic pathways and oncogenic pathways than sorafenib (Wilhelm et al., 2011). Some research studies suggested that sequential therapy with sorafenib and regorafenib can be considered to prolong survival time. In the pivotal RESORCE trial, researchers reported median OS, median PFS, and median time to progression (TTP) of 10.6, 3.1, and 3.2 months, respectively (Bruix et al., 2017). A multicenter retrospective study in Japan described the median OS, PFS, and TTP in patients who received sequential therapy with sorafenib and regorafenib for advanced HCC to be 17.3, 6.9, and 6.9 months, respectively (Ogasawara et al., 2020). Another real-world sequential therapy program with sorafenib and regorafenib for advanced HCC conducted in Korea observed median OS, PFS, and TTP of 10.0, 2.7, and 2.6 months, respectively (Lee et al., 2021). Asia-Pacific guidelines also recommended regorafenib as a second-line treatment (Omata et al., 2017).

Due to treatment advancement, immunotherapy is an emerging area. A major breakthrough included antibodies targeting negative regulators of T cells, which restore the cytotoxic ability of T cells to destroy tumor cells by blocking the programmed death (PD)-1 receptor. Camrelizumab is one of the PD-1 inhibitors, which was made in China. In a multicenter, open-label, parallel-group, randomized, phase II trial, the researchers reported that objective response occurred in 14.7% of 217 patients and the overall survival probability at 6 months was 74.4% (Qin et al., 2020). Moreover, some studies reported that camrelizumab combined with target therapy or chemotherapy can synergistically increase efficacy in advanced HCC (Qing et al., 2021). Wei F et al. demonstrated that the median PFS of the lenvatinib plus camrelizumab group was significantly longer than that of the lenvatinib group (8.0 vs 4.0 months). Additional, lenvatinib plus camrelizumab had the higher ORR (28.57% vs 7.41%) and disease control rate (DCR) (71.43% vs 51.85%) (Wei et al., 2021). Yuan G et al. compared the

efficacy and tolerability of camrelizumab and apatinib (C + A) for HCC patients with PVTT. They described that the ORR and DCR were 44.0% and 75.0%, respectively and thought C + A was a promising treatment for HCC with PVTT (Yuan et al., 2020). A multicenter phase Ib/II study about camrelizumab combined with FOLFOX4 for advanced HCC found that the ORR and DCR were 29.4% and 79.4%, respectively. The median duration of response (DOR), PFS, and OS were 6.9, 7.4, and 11.7 months, respectively (Li et al., 2021).

Regarding conversion therapy, there are still some difficult questions to answer, and one is how long the treatment is needed in order to judge the effect. An expert consensus believes that ICIs combined with TKIs have a high surgical conversion rate, and patients with effective treatment generally can be successfully converted after 3-7 treatment cycles (about half a year) (Alliance of Liver Cancer Conversion Therapy et al., 2021; Professional Committee for Prevention and Control of Hepatobiliary and Pancreatic Diseases of Chinese Preventive Medicine Association, 2021). Surgical indications include the following: Child-Pugh grade A or B liver function; adequate residual liver volume after resection, non-cirrhotic patients ≥35% standard liver volume, and cirrhosis patients ≥45% standard liver volume; ICG 15-min tributary rate <20%; the outflow and inflow tract of the liver were intact after the operation; the biliary tract structure was intact after the operation, and the drainage was smooth; the ECOG-PS score was 0–1; and the ASA rating was not higher than 3 (Alliance of Liver Cancer Conversion Therapy et al., 2021; Professional Committee for Prevention and Control of Hepatobiliary and Pancreatic Diseases of Chinese Preventive Medicine Association, 2021). Another question is whether it is still necessary to use a conversion therapy regimen after surgical resection. If it needs to be used, how long will it continue? One expert consensus suggests that ICIs or ICIs combined with TKIs should continue to be given for 6–12 months from 1 month after surgery (Professional Committee for Prevention and Control of Hepatobiliary and Pancreatic Diseases of Chinese Preventive Medicine Association, 2021). Another expert consensus thinks that we can choose the original plan or part of the drug adjuvant treatment in the original plan as appropriate for >6 months. If there is no tumor recurrence and metastasis after two consecutive imaging examinations, and the tumor markers remain normal for 3 months, consider stopping the drug (Alliance of Liver Cancer Conversion Therapy et al., 2021).

Our case reports a patient who was diagnosed with advanced HCC with PVTT and lung metastasis, and successfully implemented conversion therapy. The patient underwent 1 year of conversion therapy, which is far beyond the guideline and previous reports of half a year of conversion therapy. According to previous reports, if patients do not receive effective treatment, the survival time is less than 3 months. However, we used chemotherapy combined with targeted therapy and immunotherapy, and then the patient successfully underwent radical surgery and survived for 6 months without recurrence. For all patients with advanced HCC, this promising result indicates an important step toward a new paradigm of systemic therapy for advanced HCC, and also shows that advanced liver cancer treatment also has the option of radical surgery. Especially, we suggest if the patient is unable to undergo radical surgery and is in a good general condition, the conversion therapy should be as long as possible, which is different from current opinions.

CONCLUSION

Now that the treatment of liver cancer has entered the era of targeted therapy combined with immunotherapy, the results obtained from our case show that conversion therapy is promising for tumor control. However, HCC is still a complex disease that requires continuous hard work to improve its prognosis. Further studies are needed to confirm our findings.

DATA AVAILABILITY STATEMENT

The original contributions presented in the study are included in the article/Supplementary Material, further inquiries can be directed to the corresponding authors.

ETHICS STATEMENT

Written informed consent was obtained from the individual(s) for the publication of any potentially identifiable images or data included in this article.

AUTHOR CONTRIBUTIONS

Q-YX, H-YL, M-XP, and S-JF were the main authors of the manuscript. They were involved in the collection of all data and drafting the manuscript. Z-YG, Y-PW, G-LH, and LC summarized each section, and edited the images of the article. All authors contributed to the interpretation of data and critically revised the manuscript. All authors read and approved the final manuscript.

FUNDING

The work was supported by a grant from the Medical Scientific Research foundation of Guangdong Province of China (No. A2020613), and a grant from the National Natural Science Foundation of China (No.82072627). The funder had no role in the study design, data collection and analysis, decision to publish, or preparation of the manuscript.

REFERENCES

Alliance of Liver Cancer Conversion Therapy (2021). Chinese Expert Consensus on Conversion Therapy in Hepatocellular Carcinoma (2021 Edition). *Chin. J. Dig. Surg.* 20 (6), 600–616.

Bruix, J., Qin, S., Merle, P., Granito, A., Huang, Y.-H., Bodoky, G., et al. (2017). Regorafenib for Patients with Hepatocellular Carcinoma Who Progressed on Sorafenib Treatment (RESORCE): a Randomised, Double-Blind, Placebo-Controlled, Phase 3 Trial. *The Lancet* 389 (10064), 56–66. doi:10.1016/S0140-6736(16)32453-9

Chen, M. S., Yuan, Y. F., Guo, R. P., Shi, M., Huang, J. H., Zhao, M., et al. (2021). Application of Hepatic Arterial Infusion Chemotherapy in the Conversion Therapy of Hepatocellular Carcinoma-Eexperience of Sun Yat-Sen University Cancer Center. *Chin. J. Front. Med. Sci.* 13 (3), 70–76.

Chen, W., Zheng, R., Baade, P. D., Zhang, S., Zeng, H., Bray, F., et al. (2016). Cancer Statistics in China, 2015. *CA: A Cancer J. Clinicians* 66 (2), 115–132. doi:10.3322/caac.21338

Cheng, A.-L., Kang, Y.-K., Chen, Z., Tsao, C.-J., Qin, S., Kim, J. S., et al. (2009). Efficacy and Safety of Sorafenib in Patients in the Asia-Pacific Region with Advanced Hepatocellular Carcinoma: a Phase III Randomised, Double-Blind, Placebo-Controlled Trial. *Lancet Oncol.* 10 (1), 25–34. doi:10.1016/S1470-2045(08)70285-7

He, M., Li, Q., Zou, R., Shen, J., Fang, W., Tan, G., et al. (2019). Sorafenib Plus Hepatic Arterial Infusion of Oxaliplatin, Fluorouracil, and Leucovorin vs Sorafenib Alone for Hepatocellular Carcinoma with Portal Vein Invasion. *JAMA Oncol.* 5 (7), 953–960. doi:10.1001/jamaoncol.2019.0250

Korean Liver Cancer Study Group (2014). 2014 Korean Liver Cancer Study Group-National Cancer Center Korea Practice Guideline for the Management of Hepatocellular Carcinoma. *Korean J. Radiol.* 16 (3), 465–522. doi:10.3348/kjr.2015.16.3.465

Kudo, M., Kitano, M., Sakurai, T., and Nishida, N. (2015). General Rules for the Clinical and Pathological Study of Primary Liver Cancer, Nationwide Follow-Up Survey and Clinical Practice Guidelines: The Outstanding Achievements of the Liver Cancer Study Group of Japan. *Dig. Dis.* 33 (6), 765–770. doi:10.1159/000439101

Lee, M. J., Chang, S. W., Kim, J. H., Lee, Y.-S., Cho, S. B., Seo, Y. S., et al. (2021). Real-world Systemic Sequential Therapy with Sorafenib and Regorafenib for Advanced Hepatocellular Carcinoma: a Multicenter Retrospective Study in Korea. *Invest. New Drugs* 39 (1), 260–268. doi:10.1007/s10637-020-00977-4

Li, H., Qin, S., Liu, Y., Chen, Z., Ren, Z., Xiong, J., et al. (2021). Camrelizumab Combined with FOLFOX4 Regimen as First-Line Therapy for Advanced Hepatocellular Carcinomas: A Sub-cohort of a Multicenter Phase Ib/II Study. *Dddt* 15, 1873–1882. doi:10.2147/DDDT.S304857

Lin, D.-X., Zhang, Q.-Y., Li, X., Ye, Q.-W., Lin, F., and Li, L.-L. (2011). An Aggressive Approach Leads to Improved Survival in Hepatocellular Carcinoma Patients with portal Vein Tumor Thrombus. *J. Cancer Res. Clin. Oncol.* 137 (1), 139–149. doi:10.1007/s00432-010-0868-x

Liu, B.-J., Gao, S., Zhu, X., Guo, J.-H., Kou, F.-X., Liu, S.-X., et al. (2021). Combination Therapy of Chemoembolization and Hepatic Arterial Infusion Chemotherapy in Hepatocellular Carcinoma with Portal Vein Tumor Thrombosis Compared with Chemoembolization Alone: A Propensity Score-Matched Analysis. *Biomed. Res. Int.* 2021, 1–13. doi:10.1155/2021/6670367

Llovet, J. M., Burroughs, A., and Bruix, J. (2003). Hepatocellular Carcinoma. *The Lancet* 362 (9399), 1907–1917. doi:10.1016/s0140-6736(03)14964-1

Llovet, J. M., Ricci, S., Mazzaferro, V., Hilgard, P., Gane, E., Blanc, J.-F., et al. (2008). Sorafenib in Advanced Hepatocellular Carcinoma. *N. Engl. J. Med.* 359 (4), 378–390. doi:10.1056/NEJMoa0708857

Ogasawara, S., Ooka, Y., Itokawa, N., Inoue, M., Okabe, S., Seki, A., et al. (2020). Sequential Therapy with Sorafenib and Regorafenib for Advanced Hepatocellular Carcinoma: a Multicenter Retrospective Study in Japan. *Invest. New Drugs* 38 (1), 172–180. doi:10.1007/s10637-019-00801-8

Omata, M., Cheng, A.-L., Kokudo, N., Kudo, M., Lee, J. M., Jia, J., et al. (2017). Asia-Pacific Clinical Practice Guidelines on the Management of Hepatocellular Carcinoma: a 2017 Update. *Hepatol. Int.* 11 (4), 317–370. doi:10.1007/s12072-017-9799-9

Professional Committee for Prevention and Control of Hepatobiliary and Pancreatic Diseases of Chinese Preventive Medicine Association (2021). Chinese Expert Consensus on Conversion Therapy of Immune Checkpoint Inhibitors Combined Antiangiogenic Targeted Drugs for Advanced Hepatocellular Carcinoma (2021 Edition). *Chin. J. Hepatobiliary Surg.* 27 (4), 241–251.

Qin, S., Ren, Z., Meng, Z., Chen, Z., Chai, X., Xiong, J., et al. (2020). Camrelizumab in Patients with Previously Treated Advanced Hepatocellular Carcinoma: a Multicentre, Open-Label, Parallel-Group, Randomised, Phase 2 Trial. *Lancet Oncol.* 21 (4), 571–580. doi:10.1016/S1470-2045(20)30011-5

Qing, X., Xu, W., Zong, J., Du, X., Peng, H., and Zhang, Y. (2021). Emerging Treatment Modalities for Systemic Therapy in Hepatocellular Carcinoma. *Biomark Res.* 9 (1), 64. doi:10.1186/s40364-021-00319-3

Sato, Y., Ohnuma, H., Nobuoka, T., Hirakawa, M., Sagawa, T., Fujikawa, K., et al. (2017). Conversion Therapy for Inoperable Advanced Gastric Cancer Patients by Docetaxel, Cisplatin, and S-1 (DCS) Chemotherapy: a Multi-Institutional Retrospective Study. *Gastric Cancer* 20 (3), 517–526. doi:10.1007/s10120-016-0633-1

Sung, H., Ferlay, J., Siegel, R. L., Laversanne, M., Soerjomataram, I., Jemal, A., et al. (2021). Global Cancer Statistics 2020: GLOBOCAN Estimates of Incidence and Mortality Worldwide for 36 Cancers in 185 Countries. *CA A. Cancer J. Clin.* 71 (3), 209–249. doi:10.3322/caac.21660

Takizawa, D., Kakizaki, S., Sohara, N., Sato, K., Takagi, H., Arai, H., et al. (2007). Hepatocellular Carcinoma with portal Vein Tumor Thrombosis: Clinical Characteristics, Prognosis, and Patient Survival Analysis. *Dig. Dis. Sci.* 52 (11), 3290–3295. doi:10.1007/s10620-007-9808-2

Wei, F., Huang, Q., He, J., Luo, L., and Zeng, Y. (2021). Lenvatinib Plus Camrelizumab versus Lenvatinib Monotherapy as Post-Progression Treatment for Advanced Hepatocellular Carcinoma: A Short-Term Prognostic Study. *Cmar* 13, 4233–4240. doi:10.2147/CMAR.S304820

Wilhelm, S. M., Carter, C., Tang, L., Wilkie, D., McNabola, A., Rong, H., et al. (2004). BAY 43-9006 Exhibits Broad Spectrum Oral Antitumor Activity and Targets the RAF/MEK/ERK Pathway and Receptor Tyrosine Kinases Involved in Tumor Progression and Angiogenesis. *Cancer Res.* 64 (19), 7099–7109. doi:10.1158/0008-5472.CAN-04-1443

Wilhelm, S. M., Dumas, J., Adnane, L., Lynch, M., Carter, C. A., Schütz, G., et al. (2011). Regorafenib (BAY 73-4506): a New Oral Multikinase Inhibitor of Angiogenic, Stromal and Oncogenic Receptor Tyrosine Kinases with Potent Preclinical Antitumor Activity. *Int. J. Cancer* 129 (1), 245–255. doi:10.1002/ijc.25864

Yeung, Y. P., Lo, C. M., Liu, C. L., Wong, B. C., Fan, S. T., and Wong, J. (2005). Natural History of Untreated Nonsurgical Hepatocellular Carcinoma. *Am. J. Gastroenterol.* 100 (9), 1995–2004. doi:10.1111/j.1572-0241.2005.00229.x

Yuan, G., Cheng, X., Li, Q., Zang, M., Huang, W., Fan, W., et al. (2020). Safety and Efficacy of Camrelizumab Combined with Apatinib for Advanced Hepatocellular Carcinoma with Portal Vein Tumor Thrombus: A Multicenter Retrospective Study. *Ott* 13, 12683–12693. doi:10.2147/OTT.S286169

Conflict of Interest: The authors declare that the research was conducted in the absence of any commercial or financial relationships that could be construed as a potential conflict of interest.

Advantages of publishing in Frontiers

OPEN ACCESS
Articles are free to read for greatest visibility and readership

FAST PUBLICATION
Around 90 days from submission to decision

HIGH QUALITY PEER-REVIEW
Rigorous, collaborative, and constructive peer-review

TRANSPARENT PEER-REVIEW
Editors and reviewers acknowledged by name on published articles

Frontiers
Avenue du Tribunal-Fédéral 34
1005 Lausanne | Switzerland

Visit us: www.frontiersin.org
Contact us: frontiersin.org/about/contact

REPRODUCIBILITY OF RESEARCH
Support open data and methods to enhance research reproducibility

DIGITAL PUBLISHING
Articles designed for optimal readership across devices

FOLLOW US
@frontiersin

IMPACT METRICS
Advanced article metrics track visibility across digital media

EXTENSIVE PROMOTION
Marketing and promotion of impactful research

LOOP RESEARCH NETWORK
Our network increases your article's readership